# APPROACHES FOR MODELING SATELLITE RELATIVE MOTION

A Dissertation

by

KIRK WAYNE JOHNSON

Submitted to the Office of Graduate and Professional Studies of
Texas A&M University
in partial fulfillment of the requirement for the degree of

DOCTOR OF PHILOSOPHY

| | |
|---|---|
| Chair of Committee, | Kyle T. Alfriend |
| Co-Chair of Committee, | Srinivas R. Vadali |
| Committee Members, | John E. Hurtado |
| | Igor Zelenko |
| Head of Department, | Rodney D. W. Bowersox |

December 2016

Major Subject: Aerospace Engineering

# ABSTRACT

This dissertation explores new approaches for modeling perturbed and unperturbed satellite relative motion. It extends Hoots orbit theory, an analytical averaging-method perturbation solution to the Zonal Problem, to second order. In addition, this study develops a new hybrid numerical/analytical algorithm for converting initial conditions from osculating elements to mean elements, so that a single set of osculating initial conditions may be taken as simulation inputs. Also, this study develops a new version of the Gim-Alfriend State Transition Matrix (GA STM) for linearized perturbed relative motion, in terms of the variables from Hoots theory. These variables, the Hoots elements, are advantageous (although not unique) in that they have no singularities for orbit eccentricity or inclination and they require only one solution of Kepler's Equation at each time step, even when using the GA STM. The new models are compared by simulation with orbit theories and GA STMs using the so-called nonsingular elements (which are in fact singular for zero inclination) and the equinoctial elements. This study predicts and verifies the order of magnitude of modeling error due to various sources.

This study also considers two special applications in satellite relative motion modeling. First, Projected Circular Orbit (PCO) formations, originally defined for unperturbed motion about a circular reference orbit, have important applications and are widely studied. This dissertation removes the singularity for zero inclination by implementing the PCO initial conditions in equinoctial elements, allowing PCO formations to be initialized about equatorial orbits. Furthermore, this study reveals how the choice of variables for writing the PCO initial conditions changes the geometric interpretation of the PCO phase angle parameter $\alpha$. Second, this study develops an alternative to the standard methods for mitigating along-track drift in perturbed satellite formations. The new method eliminates all along-track secular motion to first order by sacrificing one degree of freedom in the formation design.

# ACKNOWLEDGMENTS

The past three years studying at Texas A&M have been both a tremendous privilege and a great challenge. I've had the opportunity to meet and learn from some of the greatest minds in the world in a fascinating area of research. For help in accomplishing my part of the task, I owe a debt of thanks to many.

First, as always, "I thank Christ Jesus our Lord, who has given me strength" (1 Timothy 1:12).

I am extremely grateful for the support of my family. To my wife, thank you for all the innumerable ways you've helped me throughout this process–I love you, and your encouragement means more to me than I can express! To my son and daughter, thank you for your patience–I'm proud of you both, and I promise we'll play a family game once this is all over. Thanks also to all those praying for me from a distance, especially Mom and Dad.

As for my advisors, Dr. Terry Alfriend and Dr. Rao Vadali, it was an honor to learn from them and work with them. Dr. Vadali's patient guidance in our weekly meetings and his insightful way of explaining complex topics were critical to what I've accomplished. And I have likewise benefited greatly from the depth of Dr. Alfriend's knowledge and experience. It truly seems to me that they've both forgotten more about astrodynamics than I'll ever know. They have been the best teachers and mentors I could have asked for.

I also wish to thank Dr. John Hurtado and Dr. Igor Zelenko for serving on my doctoral committee. And I am grateful for the advice and assistance of those who worked with our research group during my time here: Dr. Kohei Fujimoto, Dr. Hui Yan, Dr. Inkwan Park, and especially Bharat Mahajan, who was always ready to be a cheerful sounding board for ideas.

Finally, I am thankful the US Air Force has allowed me to spend a few years studying full-time–it's been a fantastic opportunity[1].

[1]The views expressed in this document are those of the author and do not reflect the official policy or position of the United States Air Force, Department of Defense, or the U.S. Government.

# TABLE OF CONTENTS

# LIST OF FIGURES

# CHAPTER I

# INTRODUCTION AND LITERATURE REVIEW

## I.A INTRODUCTION

Satellite formations have many potential applications and advantages over individual spacecraft. For example, Projected-Circular Orbit (PCO) formations in low-Earth orbit (LEO) are useful for constant-aperture multistatic surface observations [1]. Since such formations can be stable with very little control effort over long time spans, it is desirable to predict their trajectories (relative positions and velocities) and control costs over long time periods; this requires high-accuracy analytical approximations of the relative spacecraft dynamics. Such analytical approximations could be especially useful in autonomous on-board algorithms for relative navigation and control.

For some LEO formation orbits, the zonal harmonics of Earth's gravity field are the most significant perturbations from simple two-body Keplerian dynamics–in other words, sectoral and tesseral harmonics, resonant and third-body effects, and non-conservative forces may be neglected in some applications. Another significant perturbation in some LEO orbits, especially near reentry, is atmospheric drag. However, the differential effect of drag on the relative motion of spacecraft in formation can be small, especially if the individual satellites have similar area-to-mass ratios. Neglecting all perturbations except the zonal harmonics gives the Zonal Problem of Artificial Satellite Theory, which assumes that the only external force present is the gravity due to an axially symmetric Earth.

Finding an analytic approximate solution to the Zonal Problem requires the use of a general perturbation method, in which the gravitational zonal harmonics are treated as perturbations to the Two-Body Problem. For two satellites in formation, combining such analytic solutions into a closed-form relative motion model requires further approximation.

If the approximation used to derive a given analytical model is too coarse, the results will not be sufficiently accurate for the intended application; for example, the control system may expend unnecessary

fuel compensating for errors in the dynamic model. On the other hand, if the approximation is "too accurate" (i.e., retains too many terms in a series approximation), the system may waste computational resources while providing no operational advantage.

## I.B PROBLEM DEFINITION

This study will deal with approximate solutions to the Zonal Problem and the satellite relative motion problem, stated here exactly:

In the Zonal Problem, the Hamiltonian governing the motion of a single satellite (see [2], pp. 638 and 647, and [3], Eq. 11.63) is

$$F = -\frac{\mu}{2L^2} + \sum_{k=2}^{\infty} \frac{\mu}{r} \left( \frac{R_e}{r} \right)^k J_k \, P_k(\sin \phi)$$

where $\mu$ is the Earth's gravitational parameter, $R_e$ is the Earth's average radius, $r$ is the satellite's radial distance from Earth's center, $\phi$ is its latitude, $L = \sqrt{\mu a}$ is from the set of canonical Delaunay elements, $a$ is the orbit semi-major axis, and $P_k$ is the k$^{\text{th}}$ Legendre polynomial. The $J_k$ are the zonal harmonic coefficients, found experimentally and often used as perturbation parameters in perturbation methods of solution. $J_2$ is on the order of $10^{-3}$, while $J_3$ through $J_{14}$ are on the order of $10^{-6}$ ([2], Table D-1); therefore, $J_2$ can be considered a first-order perturbation, while subsequent harmonics can be considered as second-order perturbations.

The exact nonlinear equations of satellite relative motion for the unperturbed (Keplerian) case ([3], Eq. 14.12) are

$$\begin{aligned} \ddot{x} - 2\dot{f}\left(\dot{y} - y\frac{\dot{r}}{r}\right) - x\dot{f}^2 - \frac{\mu}{r^2} &= -\frac{\mu}{r_d^3}(r + x) \\ \ddot{y} + 2\dot{f}\left(\dot{x} - x\frac{\dot{r}}{r}\right) - y\dot{f}^2 &= -\frac{\mu}{r_d^3} y \\ \ddot{z} &= -\frac{\mu}{r_d^3} z \end{aligned} \tag{1.1}$$

where $r$ and $f$ are the chief satellite's orbit radius and true anomaly, respectively, $r_d$ is the deputy satellite's orbit radius, and $\begin{bmatrix} x & y & z \end{bmatrix}^T = \underline{x}$ is the deputy's relative position in a Local-Vertical Local-Horizontal (LVLH) reference frame centered at the chief. These equations must be solved using an appropriate set of

approximations (for example, over some time span, the relative motion will be small compared to the total orbital motion) and must be modified to account for the zonal harmonic perturbations. In the absence of such a closed-form model, the single-satellite trajectories must be differenced numerically and mapped into relative space.

## I.C LITERATURE REVIEW

### I.C.1 The Zonal Problem

Many successful general-perturbation approaches to the Zonal Problem have used averaging methods. Famously, Brouwer [4] considered zonal harmonics through $J_5$ and used the von Zeipel method [5] to derive an approximate analytical solution. This solution includes expressions for the transformation from mean to osculating elements (both Delaunay and classical orbit elements) up to first order in $J_2$, along with expressions for the secular rates of the mean elements up to second order. This method requires two transformations with two separate generating functions $S$ (for short-period terms, those depending on the mean anomaly $l$) and $S^*$ (for long-period terms, those depending on the argument of perigee $g$, but not $l$). The mean secular rates are derived by taking advantage of the fact that the mean Delaunay elements are canonical with respect to the transformed Hamiltonian.

Kozai [6] used the von Zeipel method to extend Brouwer theory to zonal harmonic $J_8$ and to second order in the mean-to-osculating transformation. Lyddane [7] improved Brouwer theory by removing certain singularities for zero eccentricity and inclination. Hoots ([8], [9]) improved it still further, in part by introducing a unique nonsingular element set, the Hoots position elements:

$$y_1 = r \quad y_2 = \dot{r} \quad y_3 = r\dot{f} \quad y_4 = \sin\tfrac{i}{2}\sin(f+g) \quad y_5 = \sin\tfrac{i}{2}\cos(f+g) \quad y_6 = f+g+h \tag{1.2}$$

where $i$ is the inclination and $h$ is the right ascension of the ascending node.

Other averaging methods that have been used successfully in the Zonal Problem are those using Lie series. The method of Hori [10], as implemented by Kinoshita [11], transforms a generic variable $\epsilon$ using

successive generating functions $S$ and $S^*$ as

$$\epsilon = \epsilon' + \{\epsilon', S\} + \frac{1}{2}\{\{\epsilon', S\}, S\} + \cdots$$

$$\epsilon' = \epsilon'' + \{\epsilon'', S^*\} + \frac{1}{2}\{\{\epsilon'', S^*\}, S^*\} + \cdots$$

where the braces denote the Poisson bracket operator. In the Hori method, the Poisson brackets are interpreted as $\{b, c\} = \frac{\partial b}{\partial p_i}\frac{\partial c}{\partial q_i} - \frac{\partial b}{\partial q_i}\frac{\partial c}{\partial p_i}$ for canonical coordinates $q_i$ and conjugate momenta $p_i$. In terms of the Delaunay elements,

$$\{b, c\} = \frac{\partial b}{\partial L}\frac{\partial c}{\partial l} - \frac{\partial b}{\partial l}\frac{\partial c}{\partial L} + \frac{\partial b}{\partial G}\frac{\partial c}{\partial g} - \frac{\partial b}{\partial g}\frac{\partial c}{\partial G} + \frac{\partial b}{\partial H}\frac{\partial c}{\partial h} - \frac{\partial b}{\partial h}\frac{\partial c}{\partial H}$$

(e.g., Reference [10], Eq. 58). Kinoshita's approximate solution considered zonal harmonics through $J_4$ and included terms up to third order for the generating functions and for the mean-to-osculating transformations of the nonsingular orbit elements $(\lambda, h, q_1, q_2, L, H)$, where $\lambda = l + g$, $q_1 = e\cos g$, $q_2 = e\sin g$, $H = G\cos i$, $G = L\eta$, and $\eta = \sqrt{1 - e^2}$.

The Lie-series method of Deprit ([12], [13]), as implemented by Kamel [14], uses $\epsilon$ to denote the small perturbation parameter and expands the generating function $W$ as a power series: $W = W_1 + \epsilon W_2 + \cdots$. Variable $y$ is transformed to $x$ as

$$x = y + \epsilon\{y, W_1\} + \frac{\epsilon^2}{2}\{y, W_2\} + \frac{\epsilon^2}{2}\{\{y, W_1\}, W_1\} + \cdots$$

In the Deprit method, the Poisson brackets are interpreted as $\{b, c\} = \frac{\partial b}{\partial q_i}\frac{\partial c}{\partial p_i} - \frac{\partial b}{\partial p_i}\frac{\partial c}{\partial q_i}$. In terms of the Delaunay elements, then,

$$\{b, c\} = \frac{\partial b}{\partial l}\frac{\partial c}{\partial L} - \frac{\partial b}{\partial L}\frac{\partial c}{\partial l} + \frac{\partial b}{\partial g}\frac{\partial c}{\partial G} - \frac{\partial b}{\partial G}\frac{\partial c}{\partial g} + \frac{\partial b}{\partial h}\frac{\partial c}{\partial H} - \frac{\partial b}{\partial H}\frac{\partial c}{\partial h}$$

(Reference [12], p. 176). Alfriend and Velez [15] applied this method to the Main Problem ($J_2$ only) using a perturbation parameter $\epsilon = \frac{J_2 R_e^2}{2}$. The resulting element transformation (where $\underline{y}$ is the vector of osculating elements and $\underline{y}''$ is the vector of mean elements) is

$$\underline{y} - \underline{y}'' = \frac{J_2 R_e^2}{2}\{\underline{y}'', W_1\} + \frac{J_2^2 R_e^4}{8}\{\underline{y}'', W_2\} + \frac{J_2^2 R_e^4}{8}\{\{\underline{y}'', W_1\}, W_1\} + \mathcal{O}(J_2^3)$$

Note that this transformation is written with a single generating function. In practice, most high-order theories use two or three separate transformations, with a generating function for each one, in order to limit

the number of terms in the derivation [13]. A perturbation theory with a single transformation step produces first-order results equivalent to existing theories, but would differ at second order.

### I.C.2 Satellite Relative Motion

Satellite relative motion models have been studied extensively since Clohessy and Wiltshire [16] first linearized and solved the relative equations of motion for a chief satellite in a circular, unperturbed orbit using a formulation due to Hill [17]. The resulting HCW model is one of the simplest available; a more accurate linearized model is found in the Gim-Alfriend State Transition Matrix (GA STM) [18]. It can accommodate eccentric chief orbits and perturbed gravity fields using a succession of linear operators:

$$\begin{bmatrix} \underline{x}(t)^T & \underline{\dot{x}}(t)^T \end{bmatrix}^T = \Sigma(t) D(t) \bar{\phi}_{\bar{e}}(t, t_0) D^{-1}(t_0) \Sigma^{-1}(t_0) \begin{bmatrix} \underline{x}(t_0)^T & \underline{\dot{x}}(t_0)^T \end{bmatrix}^T \tag{1.3}$$

where $\Sigma$ is the linearized transformation matrix mapping orbit element differences to relative position and velocity coordinates, $D$ is the linearized sensitivity matrix mapping mean to osculating elements, and $\bar{\phi}_{\bar{e}}(t, t_0)$ is the state transition matrix for the mean elements. Gim and Alfriend reported solutions with $J_2$ as the only perturbation for both nonsingular elements [18] and equinoctial elements [19]. Yan, Vadali, and Alfriend extended the GA STM to include second-order perturbation effects due to $J_2^2$, $J_4$, and $J_6$ [20].

In addition to the LVLH Cartesian coordinates used in Eqs. 1.1, another common representation of satellite relative motion uses differential orbital elements [21], [22], such as $\delta a$, $\delta \eta$, or $\delta i$, where $\delta$ signifies the difference between the chief's and deputy's values. One virtue of such a representation is that it allows the condition for zero along-track drift of the relative trajectory [23] to be expressed compactly: $\delta a = 0$ for the unperturbed case, and

$$\delta a = \frac{J_2 a}{2} \left( \frac{R_e}{a} \right)^2 \left( \frac{3\eta + 4}{\eta^5} \right) \left[ \left( 1 - 3\cos^2 i \right) \delta\eta - \left( \eta \sin 2i \right) \delta i \right] \tag{1.4}$$

for a first-order $J_2$-only model (Eq. 8.15, [1]).

It is also possible to simulate satellite relative motion without forming a full STM or other closed-form model. Each satellite's trajectory can be propagated directly from the analytic theory, and the results can be differenced numerically and mapped into relative space.

*Relative Motion Parameterizations*

Besides LVLH initial conditions and orbit element differences, a variety of parameterizations have been used to describe the geometry of satellite relative orbits. Some have used the relative eccentricity vector and relative inclination vector as parameters [24], [25].

Others have taken advantage of the simplicity of the HCW solution to find geometrically meaningful parameters, such as the Relative Orbit Elements of Lovell and Tragesser [26]. One often-studied type of satellite formation–whose parameters arise from the HCW solution–is the Projected Circular Orbit (PCO) [27, 23, 1], in which the relative motion of a deputy satellite about a chief forms a repeating circular trajectory when projected onto the Earth's surface (that is, on the local horizontal plane). Such a formation could have many potential applications, such as for multi-static Earth-observation sensors.

When the chief's orbit is noncircular, the geometry of the relative trajectory changes. Some studies have found geometrically meaningful parameters for formations about eccentric orbits, such as those of Sengupta and Vadali [28] and of Jiang, Li, Baoyin, and Gao [29].

### I.C.3 Alternative Orbit Elements

Some variable sets are better suited than others for a particular problem. For linearized approximate solutions to the satellite relative motion problem, orbit element differences are better choices than, for example, Cartesian initial conditions–they better capture the nonlinearity of the problem and produce more accurate results [30]. For the Zonal Problem, orbit element sets which are not singular for any eccentricity or inclination are preferable, because they do not exclude solutions for circular or equatorial orbits and they do not suffer from numerical difficulties in neighboring orbits. Also, element sets which satisfy Hamilton's canonical equations may be preferable, in that they may permit simpler derivations of the mean-to-osculating element transformations.

Other considerations include whether a set of elements is explicit in $f$ or in $l$, the mean anomaly; this affects when and how often an analytical algorithm requires numerical solutions of Kepler's Equation. In addition, some procedures may be more complex for element sets which include more fast variables (as

| | Classical | Delaunay | Nonsingular | Equinoctial | Hoots | Poincaré | Whittaker |
|---|---|---|---|---|---|---|---|
| | $a$ | $\boldsymbol{l}$ | $a$ or $L$ | $a$ | $\boldsymbol{r}$ | $\boldsymbol{\lambda + h}$ | $\boldsymbol{r}$ |
| | $e$ | $g$ | $\boldsymbol{u}$ or $\boldsymbol{\lambda}$ | $e\sin(g+h)$ | $\boldsymbol{\dot{r}}$ | $g_p$ | $\boldsymbol{u}$ |
| | $i$ | $h$ | $i$ | $e\cos(g+h)$ | $\boldsymbol{r\dot{f}}$ | $h_p$ | $h$ |
| | $h$ | $L$ | $e\cos g$ | $\tan\frac{i}{2}\sin h$ | $\boldsymbol{y_4}$ | $L$ | $\boldsymbol{\dot{r}}$ |
| | $g$ | $G$ | $e\sin g$ | $\tan\frac{i}{2}\cos h$ | $\boldsymbol{y_5}$ | $G_p$ | $G$ |
| | $\boldsymbol{l}$ or $\mathbf{f}$ | $H$ | $h$ | $\boldsymbol{\lambda + h}$ or $\boldsymbol{u + h}$ | $\boldsymbol{u + h}$ | $H_p$ | $H$ |
| Singular in $e$? | Y | Y | N | N | N | N | N |
| Singular in $i$? | Y | Y | Y | N | N | N | Y |
| Canonical? | N | Y | N | N | N | Y | Y |
| Explicit in $f$ or $l$? | either | $l$ | either | either | $f$ | $l$ | $f$ |

**Table 1.1: Comparison of orbit element sets (fast variables in bold)**

opposed to constants of the unperturbed motion). See Table 1.1 for a comparison of several candidate sets. (Note that fast variables are shown in bold.)

The classical and Delaunay elements are easily understood geometrically and theiry mean elements are easily propagated, but they are singular for zero eccentricity and inclination. The nonsingular elements (which are in fact singular for zero inclination) have already been discussed, and they are the basis for an orbit theory and one version of the GA STM used in this study [11], [19].

This study focuses primarily on the Hoots elements defined in Eq. 1.2, developed to compute the Brouwer-theory approximate solution to the Zonal Problem without singularities and with greater computational efficiency. Hoots claimed better accuracy plus 30-35% better run time, due to eliminating several computations at each time step, including a solution of Kepler's Equation [9]. The Hoots elements will be discussed in more detail in Chapters II and IV.

The set of orbit elements known as polar nodal variables, or Hill's variables [31], or Whittaker variables [32, p. 349], are $\underline{w} = \left[r\ u\ h\ \dot{r}\ G\ H\right]$. They are canonical with respect to the Hamiltonian of the Zonal

Problem; that is, $\dot{r}$, $G$, and $H$ are the conjugate momenta for coordinates $r$, $u$, and $h$, respectively. Whittaker elements have been used to develop a number of Lie-series averaging methods in orbit theory, including the original statement of the Deprit method [13], as well as elimination of the parallax [33] and elimination of the perigee [34]. Of course, these same transformations can be posed in terms of other elements, such as the Delaunay elements [35], [36]. Likewise, the generating functions from other methods (such as the theories of Brouwer [4] or Kinoshita [11]) can be used, at least to first order in $J_2$, in a Lie-series method using Whittaker elements [37]. The primary difficulty with Whittaker elements is their singularity for zero inclination. They will be discussed more in Appendix E.

The equinoctial elements can use either the mean longitude $\Lambda = \lambda + h$ or the true longitude $\Psi = u + h$. They are also the basis for an orbit theory and one version of the GA STM used in this study [19]. Because they are well known and completely nonsingular, they are the basis of active on-going research [38].

Finally, the Poincaré elements are defined in Table 1.1, where $g_p = \sqrt{2L(1-\eta)}\cos(g+h)$, $h_p = \sqrt{2G(1-\cos i)}\cos h$, $G_p = -\sqrt{2L(1-\eta)}\sin(g+h)$, and $H_p = -\sqrt{2G(1-\cos i)}\sin h$ [2]. They are canonical and nonsingular in both $e$ and $i$. For these reasons, they may merit further investigation as a basis for modeling perturbed satellite relative motion.

### I.C.4 Evaluating Models

To evaluate the accuracy of proposed analytic approximations, Alfriend and Yan [39] developed a nonlinearity index $\nu$, which can be used as a measure of modeling error. If $\underline{\bar{y}}(t)$ is the nondimensionalized state vector from the truth model and $\underline{y}(t)$ is the nondimensionalized state vector from the analytic theory, then $\nu(t) = |\frac{\underline{\bar{y}}^T\underline{\bar{y}}}{\underline{y}^T\underline{y}} - 1|$.

It is also possible, for a given dynamical problem, to quantify the balance between model fidelity and the requirements of the control and navigation systems, as shown by Fujimoto, Alfriend, and Vadali [40]. For example, they showed how to find the number of zonal harmonics in the approximate satellite motion model at which, for a given sensor noise level, additional harmonics fail to decrease the error in the relative state estimate. They also found the level of approximation corresponding to the global minimum of a cost

function which takes into account both control effort and computation time.

## I.D OUTLINE OF REMAINING CHAPTERS

This dissertation will explore new alternatives for modeling perturbed satellite relative motion, with a focus on low Earth orbit formations. The goal is greater flexibility (by removing singularities, for example), greater simplicity and computational efficiency (by reducing the number of algorithm steps and Kepler's Equation solutions, for example), and greater accuracy (by including more perturbations and higher-order solutions).

Chapter II will extend Hoots theory, a completely nonsingular analytical orbit theory, to zonal harmonic $J_6$ and to second order in $J_2$. It will also make some minor additions to the nonsingular-elements theory used by Kinoshita and Gim, in order to compare both theories at second order in the presence of zonal harmonics through $J_4$.

Chapters III through V will deal with satellite relative satellite motion. First, in Chapter III, the geometry of the Projected Circular Orbit formation will be described in detail, and the PCO initial conditions will be reformulated to remove the singularity for zero inclination, allowing PCO formations about equatorial orbits. Next, in Chapter IV, a new version of the GA STM will be derived using Hoots elements, corresponding to the single-satellite orbit theory in Chapter II. Then, in Chapter V, the problem of preventing along-track drift will be addressed. The current state-of-the-art analytical approximations for drift prevention will be compared to several alternatives, and a method will be developed to eliminate along-track secular motion by sacrificing one degree of freedom in the formation geometry. This chapter will examine drift in PCO formations, but it will also include a case study of relative motion about a spacecraft in a high-eccentricity orbit.

In Chapter VI, the sources of modeling error will be analyzed. Since the analytical models in this study necessarily involve certain approximations, it is important to understand how much accuracy is lost for each one. Finally, Chapter VII will compare additional simulation results among various orbit theories and relative motion models.

# CHAPTER II

# EXTENDED HOOTS THEORY

## II.A INTRODUCTION

As described above, Hoots [9] improved Brouwer's von Zeipel method solution to the Zonal Problem, in part by introducing the Hoots elements defined in Eq. 1.2. Hoots first derived corrections (mean-to-osculating conversions) for his position elements $\underline{y}$ in terms of differential classical orbit elements $\underline{\delta oe}$ ([9], Eqs. 7). He next used Brouwer's long- and short-period corrections to the classical elements ([4], pp. 394-395) in place of $\underline{\delta oe}$ to construct the final transformation giving $\underline{y} - \underline{y}''$ in terms of the mean classical elements ([9], Eqs. 8-10).

This chapter will extend these results using a different, equivalent method. This chapter will compute new correction terms for the Hoots elements directly from other generating functions using Lie series, as did Gim for nonsingular elements ([19], Section 3.4). Specifically, it will add corrections for $J_6$ using the generating function reported by Kozai ([6], Eq. 8.1). It will then add second-order correction terms for $J_2$ through $J_4$ using the generating functions reported by Kinoshita [11]. Along with adding the second-order secular rates due to $J_6$, this will extend Hoots theory to a higher level of fidelity.

### II.A.1 Lie Series

Let $\Delta_1\underline{y}$ denote the first-order transformation of the Hoots elements, so that $\underline{y} - \underline{y}'' = \Delta_1\underline{y} + \mathcal{O}(J_2^2)$. Specifically, neglecting $J_6$ and higher harmonics, denote the transformation terms depending on $J_2$ only as $\Delta_{12}\underline{y}$, those depending on $\frac{J_3}{J_2}$ as $\Delta_{13}\underline{y}$, and those depending on $\frac{J_4}{J_2}$ as $\Delta_{14}\underline{y}$, etc., so that

$$\underline{y} - \underline{y}'' = \Delta_{12}\underline{y} + \Delta_{13}\underline{y} + \Delta_{14}\underline{y} + \Delta_{15}\underline{y} + \mathcal{O}(J_2^2) \tag{2.1}$$

These results can be related to the Lie-series methods described previously–specifically, the method

of Hori [10], which transforms a generic variable $\epsilon$ using successive generating functions $S$ and $S^*$ as

$$\epsilon = \epsilon' + \{\epsilon', S\} + \frac{1}{2}\{\{\epsilon', S\}, S\} + \cdots \tag{2.2}$$

$$\epsilon' = \epsilon'' + \{\epsilon'', S^*\} + \frac{1}{2}\{\{\epsilon'', S^*\}, S^*\} + \cdots \tag{2.3}$$

Applying this method to the Zonal Problem, substituting Eq. 2.3 into Eq. 2.2, and retaining only first-order terms gives

$$\epsilon - \epsilon'' = \{\epsilon'', S_1 + S_1^*\} + \mathcal{O}(J_2^2)$$

where the subscript 1 denotes the first-order terms within each generating function. A second subscript can indicate a partition of the terms of the long-period generating function that depend on $J_2$ only (subscript 2) from those which depend on $\frac{J_3}{J_2}$ (subscript 3) and those which depend on $\frac{J_4}{J_2}$ (subscript 4), so that $S_1^* = S_{12}^* + S_{13}^* + S_{14}^*$. Since the methods of von Zeipel and Hori are identical to first order, then, $\Delta_{12}\underline{y} = \left\{\underline{y}'', S_1 + S_{12}^*\right\}$, $\Delta_{13}\underline{y} = \left\{\underline{y}'', S_{13}^*\right\}$, and $\Delta_{14}\underline{y} = \left\{\underline{y}'', S_{14}^*\right\}$. This gives a method to extend Hoots theory to account for the first-order long-period effects of $J_6$: add $\Delta_{16}\underline{y} = \left\{\underline{y}'', S_{16}^*\right\}$ to Eq. 2.1 using $S_{16}^*$ from Kozai [6].

### II.B $J_6$ EFFECTS

The first-order corrections in Hoots theory, like those in Brouwer theory, include long-period terms with coefficients of not only $J_2$, but also $\frac{J_3}{J_2}$, $\frac{J_4}{J_2}$, and $\frac{J_5}{J_2}$. The short-period effects of harmonics higher than $J_2$ are present only at second order. This section will derive a similar long-period term with coefficient $\frac{J_6}{J_2}$, and then derive second-order mean secular rates due to $J_6$.

Kozai reports the generating function

$$S_{16}^* = -\frac{k_6\mu^4}{k_2}\frac{35e^2}{4096G^7}\frac{1-\theta^2}{1-5\theta^2}\left[20\left(1-18\theta^2+33\theta^4\right)\left(\eta^2-3\right)\sin 2g + 3e^2\left(1-\theta^2\right)\left(1-11\theta^2\right)\sin 4g\right]$$

where $\theta = \cos i = H/G$, $\eta = \sqrt{1-e^2} = G/L$, $k_6 = J_6 R_e^6/2$, and $k_2 = J_2 R_e^2/2$. After taking the partial derivatives of $y_i$ and $S_{16}^*$ with respect to the Delaunay elements and computing the Poisson bracket

operation, the elements of $\Delta_{16}\underline{y} = \left\{\underline{y}'', S_{16}^*\right\}$ are

$$\Delta_{16}y_1 = \frac{k_6}{k_2}\frac{35\mu^3 e}{1024G^6}\lambda_2\Big[5e^2\lambda_1\cos(f-2g) - 5\left(4+3e^2\right)\lambda_1\cos(f+2g)$$
$$+ 3e^2\left(1-\theta^2\right)\left(1-11\theta^2\right)\cos(f+4g)\Big]$$

$$\Delta_{16}y_2 = -\frac{k_6}{k_2}\frac{35\mu^5 e}{1024G^5L^4}\lambda_2\left(\frac{a}{r}\right)^2\Big[5e^2\lambda_1\sin(f-2g) - 5\left(4+3e^2\right)\lambda_1\sin(f+2g)$$
$$+ 3e^2\left(1-\theta^2\right)\left(1-11\theta^2\right)\sin(f+4g)\Big]$$

$$\Delta_{16}y_3 = -\frac{k_6}{k_2}\frac{35\mu^5 e}{1024G^5L^4}\lambda_2\Big\{\left(\frac{a}{r}\right)^2\Big[5e^2\lambda_1\cos(f-2g) - 5\left(4+3e^2\right)\lambda_1\cos(f+2g)$$
$$+ 3e^2\left(1-\theta^2\right)\left(1-11\theta^2\right)\cos(f+4g)\Big] + \frac{eL^2}{G^2}\left(\frac{a}{r}\right)\Big[10\left(2+e^2\right)\lambda_1\cos 2g$$
$$- 3e^2\left(1-\theta^2\right)\left(1-11\theta^2\right)\cos 4g\Big]\Big\}$$

$$\Delta_{16}y_4 = \frac{k_6}{k_2}\lambda_3\Big\{\frac{\lambda_2\lambda_7}{G^6L}\left(\frac{a}{r}\right)^2\sin\frac{i}{2}\cos(f+g) + \lambda_6\sin\frac{i}{2}\cos(f+g)$$
$$+ \frac{e}{G^8\left(1-5\theta^2\right)}\Big[\sin^2 i\sin\frac{i}{2}\cos(f+g)\sin f\left(2+e\cos f\right)$$
$$- \frac{He}{2G}\sin i\cos\frac{i}{2}\sin(f+g)\Big]\left[-40\lambda_1\left(3-\eta^2\right)\cos 2g + 12e^2\left(1-\theta^2\right)\left(1-11\theta^2\right)\cos 4g\right]\Big\}$$

$$\Delta_{16}y_5 = -\frac{k_6}{k_2}\lambda_3\Big\{\frac{\lambda_2\lambda_7}{G^6L}\left(\frac{a}{r}\right)^2\sin\frac{i}{2}\sin(f+g) + \lambda_6\sin\frac{i}{2}\sin(f+g)$$
$$+ \frac{e}{G^8\left(1-5\theta^2\right)}\Big[\sin^2 i\sin\frac{i}{2}\sin(f+g)\sin f\left(2+e\cos f\right)$$
$$+ \frac{He}{2G}\sin i\cos\frac{i}{2}\cos(f+g)\Big]\left[-40\lambda_1\left(3-\eta^2\right)\cos 2g + 12e^2\left(1-\theta^2\right)\left(1-11\theta^2\right)\cos 4g\right]\Big\}$$

$$\Delta_{16}y_6 = \frac{k_6}{k_2}\lambda_3\Big\{\lambda_6 + \frac{\lambda_2 e}{G^8}\left(\frac{aG^2}{rL^2}+1\right)\sin f\left[-40\lambda_1\left(3-\eta^2\right)\cos 2g + 12e^2\left(1-\theta^2\right)\left(1-11\theta^2\right)\cos 4g\right]$$
$$+ \frac{\lambda_2\lambda_7}{G^6L}\left(\frac{a}{r}\right)^2 + \frac{e^2\theta}{G^8}\Big[\lambda_2\left[-40\left(-18+66\theta^2\right)\left(3-\eta^2\right)\sin 2g + 12e^2\left(-24+44\theta^2\right)\sin 4g\right]$$
$$+ \frac{-2+10\lambda_2}{1-5\theta^2}\lambda_4\Big]\Big\}$$

The intermediate variables needed in the above expressions are

$$\lambda_1 = 1 - 18\theta^2 + 33\theta^4$$
$$\lambda_2 = \frac{1-\theta^2}{1-5\theta^2}$$
$$\lambda_3 = \frac{-35\mu^4}{4096}$$
$$\lambda_4 = -20\lambda_1\left(3-\eta^2\right)\sin 2g + 3e^2\left(1-\theta^2\right)\left(1-11\theta^2\right)\sin 4g$$

$$\lambda_5 = \frac{e^2\lambda_2}{G^7}\Big[-40\frac{\theta^2}{G}\left(18-66\theta^2\right)\left(3-\eta^2\right)\sin 2g + 40\frac{G\lambda_1}{L^2}\sin 2g - 6\frac{G}{L^2}\left(1-\theta^2\right)\left(1-11\theta^2\right)\sin 4g$$
$$+ 6\frac{e^2H^2}{G^3}\left(12-22\theta^2\right)\sin 4g\Big]$$
$$\lambda_6 = -\left(\frac{2}{G^6L^2}+\frac{7e^2}{G^8}\right)\lambda_2\lambda_4 + \frac{2-10\lambda_2}{G^{10}\left(1-5\theta^2\right)}e^2H^2\lambda_4 + \lambda_5$$
$$\lambda_7 = \frac{2G^2}{L^3}\lambda_4 + e^2\frac{G^2}{L^3}\left[-40\lambda_1\sin 2g + 6\left(1-\theta^2\right)\left(1-11\theta^2\right)\sin 4g\right]$$

Reference [20] gives the mean secular rates due to $J_6$, found by taking partial derivatives of the $J_6$ term in the mean (doubly averaged) Hamiltonian. These, together with the first-order long-period corrections given above, extend Hoots theory to include zonal harmonics $J_2$ through $J_6$.

## II.C SECOND-ORDER CORRECTIONS

Kinoshita's Hori-method solution [11] considered zonal harmonics through $J_4$ and included terms up to third order for the generating functions and for the mean-to-osculating transformations of the nonsingular orbit elements $(\lambda, h, q_1, q_2, L, H)$.

Hoots theory can similarly be extended, incorporating $J_3$ and $J_4$ into a second-order Hori-method transformation by re-writing Eqs. 2.2 and 2.3 as

$$\underline{y} - \underline{y}' = \left\{\underline{y}', S_1\right\} + \left\{\underline{y}', S_{22}+S_{23}+S_{24}\right\} + \frac{1}{2}\left\{\left\{\underline{y}', S_1\right\}, S_1\right\} \tag{2.4}$$

$$\underline{y}' - \underline{y}'' = \left\{\underline{y}'', S_{12}^*\right\} + \Delta_{13}\underline{y} + \Delta_{14}\underline{y} + \left\{\underline{y}'', S_{22}^*+S_{23}^*+S_{24}^*+S_{234}^*\right\} \tag{2.5}$$
$$+ \frac{1}{2}\left\{\left\{\underline{y}'', S_{12}^*+S_{13}^*+S_{14}^*\right\}, S_{12}^*+S_{13}^*+S_{14}^*\right\}$$

where terms higher than second order have been neglected, and the second-order generating functions use the same subscript notation (except that $S_{234}^*$ refers to the second-order long-period terms with coupled $J_3$ and $J_4$). Kinoshita's generating function $S_2$ may be used for this purpose; however, since it is expanded as a power series in eccentricity, the user must choose how many powers of $e$ to retain.

For this study, terms up to 4th order in $e$ from Kinoshita's second-order generating function $S_2$ [11] were given to computer algebra program Maxima[1]; after performing the Poisson-bracket operations, the results were retained up to 0th order in $e$. In other words, terms of order $J_2^3$ or $eJ_2^2$ were neglected. The

[1]Maxima, a Computer Algebra System. Version 5.31.2 (2013). http://maxima.sourceforge.net/

resulting corrections are listed in Appendix A.

## II.D METHOD OF SIMULATION

The extended Hoots theory, an analytical model of perturbed satellite motion, is simulated in MATLAB® for this study[2]. Its accuracy is assessed by comparing its predicted trajectory to a numerically integrated truth model.

For comparison, two other analytical models are also simulated: one using nonsingular elements, and another using equinoctial elements . The equinoctial-elements theory is labeled "Gim" in plots; it includes first-order correction terms found by Gim [19]–they are complete in eccentricity and equivalent to the $J_2$ part of Brouwer theory.

The nonsingular-elements theory, which considers $J_2$ through $J_4$, is labeled "Kinoshita" in plots, and it has several components. The first-order $J_2$ terms (complete in $e$) were also found by Gim. The first-order long-period terms due to $J_3$ and $J_4$ are derived from Kinoshita's generating functions $S^*_{13}$ and $S^*_{14}$ [11] in the same way as the Hoots-theory $J_6$ correction above: specifically,

$$\{\lambda, S^*_{13}\} = \frac{J_3}{J_2}\frac{1}{2G^3L\sqrt{G^2-H^2}}\sqrt{\frac{1-\eta}{1+\eta}}\left[2H^2L\left(1+\eta\right) - G^2L\left(1+\eta\right) + GH^2\eta - G^3\eta\right]\cos g$$

$$\{q_1, S^*_{13}\} = -\frac{J_3}{J_2}\frac{e^2}{4G^3}\frac{2H^2-G^2}{\sqrt{G^2-H^2}}\sin 2g$$

$$\{q_2, S^*_{13}\} = \frac{J_3}{J_2}\frac{1}{4G^3L\sqrt{G^2-H^2}}\left[\left(2H^2-G^2\right)Le^2\left(\cos 2g+1\right) + 2G\eta\left(H^2-G^2\right)\right]$$

$$\{h, S^*_{13}\} = -\frac{J_3}{J_2}\frac{He}{2G^2\sqrt{G^2-H^2}}\cos g$$

and

$$\begin{aligned}\{\lambda, S^*_{14}\} = \frac{J_4}{J_2}\frac{1}{32G^6L}\Big[&10G\left(H^2-G^2\right)\left(\eta-1\right)\frac{7H^2-G^2}{5H^2-G^2} \\ &+ \frac{5e^2}{\left(5H^2-G^2\right)^2}\Big(175H^6L - 169G^2H^4L + 45G^4H^2L - 3G^6L + 70GH^6 - 94G^3H^4 \\ &+ 26G^5H^2 - 2G^7\Big)\Big]\sin 2g\end{aligned}$$

$$\{q_1, S^*_{14}\} = \frac{J_4}{J_2}\frac{1}{64G^6L\left(5H^2-G^2\right)^2}\left[b_1\left(\cos 3g - \cos g\right) - b_2\cos g\right]$$

$$\{q_2, S^*_{14}\} = \frac{J_4}{J_2}\frac{1}{64G^6L\left(5H^2-G^2\right)^2}\left[b_1\left(\sin 3g + \sin g\right) + b_2\sin g\right]$$

[2]MATLAB is a registered trademark of The MathWorks, Inc.

$$\{h, S_{14}^*\} = -\frac{J_4}{J_2}\frac{5He^2}{16G^5}\frac{35H^4 - 14G^2H^2 + 3G^4}{\left(5H^2 - G^2\right)^2}\sin 2g$$

where all variables are mean (the double-prime symbol was dropped for brevity) and

$$b_1 = 5e^3L\left(175H^6 - 169G^2H^4 + 45G^4H^2 - 3G^6\right)$$

$$b_2 = 20e\eta G\left(H^2 - G^2\right)\left(5H^2 - G^2\right)\left(7H^2 - G^2\right)$$

Note that the presence of $\sqrt{G^2 - H^2}$ in the denominator of the $J_3$ corrections indicates a singularity for 0 inclination. The second-order short-period ($J_2$) and long-period ($J_2$ through $J_4$) correction terms are directly from Kinoshita [11]. The short-period $J_3$ and $J_4$ correction terms are derived from Kinoshita's generating functions $S_{23}$ and $S_{24}$ in the same way as the Hoots-theory second-order corrections above; they are listed in Appendix A. Although Kinoshita reported terms up to fourth order in $e$, the simulations in this study include only the terms zeroth order in $e$.

The simulation can accept as inputs mean chief elements, in which case a mean-to-osculating transformation must be performed on the initial conditions before numerically integrating–thereby introducing some error into the truth model (on the order of the neglected perturbation terms). It can also accept osculating chief elements, in which case an osculating-to-mean transformation must be performed on the initial conditions prior to propagating the analytical theory. This is accomplished by a numerical root-solving algorithm using MATLAB's fsolve function and the full second-order transformation; but fsolve must be seeded by an initial guess, which is found by inverting the first-order $J_2$-only corrections terms (i.e., using $-J_2$ as the perturbation parameter).

The flowchart in Figure 2.1 illustrates the simulation algorithm when the inputs are osculating classical elements. Note that after the mean elements are propagated, the solution at each time step requires additional numerical solutions of Kepler's Equation, relating time to the chief's true anomaly. The Hoots elements and equinoctial elements require one such solution to transform the mean elements, and the nonsingular elements require one to transform the osculating elements. If the equinoctial elements were to use mean longitude $\Lambda$, instead of true longitude $\Psi$, as the fast variable, then the required Kepler's Equation solution would move from the mean-element space to the osculating-element space. This would create the same

problem which the nonsingular elements have: knowledge of the mean true anomaly at time $t$ is required in order to compute the GA STM for relative motion [19]. Here, only the Hoots elements and the equinoctial elements using $\Psi$ have access to this information without an extra solution of Kepler's Equation.

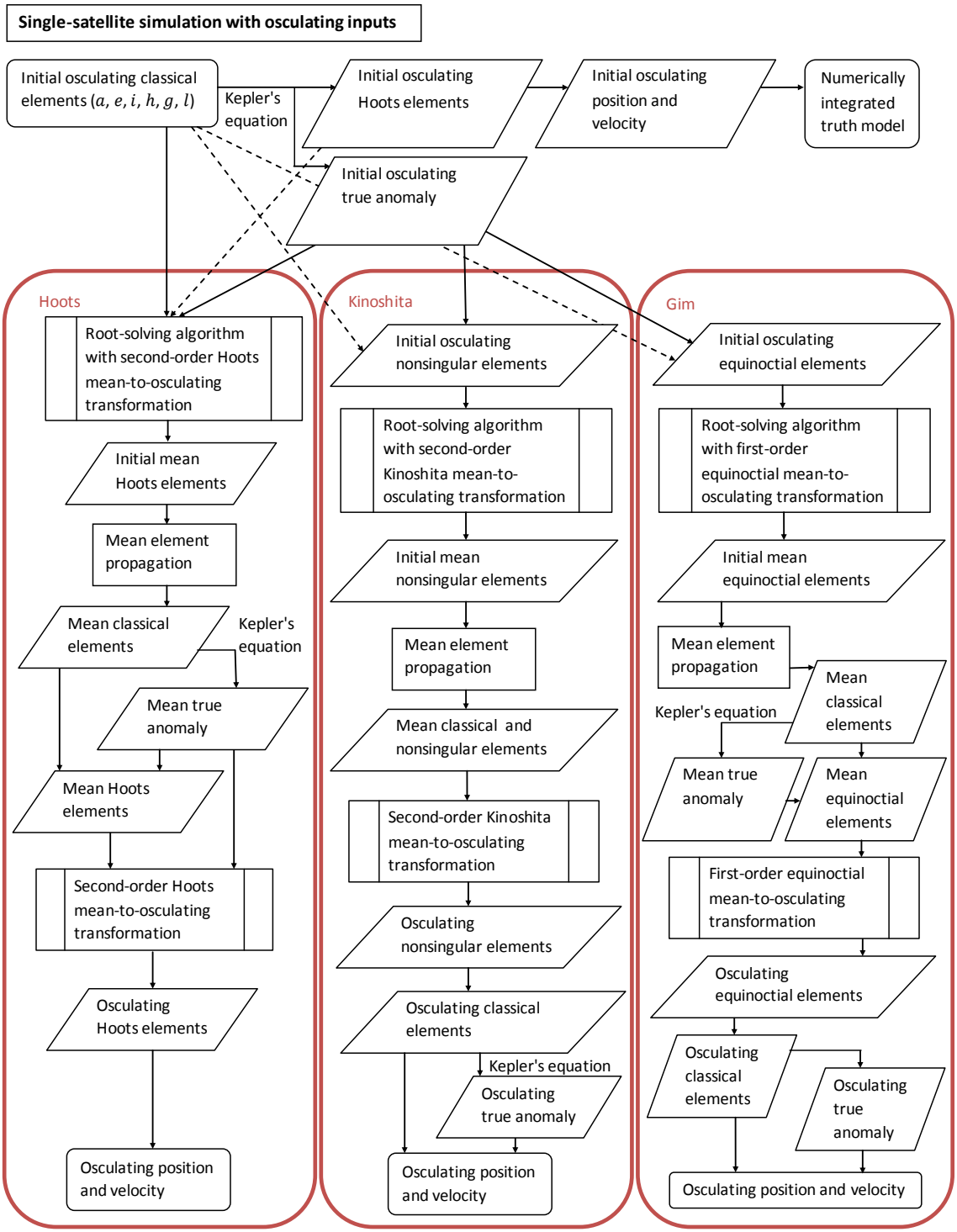


**Figure 2.1: Simulation algorithm flowchart**

# CHAPTER III

# PROJECTED CIRCULAR ORBITS

## III.A BACKGROUND

The Projected Circular Orbit (PCO) formation was derived originally [27] from a relative motion model with several assumptions: 1) no perturbations are present, 2) the solution is linearized in the relative coordinates, 3) the relative motion is bounded (no drift), and 4) the chief's orbit is circular. When a real formation is initialized using a PCO definition (a set of constraints on the initial relative coordinates), the degree to which these assumptions are violated corresponds to the degree to which the projected motion departs from a repeating circular shape. In the presence of the zonal harmonics of the Earth's gravitational field, choosing the satellites' mean elements to satisfy a PCO definition produces a close approximation of a projected circle for a limited period of time. When the chief's orbit has large eccentricity or if the formation is very large, the projection of the relative trajectory may be skewed into a noncircular shape.

The remainder of this study will use the name "PCO" to indicate any formation initialized with PCO definition constraints, regardless of whether the circular-chief or other assumptions are violated. Stated another way, the "projected circle" was used to obtain initial conditions for these formations, even when they are flown in conditions–such as eccentric chief orbits–that cause the projected shape to be noncircular. For an alternate approach, in which a formation about an eccentric chief orbit has a horizontal-plane projection as nearly circular as possible, see Reference [28].

## III.B BOUNDED, LINEARIZED, UNPERTURBED RELATIVE MOTION FOR CIRCULAR CHIEF ORBITS

The earliest and most-studied model of unperturbed satellite relative motion is the Hill-Clohessy-Wiltshire (HCW) model, which is linearized in the intial LVLH coordinates and assumes a circular chief

orbit [17, 16]. Its position solution is

$$x(t) = \left(4x_0 + \frac{2\dot{y}_0}{n}\right) + \frac{\dot{x}_0}{n}\sin nt \; - \left(3x_0 + \frac{2\dot{y}_0}{n}\right)\cos nt$$

$$y(t) = -\left(6nx_0 + 3\dot{y}_0\right)t \; + \left(y_0 - \frac{2\dot{x}_0}{n}\right) + \left(6x_0 + \frac{4\dot{y}_0}{n}\right)\sin nt \; + \frac{2\dot{x}_0}{n}\cos nt$$

$$z(t) = \frac{\dot{z}_0}{n}\sin nt \; + z_0 \cos nt$$

where $n = \sqrt{\mu/a^3}$ is the chief's mean motion and the subscript 0 denotes the initial time $t_0 = 0$. If the relative orbit is bounded (that is, if the initial conditions satisfy $\dot{y}_0 = -2nx_0$), then the solution can be rewritten in harmonic form as

$$\begin{aligned} x(t) &= \rho_x \sin\left(nt + \alpha_x\right) \\ y(t) &= \rho_y + 2\rho_x \cos\left(nt + \alpha_x\right) \\ z(t) &= \rho_z \sin\left(nt + \alpha_z\right) \end{aligned} \tag{3.1}$$

where the five parameters are

$$\rho_x = \frac{1}{n}\sqrt{\dot{x}_0^2 + x_0^2 n^2}$$

$$\rho_y = y_0 - \frac{2\dot{x}_0}{n}$$

$$\rho_z = \frac{1}{n}\sqrt{\dot{z}_0^2 + z_0^2 n^2}$$

$$\alpha_x = \mathrm{atan2}(nx_0, \dot{x}_0)$$

$$\alpha_z = \mathrm{atan2}(nz_0, \dot{z}_0)$$

[1], similar to the Relative Orbit Elements of Reference [26]. Here, these parameters are expressed in terms of LVLH coordinates at the initial time. It is clear from examining Eq. 3.1 that when $nt + \alpha_x = 0$, the deputy is at the maximum along-track position. Likewise, when $nt + \alpha_x = \pi/2$, the deputy has moved clockwise (as viewed from "above", or the positive $z$-axis) to the maximum radial position. So $\alpha_x$ is related to the initial physical angle of the deputy in the chief's orbit plane, measured clockwise from the $+y$-axis, when $t = 0$. At that time, Eq. 3.1 reveals that $x_0 = \rho_x \sin\alpha_x$ and $y_0 - \rho_y = 2\rho_x \cos\alpha_x$. But the initial physical angle is $\theta_x = \mathrm{atan2}(x_0, y_0 - \rho_y)$. Thus the relationship between the physical angle and the phase angle is $2\tan\theta_x = \tan\alpha_x$, leading to an equivalent definition of $\alpha_x$:

$$\alpha_x = \mathrm{atan2}(2x_0, y_0 - \rho_y)$$

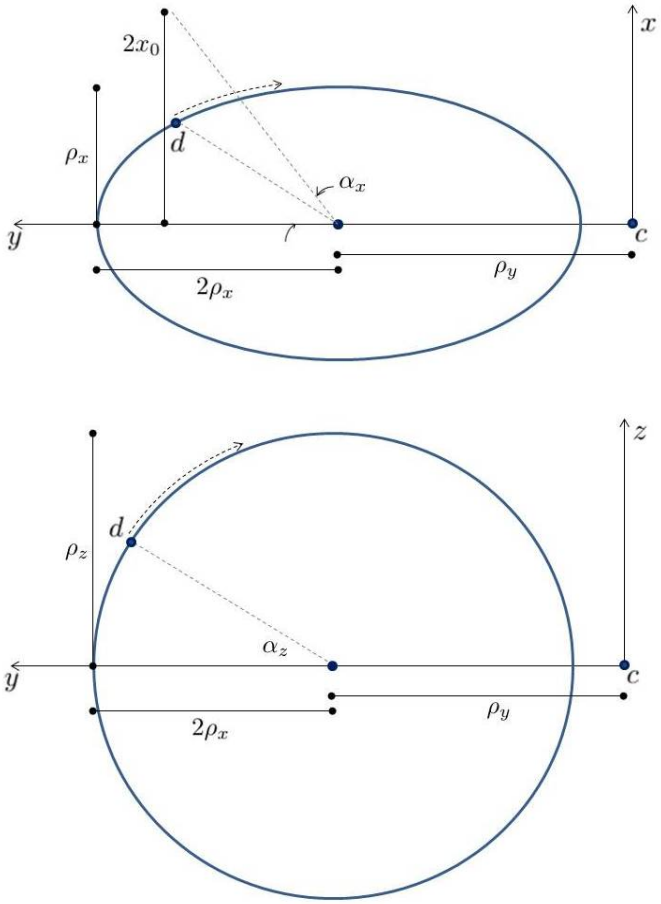


**Figure 3.1: HCW relative orbit geometry at $t = 0$ when $\alpha_z = \alpha_x$ and $\rho_z = 2\rho_x$**

See the illustration in Figure 3.1. Similarly, $\alpha_z$ is related to the clockwise angle in the horizontal plane (the $y$-$z$ plane), measured from the $+y$-axis, when $t = 0$. Since $z_0 = \rho_z \sin\alpha_z$, the initial physical angle is $\theta_z = \text{atan2}(\rho_z \sin\alpha_z, 2\rho_x \cos\alpha_x)$. The figure illustrates the special case when $\alpha_z = \alpha_x$ and $\rho_z = 2\rho_x$ (two of the PCO constraints, as shown later), so that $\theta_z = \alpha_z$.

Another satelllite relative motion model, the unit sphere approach, is written in terms of differential classical orbit elements [41, 1]. When linearized in the differential elements, the position solution becomes

$$x = r_d - r_c$$

$$y = r_d\,(\delta u + \delta h \cos i_c)$$

$$z = r_d\,(-\delta h \sin i_c \cos u_d + \delta i \sin u_d)$$

[1], where $r$ is the orbit radius, $u = f + g$ is the argument of latitude, and the subscripts $c$ and $d$ denote values for the chief and deputy, respectively. Writing this solution in the same form as Eqs. 3.1 would be one way to find a geometric interpretation of the relative orbit parameters (by yielding expressions for the parameters in terms of the differential elements). Besides the unit sphere method, other theories which express linearized unperturbed satellite relative motion in terms of differential orbit elements could be analyzed using a similar process to the one below.

Assuming bounded relative motion ($\delta a = 0$) and a circular chief orbit ($e_c = 0$ and $r_c = a_c$), and neglecting terms of second order in the coordinates,

$$r_d = a_c \left(1 - \delta e \cos l_d\right)$$

where $l$ is mean anomaly. Then the unit-sphere solution becomes, to first order,

$$x = -a_c \, \delta e \cos l_d$$

$$y = a_c \left(\delta u + \delta h \cos i_c\right)$$

$$z = a_c \left(-\delta h \sin i_c \, \cos u_d + \delta i \sin u_d\right)$$

Using the small-eccentricity approximation $\delta u = \delta\lambda + 2\,\delta e \sin l_d$, where $\lambda = l + g$ (which is reasonable since it is already assumed that $e_c = 0$ and that $e_d = \delta e$ is first-order), and considering the mean anomaly as $l = n\left(t - t_0\right) + l_0$ (so that $\lambda = n\left(t - t_0\right) + \lambda_0$ also),

$$x = -a_c \, \delta e \cos\left[n\left(t - t_0\right) + l_{d,0}\right]$$

$$y = a_c \left\{\delta\lambda_0 + \delta h \cos i_c + 2\,\delta e \sin\left[n\left(t - t_0\right) + l_{d,0}\right]\right\}$$

since, under these assumptions, the chief and deputy have the same mean motion $n$. Assuming, without loss of generality, that $t_0 = 0$, and replacing $l_{d,0}$ with $\lambda_{d,0} - g_d$,

$$x = -a_c \, \delta e \cos\left(nt + \lambda_{c,0} + \delta\lambda_0 - g_d\right)$$

$$y = a_c \left[\delta\lambda_0 + \delta h \cos i_c + 2\,\delta e \sin\left(nt + \lambda_{c,0} + \delta\lambda_0 - g_d\right)\right]$$

Then, using $q_1 = e\cos g$ and $q_2 = e \sin g$, so that $q_{2,c} = q_{1,c} = 0$, and noting that $\delta\lambda_0$ is a small angle,

$$x = a_c \, \delta e \sin\left[nt + \lambda_{c,0} - \operatorname{atan2}(\delta q_2, \delta q_1) - \pi/2\right]$$

$$y = a_c \left\{\delta\lambda_0 + \delta h \cos i_c + 2\,\delta e \cos\left[nt + \lambda_{c,0} - \operatorname{atan2}(\delta q_2, \delta q_1) - \pi/2\right]\right\}$$

to first order. Thus, comparing this result to Eqs. 3.1, the in-plane relative motion parameters are

$$\begin{aligned} \rho_x &= a_c\,\delta e \\ \rho_y &= a_c\left(\delta\lambda_0 + \delta h\cos i_c\right) \\ \alpha_x &= \lambda_{c,0} - \mathrm{atan2}(\delta q_2, \delta q_1) - \pi/2 \end{aligned} \tag{3.2}$$

Note that if $t = 0$ at the chief's ascending node (so that $\lambda_{c,0} = 0$), then $\alpha_x = -\mathrm{atan2}(\delta q_2, \delta q_1) - \pi/2$. If, in addition, the deputy's perigee is at the ascending node (so that $\mathrm{atan2}(\delta q_2, \delta q_1) = 0$), then $\alpha_x = -\pi/2$.

Expressions for the cross-track parameters $\rho_z$ and $\alpha_z$ can be found similarly. Writing the sum in the $z$-equation as a harmonic form yields

$$z = a_c\sqrt{\delta i^2 + \delta h^2\sin^2 i_c}\,\sin\left[u_d + \mathrm{atan2}(-\delta h\sin i_c, \delta i)\right]$$

Since $u_d = n\left(t - t_0\right) + \lambda_{c,0} + \delta u$, and $\delta u$ is a small angle,

$$z = a_c\sqrt{\delta i^2 + \delta h^2\sin^2 i_c}\,\sin\left[nt + \lambda_{c,0} + \mathrm{atan2}(-\delta h\sin i_c, \delta i)\right]$$

and therefore the cross-track relative motion parameters are

$$\begin{aligned} \rho_z &= a_c\sqrt{\delta i^2 + \delta h^2\sin^2 i_c} \\ \alpha_z &= \lambda_{c,0} + \mathrm{atan2}(-\delta h\sin i_c, \delta i) \end{aligned} \tag{3.3}$$

Note that if $t = 0$ at the chief's ascending node, then $\alpha_z = \mathrm{atan2}(-\delta h\sin i_c, \delta i)$. If, in addition, there is no inclination difference, so that the cross-track motion is due entirely to a difference in ascending nodes, $\alpha_z = \pm\,\pi/2$. Alternatively, when $t = 0$ at the chief's ascending node, if both satellites share an ascending node (or if the chief is in an equatorial orbit), so that the cross-track motion is due entirely to the inclination difference, then $\alpha_z = 0$ or $\pi$.

### III.C PCO SOLUTIONS

Eqs. 3.2 and 3.3 define the parameters of bounded HCW relative motion in terms of differential nonsingular elements. It is easy to see from Figure 3.1 that the projection of this relative trajectory in the

horizontal plane must be a circle centered about the chief if these parameters are related as

$$\rho_y = 0$$

$$\rho_z = 2\rho_x$$

$$\alpha_z = \alpha_x$$

[27]. These constraints, along with the boundedness contstraint, constitute the set of four initialization constraints defining a PCO. The two additional degrees of freedom are used to choose arbitrary values for parameters $\rho$ and $\alpha$, so that we can write the full set of constraints (the PCO definition) as

$$\begin{aligned} &\delta a = 0 \quad \alpha_x = \alpha + \lambda_{c,0} \quad \alpha_z = \alpha + \lambda_{c,0} \\ &\rho_y = 0 \qquad \rho_x = \tfrac{1}{2}\rho \qquad\quad \rho_z = \rho \end{aligned} \tag{3.4}$$

Of course, in order to prevent along-track drift, the boundedness constraint $\delta a = 0$ can be modified to account for perturbations from two-body gravity, as discussed in Chapter V. Note that, with this definition of $\alpha$, Eq. 3.1 can be rewritten as

$$x(t) = \rho_x \sin(\lambda_c + \alpha)$$

$$y(t) = \rho_y + 2\rho_x \cos(\lambda_c + \alpha)$$

$$z(t) = \rho_z \sin(\lambda_c + \alpha)$$

as in Reference [42]. Just as $\alpha_x$ and $\alpha_z$ are phase angles corresponding to the initial time (when $t = 0$), $\alpha$ is a phase angle corresponding to the time of the chief's equator crossing (when $\lambda_c = 0$). Furthermore, using $\alpha$, as defined here, brings the circular-chief case from Reference [43] into agreement with Eqs. 3.2 and 3.3 above.

The constraints in Eqs. 3.4 can be written in terms of the differences in the nonsingular elements ($a$, $\lambda$, $i$, $q_1$, $q_2$, $h$). The boundedness condition is unchanged, and $\rho_y = 0$ becomes $\delta\lambda_0 = -\delta h \cos i_c$. The cross-track constraints become $\sqrt{\delta i^2 + \delta h^2 \sin^2 i_c} = \rho/a_c$ and $\mathrm{atan2}(-\delta h \sin i_c, \delta i) = \alpha$. Likewise, the $\rho_x$ constraint becomes $\sqrt{\delta q_1^2 + \delta q_2^2} = \rho/(2a_c)$, since in the case of a circular chief orbit $e_d = \delta e$, $q_{1,d} = \delta q_1$, and $q_{2,d} = \delta q_2$. Finally, using the trigonometric property that $-\mathrm{atan2}(A, B) - \pi/2 = \mathrm{atan2}(-B, -A)$, the constraint on $\alpha_x$ becomes $\mathrm{atan2}(-\delta q_1, -\delta q_2) = \alpha$. These can be solved for the differential elements to

form the PCO definition

$$\begin{aligned}
\delta a &= 0 \\
\delta\lambda_0 &= \frac{\rho}{a_c}\cot i_c \sin\alpha \\
\delta i &= \frac{\rho}{a_c}\cos\alpha \\
\delta q_1 &= -\frac{\rho}{2a_c}\sin\alpha \\
\delta q_2 &= -\frac{\rho}{2a_c}\cos\alpha \\
\delta h &= -\frac{\rho}{a_c}\csc i_c \sin\alpha
\end{aligned} \tag{3.5}$$

as found in References [1] and [42]. Of course, this definition is singular for equatorial chief orbits.

To avoid the equatorial singularity, Eqs. 3.4 can be written in terms of differences in the equinoctial elements ($a$, $\tilde{q}_1 = e\cos(g+h)$, $\tilde{q}_2 = e\sin(g+h)$, $p_1 = \tan i/2\,\cos h$, $p_2 = \tan i/2\,\sin h$, $\Lambda$), where $\Lambda = l + g + h$ is the mean longitude. But first the constraints must be modified (since $\lambda_{c,0}$ is undefined for equatorial orbits) by introducing phase angle $\alpha_I = \alpha - h_c$. Just as $\alpha$ corresponds to the time of the chief's equator crossing, $\alpha_I$ corresponds to the time when the chief passes the 1-direction of the inertial reference frame, the ECI X-axis (conventionally the vernal equinox, or the First Point of Aries, denoted $\Upsilon$ [2])–that is, the point at which $\Lambda_c = 0$. The constraints are then

$$\delta a = 0 \quad \alpha_x = \alpha_I + \Lambda_{c,0} \quad \alpha_z = \alpha_I + \Lambda_{c,0}$$

$$\rho_y = 0 \qquad \rho_x = \tfrac{1}{2}\rho \qquad\qquad \rho_z = \rho$$

The nonsingular elements can be mapped into equinoctial elements using the formulas

$$\lambda = \Lambda - h \qquad\qquad \delta\lambda = \delta\Lambda - \delta h$$

$$i = 2\,\mathrm{atan2}\sqrt{p_1^2 + p_2^2} \qquad\qquad \delta i = \frac{2(p_1\,\delta p_1 + p_2\,\delta p_2)}{\sqrt{p_1^2+p_2^2}\left(1+p_1^2+p_2^2\right)}$$

$$h = \mathrm{atan2}(p_2, p_1) \qquad\qquad \delta h = \frac{p_1\,\delta p_2 - p_2\,\delta p_1}{p_1^2+p_2^2}$$

$$\delta q_1 = \frac{1}{\sqrt{p_1^2+p_2^2}}\left[\delta h\left(\tilde{q}_2 p_1 - \tilde{q}_1 p_2\right) + \delta\tilde{q}_1 p_1 + \delta\tilde{q}_2 p_2\right] \quad \delta q_2 = \frac{-1}{\sqrt{p_1^2+p_2^2}}\left[\delta h\left(\tilde{q}_1 p_1 + \tilde{q}_2 p_2\right) + \delta\tilde{q}_1 p_2 + \delta\tilde{q}_2 p_1\right]$$

In terms of equinoctial elements, then, $\rho_y = 0$ becomes

$$\delta\Lambda_0 = \frac{p_{1,c}\,\delta p_2 - p_{2,c}\,\delta p_1}{p_{1,c}^2 + p_{2,c}^2}\left[1 - \cos\left(2\,\mathrm{atan2}\sqrt{p_{1,c}^2 + p_{2,c}^2}\right)\right]$$

For the cross-track motion, the $\alpha_z$ constraint becomes

$$\text{atan2}[-(p_{1,c}\,\delta p_2 - p_{2,c}\,\delta p_1),\, p_{1,c}\,\delta p_1 + p_{2,c}\,\delta p_2] = \alpha_I + \text{atan2}(p_{2,c},\, p_{1,c})$$

and the $\rho_z$ constraint becomes

$$\frac{1}{\sqrt{p_{1,c}^2 + p_{2,c}^2}} \sqrt{\frac{4\left(p_{1,c}\,\delta p_1 + p_{2,c}\,\delta p_2\right)^2}{\left(1 + p_{1,c}^2 + p_{2,c}^2\right)^2} + \frac{\left(p_{1,c}\,\delta p_2 - p_{2,c}\,\delta p_1\right)^2}{p_{1,c}^2 + p_{2,c}^2} \sin^2\left(2\,\text{atan2}\sqrt{p_1^2 + p_2^2}\right)} = \frac{\rho}{a_c}$$

In-plane, the $\alpha_x$ constraint becomes

$$\text{atan2}[-(\delta\tilde{q}_1 p_{1,c} + \delta\tilde{q}_2 p_{2,c}),\, -(-\delta\tilde{q}_1 p_{2,c} + \delta\tilde{q}_2 p_{1,c})] = \alpha_I + \text{atan2}(p_{2,c}, p_{1,c})$$

and the $\rho_x$ constraint becomes

$$\frac{\rho}{2a_c} = \sqrt{\delta\tilde{q}_1^2 + \delta\tilde{q}_2^2}$$

since the chief's orbit is circular. After some algebra, this system of equations can be solved for the differential equinoctial elements to form the PCO definition

$$\begin{aligned}
\delta a &= 0 \\
\delta\tilde{q}_1 &= -\frac{\rho}{2a_c}\sin\alpha_I \\
\delta\tilde{q}_2 &= -\frac{\rho}{2a_c}\cos\alpha_I \\
\delta p_1 &= \frac{\rho}{2a_c}\left(1 + p_{1,c}^2 + p_{2,c}^2\right)\cos\alpha_I \\
\delta p_2 &= -\frac{\rho}{2a_c}\left(1 + p_{1,c}^2 + p_{2,c}^2\right)\sin\alpha_I \\
\delta\Lambda_0 &= \frac{2\left(p_{1,c}\,\delta p_2 - p_{2,c}\,\delta p_1\right)}{1 + p_{1,c}^2 + p_{2,c}^2}
\end{aligned}$$

## III.D CONCLUSIONS

This chapter has described in detail the satellite formation known as a Projected Circular Orbit, which, in unperturbed motion, projects a circular trajectory onto the horizontal plane. This chapter makes several contributions to the study of PCOs.

First, this chapter described the parameters of bounded, linearized, unperturbed relative motion for circular chief orbits in terms of differential orbit elements (Eqs. 3.2 and 3.3). In addition, this chapter described the geometric interpretation of the deputy's phase angle $\alpha$, including its relationship to the physical

angle in each plane, and resolved the ambiguity among its three possible definitions: the phase angle at $t = 0$ (as used in Chapter 5 of Reference [1]), that at the time of the chief's equator crossing (as in Chapter 6 of Reference [1]), and that at the time when the chief passes the ECI X-axis (as needed for equatorial orbits).

Finally, this chapter stated the PCO definition as a set of 6 constraints on the relative initial conditions (Eq. 3.4), using them to re-derive the PCO definition in terms of nonsingular elements and to derive the PCO definition in terms of equinoctial elements.

In future research, the same analysis performed here for PCO formations could be performed for other formation types (such as a general circular orbit, GCO [42], where $\rho_z = \sqrt{3}\rho_x$).

# CHAPTER IV

# RELATIVE STATE TRANSITION MATRIX IN TERMS OF HOOTS ELEMENTS

## IV.A BACKGROUND

This chapter aims to extend the Gim-Alfriend State Transition Matrix (GA STM) [18], a linearized satellite relative motion model. The GA STM can accommodate eccentric chief orbits and perturbed gravity fields using a succession of linear operators:

$$\begin{bmatrix} \underline{r}(t)^T & \underline{v}(t)^T \end{bmatrix}^T = \Sigma(t)D(t)\bar{\phi}_{\bar{y}}(t,t_0)D^{-1}(t_0)\Sigma^{-1}(t_0)\begin{bmatrix} \underline{r}(t_0)^T & \underline{v}(t_0)^T \end{bmatrix}^T \tag{4.1}$$

where $\Sigma$ is the linearized transformation matrix mapping orbit element differences to relative position and velocity coordinates, $D$ is the linearized sensitivity matrix mapping mean to osculating elements, $\bar{\phi}_{\bar{y}}(t,t_0)$ is the state transition matrix for the mean elements, and $\underline{r}(t)$ and $\underline{v}(t)$ are the deputy satellite's relative position and velocity in a Local-Vertical Local-Horizontal (LVLH) reference frame centered at the chief.

As a first step, this chapter will reformulate the GA STM for the Main Problem using the Hoots position elements [9], developed to compute the Brouwer-theory approximate solution [4] without singularities and with greater computational efficiency. The Hoots position elements describing a satellite's orbit were defined in Eq. 1.2, and are restated here:

$$y_1 = r \qquad y_2 = \dot{r} \qquad y_3 = r\dot{f}$$

$$y_4 = \sin\tfrac{i}{2}\sin(f+g) \quad y_5 = \sin\tfrac{i}{2}\cos(f+g) \quad y_6 = f+g+h$$

The vector of osculating Hoots position elements will be denoted $\underline{y}$, and the vector of mean elements $\underline{y}''$.

## IV.B SENSITIVITY MATRIX $D$

The sensitivity matrix $D(t)$ is defined as $D = \frac{\partial \underline{y}}{\partial \underline{y}''}$, the Jacobian of the osculating elements with respect to the mean elements. Considering the osculating elements as a vector of nonlinear functions of the mean elements, and expanding the elements for a deputy satellite as a Taylor series about the reference or chief satellite, yields the following: $\underline{y}_d(t) = \underline{y}_c(t) + \frac{\partial \underline{y}}{\partial \underline{y}''}\big|_{\underline{y}''_c}\left(\underline{y}''_d(t) - \underline{y}''_c(t)\right) + \cdots$. This shows that $D$

can function as a linearized operator for relative motion, mapping the differences in mean Hoots position elements into differential osculating Hoots elements: $\underline{\delta y}(t) = D(t)\left[\underline{y}''_d(t) - \underline{y}''_c(t)\right]$. Importantly, this relationship can be inverted at the initial time, providing a way to convert osculating initial conditions to mean relative initial conditions: $\underline{\delta y}''(t_0) = D^{-1}(t_0)\left[\underline{y}_d(t_0) - \underline{y}_c(t_0)\right]$.

Given correction terms $\underline{y} - \underline{y}''$ from the mean-to-osculating transformation of a particular perturbation theory, we can compute the sensitivity matrix as $D = \mathbb{1}_{6x6} + \frac{\partial(\underline{y} - \underline{y}'')}{\partial \underline{y}''}$, where $\mathbb{1}$ is the identity matrix. If the perturbation theory uses successive transformations (for example, long-period and short-period corrections), then we can apply the $D$ operators in succession:

$$D = D^{SP}D^{LP} = \frac{\partial \underline{y}}{\partial \underline{y}'}\frac{\partial \underline{y}'}{\partial \underline{y}''} = \left(\mathbb{1}_{6x6} + \frac{\partial(\underline{y} - \underline{y}')}{\partial \underline{y}'}\right)\left(\mathbb{1}_{6x6} + \frac{\partial(\underline{y}' - \underline{y}'')}{\partial \underline{y}''}\right) \tag{4.2}$$

It is possible to compute $D$ based on the first-order $J_2$-only corrections from Hoots theory as a single-step transformation, consistent with the approaches in References [9] and [15]. This is equivalent to writing Eq. 4.2 as

$$D = \mathbb{1}_{6x6} + \frac{\partial(\underline{y} - \underline{y}')}{\partial \underline{y}'} + \frac{\partial(\underline{y}' - \underline{y}'')}{\partial \underline{y}''} + \mathcal{O}\left(J_2^2\right) \tag{4.3}$$

where the product $\frac{\partial(\underline{y} - \underline{y}')}{\partial \underline{y}'}\frac{\partial(\underline{y}' - \underline{y}'')}{\partial \underline{y}''}$ has been neglected as second-order in $J_2$, and then further neglecting the difference $\frac{\partial(\underline{y} - \underline{y}')}{\partial \underline{y}'} - \frac{\partial(\underline{y} - \underline{y}')}{\partial \underline{y}''}$:

$$D = \mathbb{1}_{6x6} + \frac{\partial(\underline{y} - \underline{y}'')}{\partial \underline{y}''} + \mathcal{O}\left(J_2^2\right)$$

This study will follow similar notation to that of Reference [18], so that, for a first-order perturbation theory solution, Eq. 4.3 becomes

$$D = \mathbb{1}_{6x6} + D^{(lp)} + D^{(sp)}$$

where $D^{(lp)} = \frac{\partial(\underline{y}' - \underline{y}'')}{\partial \underline{y}''}$ and $D^{(sp)} = \frac{\partial(\underline{y} - \underline{y}')}{\partial \underline{y}'}$. The correction terms $(\underline{y}' - \underline{y}'')$ and $(\underline{y} - \underline{y}')$ can be transformed from classical orbit elements to Hoots elements using the following relationships (all derived from Eqs. 1.2): $\sin u = \frac{y_4}{\sin i/2}$, $\cos u = \frac{y_5}{\sin i/2}$, $\sin i/2 = \sqrt{y_4^2 + y_5^2}$, $\cos i/2 = \sqrt{1 - y_4^2 - y_5^2}$, $\sin f = \frac{y_2\eta}{nae}$, $\cos f = 1/e\left(\frac{a\eta^2}{y_1} - 1\right)$, and $a = \frac{y_1^2 y_3^2}{\mu\eta^2}$. Solving these relations for the final variable, $e$, yields a 4th-order polynomial whose only root on $e \in [0, 1)$ is $e = \frac{1}{\mu}\sqrt{y_1^2 y_3^4 + y_1^2 y_2^2 y_3^2 - 2\mu y_1 y_3^2 + \mu^2}$.

Once this transformation is complete, forming matrices $D^{(lp)}$ and $D^{(sp)}$ is a straightforward matter of taking partial derviatives. Note that using mean elements $\underline{y}''$, rather than intermediate elements $\underline{y}'$, as inputs when computing $D^{(sp)}$ constitutes yet another approximation, introducing error of second order in $J_2$. The elements of both matrices $D^{(lp)}$ and $D^{(sp)}$ are listed in Appendix B.

### IV.C MEAN STATE TRANSITION MATRIX $\bar{\phi}_{\bar{y}}$

Considering the state $\underline{y}''(t)$ as a vector function of the initial conditions, and expanding the state for a deputy satellite as a Taylor series about the chief, yields the following:

$$\underline{y}_d''(t) = \underline{y}_c''(t) + \frac{\partial \underline{y}''(t)}{\partial \underline{y}''(t_0)}\Big|_{\underline{y}_c''(t_0)} \left(\underline{y}_d''(t_0) - \underline{y}_c''(t_0)\right) + \cdots$$

or $\underline{\delta y}''(t) = \frac{\partial \underline{y}''(t)}{\partial \underline{y}''(t_0)}\Big|_{\underline{y}_c''(t_0)} \underline{\delta y}''(t_0) + \cdots$. This shows that $\bar{\phi}_{\bar{y}}(t, t_0) = \frac{\partial \underline{y}''(t)}{\partial \underline{y}''(t_0)}\Big|_{\underline{y}_c''(t_0)}$ is the linearized relative state transition matrix (STM), so that (neglecting terms of second order in the relative coordinates) $\underline{\delta y}''(t) = \bar{\phi}_{\bar{y}}(t, t_0)\underline{\delta y}''(t_0)$.

Finding the partial derivatives of $\underline{y}''(t)$ with respect to the initial conditions is most conveniently accomplished through a change of variables to a set of elements $\underline{x}$ used by Lyddane [7]:

$$x_1 = a \qquad x_2 = e\sin l \qquad x_3 = e\cos l$$

$$x_4 = \sin\tfrac{i}{2}\sin h \quad x_5 = \sin\tfrac{i}{2}\cos h \quad x_6 = l + g + h$$

where $a$ is the semi-major axis and $l$ is the mean anomaly. Then we can say that

$$\frac{\partial \underline{y}''(t)}{\partial \underline{y}''(t_0)} = \frac{\partial \underline{y}''(t)}{\partial \underline{x}''(t)} \frac{\partial \underline{x}''(t)}{\partial \underline{x}''(t_0)} \frac{\partial \underline{x}''(t_0)}{\partial \underline{y}''(t_0)}$$

Hoots found the partial derivatives of $\underline{y}$ with respect to $\underline{x}$ [8], and these can be assembled into $\mathcal{J} = \frac{\partial \underline{y}}{\partial \underline{x}}$, the geometric transformation between the two sets, which has the same form whether computed using mean, intermediate, or osculating elements (i.e., $\frac{\partial \underline{y}''}{\partial \underline{x}''} = \frac{\partial \underline{y}'}{\partial \underline{x}'} = \frac{\partial \underline{y}}{\partial \underline{x}}$). $\underline{x}$ is expressed in terms of the initial conditions as

$$x_1''(t) = x_1''(t_0)$$

$$x_2''(t) = x_2''(t_0)\cos\left[\left(n'' + \dot{l}_p''\right)(t - t_0)\right] + x_3''(t_0)\sin\left[\left(n'' + \dot{l}_p''\right)(t - t_0)\right]$$

$$x_3''(t) = -x_2''(t_0)\sin\left[\left(n'' + \dot{l}_p''\right)(t - t_0)\right] + x_3''(t_0)\cos\left[\left(n'' + \dot{l}_p''\right)(t - t_0)\right]$$

$$x_4''(t) = x_4''(t_0)\cos\left[\dot{h}_p''(t-t_0)\right] + x_5''(t_0)\sin\left[\dot{h}_p''(t-t_0)\right]$$

$$x_5''(t) = -x_4''(t_0)\sin\left[\dot{h}_p''(t-t_0)\right] + x_5''(t_0)\cos\left[\dot{h}_p''(t-t_0)\right]$$

$$x_6''(t) = x_6''(t_0) + \left(n'' + \dot{l}_p'' + \dot{g}_p'' + \dot{h}_p''\right)(t-t_0)$$

where $n = \sqrt{\mu/a^3}$ is the mean motion (so that $n'' = \sqrt{\mu/x_1''(t_0)^3}$) and the subscript $p$ indicates the secular rates due to perturbations. Brouwer theory [4] finds these secular rates by taking advantage of the fact that the mean Delaunay elements (which include $l''$, $g''$, and $h''$) are canonical with respect to the transformed Hamiltonian. In terms of $\underline{x}(t_0)$, they are (to first order in $J_2$)

$$\dot{l}_p'' = R_e^2 J_2 \sqrt{\mu}\frac{-3\left(6x_5''(t_0)^4 + 12x_4''(t_0)^2x_5''(t_0)^2 - 6x_5''(t_0)^2 + 6x_4''(t_0)^4 - 6x_4''(t_0)^2 + 1\right)}{2x_1''(t_0)^{7/2}\sqrt{-x_3''(t_0)^2 - x_2''(t_0)^2 + 1}\,\left(x_3''(t_0)^2 + x_2''(t_0)^2 - 1\right)}$$

$$\dot{g}_p'' = R_e^2 J_2 \sqrt{\mu}\frac{3\left(5x_5''(t_0)^4 + 10x_4''(t_0)^2x_5''(t_0)^2 - 5x_5''(t_0)^2 + 5x_4''(t_0)^4 - 5x_4''(t_0)^2 + 1\right)}{x_1''(t_0)^{7/2}\left(x_3''(t_0)^2 + x_2''(t_0)^2 - 1\right)^2}$$

$$\dot{h}_p'' = R_e^2 J_2 \sqrt{\mu}\frac{3\left(2x_5''(t_0)^2 + 2x_4''(t_0)^2 - 1\right)}{2x_1''(t_0)^{7/2}\left(x_3''(t_0)^2 + x_2''(t_0)^2 - 1\right)^2}$$

Let $\bar{\phi}_{\bar{x}}(t,t_0) = \frac{\partial \underline{x}''(t)}{\partial \underline{x}''(t_0)}$. Then $\bar{\phi}_{\bar{y}}(t,t_0) = \mathcal{J}(t)\bar{\phi}_{\bar{x}}(t,t_0)\mathcal{J}^{-1}(t_0)$, where all initial conditions are for the chief satellite. The elements of $\mathcal{J}$ and $\bar{\phi}_{\bar{x}}(t,t_0)$ are listed in Appendix C.

Note that $\underline{x}$ and $\bar{\phi}_{\bar{x}}(t,t_0)$ are nonlinear functions of the perturbed mean secular rates and will have to be re-derived to account for $J_2^2$ or higher zonal harmonics.

### IV.D RELATIVE TRANSFORMATION MAP $\Sigma$

Reference [18] reports expressions for a deputy satellite's relative position $\underline{r}(t)$ and velocity $\underline{v}(t)$ in terms of the chief's osculating nonsingular elements ($a$, $u = f + g$, $i$, $q_1 = e\cos g$, $q_2 = e\sin g$, and $h$) and the deputy's relative osculating nonsingular elements ($\delta a$, $\delta u$, $\delta i$, $\delta q_1$, $\delta q_2$, and $\delta h$) as

$$\begin{bmatrix} x \\ y \\ z \end{bmatrix} = \begin{bmatrix} \frac{r}{a}\delta a + \frac{r^2}{p}\left(q_1\sin u - q_2\cos u\right)\delta u - \frac{r}{p}\left[\left(2aq_1 + r\cos u\right)\delta q_1 + \left(2aq_2 + r\sin u\right)\delta q_2\right] \\ r\left(\delta u + \delta h\cos i\right) \\ r\left(\delta i\sin u - \delta h\sin i\cos u\right) \end{bmatrix}$$

$$\begin{bmatrix} \dot{x} \\ \dot{y} \\ \dot{z} \end{bmatrix} = \begin{bmatrix} \delta v_r - v_t\left(\delta u + \delta h \cos i\right) + \omega_n y \\ \delta v_t + v_r\left(\delta u + \delta h \cos i\right) - \omega_n x + \omega_r z \\ v_r\left(\delta i \sin u - \delta h \sin i \cos u\right) + v_t\left(\delta i \cos u - \delta h \sin i \sin u\right) - \omega_r y \end{bmatrix}$$

where

$$\omega_r = \dot{h}\frac{\sin i}{\sin u}$$

$$\omega_n = \dot{u} + \dot{h}\cos i$$

and

$$v_r = \dot{r}$$

$$v_t = r\omega_n$$

Taking the first variation of $v_r$ and $v_t$ yields

$$\begin{aligned} \delta v_r = &-\left(\frac{n}{2\eta}\delta a - \frac{na}{\eta^2}\delta\eta\right)\left(q_1 \sin u - q_2 \cos u\right) \\ &+ \frac{an}{\eta}\left[\delta q_1 \sin u - \delta q_2 \cos u + \left(q_1 \cos u + q_2 \sin u\right)\delta u\right] \\ \delta v_t = &-\left(\frac{n}{2\eta}\delta a + \frac{na}{\eta^2}\delta\eta\right)\left(1 + q_1 \cos u + q_2 \sin u\right) \\ &+ \frac{an}{\eta}\left[\delta q_1 \cos u + \delta q_2 \sin u + \left(-q_1 \sin u + q_2 \cos u\right)\delta u\right] \end{aligned} \tag{4.4}$$

Note that Eqs. 4.4 are a correction to Eqs. 7.101 and 7.102 in Reference [1].

These expressions can be easily mapped into classical orbit elements $\underline{oe} = \begin{bmatrix} a & e & i & g & h & M \end{bmatrix}^T$ using the variations $\delta q_1 = \cos g\,\delta e - e \sin g\,\delta g$, $\delta q_2 = \sin g\,\delta e + e \cos g\,\delta g$, $\delta u = \delta g + \delta f$, and $\delta f = \frac{\partial f}{\partial e}\delta e + \frac{\partial f}{\partial M}\delta M = \frac{(2+e\cos f)\sin f}{1-e^2}\delta e + \frac{(1+e\cos f)^2}{(1-e^2)^{3/2}}\delta M$. Some terms in $\underline{v}\left(\underline{oe}(t), \underline{\delta oe}(t)\right)$ depend on the perturbed rates of change in $u$ and $h$, which can be found from Gauss's Variational Equations in terms of the perturbing acceleration vector $\underline{a}_p$ due to the Earth's gravitational zonal harmonics [3]:

$$\dot{h} = \frac{a_h\, r \sin\left(f + g\right)}{G \sin i}$$

$$\dot{u} = \frac{G}{r^2} - \dot{h}\cos i$$

where $a_h$ is the component of $\underline{a}_p$ normal to the osculating orbit plane and $G$ is the angular momentum magnitude. Neglecting harmonics beyond $J_2$, a first-order perturbation theory gives

$$a_h = -3R_e^2 J_2\, \mu \sin i \cos i\, \frac{\sin(f+g)}{r^4}$$

The differential classical elements are transformed using the linearized map $\underline{\delta \text{œ}} = \frac{\partial \underline{\text{œ}}}{\partial \underline{y}}\Big|_{\underline{y}_c} \underline{\delta y}$. This map can be found by taking the matrix inverse of the Jacobian $\frac{\partial \underline{y}}{\partial \underline{\text{œ}}}$, which is known from taking the partial derivatives of Eqs. 1.2. Specifically,

$$\frac{\partial \underline{y}}{\partial \underline{\text{œ}}} = \begin{bmatrix} \frac{\eta^2}{p/r} & -a\cos f & 0 & 0 & 0 & \frac{ae}{\eta}\sin f \\ -\frac{ne}{2\eta}\sin f & \frac{\sqrt{\mu}(p/r)^2\sin f}{\sqrt{a}\eta^3} & 0 & 0 & 0 & \frac{\sqrt{\mu}e(p/r)^2\cos f}{\sqrt{a}\eta^4} \\ \frac{n(p/r)}{-2\eta} & \frac{\sqrt{\mu}(p/r)[\cos f(p/r)-e]}{\sqrt{a}\eta^3} & 0 & 0 & 0 & \frac{\sqrt{\mu}e(p/r)^2\sin f}{-\sqrt{a}\eta^4} \\ 0 & \frac{\sin\frac{i}{2}\cos u(2+e\cos f)\sin f}{\eta^2} & \frac{\cos\frac{i}{2}\sin u}{2} & \sin\frac{i}{2}\cos u & 0 & \frac{\sin\frac{i}{2}(p/r)^2\cos u}{\eta^3} \\ 0 & -\frac{\sin\frac{i}{2}\sin u(2+e\cos f)\sin f}{\eta^2} & \frac{\cos\frac{i}{2}\cos u}{2} & -\sin\frac{i}{2}\sin u & 0 & \frac{\sin\frac{i}{2}(p/r)^2\sin u}{-\eta^3} \\ 0 & \frac{(2+e\cos f)}{\eta^2}\sin f & 0 & 1 & 1 & \frac{(p/r)^2}{\eta^3} \end{bmatrix}$$

where $p/r = 1 + e\cos f$, and

$$\left[\frac{\partial \underline{y}}{\partial \underline{\text{œ}}}\right]^{-1} = \begin{bmatrix} \frac{2(p/r)^2}{\eta^4} & \frac{2e\sin f}{n\eta} & \frac{2(p/r)}{n\eta} & 0 & 0 & 0 \\ \frac{(e+\cos f)(p/r)}{a\eta^2} & \frac{\eta\sin f}{na} & \frac{\eta(e+2\cos f+e\cos^2 f)}{na(1+e\cos f)} & 0 & 0 & 0 \\ 0 & 0 & 0 & \frac{2\sin u}{\cos\frac{i}{2}} & \frac{2\cos u}{\cos\frac{i}{2}} & 0 \\ \frac{(p/r)\sin f}{ae\eta^2} & \frac{-\eta\cos f}{nae} & \frac{\eta(2+e\cos f)\sin f}{nae(1+e\cos f)} & \frac{\cos u}{\sin\frac{i}{2}} & \frac{-\sin u}{\sin\frac{i}{2}} & 0 \\ 0 & 0 & 0 & \frac{-\cos u}{\sin\frac{i}{2}} & \frac{\sin u}{\sin\frac{i}{2}} & 1 \\ \frac{(e^2+p/r)\sin f}{-ae\eta} & \frac{\eta^2(e\cos^2 f+\cos f-2e)}{nae(1+e\cos f)} & \frac{-\eta^2(2+e\cos f)\sin f}{nae(1+e\cos f)} & 0 & 0 & 0 \end{bmatrix}$$

The elements of this matrix can likewise be transformed to use the Hoots elements, resulting in

$$\left[\frac{\partial \underline{y}}{\partial \underline{\text{œ}}}\right]^{-1} = \begin{bmatrix} \frac{2\mu^2}{k_1^2} & \frac{2\mu y_1^2 y_2}{k_1^2} & \frac{2\mu y_1^2 y_3}{k_1^2} & 0 & 0 & 0 \\ \frac{y_3^2(y_1y_3^2+y_1y_2^2-\mu)}{\mu k_2} & \frac{y_1^2y_2y_3^2}{\mu k_2} & \frac{y_1y_3(2y_1y_3^2+y_1y_2^2-2\mu)}{\mu k_2} & 0 & 0 & 0 \\ 0 & 0 & 0 & \frac{2y_4}{\sqrt{1-k_3}\sqrt{k_3}} & \frac{2y_5}{\sqrt{1-k_3}\sqrt{k_3}} & 0 \\ \frac{\mu y_2y_3}{k_2^2} & \frac{-y_1y_3(y_1y_3^2-\mu)}{k_2^2} & \frac{y_1y_2(y_1y_3^2+\mu)}{k_2^2} & \frac{y_5}{k_3} & \frac{-y_4}{k_3} & 0 \\ 0 & 0 & 0 & \frac{-y_5}{k_3} & \frac{y_4}{k_3} & 1 \\ \frac{y_2\sqrt{k_1}(k_2^2+\mu y_1y_3^2)}{-\mu k_2^2\sqrt{y_1}} & \frac{k_4\sqrt{y_1k_1}}{-\mu k_2^2} & \frac{y_2y_3\sqrt{y_1^3k_1}(y_1y_3^2+\mu)}{-\mu k_2^2} & 0 & 0 & 0 \end{bmatrix}$$

where the notation $k_1 = 2\mu - y_1y_2^2 - y_1y_3^2$, $k_2 = \sqrt{\mu^2 - k_1y_1y_3^2} = \mu e$, $k_3 = y_4^2 + y_5^2 = \sin^2\frac{i}{2}$, and $k_4 = 2k_2^2 - y_1^2y_3^4 + \mu y_1y_3^2$ has been used for brevity.

Finally, the remaining variables in the expressions for $\underline{r}(t)$ and $\underline{v}(t)$ can be transformed into Hoots

elements. The coefficients of the differential Hoots elements are then formed into matrix $\Sigma(t)$, so that

$$\begin{bmatrix} \underline{r}(t) \\ \\ \underline{v}(t) \end{bmatrix} = \Sigma(t)\, \underline{\delta y}(t)$$

The portion of the transformation due to the perturbing acceleration can be partitioned into a separate map $B(t)$, so that $\Sigma(t) = A(t) + B(t)$. The elements of $A(t)$ and $B(t)$ are listed in Appendix D.

# CHAPTER V

# PREVENTING ALONG-TRACK DRIFT

A key consideration in the design of satellite formations is preventing the spacecraft from drifting apart over time. Often, formations are most susceptible to drift in the direction of the chief's motion, or along-track. In unperturbed motion, all that is necessary to prevent drift is to match the satellites' orbit periods by matching their orbit energies–that is, by matching their semi-major axes: $\delta a = 0$. However, in the Zonal Problem, a mismatch in the mean secular rates $\dot{l}$, $\dot{g}$, or $\dot{h}$ can also lead to drift.

## V.A THREE-CONSTRAINT CONDITION

To completely eliminate drift, then, requires three constraints: $\dot{\delta l} = \dot{\delta g} = \dot{\delta h} = 0$. Expanding the mean secular rates from a perturbation theory shows that these differential rate, to first order in $J_2$, are

$$\begin{aligned}
\dot{\delta l} &= -\frac{3n}{2a}\delta a - \frac{3J_2R_e^2n}{4a^2\eta^3}\left[\frac{7}{4a}\left(3\cos 2i + 1\right)\delta a + \frac{3}{2\eta}\left(3\cos 2i + 1\right)\delta\eta + 3\sin 2i\,\delta i\right] \\
\dot{\delta g} &= -\frac{3J_2R_e^2n}{2a^2\eta^4}\left[\frac{7}{8a}\left(5\cos 2i + 3\right)\delta a + \frac{1}{\eta}\left(5\cos 2i + 3\right)\delta\eta + \frac{5}{2}\sin 2i\,\delta i\right] \\
\dot{\delta h} &= \frac{3J_2R_e^2n}{a^2\eta^4}\left[\frac{7}{4a}\cos i\,\delta a + \frac{2}{\eta}\cos i\,\delta\eta + \frac{1}{2}\sin i\,\delta i\right]
\end{aligned} \tag{5.1}$$

where $n = \sqrt{\mu/a^3}$. The relative rates depend only on the relative momentum coordinates; thus the well-known solution to the three-constraint condition is simply

$$\delta a = \delta\eta = \delta i = 0$$

The disadvantage of the three-constraint condition is that it leaves only three degrees of freedom for formation design. In general, this prevents using a formation such as a PCO, which requires five degrees of freedom to specify the geometry, leaving only one degree of freedom for drift prevention. In fact, it has been said [1, Sec. 8.1.1] that only leader-follower type formations are possible, with some cross-track oscillation. However, note that the PCO definition constraints for $\delta i$, $\delta q_1$, and $\delta q_2$ from Eq. 3.5 can be restated as

$$\delta\eta = \frac{\rho}{2a}\frac{e}{\eta}\sin\left(g_0 + \alpha\right)$$

$$\delta i = \frac{\rho}{a}\cos\alpha$$

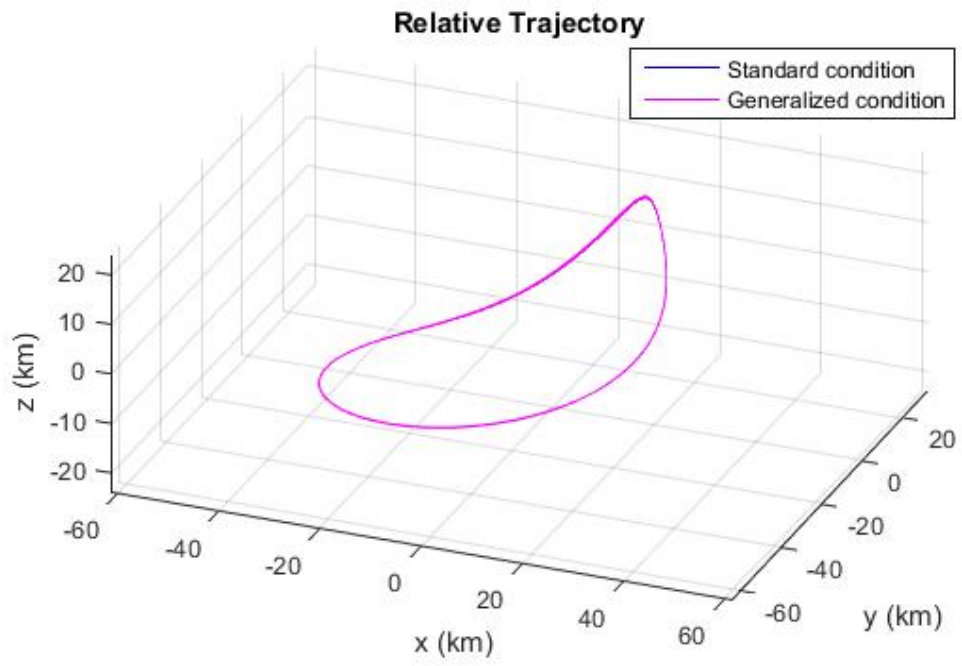


**Figure 5.1: 3D relative trajectory, $g = \pi/2$ and $\alpha = \pi/2$**

where $g_0$ is the chief's initial argument of perigee.

One consequence of this result is that if the chief's initial argument of perigee $g$ is $\pm\pi/2$, then a deputy in a PCO with $\alpha = \pm\pi/2$ will experience no along-track drift, since $\delta\eta$ and $\delta i$ will both equal $0$ (as will $\delta a$ using any of the one-constraint conditions discussed below), and therefore all the relative mean secular rates will also equal $0$. So on these particular chief orbits, the three-constraint condition happens to satisfy (trivially) the PCO constraints on $\delta a$, $\delta\eta$, and $\delta i$.

For example, consider a PCO on a highly eccentric chief orbit. As will be shown later in this chapter, for high chief eccentricity, the standard one-constraint condition on $\delta a$ to mitigate along-track drift (Eq. 5.2 below) does not perform as well by itself. But by setting $g = \pi/2$ and $\alpha = \pi/2$, the drift is removed, as shown in the 10-orbit simulation in Figure 5.1, because the three-constraint condition is satisfied. Note that this formation is not a simple leader-follower with cross-track oscillation: it is a PCO warped by the chief's eccentricity. (In this figure, the PCO radius is 20 kilometers, and the chief satellite has the following initial

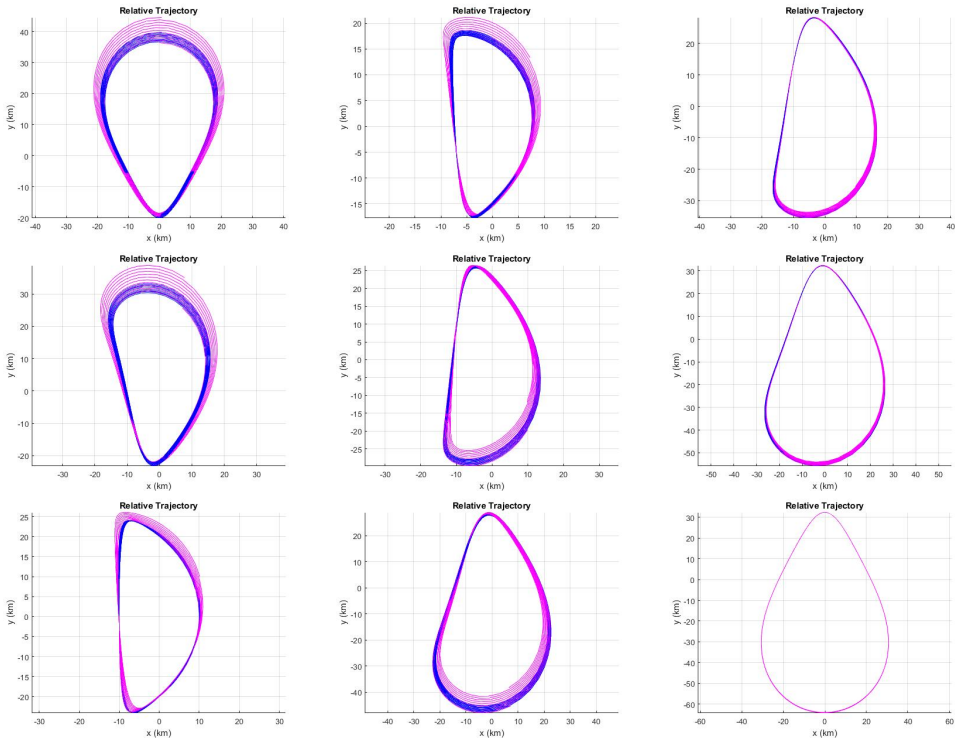


**Figure 5.2: In-plane relative trajectory, $g = 0, \pi/4, \pi/2$ and $\alpha = 0, \pi/4, \pi/2$. Standard condition blue, generalized condition magenta.**

mean elements: semi-major axis of 36,000 kilometers, eccentricity 0.8182, inclination 50 degrees, argument of perigee 90 degrees, and all others 0. The curve labeled "standard condition" uses Eq. 5.2 below to define $\delta a$, and the curve labeled "generalized condition" uses Eq. 5.10, also explained below.)

To illustrate how varying $g$ and $\alpha$ affects drift, Figure 5.2 shows the in-plane relative motion for nine variations of the above scenario. From left to right, each column uses $g$ equal to 0, $\pi/4$, and $\pi/2$, respectively. From top to bottom, each row uses $\alpha$ equal to 0, $\pi/4$, and $\pi/2$, respectively. Only the formation with $\alpha = \pi/2$ around the chief with $g = \pi/2$ (the same one illustrated in Figure 5.1) has no visible along-track drift.

The relative orbit from Figure 5.1 is very stable, especially in the in-plane coordinates; the in-plane trajectory over 1600 orbits is shown in Figure 5.3. Over such a long time scale, there is noticeable cross-track drift due to long-period effects; for this orbit the apsidal rotation period is over 4000 orbits. Scenarios such as this one suggest the need to treat long-period effects as though they were secular, in some cases, and

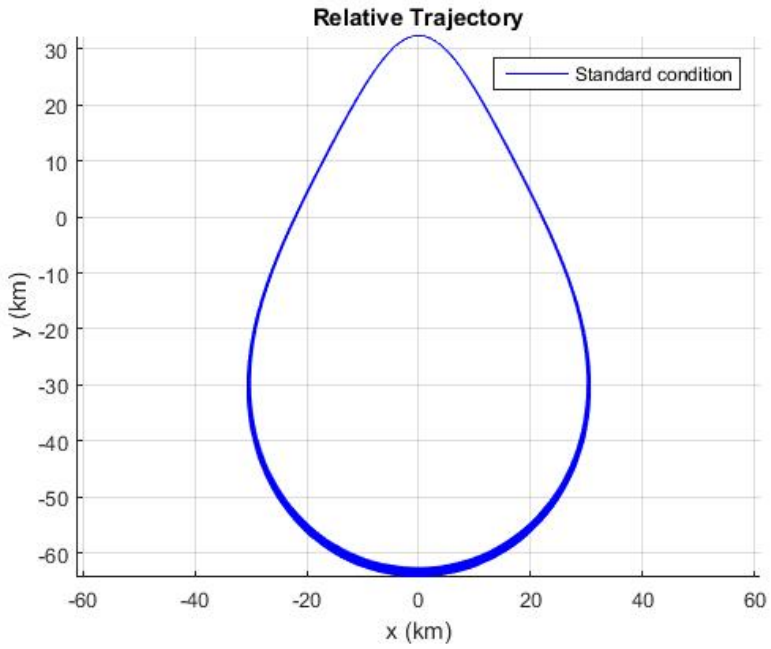


**Figure 5.3: In-plane relative trajectory over 1600 orbits, $g = \pi/2$ and $\alpha = \pi/2$**

to derive analytical methods for mitigating them.

The scenario from Figure 5.1 has the following initial mean element differences: $\delta a = \delta\eta = \delta i = 0$, $\delta h = -7.25\text{e}{-4}$, $\delta g = 10.65\text{e}{-4}$, and $\delta l = -5.99\text{e}{-4}$. By using these values, rather than the PCO definition, to initialize a formation, a similar trajectory can be produced regardless of the initial mean value of $g$. This is shown in the 30-orbit simulations in Figure 5.4, where $g_0 = \pi/3$. Here, the three-constraint condition is still satisfied, and only the cross-track motion differs from Figure 5.1, because of the different value of $g$. It is as though the long-period cross-track effect had been fast-forwarded from $g = \pi/2$ to $g = \pi/3$.

In general, of course, restrictions on the chief's initial argument of perigee are not desirable. In order to prevent along-track drift for any set of chief initial mean orbit elements, then drift must be eliminated using constraints only on the formation parameters.

## V.B TWO-CONSTRAINT CONDITIONS

One of the best known two-constraint conditions is the "$J_2$-invariant" condition [44], which prevents cross-track drift by requiring that $\dot{\delta h} = 0$ and addresses along-track drift by requiring that $\dot{\delta\lambda} = 0$, where

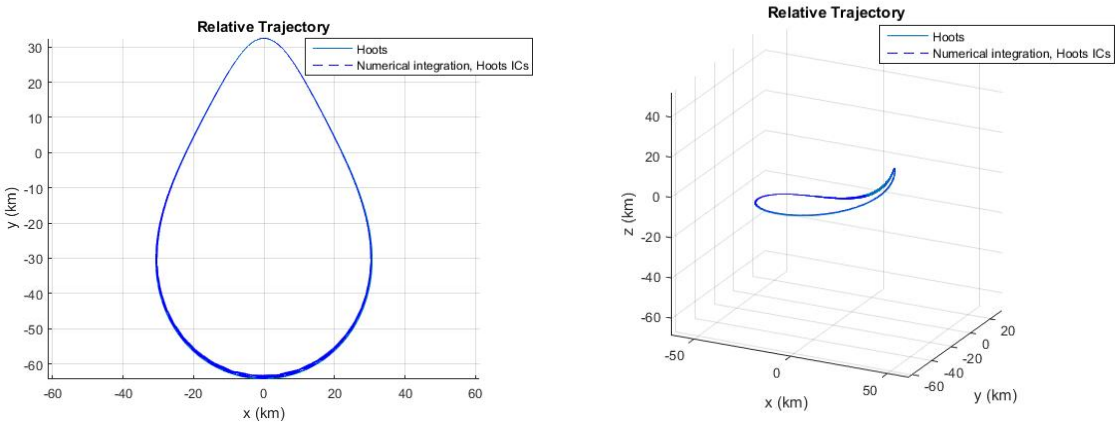


**Figure 5.4: In-plane and 3D relative trajectories, $g = \pi/3$**

$\lambda = l + g$. This "$J_2$-invariant" condition allows $\delta l$ and $\delta g$ to grow at equal and opposite rates. Its solution is

$$\delta\eta = -\frac{\eta}{4}\tan i\,\delta i$$
$$\delta a = \frac{J_2 R_e^2}{2a\eta^5}\left(4+3\eta\right)\left(1+5\cos^2 i\right)\delta\eta$$

[3, Eqs. 14.150 and 14.153]. This form is singular for polar orbits, but inverting the first equation would create a different "invariant" formation whose singularity is at zero inclination instead.

Later in this chapter, a new two-constraint condition will be developed which prevents along-track drift. However, to work with a formation, such as a PCO, which requires five degrees of freedom to specify the formation geometry, a one-constraint condition to minimize along-track drift is desirable.

## V.C STANDARD APPROACH: APPROXIMATE ANGLE RATE MATCHING

The standard condition for preventing along-track drift of a satellite formation in the presence of $J_2$ is [1]

$$\delta a = -J_2 R_e^2 \frac{3\eta+4}{4a\eta^5}\left(2\delta i\,\eta\sin 2i + 3\delta\eta\cos 2i + \delta\eta\right) \tag{5.2}$$

in which all variables are mean. This condition was derived by matching the approximate mean along-track angle rates of the deputy and chief when $\delta h$ is small: $\left(\dot{l}_d + \dot{g}_d\right)\cos\delta i + \dot{h}_d\cos i$ and $\dot{l} + \dot{g} + \dot{h}\cos i$, respectively [23]. Further assuming small $\delta i$, this resulted in the condition

$$\dot{\delta l} + \dot{\delta g} + \dot{\delta h}\cos i = 0 \tag{5.3}$$

After using mean secular rates from a first-order (in $J_2$) perturbation theory, expanding to first order in $\delta a$, $\delta\eta$, and $\delta i$, and then solving for $\delta a$, Eq. 5.3 gave rise to Eq. 5.2.

If the perturbation theory is instead a second-order theory, accounting for $J_2$, $J_4$, and $J_6$, then the second-order (in $J_2$) mean secular rates can be expanded to first order in $\delta a$, $\delta\eta$, and $\delta i$ and used in Eq. 5.3. The solution for $\delta a$ to this second-order equation will then have terms up to $\mathcal{O}(J_2^2)$ in both the numerator and denominator, but its Taylor-series expansion gives the following second-order version of the standard zero-drift condition:

$$
\begin{aligned}
\delta a = &- J_2 R_e^2 \frac{3\eta+4}{4a\eta^5}\left(2\delta i\,\eta\sin 2i + 3\delta\eta\cos 2i + \delta\eta\right) \\
&+ \frac{J_2^2 R_e^4}{512a^3\eta^9}\Big\{ -4\delta i\,\eta\Big[\left(25\eta^3 - 78\eta^2 - 231\eta - 56\right)\sin 4i + \left(-130\eta^3 - 228\eta^2 + 46\eta + 496\right)\sin 2i\Big] \\
&\qquad - \delta\eta\Big[\left(125\eta^3 - 498\eta^2 - 1281\eta - 56\right)\cos 4i \\
&\qquad\quad + \left(-1300\eta^3 - 2424\eta^2 + 1092\eta + 7392\right)\cos 2i - 425\eta^3 - 1302\eta^2 - 259\eta + 3416\Big]\Big\} \\
&+ \frac{J_4 R_e^4}{512a^3\eta^9}\Big[ -20\delta i\,\eta\left(15\eta^3 + 18\eta^2 - 15\eta - 40\right)\left(7\sin 4i + 2\sin 2i\right) \\
&\qquad - 5\delta\eta\left(15\eta^3 + 18\eta^2 - 21\eta - 56\right)\left(35\cos 4i + 20\cos 2i + 9\right)\Big] \\
&+ \frac{J_6 R_e^6}{32768a^5\eta^{13}}\Big[ -70\delta i\,\eta\left(105\eta^5 + 120\eta^4 - 350\eta^3 - 700\eta^2 + 189\eta + 756\right)\left(33\sin 6i\right. \\
&\qquad\qquad \left. + 12\sin 4i + 5\sin 2i\right) \\
&\qquad - 35\delta\eta\left(35\eta^5 + 40\eta^4 - 150\eta^3 - 300\eta^2 + 99\eta + 396\right)\left(231\cos 6i + 126\cos 4i\right. \\
&\qquad\qquad \left. + 105\cos 2i + 50\right)\Big]
\end{aligned}
$$

Note that the first term is equivalent to Eq. 5.2.

Only even zonal harmonics appear (here and in every drift-prevention formula) because, to second order in $J_2$, odd harmonics are not present in the mean Hamiltonian. As a result, the odd harmonics do not contribute to secular drift. This effect will be illustrated later (Figure 5.14).

If the chief's mean orbit is circular, then setting $\eta = 1$ reduces the first-order condition to

$$\delta a = -\frac{7J_2R_e^2}{4a}\left[2\sin 2i\,\delta i + \left(3\cos 2i + 1\right)\delta\eta\right]$$

In all cases, neglecting perturbations simply reduces to $\delta a = 0$, as expected.

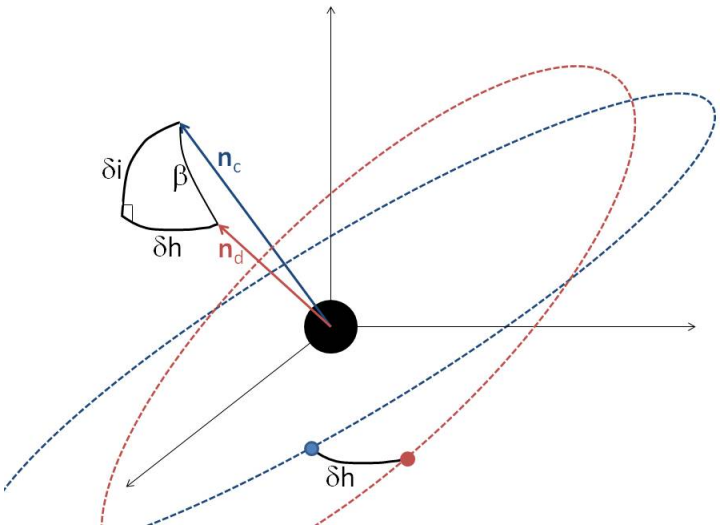


**Figure 5.5: Relative orientation of chief (blue) and deputy (red) mean orbit planes**

If the formation is large, it may be desirable to include some of the nonlinear effects due to higher-order terms in the relative coordinates, as in Section 8.2 of Reference [1].

### V.D ANGLE RATE AVERAGING

However, it is not necessary to use approximate mean angle rates to derive a zero-drift condition. The exact angle rates of the mean orbits are known. For the chief, it is $\dot{f} + \dot{g} + \dot{h}\cos i$. The rates in $f$ and $g$ are measured about the chief's orbit normal vector $\boldsymbol{n}_c$, and the rate in $h$ is measured about the inertial vertical direction and projected through angle $i$ onto $\boldsymbol{n}_c$ (see Figure 5.5). The deputy's rate in $h$ is likewise measured about the inertial vertical direction, but its rates in $f$ and $g$ are measured about its own orbit normal $\boldsymbol{n}_d$, and must therefore be projected onto $\boldsymbol{n}_c$ through the angle $\beta$ between them. As Figure 5.5 illustrates, $\beta$ is the hypotenuse of a right spherical triangle whose legs are $\delta h$ and $\delta i$; thus $\cos\beta = \cos\delta h \cos\delta i$ and the deputy's angle rate is $\left(\dot{f}_d + \dot{g}_d\right)\cos\delta h\cos\delta i + \dot{h}_d\cos i$ (where subscript $d$ indicates the deputy's elements).

Note that in the above discussion, each mean rate $\dot{f}$ is not constant, but oscillates over the course of one mean orbit unless that orbit is circular.

Furthermore, to prevent along-track drift, it is not necessary to match the chief's and deputy's oscil-

lating rates at all times. Instead, it is only necessary to match the chief's and deputy's periods. That is, after one chief orbit, the relative angular separation must not have changed. This requires that

$$\int_0^{2\pi} \left[\left(\dot{f}_d + \dot{g}_d\right)\cos\delta h\cos\delta i + \dot{h}_d\cos i\right]\,dl - \int_0^{2\pi}\left[\dot{f}+\dot{g}+\dot{h}\cos i\right]\,dl = \int_0^{2\pi}\left[\left(\dot{f}_d+\dot{g}_d\right)\cos\delta h\cos\delta i - \dot{f}-\dot{g}+\dot{\delta h}\cos i\right]\,dl = 0$$

Using a first-order approximation for small $\delta h$ and $\delta i$, this becomes

$$\int_0^{2\pi}\left[\dot{\delta f}+\dot{\delta g}+\dot{\delta h}\cos i\right]\,dl = 0$$

Since each term of the integrand except $\dot{\delta f} = \dot{f}_d - \dot{f}$ is independent of $l$, the period-matching condition is

$$\frac{1}{2\pi}\int_0^{2\pi}\dot{\delta f}\,dl + \dot{\delta g} + \dot{\delta h}\cos i = 0 \tag{5.4}$$

The first term of the period-matching condition is the time-average of $\dot{\delta f}$ over one chief orbit. $\dot{\delta f}$ may be found in terms of chief mean elements and known secular rates by computing the first variation of

$$\dot{f} = \frac{\partial f}{\partial l}\dot{l} = \frac{a^2}{r^2}\eta\dot{l}$$

This is

$$\begin{aligned}\dot{\delta f} = &-2e\left(\frac{a}{r}\right)^3\sin f\,\dot{l}\,\delta l + \eta\left(\frac{a}{r}\right)^2\dot{\delta l}\\ &+\frac{1}{2\eta^2}\frac{a}{r}\left[-e\cos 3f - 4\cos 2f - \left(\frac{4}{e}+e\right)\cos f - 2\right]\dot{l}\,\delta\eta\end{aligned} \tag{5.5}$$

and the orbit average is

$$\begin{aligned}\frac{1}{2\pi}\int_0^{2\pi}\dot{\delta f}\,dl = &-2e\,\dot{l}\,\delta l\frac{1}{2\pi}\int_0^{2\pi}\left(\frac{a}{r}\right)^3\sin f\,dl + \eta\,\dot{\delta l}\frac{1}{2\pi}\int_0^{2\pi}\left(\frac{a}{r}\right)^2\,dl\\ &+\frac{1}{2\eta^2}\dot{l}\,\delta\eta\frac{1}{2\pi}\int_0^{2\pi}\frac{a}{r}\left[-e\cos 3f - 4\cos 2f - \left(\frac{4}{e}+e\right)\cos f - 2\right]dl\end{aligned}$$

Using the property that

$$\frac{1}{2\pi}\int_0^{2\pi}\cos jf\,dl = \left(\frac{-e}{1+\eta}\right)^j(1+j\eta) \tag{5.6}$$

for $j = 1, 2, ...$ [45], it can be shown that

$$\frac{1}{2\pi}\int_0^{2\pi}\left(\frac{a}{r}\right)^2\,dl = \frac{1}{\eta}$$

$$\frac{1}{2\pi}\int_0^{2\pi}\left(\frac{a}{r}\right)^3\sin f\,dl = 0$$

$$\frac{1}{2\pi}\int_0^{2\pi}\left(\frac{a}{r}\right)\cos 3f\,dl = -\left(\frac{1-\eta}{1+\eta}\right)^{3/2}$$

$$\frac{1}{2\pi}\int_0^{2\pi}\left(\frac{a}{r}\right)\cos 2f\,dl = \frac{1-\eta}{1+\eta}$$
$$\frac{1}{2\pi}\int_0^{2\pi}\left(\frac{a}{r}\right)\cos f\,dl = -\sqrt{\frac{1-\eta}{1+\eta}}$$
$$\frac{1}{2\pi}\int_0^{2\pi}\left(\frac{a}{r}\right)\,dl = 1$$

After making these substitutions and simplifying, the $\delta\eta$ and $\delta l$ terms vanish, leaving

$$\frac{1}{2\pi}\int_0^{2\pi}\dot{\delta f}\,dl = \dot{\delta l}$$

so that Eq. 5.4 reduces to Eq. 5.3.

Thus, the only assumptions underlying Eq. 5.3 are small (first-order) $\delta h$ and $\delta i$, and the only additional assumptions underlying the standard zero-drift condition (Eq. 5.2 or its second-order version) are first-order $\delta a$ and $\delta\eta$. There is no assumption of small chief mean eccentricity; but note that this condition removes drift in the along-track angular position, not necessarily in the along-track curvilinear position.

In some cases, rate matching may be of more interest than period matching. Then, if the chief mean orbit is not circular, it will be necessary to satisfy

$$\dot{\delta f} + \dot{\delta g} + \dot{\delta h}\cos i = 0$$

at some specific point in time. This was the approach of Roscoe [46], who modified Eq. 5.2 to account for the difference between $\dot{\delta f}$ and $\dot{\delta l}$ in a particular region of interest along the chief's orbit.

## V.E CURVILINEAR RATE AVERAGING

However, matching angle rates, or integrated angle rates, only prevents angular drift, not necessarily along-track drift in a curvilinear local-vertical local-horizontal reference frame. If the satellites' orbits have non-negligible eccentricity, these quantities will be different, because the change in the deputy's orbit radius–not only the change in its angular position–has an along-track component. See the illustration in Figure 5.6 of two satellites orbiting in the same plane, where $u = f + g$ is the argument of latitude. Clearly the differential angle rate contributes to the along-track motion as $\dot{u}_d\cos\delta u - \dot{u}_c$, which can be approximated to first order as $\delta\dot{u}$. However, there is also an along-track contribution from the deputy's radial motion, $(\dot{r}_c + \delta\dot{r})\sin\delta u$,

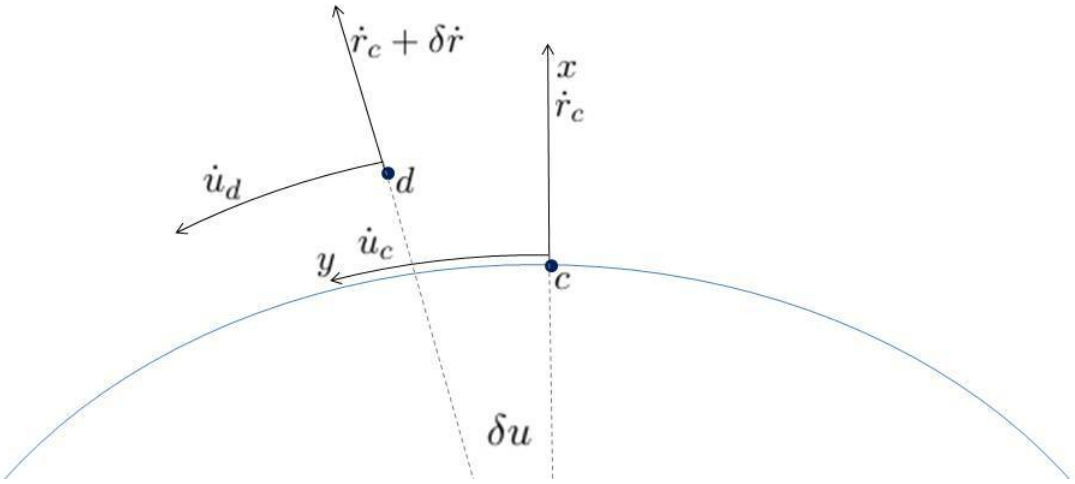


**Figure 5.6: In-plane contributions to along-track relative motion**

which is $\dot{r}_c\,\delta u$ to first order.

The curvilinear along-track position (to first order in the differential orbit elements) is [1, Eq. 7.86]

$$y = r\left(\delta f + \delta g + \delta h \cos i\right)$$

To prevent along-track drift, the following condition should be enforced:

$$\frac{1}{2\pi}\int_0^{2\pi} \dot{y}\, dl = 0 \tag{5.7}$$

The scalar time derivative of $y$ is $\dot{y} = r\left(\dot{\delta f} + \dot{\delta g} + \dot{\delta h}\cos i\right) + \dot{r}\left(\delta f + \delta g + \delta h \cos i\right)$, where $\dot{r} = \dot{l}\frac{ae}{\eta}\sin f$. Thus

$$\begin{aligned}\frac{1}{2\pi}\int_0^{2\pi} \dot{y}\, dl = \frac{1}{2\pi}\int_0^{2\pi} r\,\dot{\delta f}\, dl + \left(\dot{\delta g} + \dot{\delta h}\cos i\right)\frac{1}{2\pi}\int_0^{2\pi} r\, dl \\ + \dot{l}\frac{ae}{\eta}\frac{1}{2\pi}\int_0^{2\pi} \sin f\,\delta f\, dl + \dot{l}\frac{ae}{\eta}\left(\delta g + \delta h\cos i\right)\frac{1}{2\pi}\int_0^{2\pi}\sin f\, dl\end{aligned} \tag{5.8}$$

The last integral vanishes, removing $\delta g$ and $\delta h$ from the condition. Furthermore, it can be shown that the orbit average of $r$ is $a\left(1 + e^2/2\right)$, leaving only the integrals containing $\delta f$ and $\dot{\delta f}$.

Using the expression for $\dot{\delta f}$ from Eq. 5.5, the first of these integrals becomes

$$\frac{1}{2\pi}\int_0^{2\pi} r\,\delta\dot{f}\,dl = a\frac{1}{2\pi}\int_0^{2\pi}\left(\frac{r}{a}\right)\{-2e\left(\frac{a}{r}\right)^3\sin f\,\dot{l}\,\delta l+\eta\left(\frac{a}{r}\right)^2\dot{\delta l}$$
$$+\frac{1}{2\eta^2}\frac{a}{r}\left[-e\cos 3f-4\cos 2f-\left(\frac{4}{e}+e\right)\cos f-2\right]\dot{l}\,\delta\eta\}dl$$
$$=a\frac{1}{2\pi}\int_0^{2\pi}\{-2e\left(\frac{a}{r}\right)^2\sin f\,\dot{l}\,\delta l+\eta\left(\frac{a}{r}\right)\dot{\delta l}$$
$$+\frac{1}{2\eta^2}\left[-e\cos 3f-4\cos 2f-\left(\frac{4}{e}+e\right)\cos f-2\right]\dot{l}\,\delta\eta\}dl$$
$$=a\{-2e\dot{l}\,\delta l\frac{1}{2\pi}\int_0^{2\pi}\left(\frac{a}{r}\right)^2\sin f\,dl+\eta\,\dot{\delta l}\frac{1}{2\pi}\int_0^{2\pi}\left(\frac{a}{r}\right)\,dl$$
$$+\frac{\dot{l}\,\delta\eta}{2\eta^2}[-e\frac{1}{2\pi}\int_0^{2\pi}\cos 3f dl-4\frac{1}{2\pi}\int_0^{2\pi}\cos 2f dl$$
$$-\left(\frac{4}{e}+e\right)\frac{1}{2\pi}\int_0^{2\pi}\cos f dl-2\frac{1}{2\pi}\int_0^{2\pi}dl]\}$$

Using Eq. 5.6, it can be shown that

$$\frac{1}{2\pi}\int_0^{2\pi}\left(\frac{a}{r}\right)^2\sin f\,dl=0$$

This result, along with others obtained previously, results in

$$\frac{1}{2\pi}\int_0^{2\pi} r\,\delta\dot{f}\,dl=a\eta\,\dot{\delta l}+a\dot{l}\,\delta\eta$$

Three of the integrals from Eq. 5.8 have now been found. The final integral is

$$\frac{1}{2\pi}\int_0^{2\pi}\sin f\,\delta f\,dl=\frac{1}{2\pi}\int_0^{2\pi}\sin f\left(\frac{\partial f}{\partial l}\delta l+\frac{\partial f}{\partial\eta}\delta\eta\right)\,dl$$
$$=\frac{1}{2\pi}\int_0^{2\pi}\sin f\left[\eta\left(\frac{a}{r}\right)^2\delta l-\frac{(2+e\cos f)\sin f}{\eta e}\delta\eta\right]\,dl$$
$$=\eta\,\delta l\frac{1}{2\pi}\int_0^{2\pi}\left(\frac{a}{r}\right)^2\sin f\,dl-\frac{1}{\eta e}\frac{1}{2\pi}\int_0^{2\pi}(2+e\cos f)\sin^2 f\,\delta\eta\,dl$$

Since the first integral here vanishes,

$$\frac{1}{2\pi}\int_0^{2\pi}\sin f\,\delta f\,dl=-\frac{1}{2\eta e}\delta\eta\frac{1}{2\pi}\int_0^{2\pi}\left(2+\frac{e}{2}\cos f-2\cos 2f-\frac{e}{2}\cos 3f\right)dl$$

After once more applying Eq. 5.6 and simplifying, it turns out that

$$\frac{1}{2\pi}\int_0^{2\pi}\sin f\,\delta f\,dl=-\frac{\eta}{e}\delta\eta$$

Thus we can rewrite Eq. 5.8 as

$$\frac{1}{2\pi}\int_0^{2\pi} \dot{y}\, dl = a\eta\,\dot{\delta l} + a\dot{l}\,\delta\eta + a\left(1+\frac{e^2}{2}\right)\left(\dot{\delta g} + \dot{\delta h}\cos i\right) + \dot{l}\frac{ae}{\eta}\left(-\frac{\eta}{e}\delta\eta\right)$$
$$= a\eta\,\dot{\delta l} + a\left(1+\frac{e^2}{2}\right)\left(\dot{\delta g} + \dot{\delta h}\cos i\right)$$

To accord with the new condition for preventing along-track drift, Eq. 5.7, this quantity should be set equal to 0. Thus Eq. 5.3 is replaced with

$$\eta\,\dot{\delta l} + \left(1+\frac{e^2}{2}\right)\left(\dot{\delta g} + \dot{\delta h}\cos i\right) = 0 \tag{5.9}$$

After using mean secular rates from a first-order (in $J_2$) perturbation theory, expanding to first order in $\delta a$, $\delta\eta$, and $\delta i$, and then solving for $\delta a$, Eq. 5.9 gives rise to the following generalized condition:

$$\delta a = -J_2 R_e^2 \frac{1}{4a\eta^5}\frac{\eta^2+6}{\eta}\left(2\delta i\,\eta\sin 2i + 3\delta\eta\cos 2i + \delta\eta\right) \tag{5.10}$$

A second-order perturbation theory accounting for zonal harmonics through $J_6$ yields the following second-order generalized condition:

$$\begin{aligned}
\delta a = &- J_2 R_e^2 \frac{1}{4a\eta^5}\frac{\eta^2+6}{\eta}\left(2\delta i\,\eta\sin 2i + 3\delta\eta\cos 2i + \delta\eta\right) \\
&+ \frac{J_2^2 R_e^4}{256a^3\eta^{11}}\Big\{ -4\delta i\,\eta\big[\left(5\eta^5 - 12\eta^4 + 5\eta^3 + 210\eta - 378\right)\sin 4i \\
&\qquad + \left(-26\eta^5 - 8\eta^4 - 162\eta^3 + 540\eta - 252\right)\sin 2i\big] \\
&\qquad - \delta\eta\big[\left(25\eta^5 - 72\eta^4 - 10\eta^3 + 1470\eta - 2268\right)\cos 4i \\
&\qquad + \left(-260\eta^5 - 96\eta^4 - 1800\eta^3 + 7560\eta - 3024\right)\cos 2i \\
&\qquad - 85\eta^5 - 88\eta^4 - 750\eta^3 + 4410\eta - 2772\big]\Big\} \\
&+ \frac{J_4 R_e^4}{256a^3\eta^{10}}\big[ -20\delta i\,\eta\left(3\eta^4 + 16\eta^2 - 30\right)\left(7\sin 4i + 2\sin 2i\right) \\
&\qquad - 5\delta\eta\left(3\eta^4 + 17\eta^2 - 42\right)\left(35\cos 4i + 20\cos 2i + 9\right)\big] \\
&+ \frac{3J_6 R_e^6}{32768a^5\eta^{14}}\big[ -70\delta i\,\eta\left(15\eta^6 + 60\eta^4 - 413\eta^2 + 378\right)\left(33\sin 6i + 12\sin 4i + 5\sin 2i\right) \\
&\qquad - 35\delta\eta\left(5\eta^6 + 20\eta^4 - 183\eta^2 + 198\right)\left(231\cos 6i + 126\cos 4i + 105\cos 2i + 50\right)\big]
\end{aligned}$$

Note that the first term is equivalent to Eq. 5.10.

The impact of replacing the standard condition, Eq. 5.2, with Eq. 5.10 is shown in Figure 5.7. The plot in the lower left displays the orbit-averaged value of along-track coordinate $y$ for both types of

formations. The averaging is a simple numerical mean of the $y$-value at each time step. This simulation is for the same scenario as Figure 5.1, except that $g = 0$ and $\alpha = 0$. The generalized condition consistently shows slightly smaller drift in the orbit-averaged value of $y$, in that the slope from orbit 1 to orbit 10 is slightly less. However, this is not always the best metric for drift, as shown by the upper plot in Figure 5.7, illustrating the in-plane motion over ten orbits. Even though the average value is drifting less, the worst-case drift is at the chief's perigee (the point in the relative orbit corresponding to the maximum $y$-value): here, the generalized condition worsens the drift. The reason for the discrepancy is that near apogee, where the satellites spend much more time, the generalized condition slightly lessens the drift, as shown in the close-up in the lower right-hand plot.

Thus, curvilinear rate averaging produces a different result than angle rate matching, but not necessarily a better one. A different drift-prevention condition is still desirable.

## V.F ELIMINATING THE SECULAR ALONG-TRACK MOTION

Again, the curvilinear along-track position (to first order in the differential orbit elements) is [1, Eq. 7.86]

$$y = r\left(\delta f + \delta g + \delta h \cos i\right)$$

For the most general method to prevent along-track drift, consider the variables above as mean and select formation parameters (differential orbit elements) which eliminate any secular terms. Expanding,

$$\begin{aligned}
y &= r\,\delta f + r\left(\delta g + \delta h \cos i\right) \\
&= r\left(\frac{\partial f}{\partial l}\delta l + \frac{\partial f}{\partial \eta}\delta\eta\right) + r\left(\delta g + \delta h \cos i\right) \\
&= r\left[\eta\left(\frac{a}{r}\right)^2 \delta l - \frac{\left(2 + e\cos f\right)\sin f}{\eta e}\delta\eta\right] + r\left(\delta g + \delta h \cos i\right) \\
&= a\eta\,\delta l\left(\frac{a}{r}\right) - \frac{2\sin f}{\eta e}\frac{a\eta^2}{1 + e\cos f}\delta\eta - \frac{e\cos f \sin f}{\eta e}\frac{a\eta^2}{1 + e\cos f}\delta\eta + \left(\delta g + \delta h\cos i\right)\frac{a\eta^2}{1 + e\cos f} \\
&= -\frac{2a\eta}{e}\delta\eta\frac{\sin f}{1 + e\cos f} - a\eta\,\delta\eta\frac{\cos f \sin f}{1 + e\cos f} + \frac{a}{\eta}\delta l\left(1 + e\cos f\right) + a\eta^2\left(\delta g + \delta h\cos i\right)\frac{1}{1 + e\cos f}
\end{aligned}$$

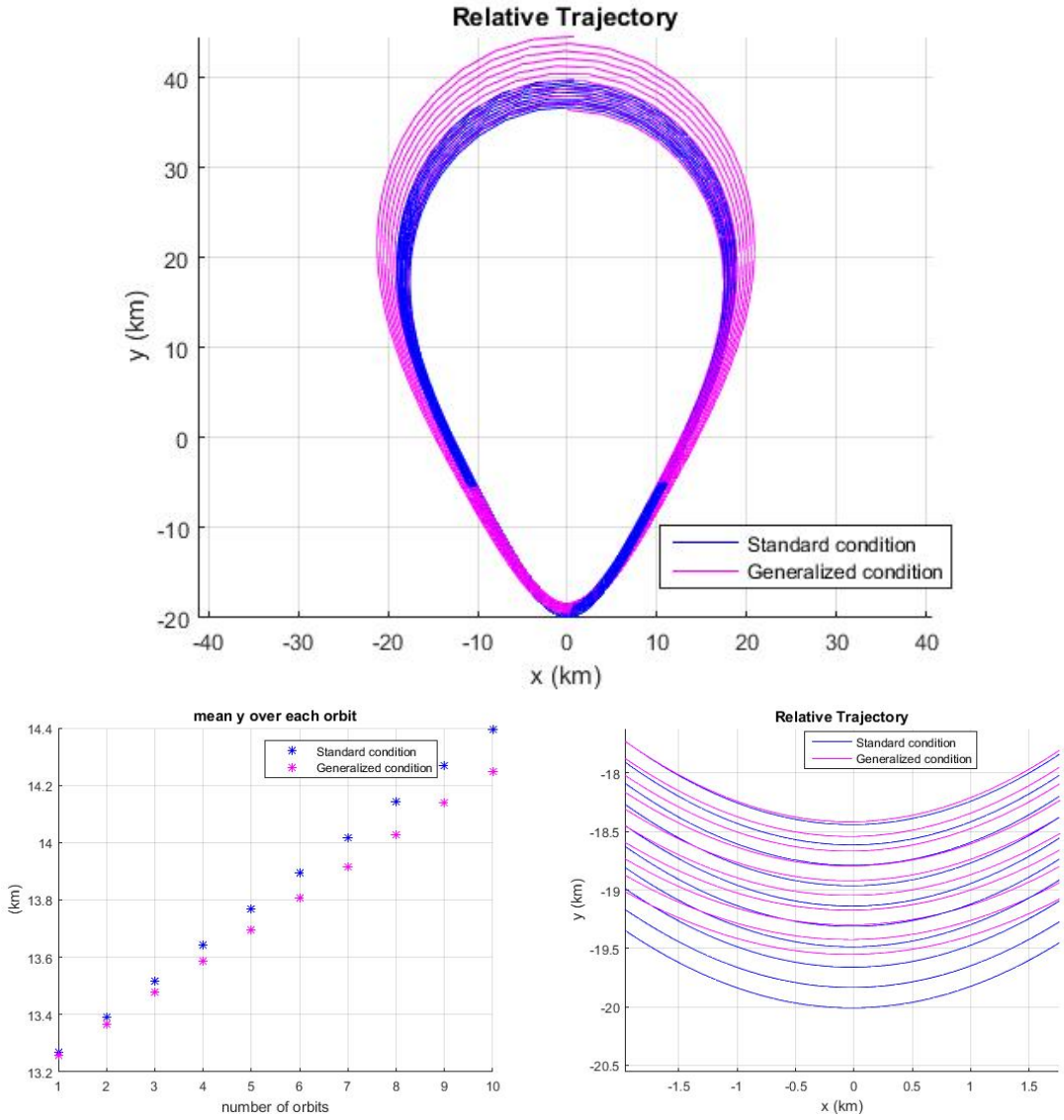


**Figure 5.7: Drift, $e = 0.8182$**

The first two terms are periodic, and the final two terms depend on the mean secular rates through

$$\delta l = \delta l_0 + \dot{\delta l}\,(t - t_0)$$

$$\delta g = \delta g_0 + \dot{\delta g}\,(t - t_0)$$

$$\delta h = \delta h_0 + \dot{\delta h}\,(t - t_0)$$

where the subscript 0 represents values at the initial time. Thus $y$ can be written as

$$y = y_{constant} + y_{periodic} + y_{secular}$$

where

$$y_{constant} = \frac{a}{\eta}\left(\delta l_0 - \dot{\delta l}\, t_0\right)$$

$$y_{periodic} = \left(-\frac{2a\eta}{e}\frac{\sin f}{1 + e\cos f} - a\eta\frac{\cos f \sin f}{1 + e\cos f}\right)\delta\eta + \frac{ae}{\eta}\left(\delta l_0 - \dot{\delta l}\, t_0\right)\cos f + a\eta^2\left[\delta g_0 - \dot{\delta g}\, t_0 + \left(\delta h_0 - \dot{\delta h}\, t_0\right)\cos i\right]\frac{1}{1 + e\cos f}$$

and

$$y_{secular} = \dot{\delta l}\left(\frac{a}{\eta}t + \frac{ae}{\eta}t\cos f\right) + a\eta^2\left(\dot{\delta g} + \dot{\delta h}\cos i\right)\frac{t}{1 + e\cos f} \tag{5.11}$$

Along-track drift can be prevented by eliminating $y_{secular}$, which contains all the secular and mixed-secular terms. Note that for circular chief orbits, $y_{secular} = a\left(\dot{\delta l} + \dot{\delta g} + \dot{\delta h}\cos i\right)t$.

The secular and nonsecular components of $y$ are illustrated in Figure 5.8 for a PCO formation with a radius of 20 km, where the chief satellite has the following initial mean elements: semi-major axis of 36,000 km, eccentricity 0.8182, inclination 50 degrees, and all others 0 (the same scenario as in Figure 5.7). All three simulations use numerical integration accounting for the $J_2$ perturbation, but the value of $\delta a$ is computed differently in each plot. The values of $y_{secular}$ shown here are approximate, in that the mean secular rates are computed only to first-order in $J_2$, and in that osculating values of the true anomaly $f$ are used instead of mean values in Eq. 5.11. However, to the scale of these plots, removing $y_{secular}$ from $y$ removes all drift.

Inspecting Eq. 5.11 reveals that $y_{secular}$ depends on time $t$, chief orbit elements $a$, $e$, and $i$, and relative secular rates $\dot{\delta l}$, $\dot{\delta g}$, and $\dot{\delta h}$. Using the expressions for these relative rates from Eq. 5.1, $y_{secular}$ depends on $t$, $a$, $e$, $i$, and formation parameters $\delta a$, $\delta\eta$, and $\delta i$. In a PCO formation, some of these parameters

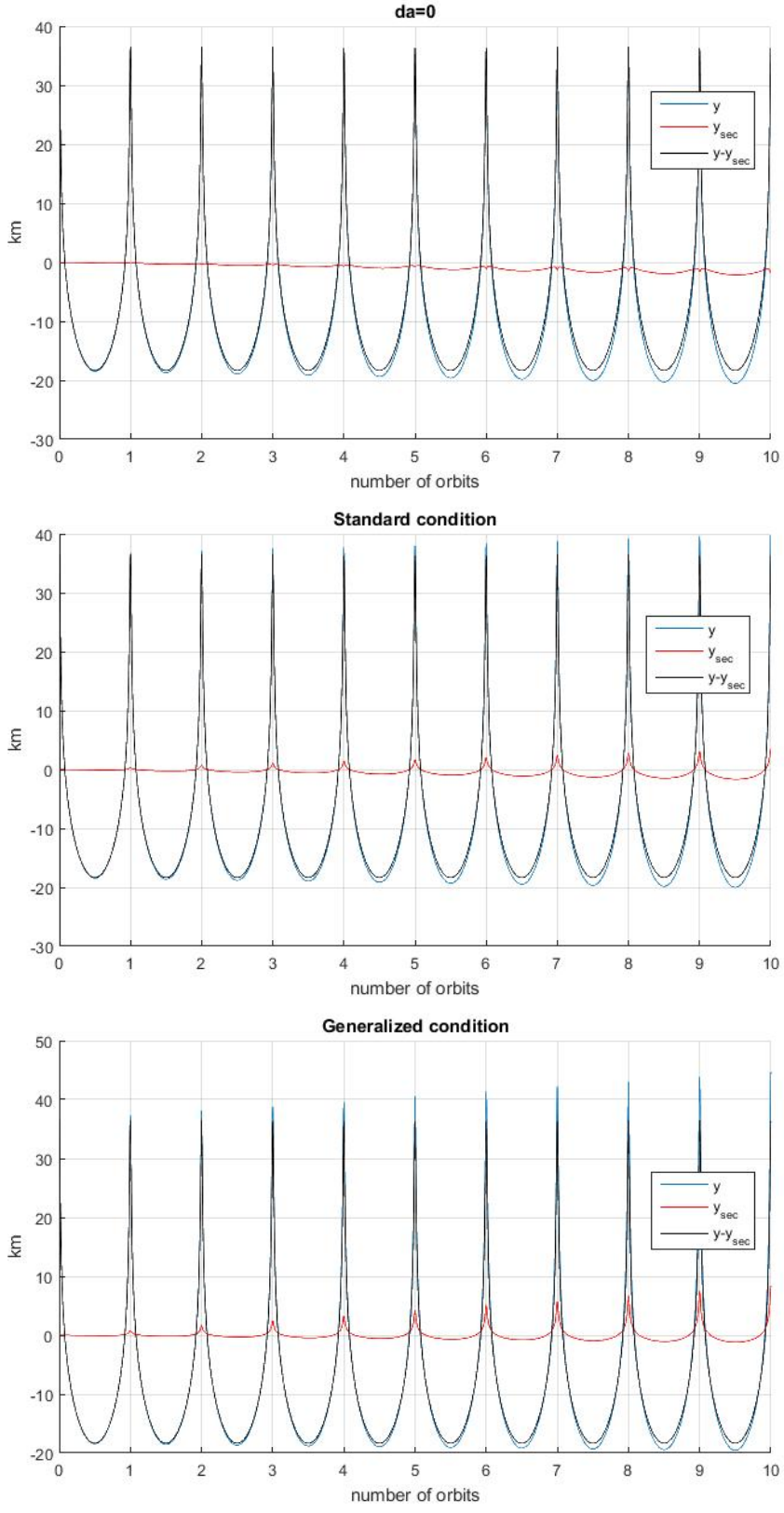


**Figure 5.8: Along-track secular and nonsecular components**

are dictated by PCO radius $\rho$ and initial deputy phase angle $\alpha$. Thus when a PCO definition is enforced, $y_{secular}$ depends on time, chief initial orbit elements $a$, $e$, $i$, and $g_0$, and formation parameters $\delta a$, $\rho$, and $\alpha$.

### V.F.1 Two Constraints

Obviously, a three-constraint condition of the kind discussed earlier in this chapter would cause $y_{secular}$ to vanish. However, since the mean secular rates are functions of $\delta a$, $\delta\eta$, and $\delta i$, a satellite formation can easily be designed to eliminate $y_{secular}$ using the two constraints

$$\begin{aligned} \dot{\delta l} &= 0 \\ \dot{\delta g} + \dot{\delta h}\cos i &= 0 \end{aligned} \tag{5.12}$$

Note that for circular chief orbits, the standard condition (solving Eq. 5.3, $\dot{\delta l} + \dot{\delta g} + \dot{\delta h}\cos i = 0$, to find $\delta a$) completely eliminates along-track drift. Solving Eqs. 5.12 for $\delta a$ and $\delta\eta$ gives, to first order in $J_2$,

$$\begin{aligned} \delta a &= 0 \\ \delta\eta &= -\frac{2\eta\sin 2i}{3\cos 2i+1}\delta i \\ &\quad -\frac{J_2 R_e^2 \sin i}{128a^2\eta^3}\frac{5\left(3\eta^2-28\right)\sin 6i + 4\left(93\eta^2-580\right)\sin 4i + \left(363\eta^2-2620\right)\sin 2i}{9\cos 4i + 12\cos 2i + 11}\delta i \end{aligned}$$

or, to zeroth order in $J_2$,

$$\begin{aligned} \delta a &= 0 \\ \delta\eta &= -\frac{2\eta\sin 2i}{3\cos 2i+1}\delta i \end{aligned} \tag{5.13}$$

This solution has a singularity at mean chief inclination values of approximately 54.7 degrees, which is the same value for which the first-order term in the mean secular rate of the mean anomaly vanishes, so that $\dot{l} = n + \mathcal{O}(J_2^2)$ (just as the critical inclination, approximately 63.4 degrees, causes the mean secular rate of the argument of perigee to vanish at first order, so that $\dot{g} = \mathcal{O}(J_2^2)$).

The second of Eqs. 5.13 can be inverted to give a solution for $\delta a$ and $\delta i$ in terms of $\delta\eta$. Specifically, to zeroth order in $J_2$,

$$\begin{aligned} \delta a &= 0 \\ \delta i &= -\frac{3\cos 2i+1}{2\eta\sin 2i}\delta\eta \end{aligned} \tag{5.14}$$

This formation's singularity occurs for polar orbits (for which $\dot{h} = \mathcal{O}(J_2^2)$). Figure 5.9 replicates Figure

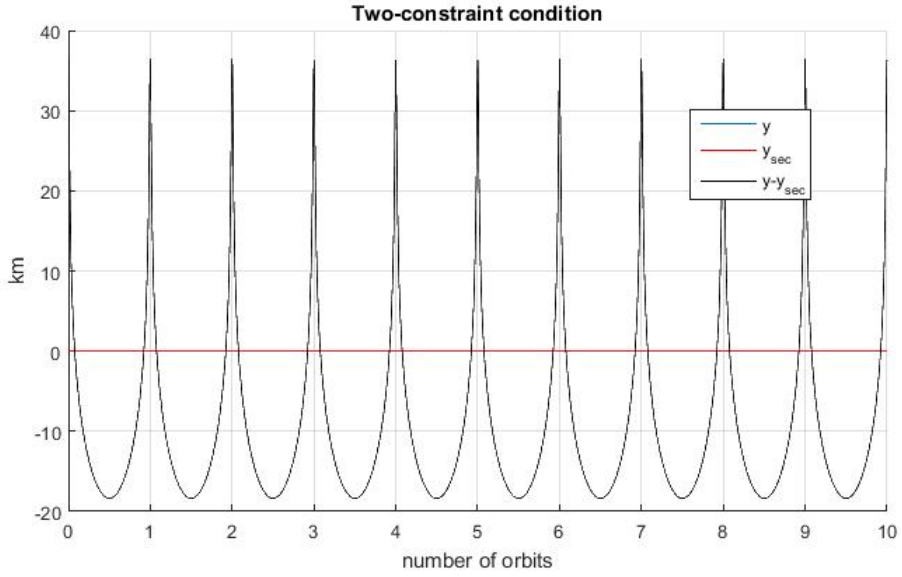


**Figure 5.9: Along-track secular and nonsecular components, two constraints**

5.8, but with Eqs. 5.14 providing $\delta a$ and replacing the PCO definition of $\delta i$. The plot shows that the secular component of $y$ has been completely removed, and there is no drift.

Note that for either formation (Eqs. 5.13 or Eqs. 5.14), substituting either one of the conditions into the standard condition, Eq. 5.2, or into the generalized condition, Eq. 5.10, yields the other. In other words, this two-constraint solution is a subset of both approximate solutions given previously.

Note also that the two-constraint solution presented here is different from the two-constraint "$J_2$-invariant" condition [44] discussed earlier in this chapter.

*Case Study*

Suppose a chief satellite is in a geostationary transfer orbit (GTO; perhaps after suffering an apogee kick motor failure, for example) with mean classical elements as follows: semi-major axis 24,432 kilometers; eccentricity 0.72577; inclination 28.5 degrees; all others 0. Suppose further that a servicing vehicle enters a relative orbit (perhaps designed for circumnavigation and inspection) with mean differential elements as follows: $\delta a = 0, \delta e = 0, \delta i = 1\text{e}{-5}, \delta h = 8\text{e}{-6}, \delta g = -5\text{e}{-6}, \delta l = -5\text{e}{-6}$. This relative orbit is depicted in LVLH coordinates in Figure 5.10, computed by directly differencing numerically integrated trajectories

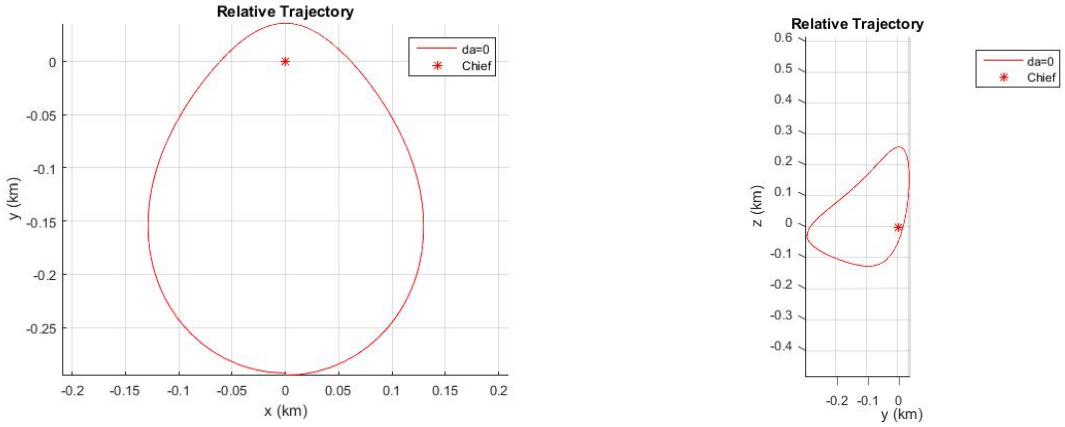


**Figure 5.10: 1 relative orbit, $\delta a = 0$**

(including the effect of $J_2$) for both the chief and the servicer.

However, this relative orbit is subject to drift due to $J_2$. Over twenty orbits, the relative trajectory appears as in Figure 5.11. To prevent this drift, the formation could be changed using any of the conditions discussed so far. Figure 5.12 shows three such attempts: the standard condition on $\delta a$ (Eq. 5.2), the two-constraint solution offered here for $\delta a$ and $\delta \eta$ (Eq. 5.13), and the "$J_2$-invariant" conditions on $\delta a$ and $\delta \eta$. Note that all three formations share the same values of $\delta i$, $\delta h$, $\delta g$, and $\delta l$.

Inspecting Figure 5.12 shows that the standard condition preserves the geometry of the original formation in Figure 5.10 and improves along-track drift slightly. The "$J_2$-invariant" condition changes the formation shape slightly and still experiences some along-track drift. The new two-constraint condition changes the formation shape more, but eliminates the along-track drift. The secular and nonsecular components of the along-track motion are plotted in Figure 5.13 for all three conditions, showing that only the new two-constraint condition eliminates $y_{secular}$.

*Demonstration of Second-order Effects*

Since the two-constraint approach removes drift due to first-order $J_2$, it provides a convenient way to demonstrate drift due to $J_2^2$ and higher harmonics. For example, it can be used to illustrate that odd zonal harmonics do not contribute to drift, as previously noted. Figure 5.14 shows the drift in a large (80-kilometer scale) formation computed by numerical integration using four different force models: two-body

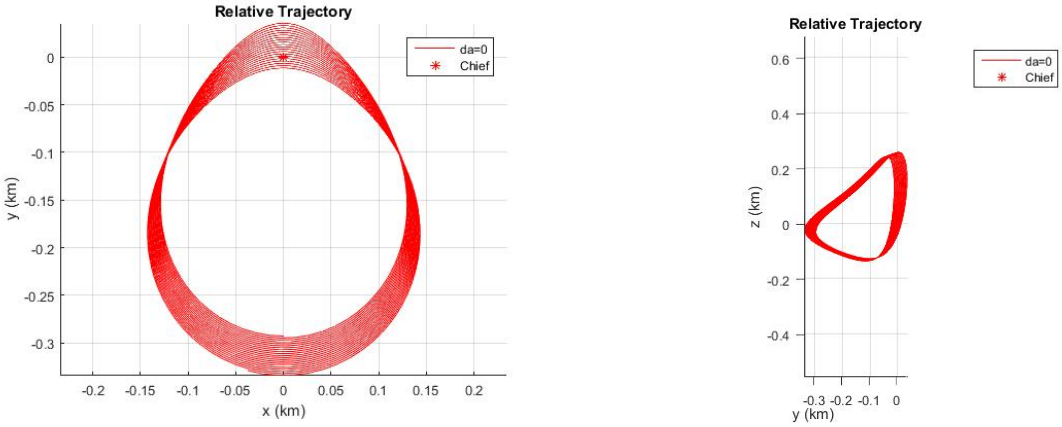


**Figure 5.11: 20 relative orbits, $\delta a = 0$**

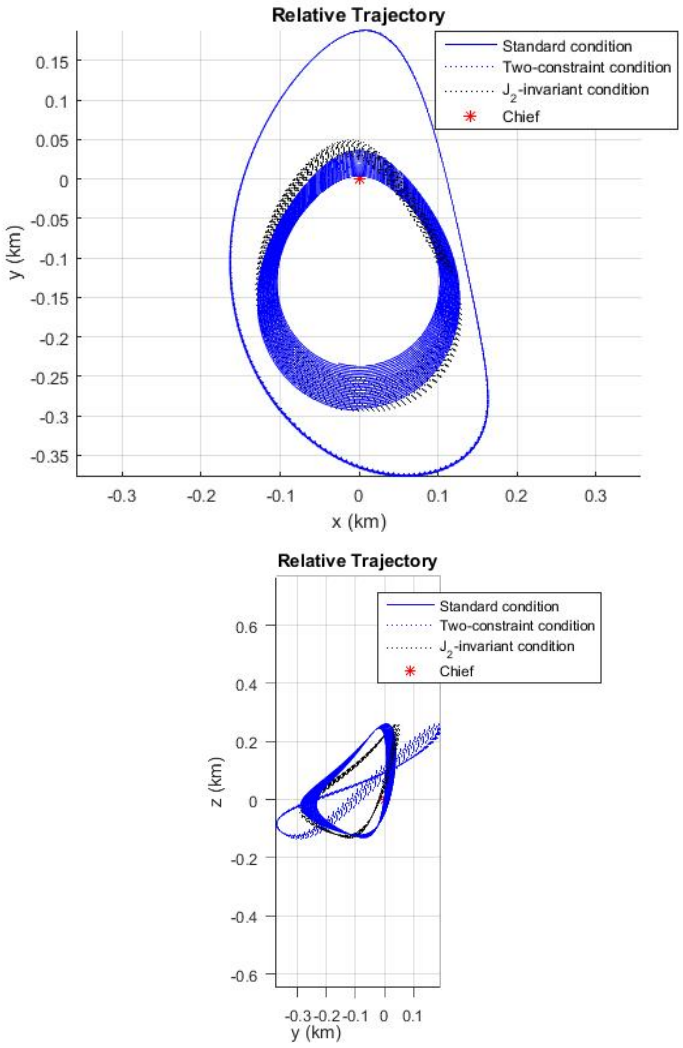


**Figure 5.12: 20 relative orbits, three different drift-prevention strategies**

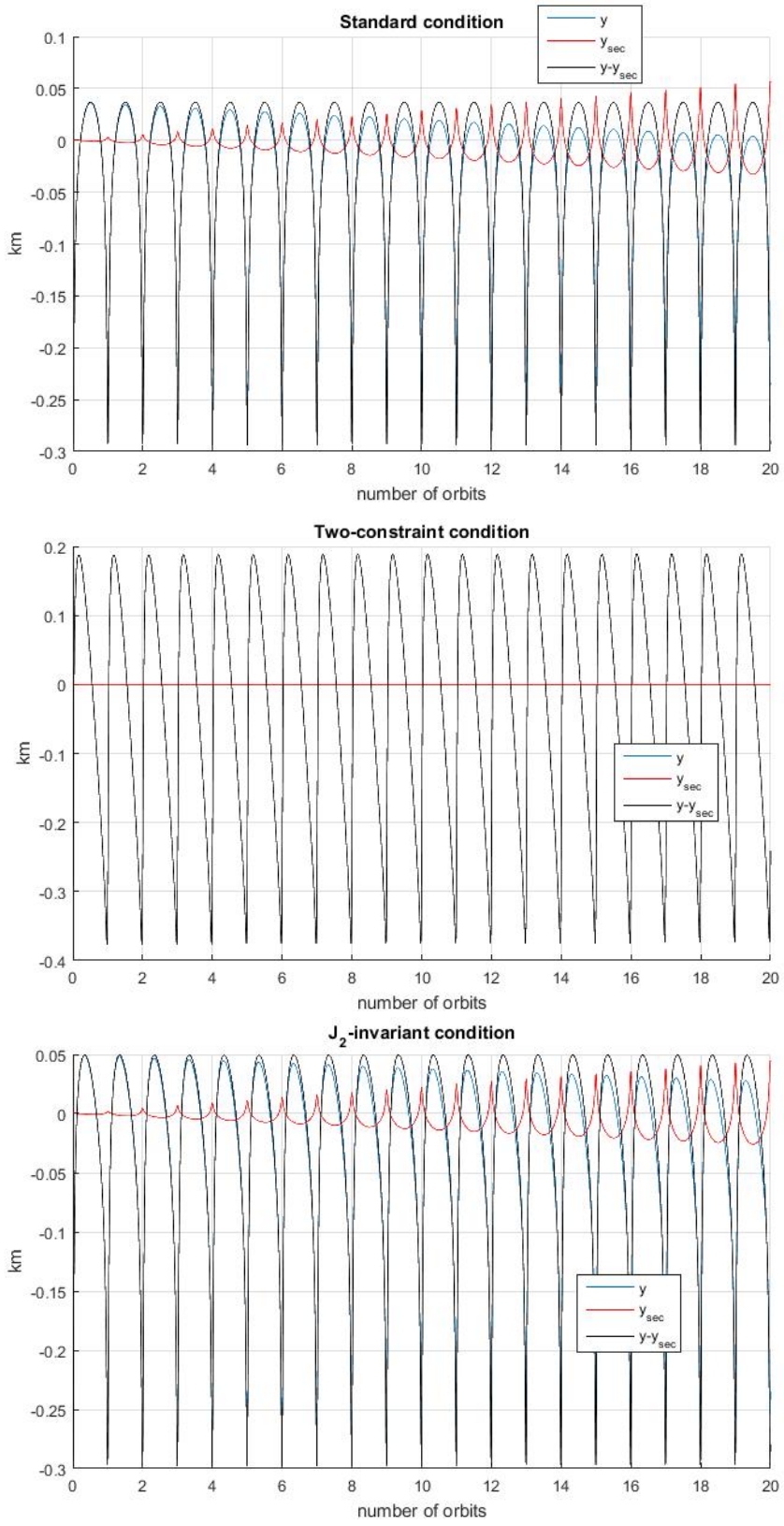


**Figure 5.13: Along-track secular and nonsecular components for the GTO case study**

gravity; $J_2$ only; even harmonics through $J_6$; and finally, both even and odd harmonics through $J_6$. For this scenario, the chief's mean orbit has semi-major axis 7100 kilometers, eccentricity 0.1, and inclination 50 degrees; the deputy's mean relative equinoctial elements are $\delta a = 0$, $\delta\Lambda = 0$, $\delta\tilde{q}_1 = 0.005732875360449$, $\delta\tilde{q}_2 = -7.042253521126760\text{e}{-05}$, $\delta p_1 = 8.573541070802810\text{e}{-05}$, and $\delta p_2 = 0$ (equivalent to modifying a 1-kilometer PCO with Eq. 5.13). The drift is measured here by showing the change in the maximum and minimum values of $y$ (the curvilinear along-track coordinate) for each relative orbit. To make the trends easier to see, the negative portions of the $y$-curve (which contain the minima) are reflected into the positive domain via a simple absolute value function, and the local maxima of $|y|$ are displayed. For the two lower plots, the mean-to-osculating transformation on the initial conditions is prevented from considering any harmonics higher than $J_2$, so that all three perturbed cases have the same initial osculating conditions.

The results show that, as expected, $J_2^2$ causes some drift (top right), adding $J_4$ and $J_6$ to the numerically integrated solution increases the drift (bottom left), and adding $J_3$ and $J_5$ does not increase the drift further (bottom right).

### V.F.2 One Constraint

The two-constraint approach is not possible for a formation that allows only one additional constraint, such as a PCO. In this case, drift cannot be perfectly eliminated, but it can be minimized. The differential semi-major axis resulting in minimum along-track drift is then

$$\arg\min_{\delta a} \int_0^\infty y_{secular}^2 \, dt$$

This study has not pursued the minimization approach, but it remains a viable line of inquiry for future research.

## V.G CONCLUSIONS

In the field of satellite formation flying, the need to prevent along-track drift due to zonal harmonic gravitational perturbations has long been known. The present chapter makes several contributions to the analysis of this problem.

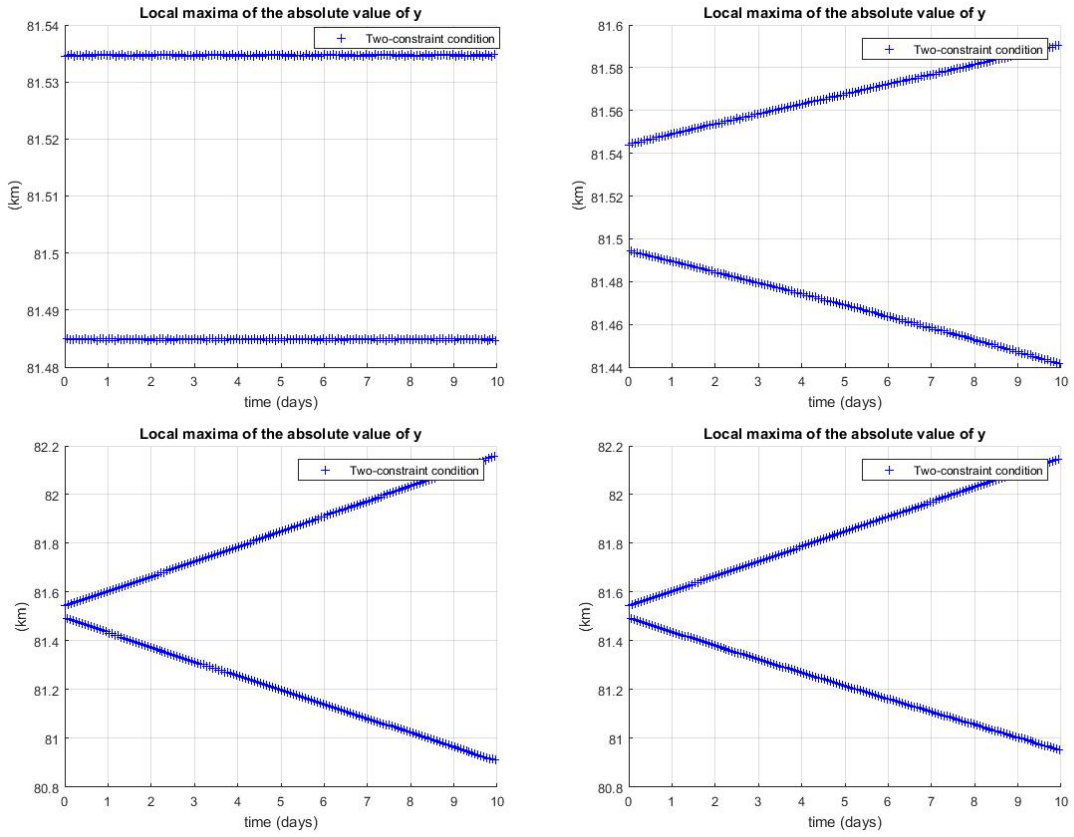


**Figure 5.14: Drift in the extrema of $y$ for four cases. The cases are two-body gravity (top left), $J_2$ (top right), even harmonics (bottom left), and even and odd harmonics (bottom right).**

First, this chapter found relative orbits where the three-constraint condition for no drift can also satisfy the PCO definition constraints, for certain values of $g_0$. Next, this chapter showed that the standard approach for mitigating along-track drift, based on matching the approximate mean angle rates of chief and deputy satellites, is equivalent to matching the orbit-averaged mean angle rates. This chapter also derived a generalized condition based on matching the orbit-averaged rates of change of the curvilinear along-track position; this new condition performs better at mitigating orbit-averaged drift, but not necessarily at mitigating worst-case drift. Furthermore, this chapter extended both the standard and generalized conditions to second order in $J_2$.

Finally, and most importantly, this chapter found the expression for secular along-track motion and developed a way to remove it for any chief orbit via a two-constraint solution, although it removes one degree of freedom from the formation design. In future work, a one-constraint approximation may be found by minimizing the secular along-track motion.

# CHAPTER VI

# SOURCES OF MODELING ERROR

This chapter will analyze the following sources of error in modeling satellite motion: 1) Numerical integration amplifying input noise; 2) Linearized relative coordinates; 3) Approximate solutions to the Zonal Problem; 4) Truncation due to Kepler's Equation; and 5) Singularities. These errors will be illustrated graphically using a variety of MATLAB-generated error plots. One additional way to illustrate error, not pursued in this chapter, would be to use the Yan-Alfriend modeling error index [39].

## VI.A NUMERICAL INTEGRATION AMPLIFYING INPUT NOISE

In the satellite motion simulation results shown here, to generate the truth model, MATLAB's numerical integrator ode45 solves for each satellite's ECI absolute position and velocity vectors as a function of time, $\underline{r}(t)$ and $\underline{v}(t)$. The code constrains ode45 to use an evenly spaced time array.

In simulations of the Two-Body Problem, analytical solutions are all nearly identical, with almost machine precision–see Figure 6.1 for a simulation where $J_2 = 0$, the semi-major axis is 7100 kilometers, the eccentricity is 0, the inclination is 45 degrees, and ode45's relative tolerance is 3e-14; the plot shows differences in one of the satellite's ECI position coordinates measured in canonical (dimensionless) Distance Units (DU). If the analytical models are all compared to the same numerical solution, therefore, they have nearly identical (very small) error profiles–see Figure 6.2, which shows position and velocity errors in kilometers and kilometers per second.

This error profile is insensitive to the number of time steps. The shape of the error profile is sensitive to eccentricity. The scale of the error profile is somewhat sensitive to the orbit selected (especially orbit size) and very sensitive to the tolerance settings for ode45, but it is qualitatively the same for a given value of eccentricity. (Reducing the absolute tolerance for ode45 below about 1e-15 does not change the error profile, and the relative tolerance cannot be changed below about 2.3e-14.) In fact, for low eccentricities each ECI component of $\underline{r}(t)$ and $\underline{v}(t)$ is qualitatively similar. See Figure 6.3, which shows position and

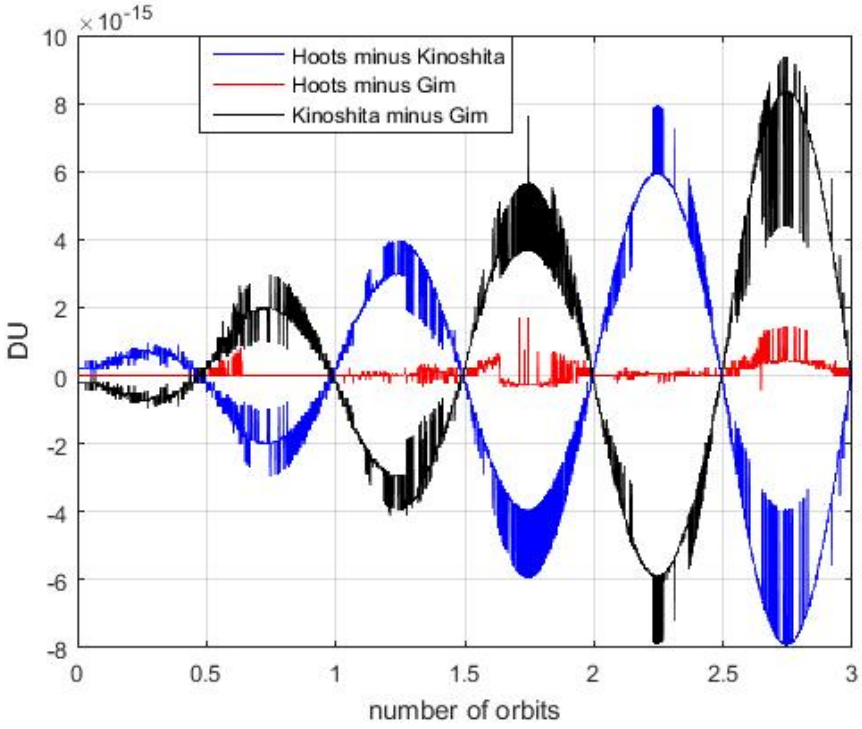


**Figure 6.1: Differences in analytically propagated ECI x-coordinate**

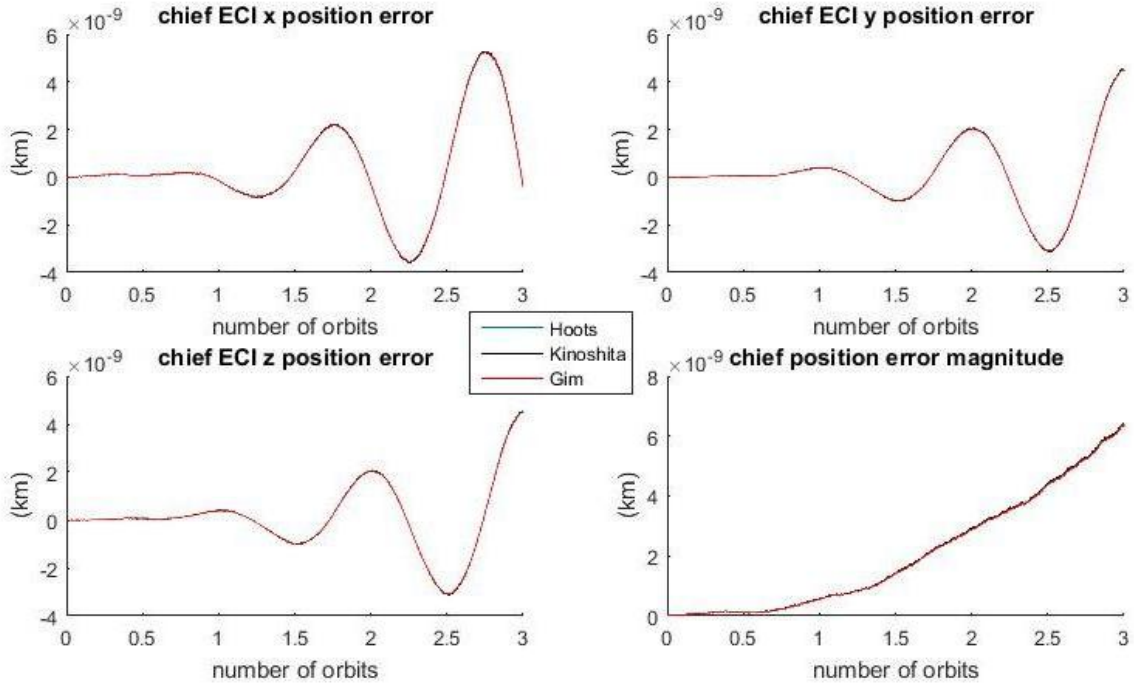


**Figure 6.2: Error: 3 analytical models vs. single numerical solution**

velocity errors for a scenario identical to that in Figures 6.1 and 6.2, except that ode45's relative tolerance is now 1e-8. Note that the errors (like the tolerance) are now almost six orders of magnitude greater.

However, generating a separate numerical solution to compare against each analytical solution changes this result. Even though there are no perturbations, and thus each numerical solution should be equivalent, the error profiles differ noticeably (while all are still small). This can be seen in Figure 6.4 (in which ode45's relative tolerance has been returned to 3e-14). This means the numerical solutions themselves are different.

The cause of these errors is ode45's amplification of input noise. When all the inputs are the same (to 15 significant figures), and the relative tolerance is 3e-14, the first point in each solution is identical to the initial conditions (again to 15 significant figures), but the final points (tested using 3-orbit simulations) are consistent only to 11 or 12 significant figures. Each time ode45 propagates the "truth model", it amplifies discrepancies on the order of 1e-16 into this level of error. See the differences in the separately computed, but nominally identical, numerical solutions in Figure 6.5 (measured in DU).

Direct-differencing relative motion results follow a similar pattern, as in Figures 6.6 and 6.7, which show the errors in relative position based on a single numerical solution and separate numerical solutions, respectively. The simulation is for a Projected Circular Orbit (PCO) formation with a radius of 1 kilometer and a deputy initial phase angle of 0.

Again, all this error is mapped from error in the ode45-generated truth trajectories, which arise because of noise in the initial conditions, which originates as round-off error when $\underline{r}(t_0)$ and $\underline{v}(t_0)$ are computed from different variables.

## VI.B LINEARIZED RELATIVE COORDINATES

The errors shown thus far are small–negligibly small for most applications. However, relative motion results computed analytically via a State Transition Matrix (STM) necessarily include more error, due to the truncation at first order in the relative coordinates. For a PCO, the scale of the STM errors increases with the square of the PCO radius. This linearization error may dominate the error in the numerical solutions

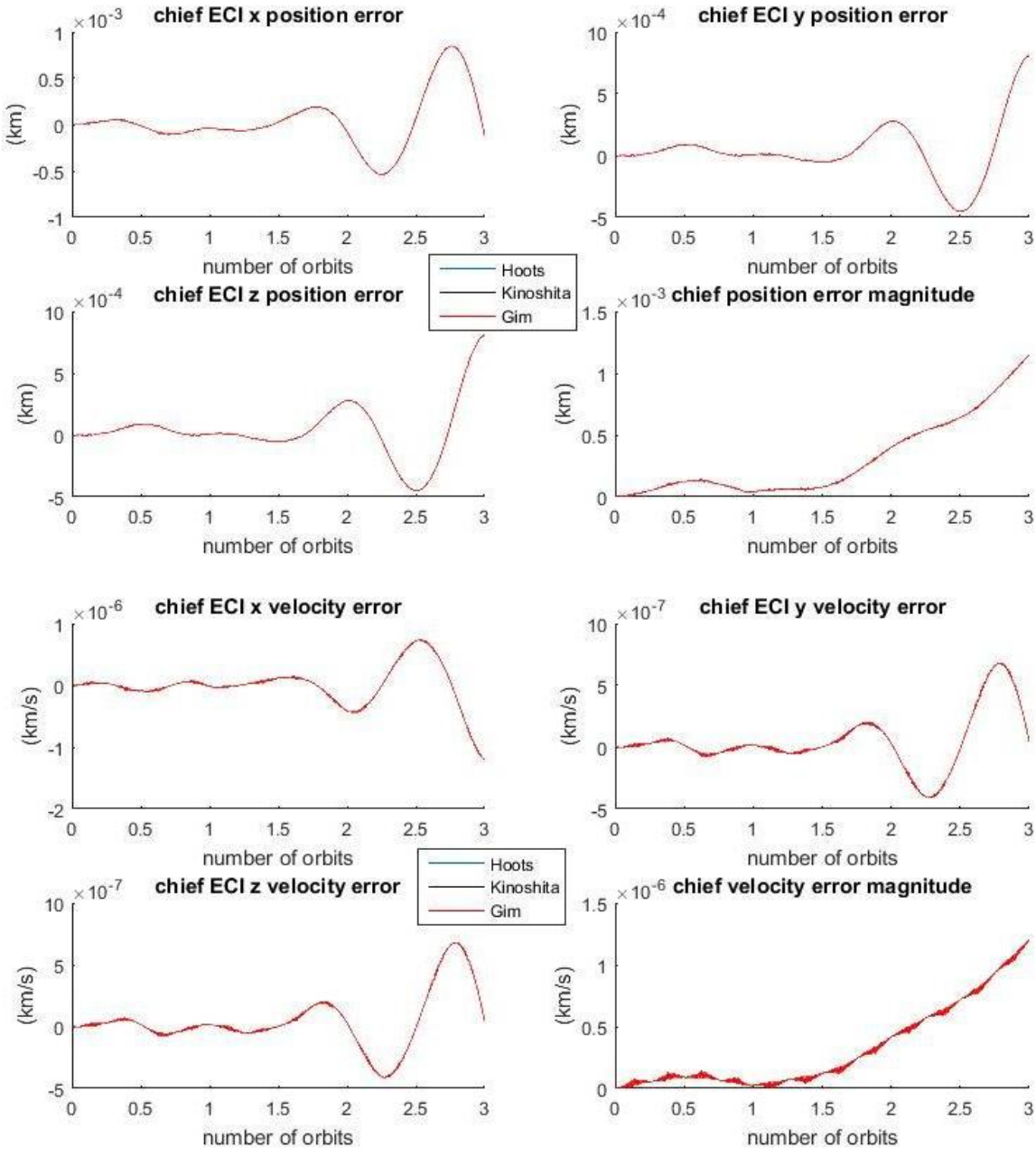


**Figure 6.3: Error with reltol=1e-8**

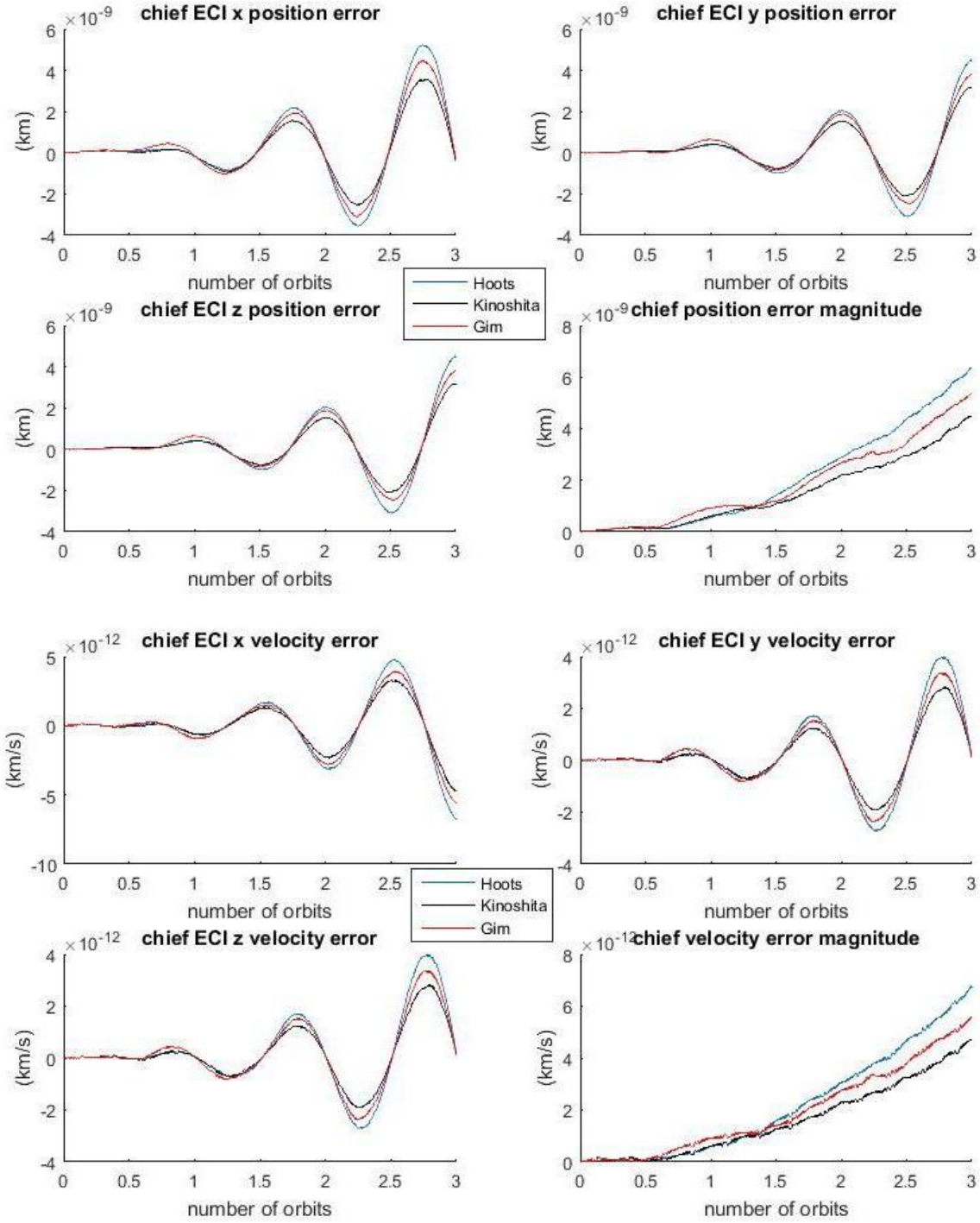


**Figure 6.4: Error: each of 3 analytical models vs. its own corresponding numerical solution**

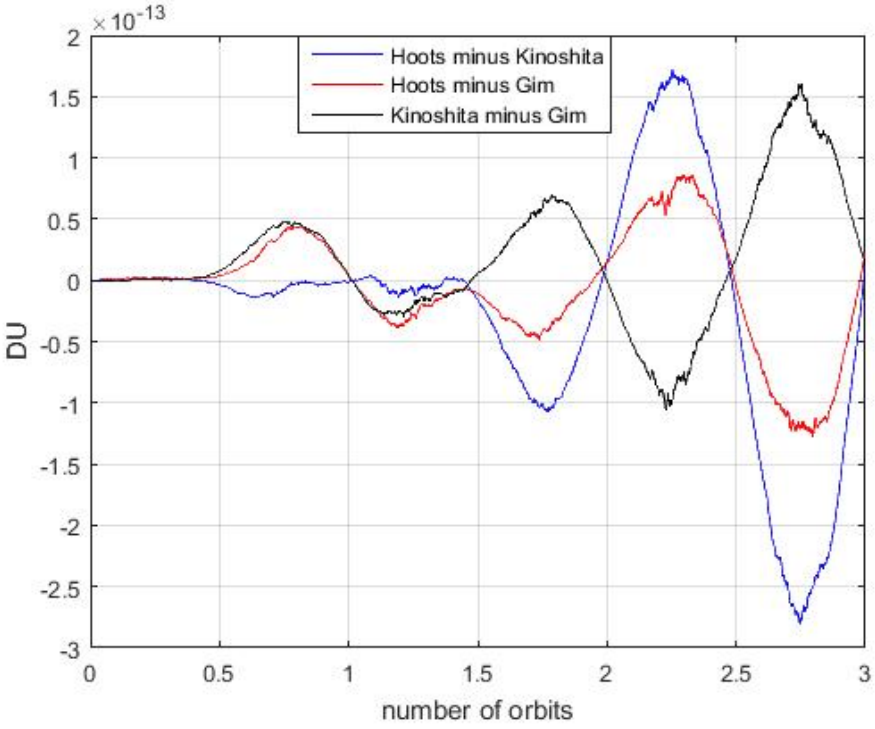


**Figure 6.5: Differences in numerically propagated ECI x-coordinate**

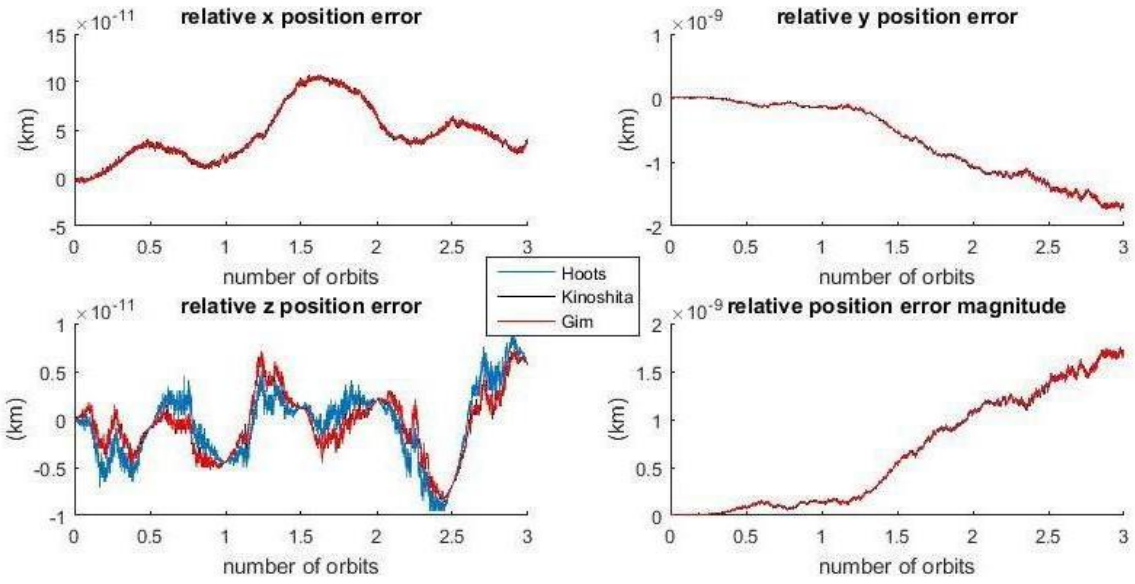


**Figure 6.6: Direct-differencing error: 3 analytical models vs. single numerical solution**

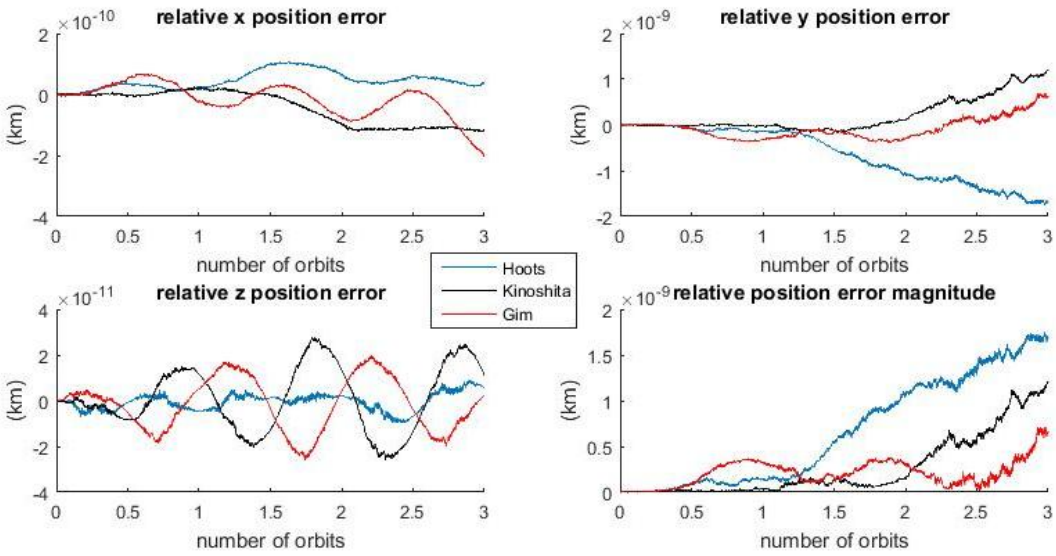


**Figure 6.7: Direct-differencing error: each of 3 analytical models vs. its own corresponding numerical solution**

discussed above. Different chief orbits and different formations lead to different error profiles for STM-based relative trajectories.

For versions of the Gim-Alfriend STM (GA STM) in different variables, the linearization occurs in different variables, and therefore the linearization error can have a different structure, as in the cross-track motion for the case shown in Figure 6.8.

Numerically, these differences in STM-based trajectories manifest through differences in the LVLH initial conditions–that is to say, the STMs themselves are very close at a given time $t$, but $X(t) = \Phi(t, t_0)X(t_0)$ is different for each version of the STM because $X(t_0)$ is different for each version. (Here $\Phi(t, t_0)$ is the GA STM and $X(t)$ is the vector of curvilinear LVLH relative coordinates.) This is evident in Figure 6.8 in the form of a bias, or nonzero mean, for some of the error components. The theoretical explanation for this finding follows:

$X(t_0)$ is the initial condition to be used for the linearized propagation in LVLH coordinates. Therefore, in order to produce accurate results, it must be found via a linearized transformation from the differential orbit elements ($X(t_0) = \Sigma(t_0)\underline{\delta\epsilon}(t_0)$ for element set $\underline{\epsilon}$), rather than via the exact nonlinear transforma-

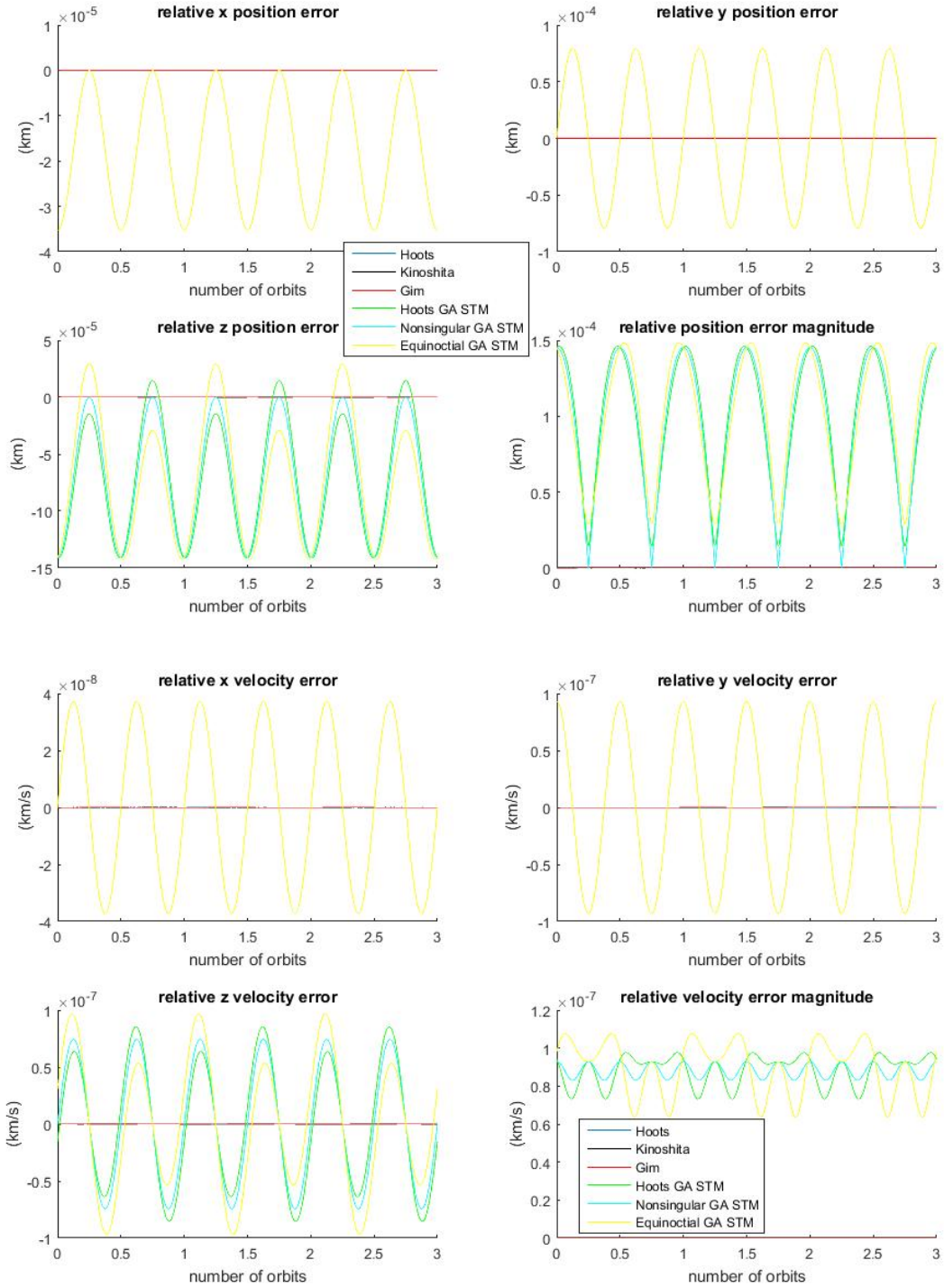


**Figure 6.8: PCO relative error, including STMs**

tion ($\underline{\delta\epsilon}(t_0) \rightarrow X(t_0)$)–that is, the initial conditions for the linearized propagation must be calibrated [47]. It may seem counterintuitive that introducing error to the initial conditions would produce more accurate results, but this was how Gim and Alfriend used the GA STM from the beginning; they pointed out in their results "small initial biased errors as a result of the linearization in the geometric method." [18]

The calibrated initial conditions are only accurate to first order in the formation size–that is, for a PCO, they will differ from "exact" LVLH initial conditions by quantities on the order of $\rho^2/R_e$ in dimensional coordinates. For $\rho$ equal to 1 kilometer, this means the STM-based trajectory will have position error on the order of 15 centimeters (consistent with Figure 6.8).

For this same scenario, the relative velocity vector has a magnitude $v_{rel}$ around 1 meter per second; thus the STM-based trajectory will have velocity error on the order of $v_{rel}^2/v_{ref}$, where $v_{ref} = \sqrt{\mu/R_e}$; this predicted error value is about 1e-7 kilometers per second, also consistent with Figure 6.8. (The expressions for order-of-magnitude error predictions have been derived by squaring the nondimensionalized quantity, and then re-dimensionalizing. The result is always quantity squared, divided by reference value.)

Thus the scale of the linearization error for each STM version is expected to be similar, but the actual error profiles may differ. If we calibrate the initial conditions for each version of the GA STM using its own set of elements and its own elements-to-LVLH map $\Sigma$, then the linearization errors will be different for each one, and we may expect differences among the STM-based trajectories with the same order of magnitude (e.g., 15-centimeter scale for a 1-kilometer PCO formation).

To reinforce the observation that the initial conditions should be calibrated, Figure 6.9 recreates Figure 6.8, but replacing the calibrated initial conditions with "true" initial conditions (specifically, the numerical solutions at $t_0$, mapped into LVLH space using the full nonlinear transformation). Note that the size of the bounded errors has increased several times (up to a factor of 4 for the error in $x$), and the position error now grows secularly, due to unbounded error in $y$. Note also that since all three versions of the GA STM received equal values of $X(t_0)$, their error plots are indistinguishable.

So regardless of the variables chosen, there is a certain base level of linearization error present in any STM-based relative trajectory (assuming the initial conditions are correctly calibrated). But the calibration

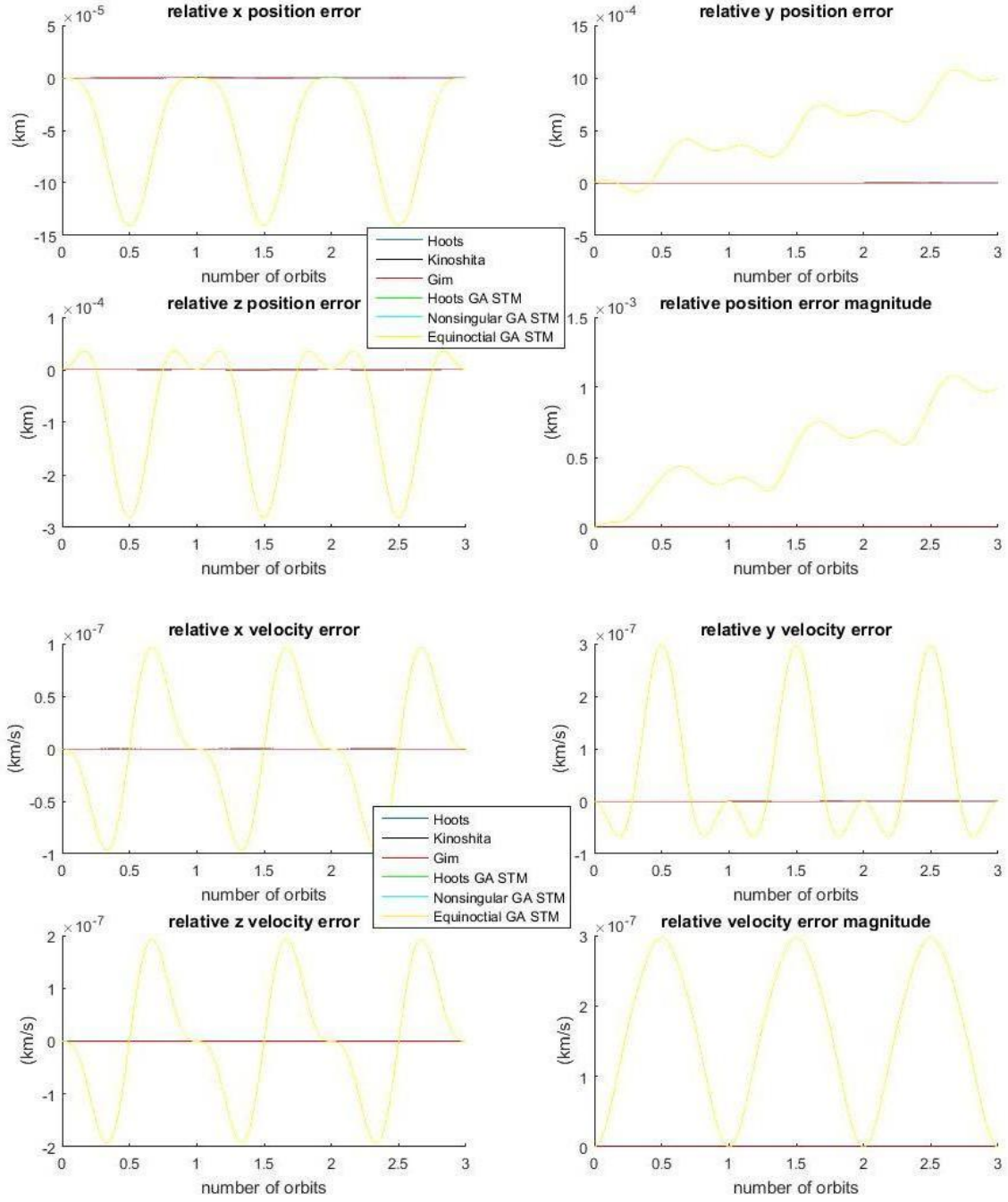


**Figure 6.9: PCO relative error with uncalibrated initial conditions**

itself leads to a slightly different error profile depending on the variables chosen.

## VI.C APPROXIMATE SOLUTIONS TO THE ZONAL PROBLEM

### VI.C.1 Zeroth- and First-order Models

*Osculating Inputs*

All the errors discussed thus far have been present in simulations of the Two-Body Problem. When the Earth's gravitational field is not assumed to be uniform (specifically, when the disturbing potential due to zonal harmonics is considered), then analytical models contain still more error, because they depend on approximate solutions to the motion using perturbation methods. Methods with different levels of fidelity will introduce different degrees of error. In averaging methods such as those used by Brouwer [4] and Kozai [6], it is known that the first-order terms in the generating function are proportional to $J_2/a^{3/2}$, and the second-order $J_2$ terms are proportional to $J_2^2/a^{7/2}$ (where $a$ must be in dimensionless units). Therefore, in single-satellite propagations, solutions that are first-order in $J_2$ should introduce error on the order of $J_2^2/a^{7/2}$. For an orbit with a semi-major axis of 7100 kilometers, this level of error is approximately 8e-7 in dimensionless units, or about 5 meters in distance. This is indeed seen in coordinates that are not subject to drift (such as semi-major axis, eccentricity, inclination, and circular-orbit radius); coordinates that experience drift due to mismatched periods, apsidal rotation, or nodal precession (such as right ascension of the ascending node, argument of perigee, and mean anomaly) can quickly exceed this error scale. See, for example, Figure 6.10, showing the magnitude error for the radius of a satellite in a circular orbit, where the truth model includes the effects of $J_2$ only. See also Figure 6.11, showing the error in each of the osculating classical elements; to avoid the singularity for circular orbits, the eccentricity is set to 0.02.

Likewise, solutions that neglect $J_2$ introduce error on the order of $J_2/a^{3/2}$, which is about 6 kilometers for a semi-major axis of 7100 kilometers. This is seen in Figure 6.12, showing the magnitude error from a two-body analytical model for a circular orbit.

Adding eccentricity changes the error profile, as seen in Figure 6.13, showing the classical element error over ten orbits for an eccentricity of 0.1, using first-order models. This figure shows that some theories

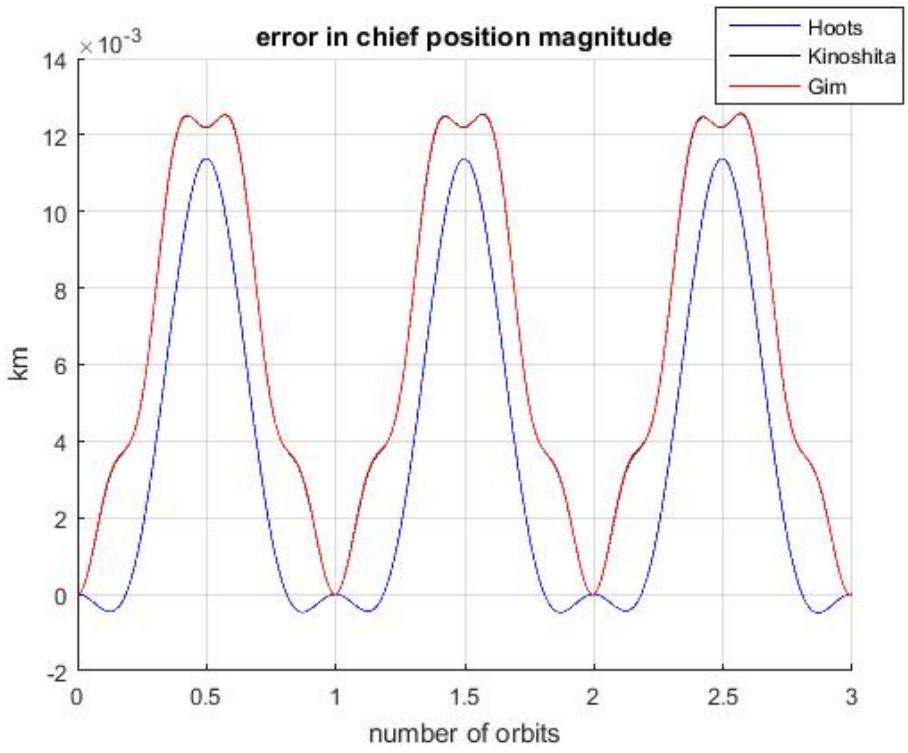


**Figure 6.10: Error in magnitude of chief radius with $J_2$ (first-order models)**

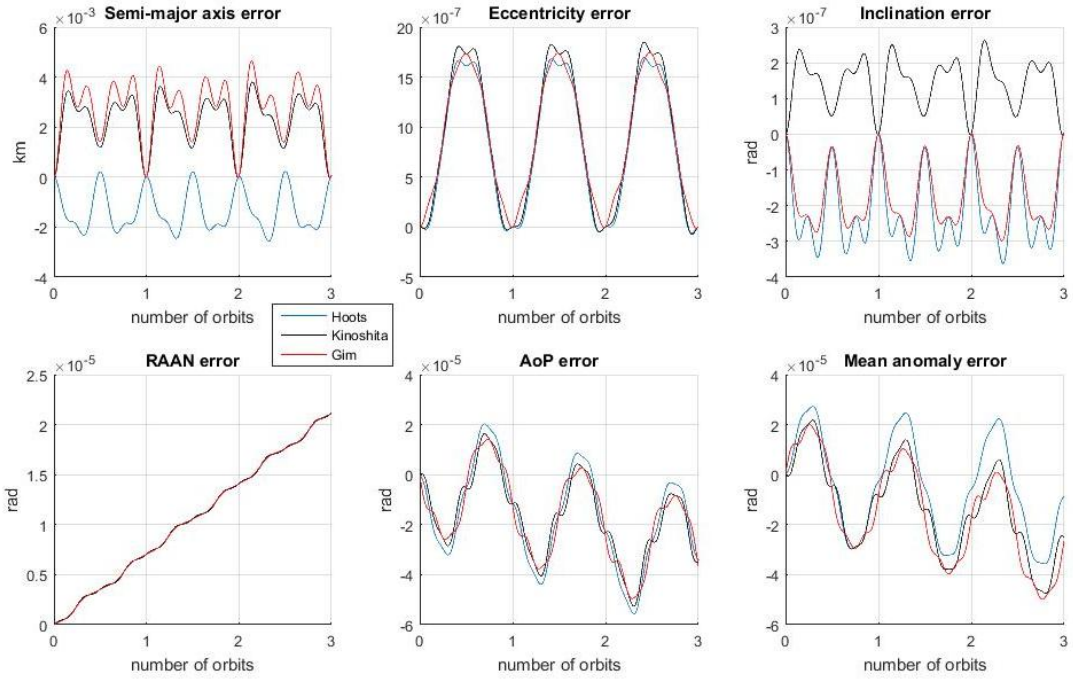


**Figure 6.11: Error in chief's osculating classical elements, $e = 0.02$**

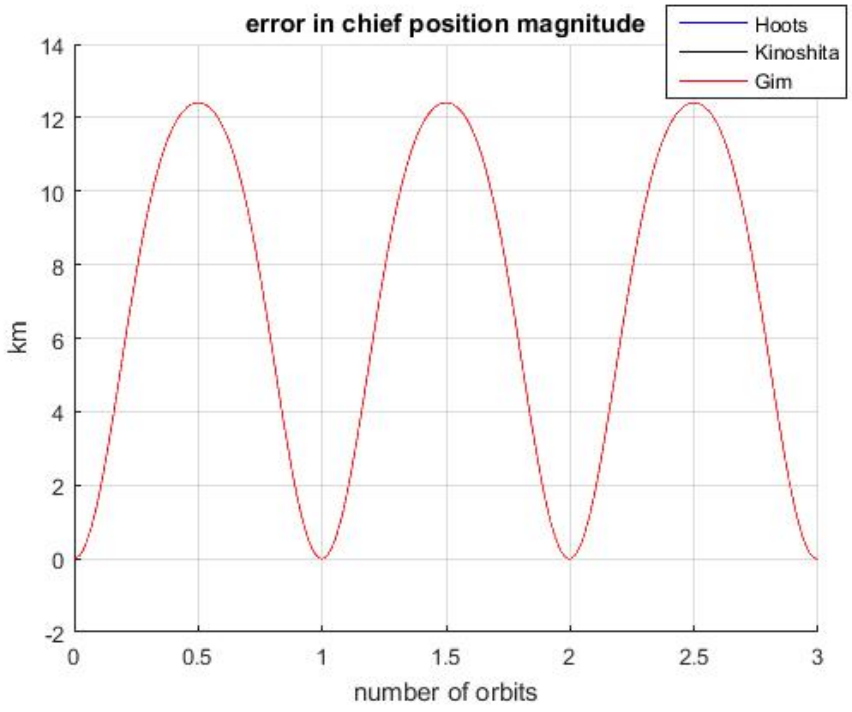


**Figure 6.12: Error in magnitude of chief radius with $J_2$ (zeroth-order model)**

have noticeably lower error than others for certain cases; here this is due to the mean anomaly error growing much more slowly for Hoots theory. This unbounded mean anomaly error causes the corresponding ECI error shown in the lower portion of the figure.

When the simulation's inputs are considered to be osculating initial conditions, then the numerical integration need be performed only once, and each analytical solution can be compared to this single truth model; this was done for Figures 6.10 through 6.13. Most of the error differences are attributable to the osculating-to-mean transformation performed on the initial conditions for each of the analytical models. To show this, Figure 6.13 is repeated in Figure 6.14, but with all three models forced to used the mean initial conditions found via Kinoshita theory–most of the error differences have vanished.

Note that it is not always Hoots theory which provides the best transformation of the initial conditions. If the inclination is changed from 45 degrees to 20 degrees, and the argument of perigee is changed from 0 to 70 degrees, then the errors appear as in Figure 6.15.

These results show that no choice of variables guarantees lower error in single-satellite propagation

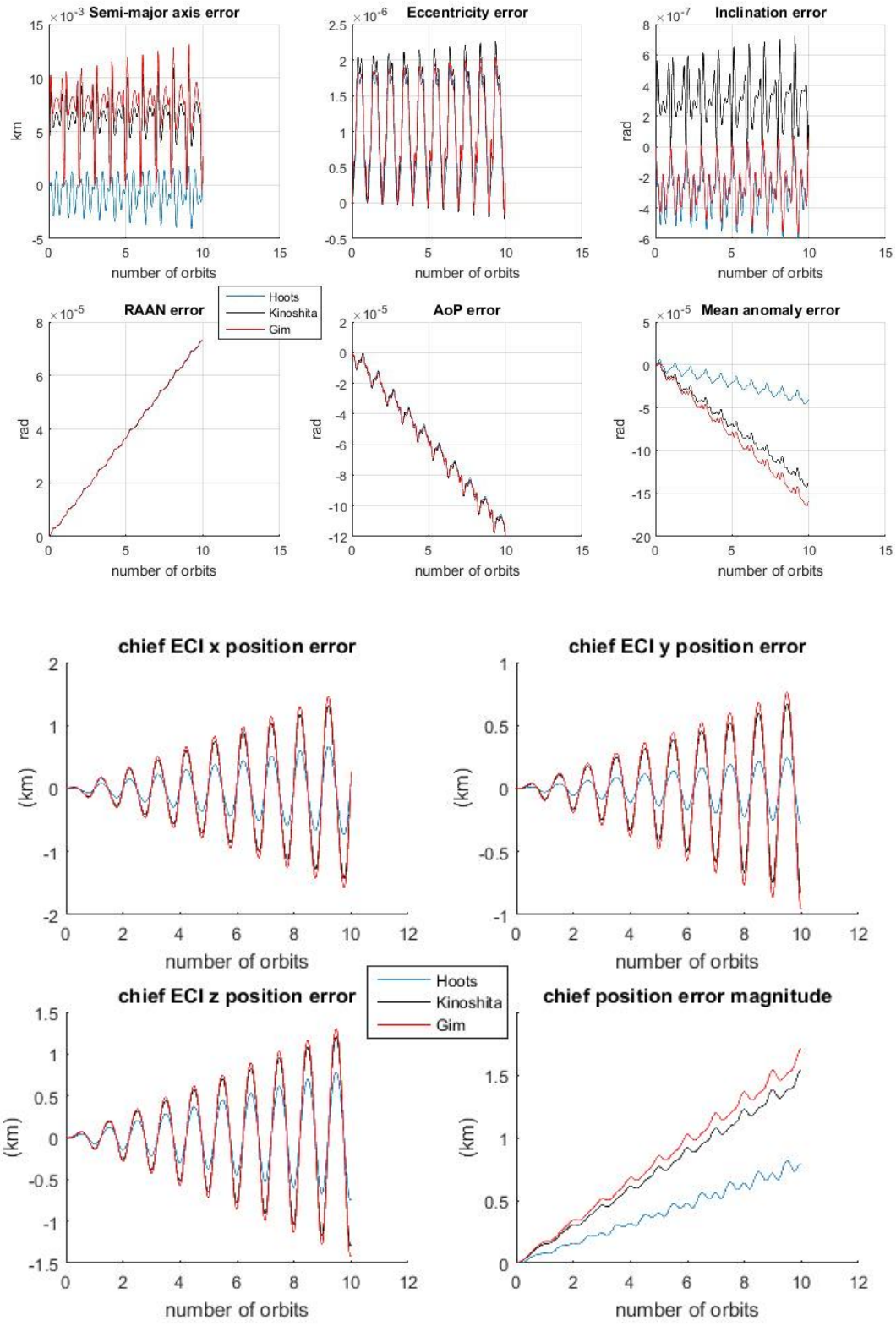


**Figure 6.13: Error in chief's osculating classical elements and ECI coordinates, $e = 0.1$**

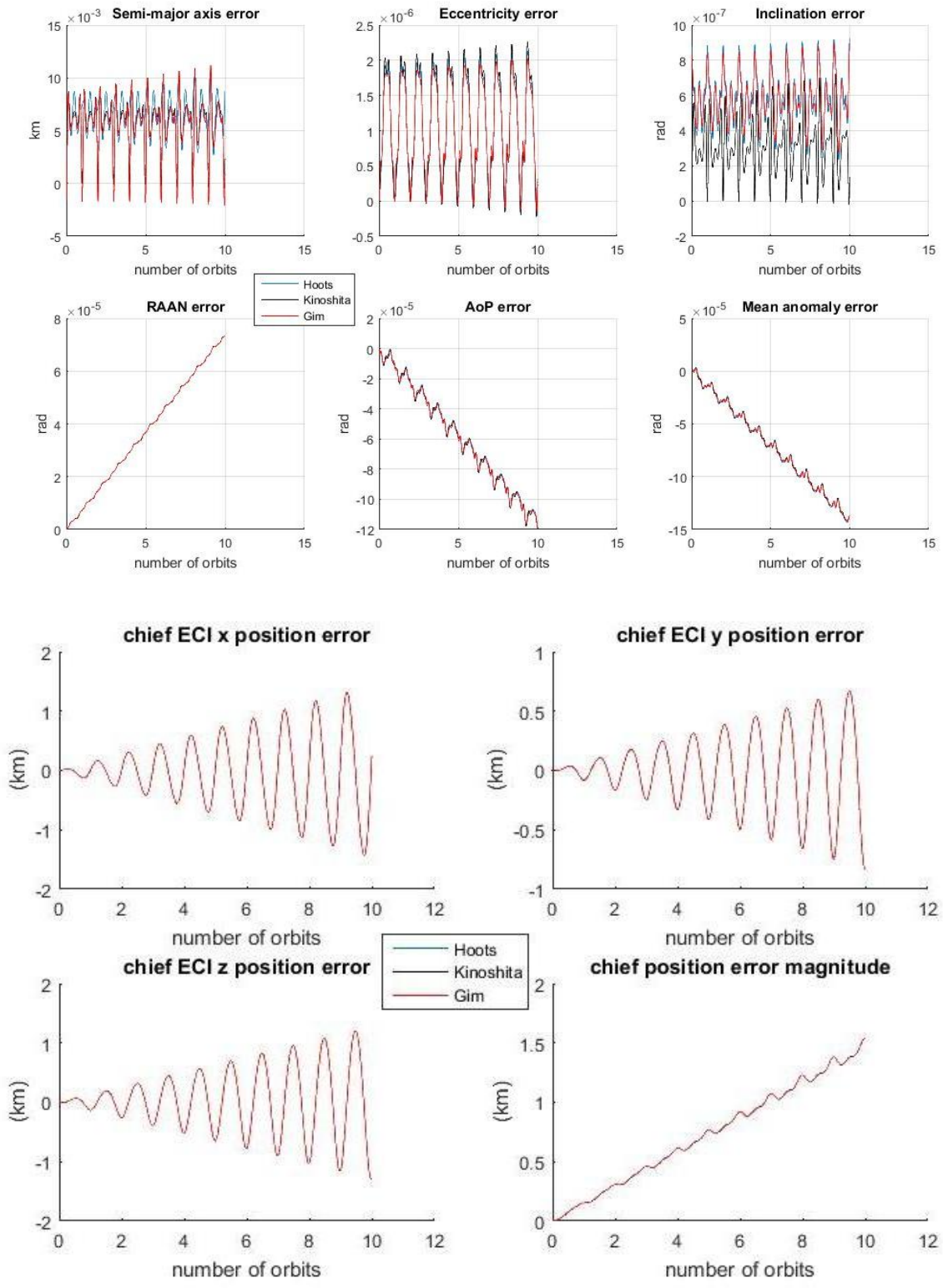


**Figure 6.14: Error with all models using Kinoshita-theory initial conditions, $e = 0.1$**

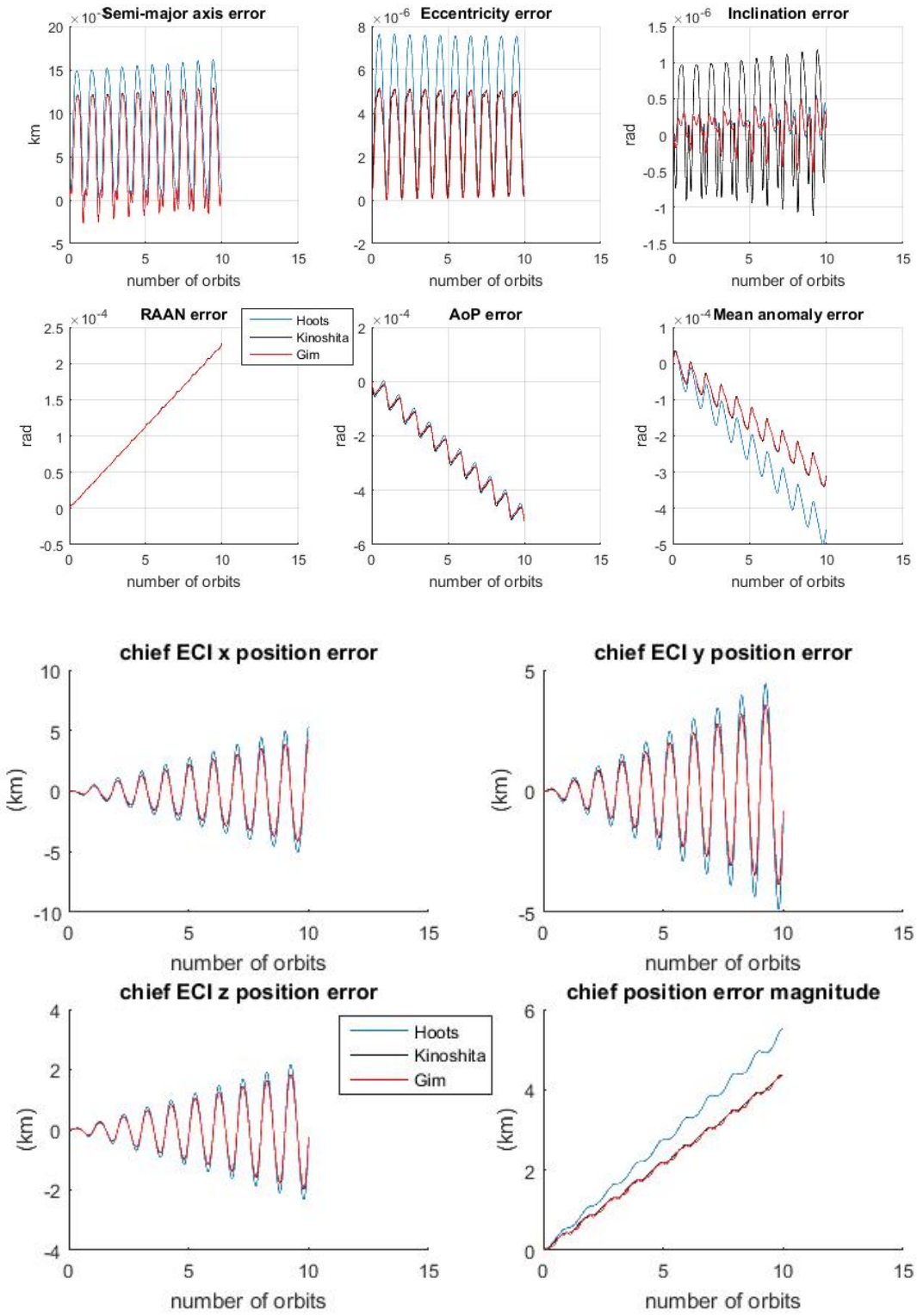


**Figure 6.15: Error in chief's osculating classical elements and ECI coordinates, $i = 20°, g = 70°$**

for all orbits. The error is dominated by a "drift" between the analytical solution and the truth model in those coordinates subject to secular changes; this drift is caused by errors of second order in the initial conditions, due to the approximate nature of the osculating-to-mean corrections. Each theory uses corrections for its own set of variables, and therefore different theories introduce different errors. However, no variable set can be universally superior, because the errors are propagated differently in different orbits.

In a sense, the osculating-to-mean transformation is analogous to the linearizing transformation (or calibration) performed on initial conditions prior to propagation using a linearized model. If the analytical model performs no mean-to-osculating or osculating-to-mean transformations, but simply propagates the osculating initial conditions using the perturbed mean orbit rates, then of course the results will be poor, as shown in Figure 6.16, which simulates the same conditions as in Figure 6.13. Note that only one set of error curves is plotted, since the mean rates are identical for all the analytical theories.

*Mean Inputs*

Alternatively, when the inputs are considered to be mean initial conditions, then a mean-to-osculating transformation must be performed, yielding different osculating initial conditions depending on which perturbation theory is used; thus each analytical model must be compared to its own truth model, with the corresponding set of initial conditions. A first-order transformation still introduces second-order error into the initial conditions; for example, a simulation identical to that which produced Figure 6.13, except that the inputs are taken as mean, produces error plots indistinguishable from Figure 6.13. If the simulation forces all three analytical models to use the same truth model, based on initial conditions computed from Hoots theory, then the results are as shown in Figure 6.17: the error curves are nearly identical for all three models, but their scale has not changed from Figure 6.13.

*Relative Motion*

Some of this error due to neglected zonal harmonic effects is common to both the chief and deputy satellites; therefore in relative-motion propagations, the error is lower. Compare Figure 6.10 to Figure 6.18, which shows the error in the relative separation distance for a PCO formation with a 1-kilometer radius and

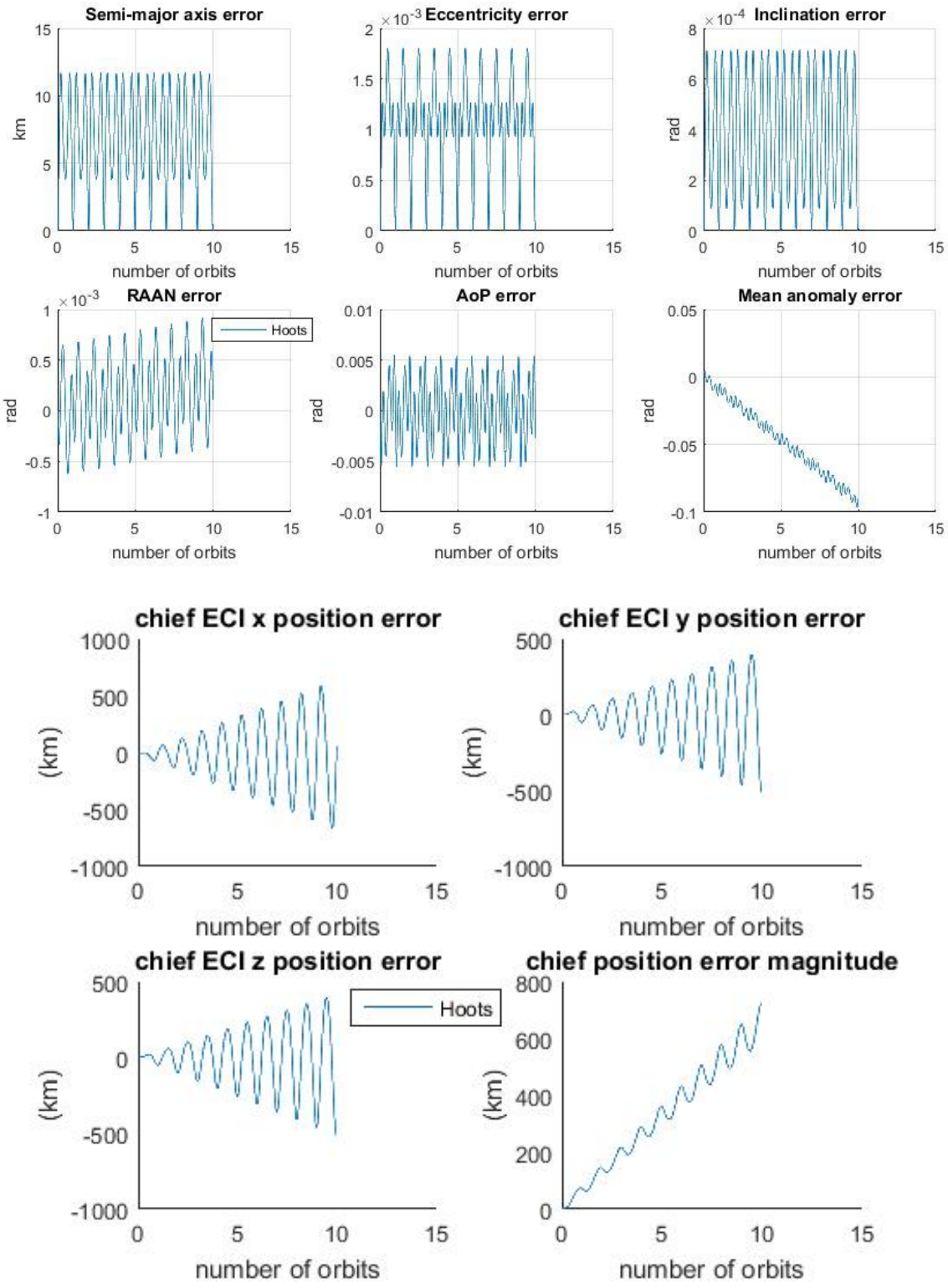


**Figure 6.16: Error without mean-to-osculating transformations**

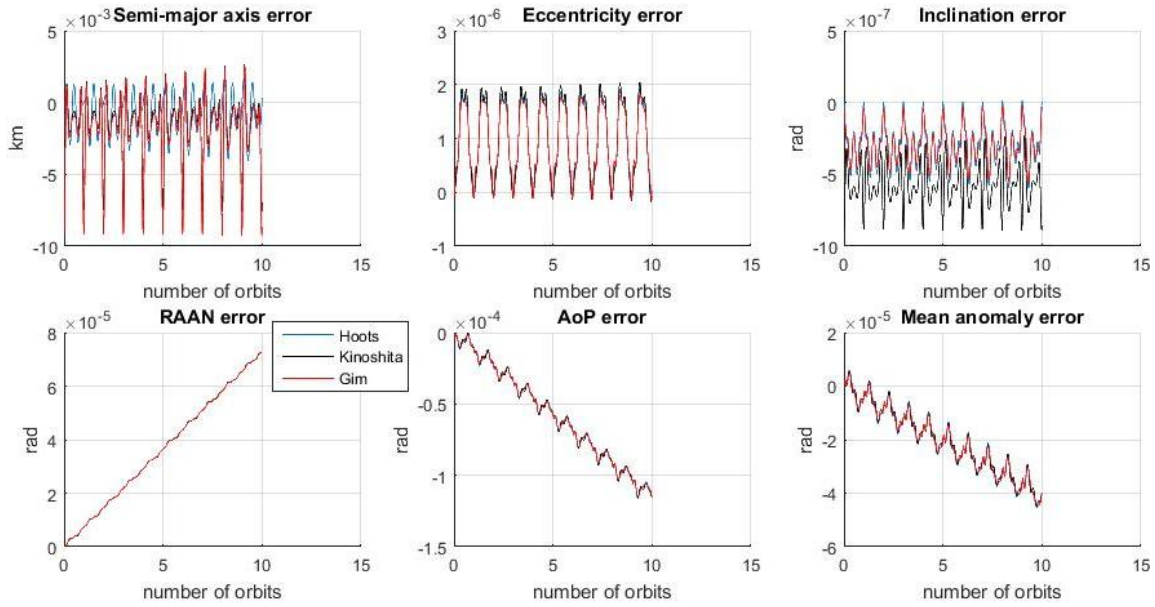


**Figure 6.17: Error in chief's osculating classical elements vs. truth model with Hoots-theory ICs**

a chief in a circular orbit, as predicted by direct differencing. Figure 6.18 also shows the LVLH components of the relative position error for the same formation; note that the error is dominated by along-track drift, which accounts for the secular growth in all the relative error metrics. Over the first orbit, however, the error in the relative separation distance is two orders of magnitude smaller than the corresponding single-satellite error in Figure 6.10.

This perturbed relative error is linear with formation size: see Figure 6.19, which shows the error for a PCO formation with a 10-kilometer radius–the error has also grown by a factor of 10. This linear relationship is expected, as can be shown by a short derivation. In a short-period generating function such as Kozai's [6], the $J_2^2$ term actually has a coefficient of $J_2^2/(a^{7/2}\eta^9)$. Therefore, the error in a first-order direct-differencing relative motion model is

$$\mathcal{O}\left(\frac{J_2^2}{(a+\delta a)^{7/2}(\eta+\delta\eta)^9} - \frac{J_2^2}{a^{7/2}\eta^9}\right)$$

Using binomial expansions for $(a+\delta a)^{-7/2}$ and $(\eta+\delta\eta)^{-9}$, since $\delta a/a$ and $\delta\eta/\eta$ are small, the error is

$$\mathcal{O}\left(\frac{J_2^2}{a^{7/2}\eta^9}\left[-\frac{7}{2}\frac{\delta a}{a} - 9\frac{\delta\eta}{\eta} + \cdots\right]\right)$$

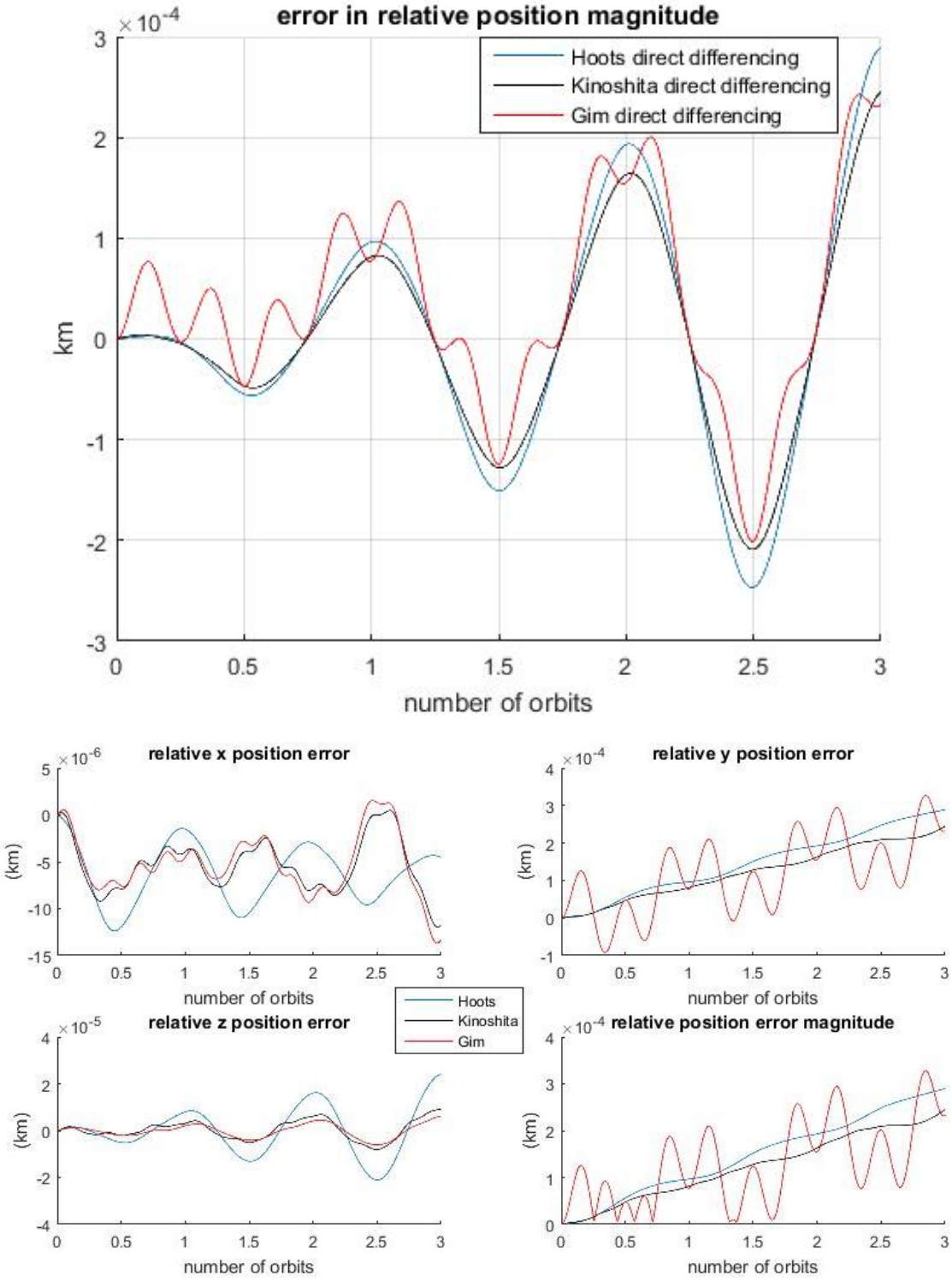


**Figure 6.18: Magnitude and LVLH relative position error, direct differencing**

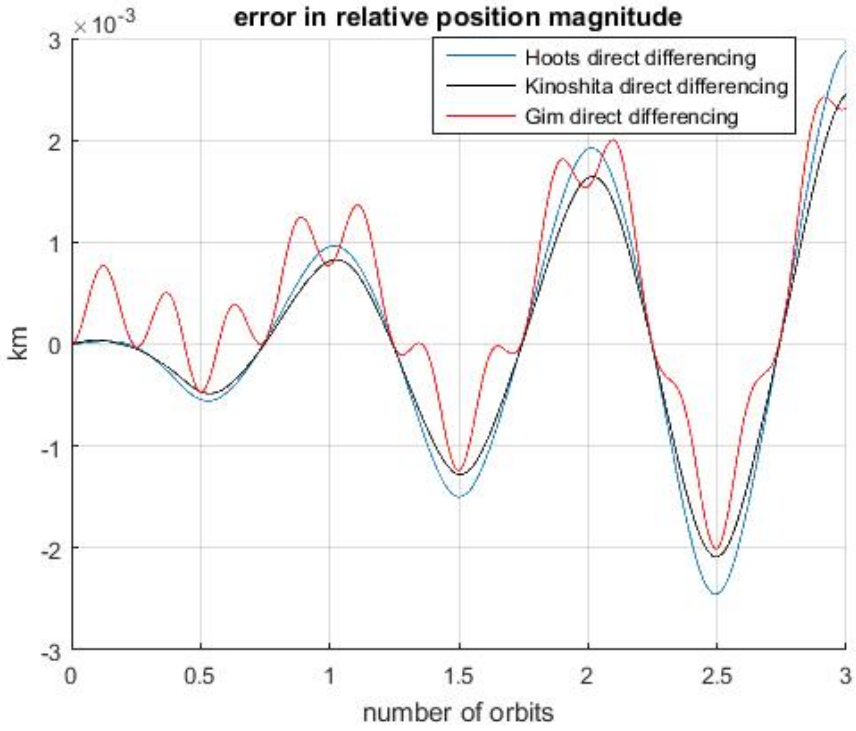


**Figure 6.19: Relative magnitude error, direct differencing, $\rho = 10$ kilometers**

The initial conditions for a PCO either set $\delta a$ to 0, in which case the relative error is proportional to $\delta\eta$, or else use a drift-mitigation condition on $\delta a$, where $\delta a = c_1\,\delta i + c_2\,\delta\eta$, and $c_1$ and $c_2$ are constant functions of the chief's orbit elements. In this latter case, the relative error has one term proportional to $\delta i$ and one proportional to $\delta\eta = -\frac{1}{\eta}\left(q_1\delta q_1 + q_2\delta q_2\right)$. But in these same initial conditions, $\delta i$, $\delta q_1$, and $\delta q_2$ are all proportional to $\rho$ (as in Eq. 3.5). Thus, in the expression giving the order of magnitude of relative error, every term is linearly proportional to $\rho$.

As with the perturbed single-satellite error, considering the inputs as mean initial conditions does not noticeably change the perturbed relative position error; Figure 6.18 would be essentially unchanged with mean inputs. Also like the single-satellite error, simulating with mean inputs but forcing all three analytical theories to use the same numerically integrated truth model produces errors like those in Figure 6.20–the scale of the error is unchanged, but the error differences between theories are smaller. This shows that a portion of the relative error is due to propagating small errors in the initial conditions.

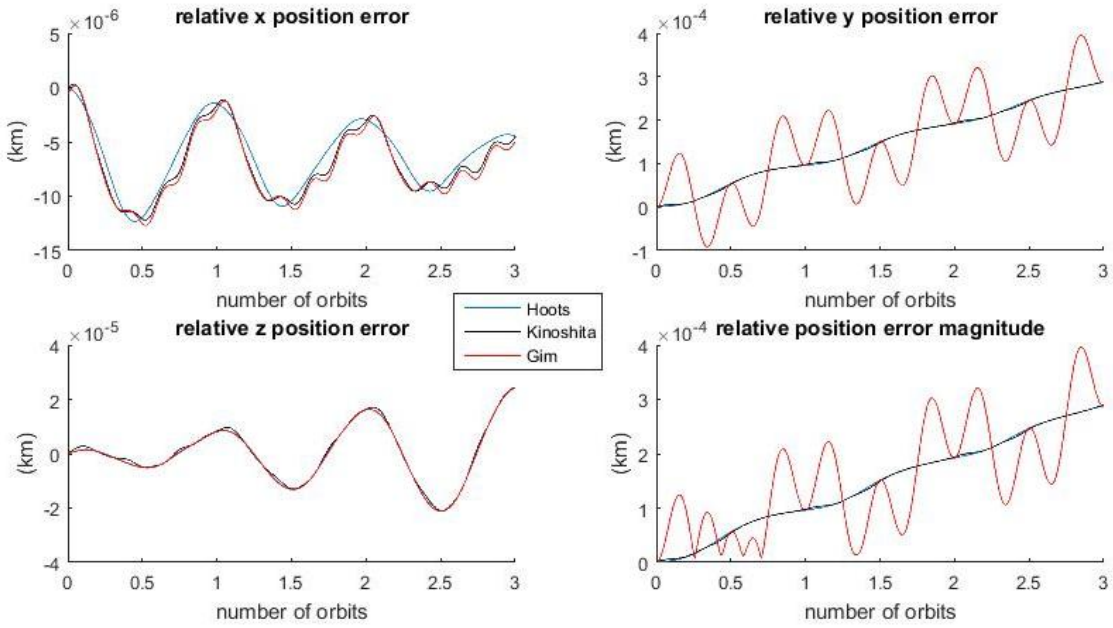


**Figure 6.20: Perturbed direct-differencing error: 3 analytical models vs. single numerical solution**

Including the results from all three versions of the GA STM changes Figure 6.18 to Figure 6.21. For this formation, the STM errors are comparable to the direct-differencing errors. For a 10-kilometer PCO (see Figure 6.22), the direct-differencing errors increase by one order of magnitude, as expected due to the neglected second-order $J_2$ effects; and the STM errors increase by about two orders of magnitude, as expected due to the dominant linearization error.

*Higher Harmonics*

If the simulation accounts for zonal harmonics higher than $J_2$, but the analytical models contain only first-order terms in the mean-to-osculating correction (including short-period terms with $J_2$ and long-period terms with $J_3/J_2$, etc.), then the single satellite errors should still be roughly on the order of $J_2^2/a^{7/2}$. This is indeed shown for first-order Hoots and Kinoshita theory in Figures 6.23 and 6.24; note that the errors here are the same scale as in Figures 6.13 and 6.18. The same is true when $J_5$ and $J_6$ are included, as shown in Figure 6.25 (the relative-motion error plots would show no perceptible difference from the Hoots-theory curves in Figure 6.24).

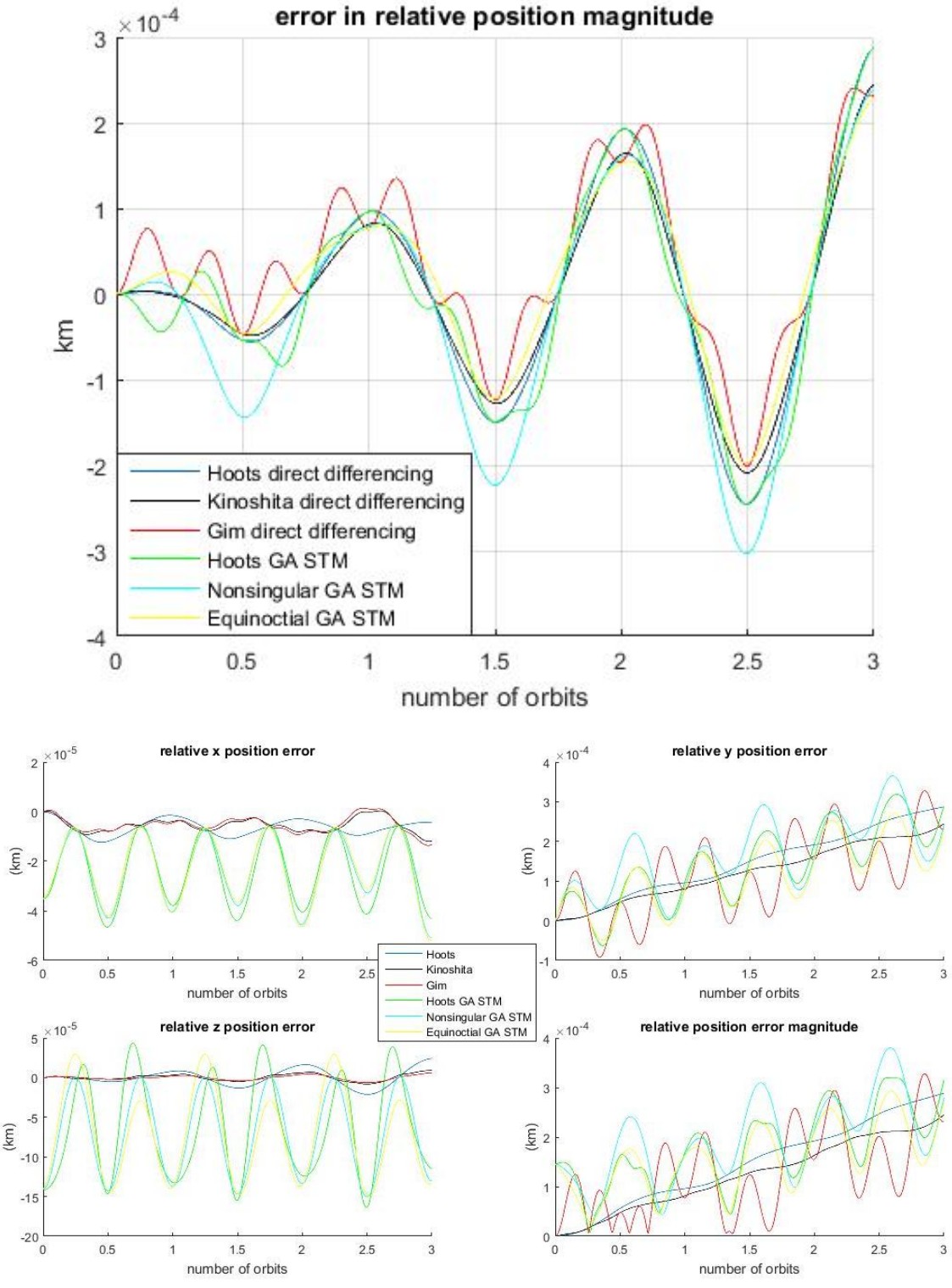


**Figure 6.21: Magnitude and LVLH relative position error, direct differencing and STMs**

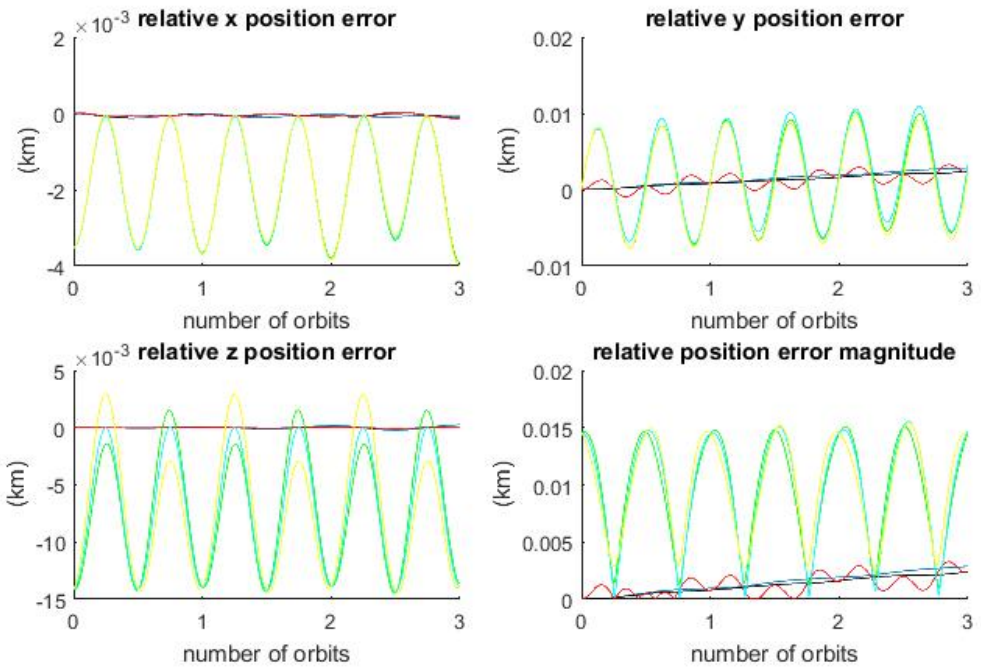


**Figure 6.22: LVLH relative position error, $\rho = 10$ kilometers**

Note that even though Figure 6.23 shows Hoots-theory error as significantly lower than Kinoshita-theory error, this is simply an artifact of how the different initial-condition errors are propagated in this orbit. In another orbit, the effect could be reversed.

### VI.C.2 Second-order Models

In a high-order averaging method solution to the Zonal Problem, the third-order terms of the generating function are proportional to $J_2^3/a^{11/2}$ [11]. Thus, this is the theoretical level of error to expect from a second-order analytical model: for a 7100-kilometer semi-major axis, this is approximately 7e-10 in dimensionless units, or about 4 millimeters in distance. However, since the second-order models used for this study also neglect terms that are second-order in $J_2$ but first-order in $e$, then the actual error seen is on the order of $eJ_2^2/a^{7/2}$. For a 7100-kilometer semi-major axis and an eccentricity of 0.02, this is approximately 2e-8, or about 10 centimeters. This can be seen in Figure 6.26, which recreates Figures 6.10 and 6.11, but with second-order analytical models.

Of course, adding the effects of $J_3$ and $J_4$ increases the error, since the analytical models also neglect

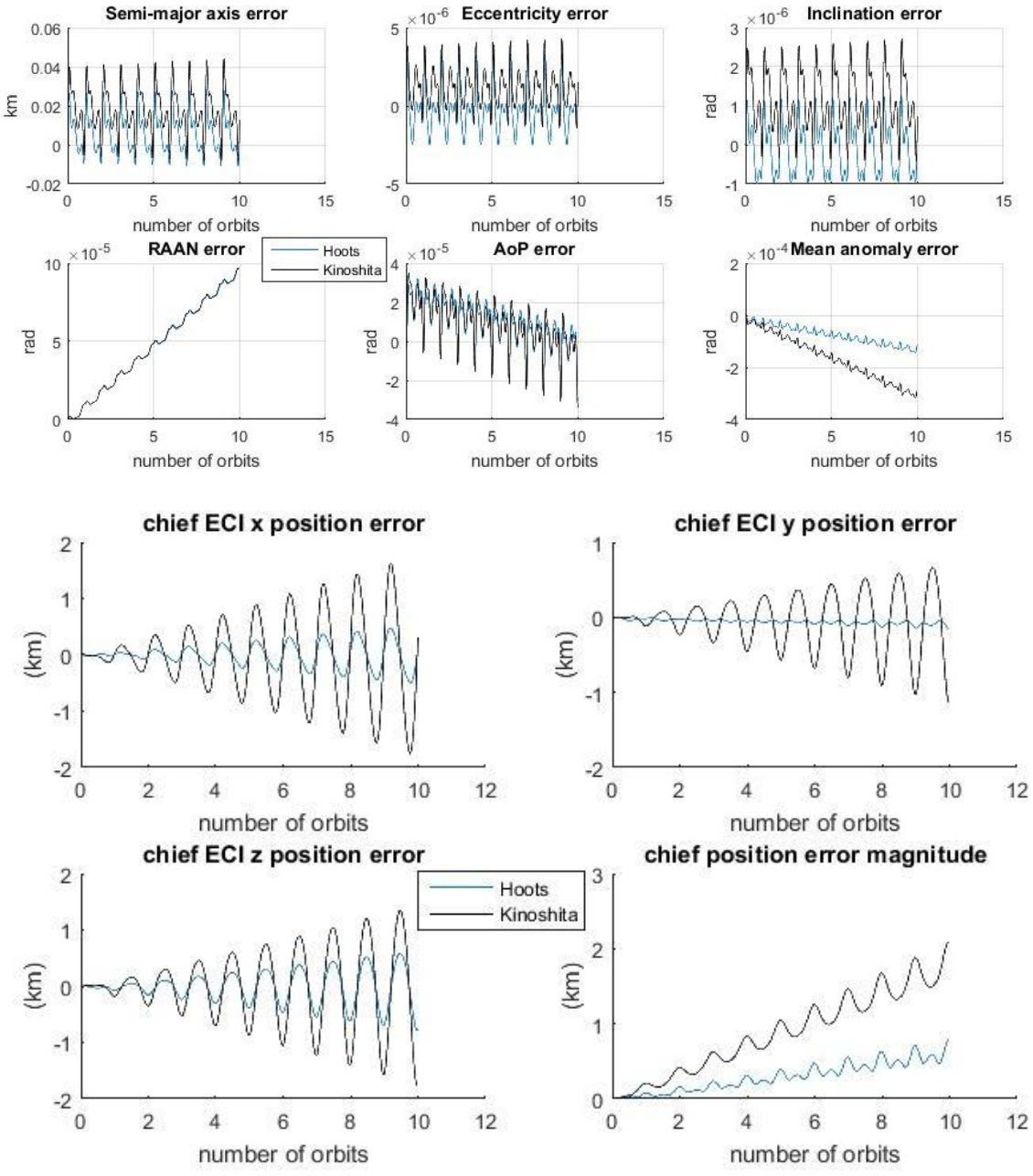


**Figure 6.23: Error in chief's osculating classical elements and ECI coordinates, $e = 0.1$, $J_2$ through $J_4$, first order**

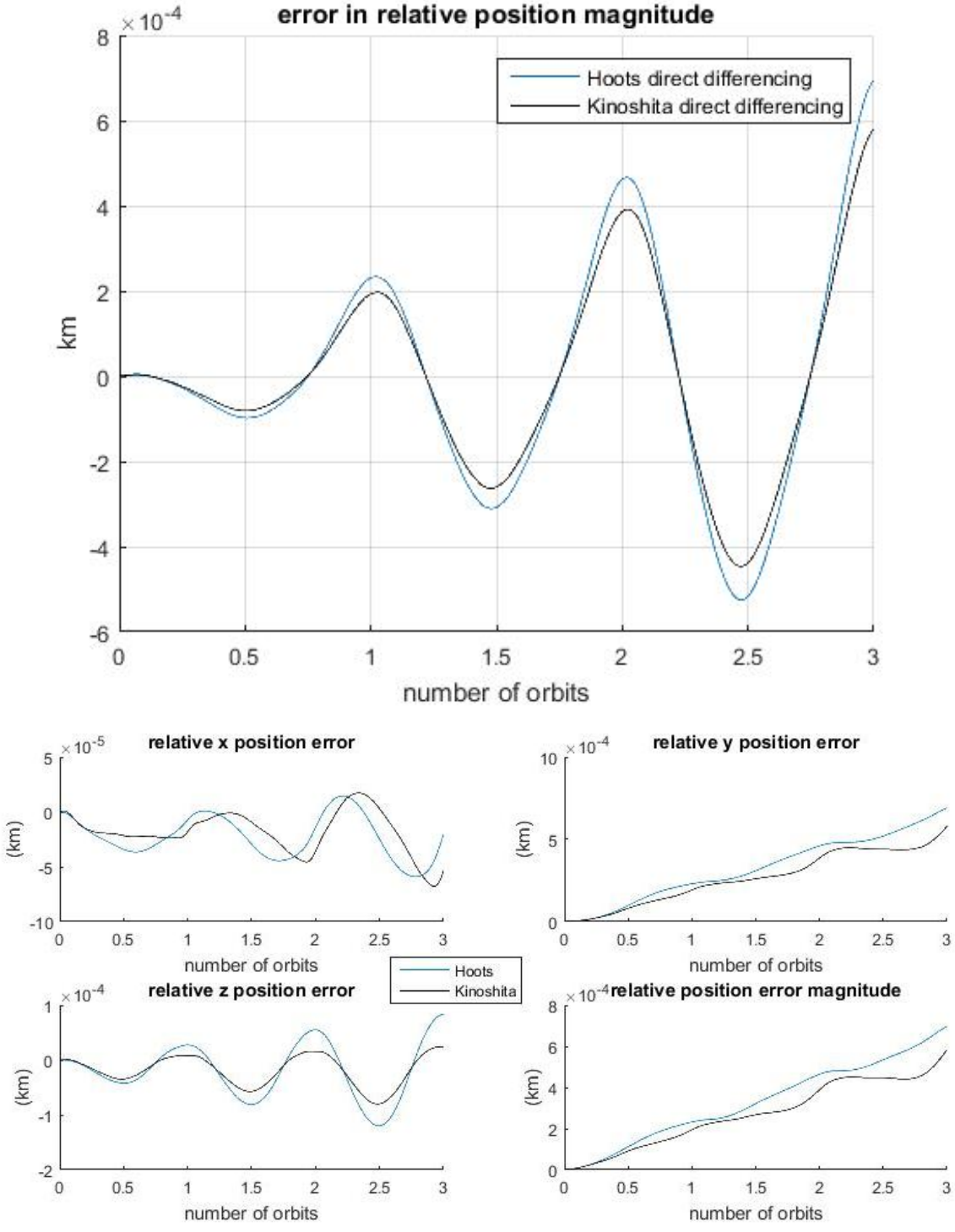


**Figure 6.24: Magnitude and LVLH relative position error, $e = 0.1$, $J_2$ through $J_4$, first order**

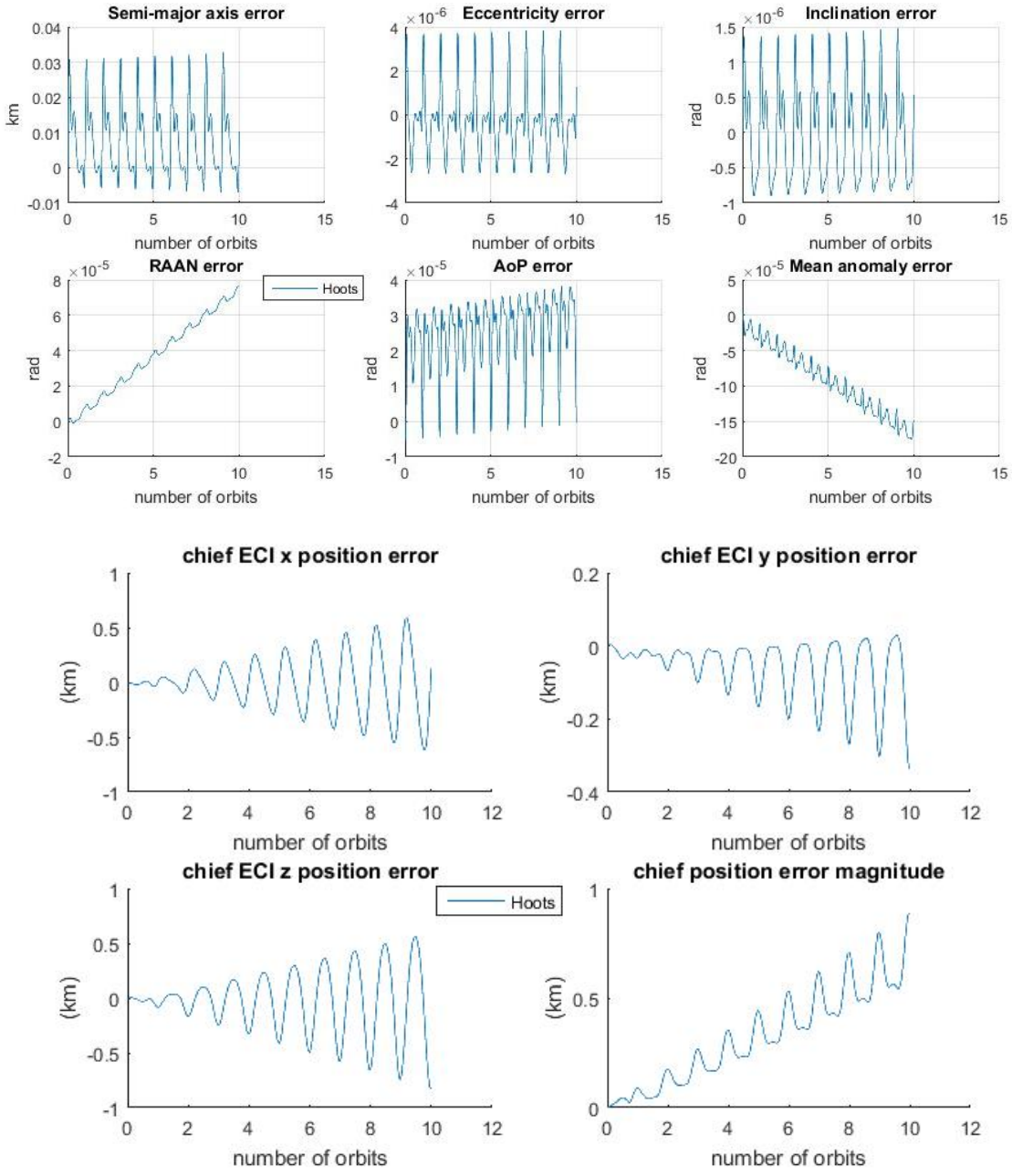


**Figure 6.25: Error in chief's osculating classical elements and ECI coordinates, $e = 0.1$, $J_2$ through $J_6$, first order**

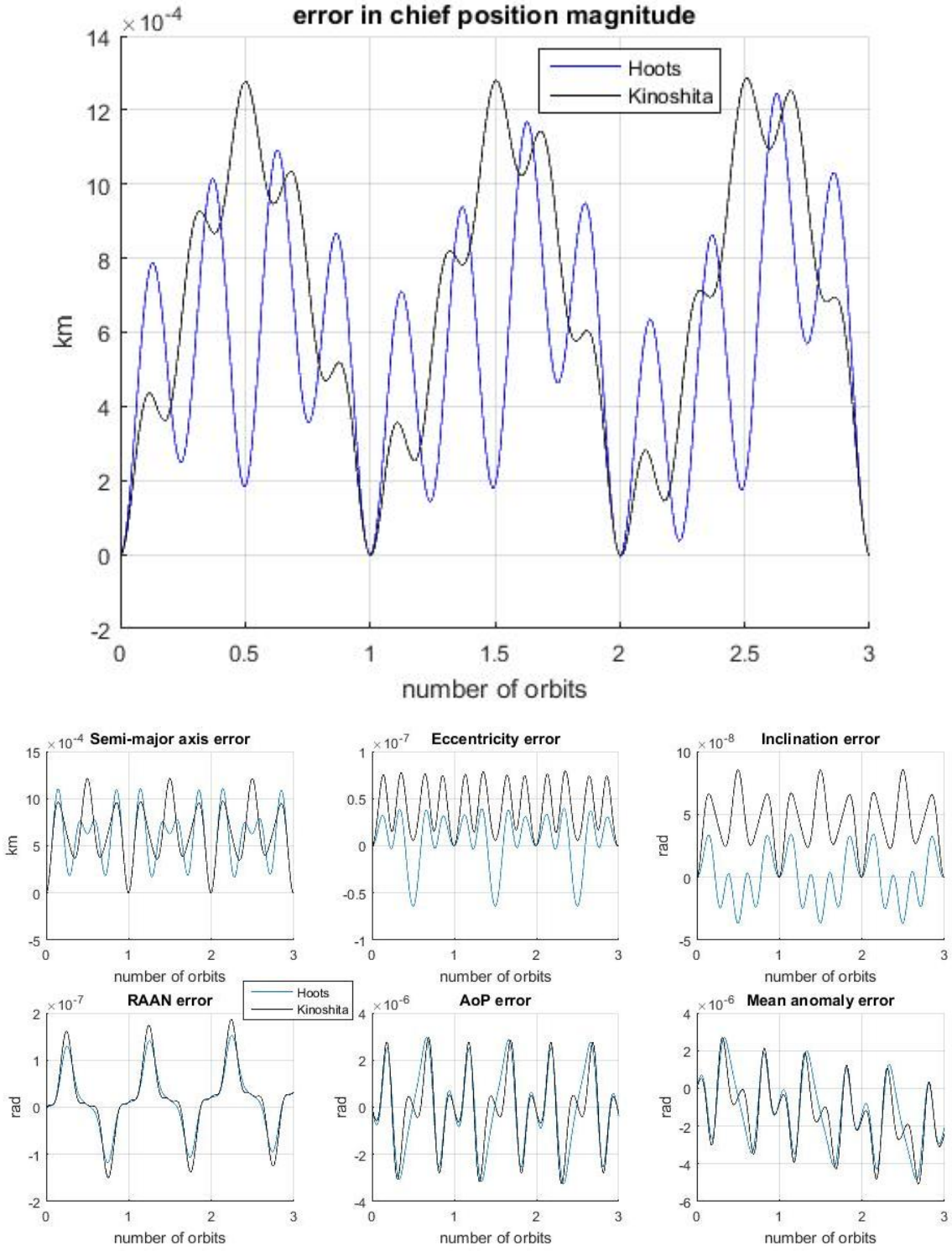


**Figure 6.26: Error in chief's radius and classical elements, $e = 0.02$, $J_2$, second order**

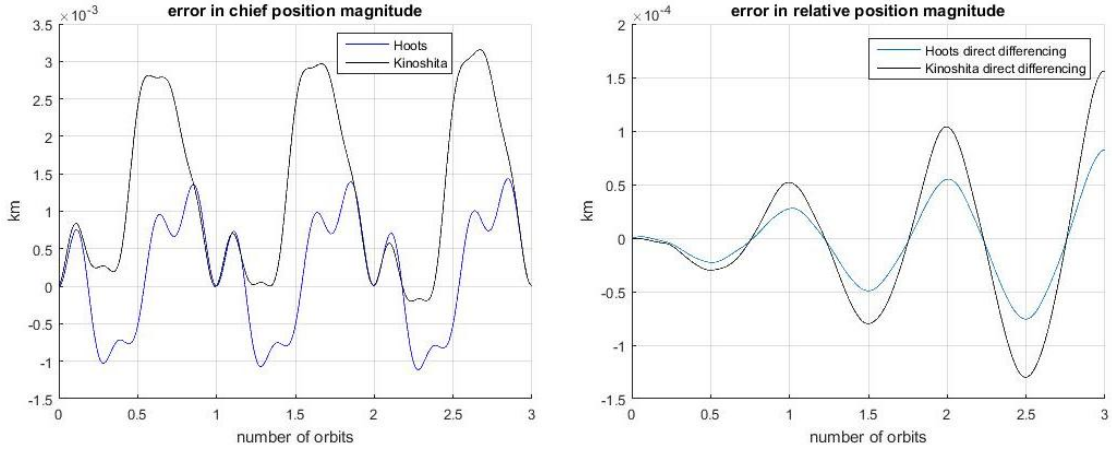


**Figure 6.27: Error in absolute and relative position magnitude, $e = 0.02$, $J_2$ through $J_4$, second order**

terms proportional to $eJ_3$ and $eJ_4$: see Figure 6.27, which recreates the radial error portion of Figure 6.26, but with $J_3$ and $J_4$ added to both analytical and truth models. The second plot in Figure 6.27 shows that the majority of the error is common to both chief and deputy satellites, so that the relative error from direct-differencing is much smaller than the single-satellite error.

## VI.D KEPLER'S EQUATION

One source of error in any analytical satellite theory comes from solving Kepler's Equation numerically, necessary in order to relate time to a satellite's true anomaly. The simulations in this study usually used a solution tolerance of 1.5e-14; anything smaller tended to cause problems with convergence. However, this does not necessarily mean that the resulting error is on the order of 1.5e-14; it depends on the parameters of the problem. In general, the higher the eccentricity, the higher the likely error. However, for tolerances as tight as 1.5e-14, the eccentricity must be extremely high before there is a noticeable increase in error. For three cases of eccentricity, and 500 randomly chosen values of true anomaly for each case, the Kepler Equation solver used in this study produced the errors shown in Figure 6.28.

This study used three different analytical models of satellite motion, with three different sets of variables: Hoots elements, nonsingular elements, and equinoctial elements. Each model required Kepler's

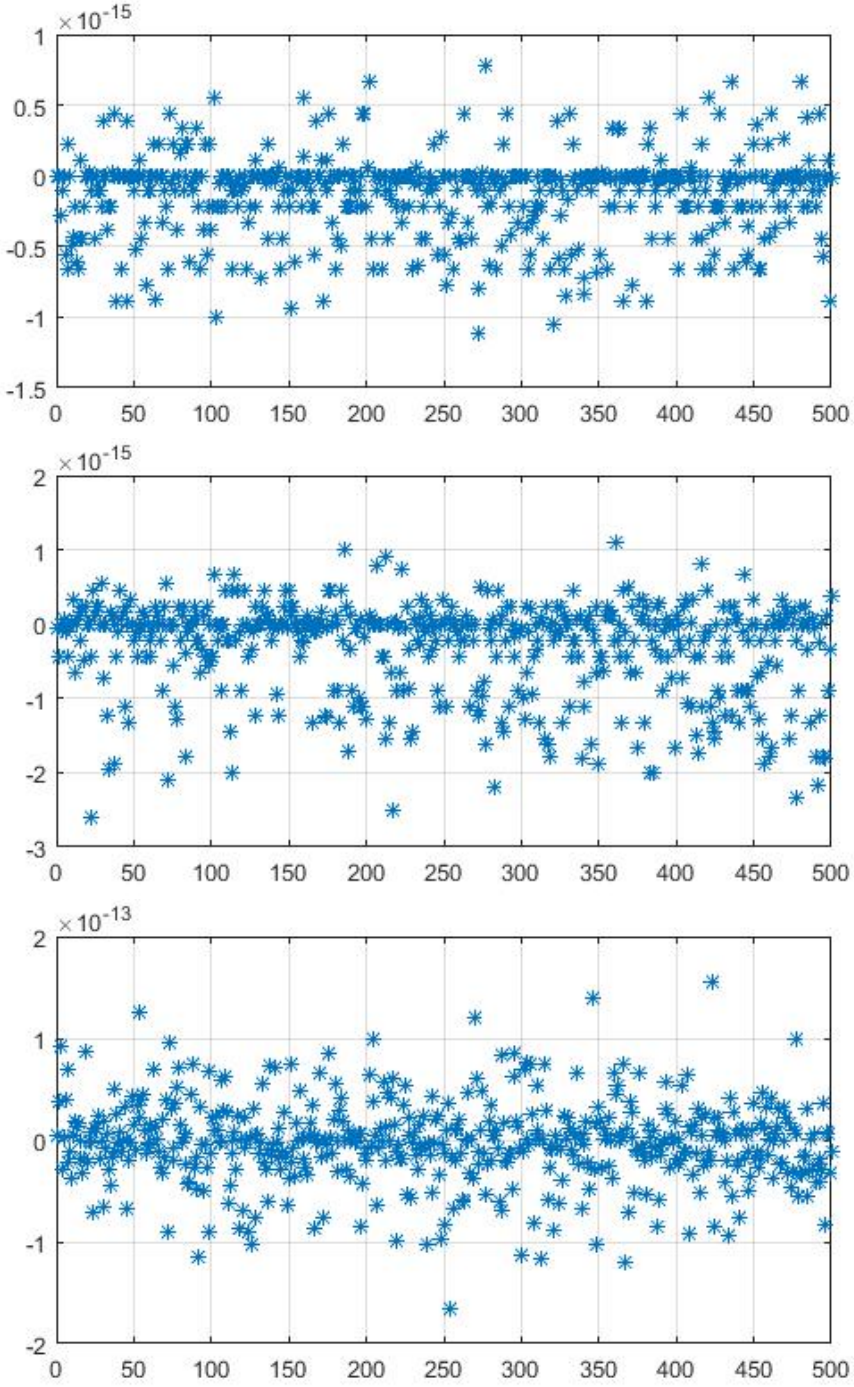


**Figure 6.28: Error from Kepler's Equation (tolerance 1.5e-14). $e = 0.001$ (top), $e = 0.82$ (middle), $e = 0.999$ (bottom)**

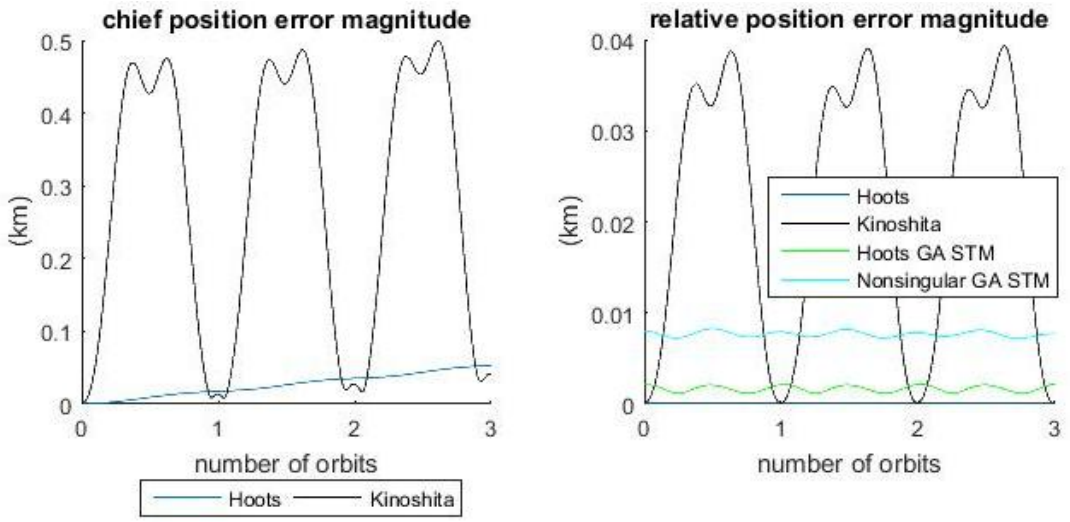


**Figure 6.29: Error from second-order theories and from GA STMs, near equatorial**

Equation to be solved at different times (see Figure 2.1). Theoretically, a greater number of numerical Kepler's Equation solutions could contribute greater error; however, with sufficiently tight tolerances, the error is significantly smaller than third order in $J_2$, and therefore not noticeable. The primary advantage of avoiding additional Kepler's Equation solutions, therefore, is computational cost, not accuracy.

## VI.E SINGULARITIES

Of course, simulating conditions at or near a singularity for one of the element sets will cause numerical problems. For example, Kinoshita theory and the nonsingular-elements version of the GA STM are both singular for zero inclination. For two-body simulations, these models fail for inclinations of 6e-7 degrees or less; in simulations of the Zonal Problem, there are inclination values which are not small enough to cause the models to fail, but are small enough to cause significant numerical inaccuracy. For example, see the errors in Figure 6.29, a simulation with $J_2$-$J_4$, osculating inputs, second-order analytical models, and a chief inclination of 0.9 degrees. In this figure, the models which use the "nonsingular" elements have significantly higher error.

# CHAPTER VII

# COMPARISON OF MODEL RESULTS

This study's goals for an analytic theory are to preserve the simplicity and computational efficiency of Hoots theory, and to increase accuracy by extending the theory to more zonal harmonics and higher-order approximation.

This chapter includes MATLAB simulations of three kinds: single-satellite orbit propagations (computed either numerically or via an analytical theory, such as the extended Hoots theory in Eqs. 2.4 and 2.5), relative motion trajectories computed from the Hoots-element version of the GA STM, Eq. 4.1, and relative motion trajectories computed by direct differencing. The direct differencing method computes the absolute motion of a chief and deputy satellite via single-satellite propagation, differences these trajectories numerically, and then maps the differences into relative space. Computing the relative trajectory this way forms a rough lower bound on the error for closed-form relative motion approximations. The numerical and direct-differencing results, as well as the initial conditions for the STM, are all transformed from orthogonal to curvilinear LVLH coordinates.

The STM is derived from a theory that is first order in $J_2$, but its elements depend on the chief satellite's motion, which can be computed using different physics–for example, a second-order theory. In practice, the chief's properties could be obtained from a precise orbit determination, rather than an analytical model. For example, a chief satellite in LEO may use a GPS navigation system to determine its own osculating orbit elements, and then use that information to populate the STM for a deputy satellite's relative motion.

The error in each analytic theory error is found by differencing with the corresponding numerically integrated truth trajectory, just as in Chapter VI. In the plots below, the extended Hoots theory (where the mean-to-osculating transformation occurs in Hoots-element space) is compared against the alternate perturbation theories labeled "Kinoshita" (using the so-called nonsingular elements) and "Gim" (using equinoctial elements)–see the descriptions in Chapter II. These comparisons are depicted graphically by showing four

different metrics as a function of time: position and velocity error norms for both chief satellite absolute position and deputy satellite relative position.

In the subsequent relative-motion plots, the GA STM results are compared with direct-differencing results in similar graphical comparisons.

## VII.A COMPARISONS OF FIRST- AND SECOND-ORDER MODELS

The plots in this section are chosen to illustrate representative results. Unless otherwise stated, each plot uses the following simulation parameters:

- Inputs are considered to be osculating initial conditions
- 8 chief orbits
- Near-PCO formation[1]: relative orbit size 1 km, initial deputy phase angle 0
- Chief initial conditions: semi-major axis 7100 km, $e = 0.01$, $g = 0$, $h = 0$, mean anomaly $0$, inclination 50 degrees

The first pair of figures (Figures 7.1 and 7.2) illustrates the importance of including in an orbit theory the first-order long-period correction terms due to higher harmonics, of the kind derived in Chapter II for the nonsingular-elements theory. In both of these figures, the truth model accounts for harmonics through $J_4$, the analytical models are first-order, and the relative motion results are from direct differencing. In Figure 7.2, the Hoots and Kinoshita orbit theories include the $J_3$ and $J_4$ long-period terms, but in Figure 7.1, they do not. In each case, the error curves with $J_3$ and $J_4$ are lower than those without.

Figure 7.3 illustrates the importance of the second-order correction terms derived in Chapter II for Hoots theory. The error curves are all much smaller than in Figure 7.2, although the only change was adding second-order terms to the analytical models.

[1]The zero-drift constraint on $\delta a$ is turned off.

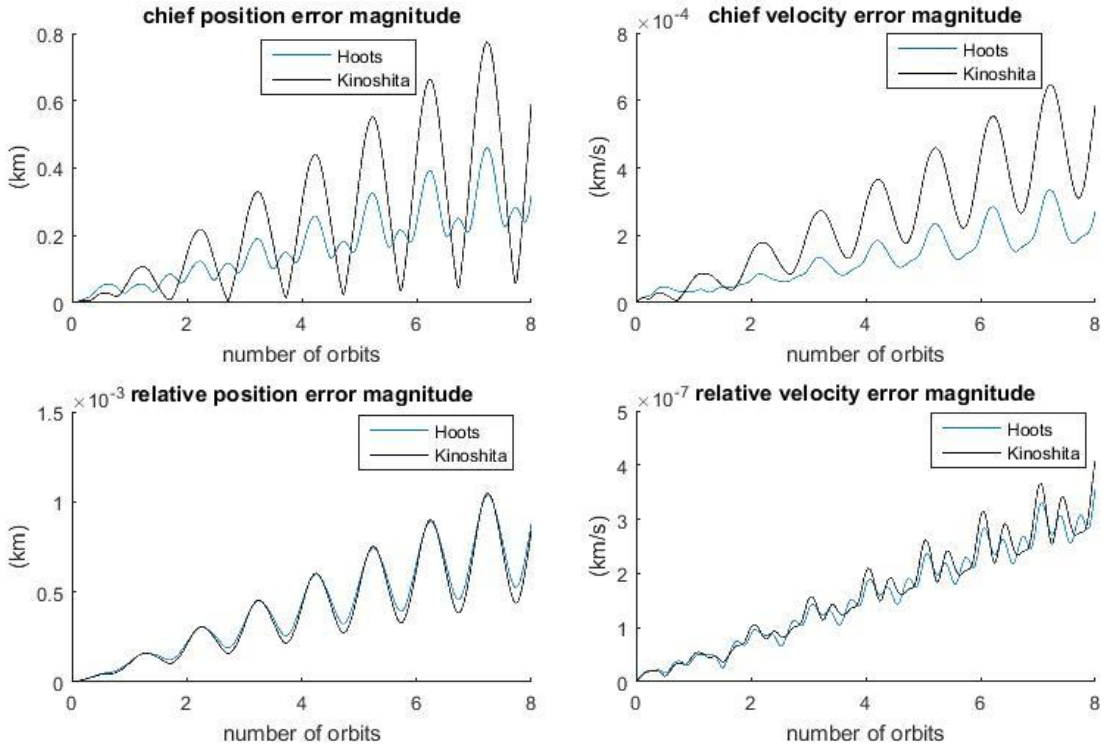


**Figure 7.1: First-order theory: truth model through $J_4$, analytical model $J_2$ only**

## VII.B COMPARISONS OF GA STM USING HOOTS, NONSINGULAR, AND EQUINOCTIAL ELEMENTS

In Figure 7.4, the analytical models shown include direct differencing of the absolute-motion results from Hoots and Kinoshita theory, as well as relative motion computed from the Hoots-elements version of the GA STM. Both numerical and analytical models consider $J_2$ as the only perturbation, and the given initial conditions are considered as osculating elements. The chief and deputy orbit parameters are the same as in the previous section. In this scenario, the GA STM shows error characteristics competitive with the direct differencing models.

The new version can also be compared against previous versions of the GA STM formulated in terms of nonsingular elements and equinoctial elements. Figure 7.5 shows results from a chief satellite in a near-circular low-Earth orbit like that illustrated in Chapter 5 of Reference [19]; the LVLH components and the magnitude of the relative position error over one day are shown for all three STMs, as well as for

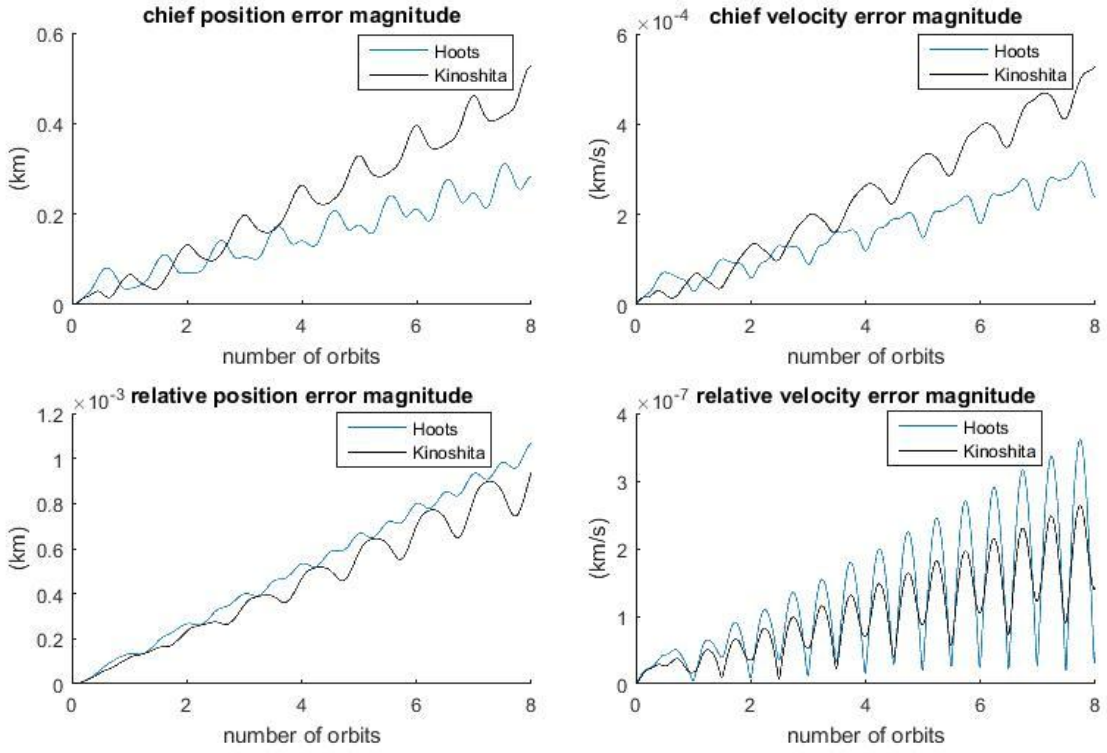


**Figure 7.2: First-order theory: truth model and analytical model through $J_4$**

all three versions of direct differencing. The truth model includes zonal harmonics through $J_5$, but each analytical model includes first-order $J_2$ only. The chief has the following initial osculating elements: $a$ is 7100 kilometers, $u$ is 170 degrees, $i$ is 70 degrees, $q_1$ is 4.698e-3, $q_2$ is 1.710e-3, and $h$ is 45 degrees. The differential nonsingular elements are as follows: $\delta a$ is -1.299 meters, $\delta u$ is 3.761e-3 degrees, $\delta i$ is -3.991e-3 degrees, $\delta q_1$ is 6.347e-6, $\delta q_2$ is 3.492e-5, and $\delta h$ is 7.489e-4 degrees. As the figure shows, for this case, the STM errors are not significantly greater than those for direct differencing.

The eccentric low-Earth orbit scenario from Reference [19] is recreated in Figure 7.6. Here, the chief has the following initial osculating elements: $a$ is 8500 kilometers, $u$ is 170 degrees, $i$ is 70 degrees, $q_1$ is 9.397e-2, $q_2$ is 3.420e-2, and $h$ is 45 degrees. The differential nonsingular elements are as follows: $\delta a$ is -103.624 meters, $\delta u$ is -1.104e-3 degrees, $\delta i$ is 7.076e-4 degrees, $\delta q_1$ is 4.262e-5, $\delta q_2$ is 9.708e-6, and $\delta h$ is 3.227e-3 degrees. In this one-day simulation, the STMs perform slightly worse than the direct differencing models.

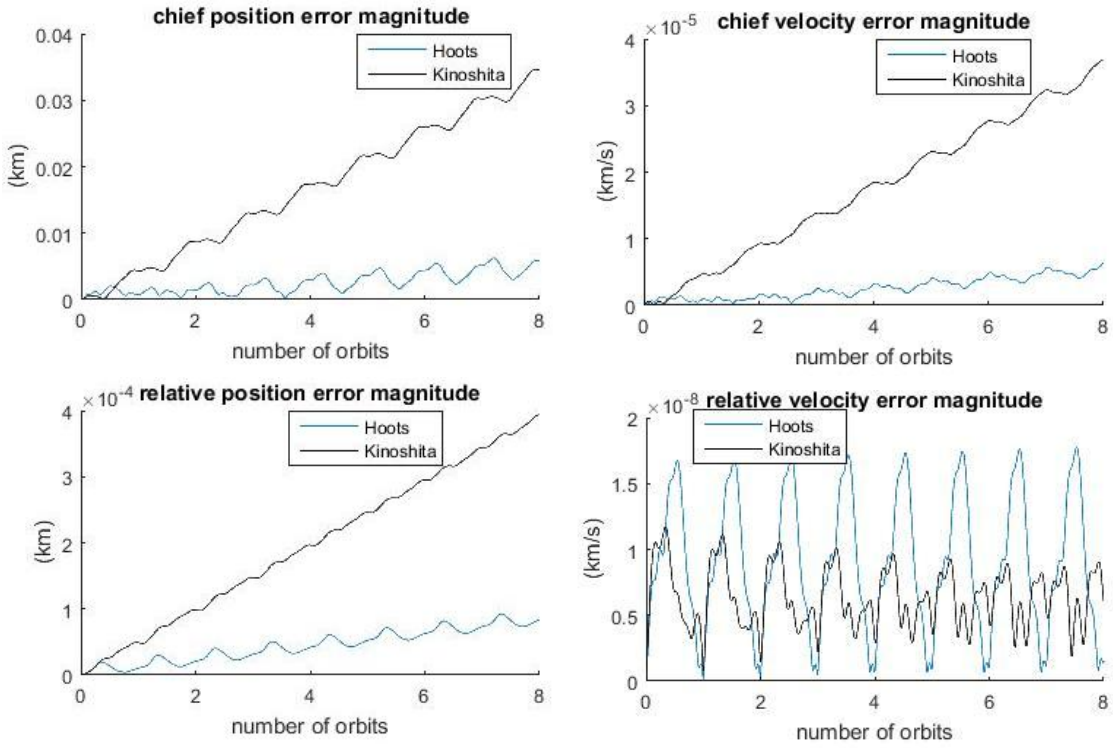


**Figure 7.3: Second-order theory: truth model and analytical model through $J_4$**

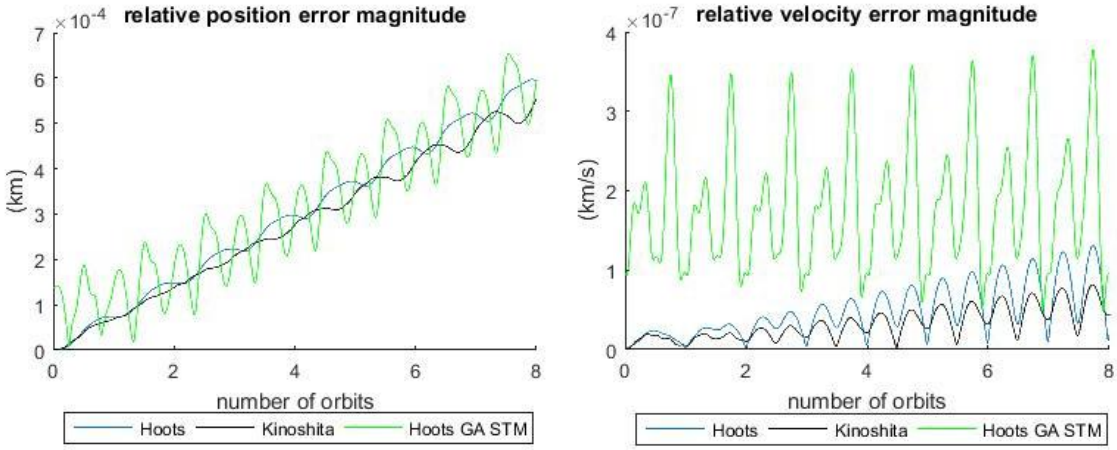


**Figure 7.4: First-order theory: Direct differencing vs. GA STM**

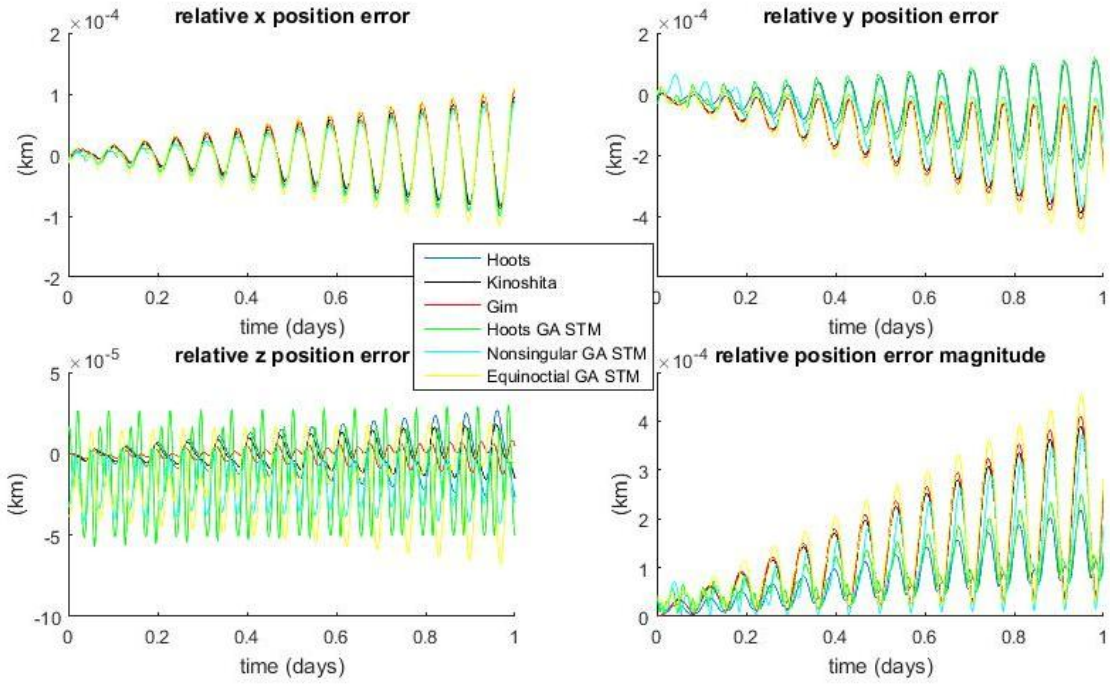


**Figure 7.5: Relative position error for near-circular orbit**

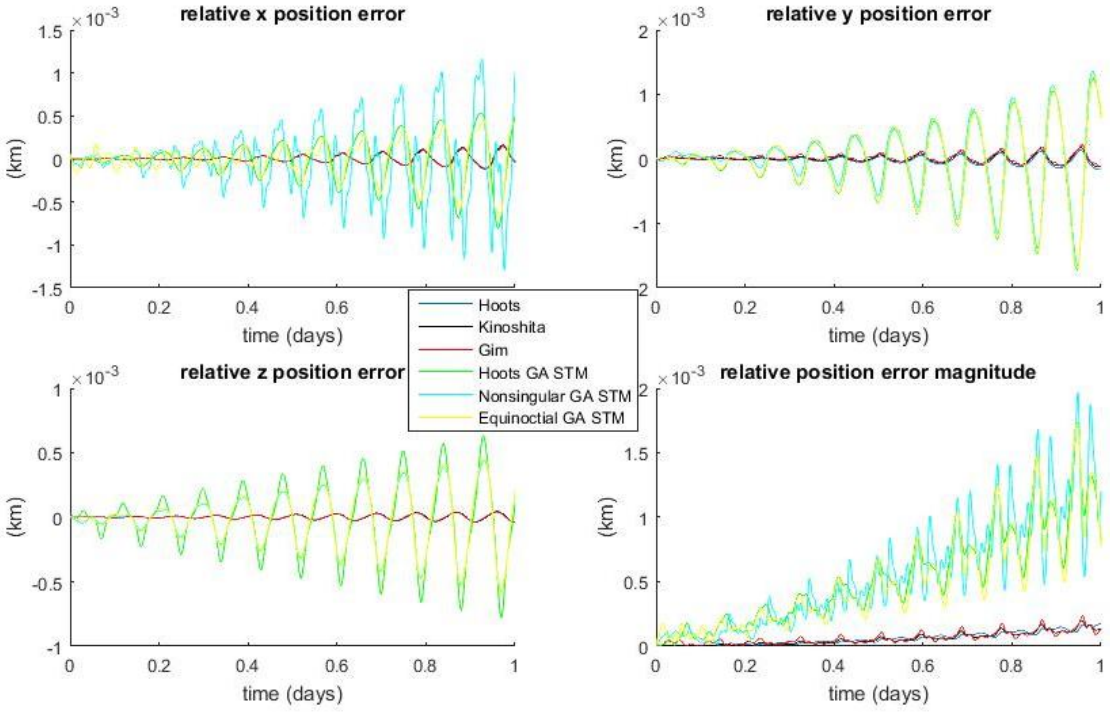


**Figure 7.6: Relative position error for eccentric orbit**

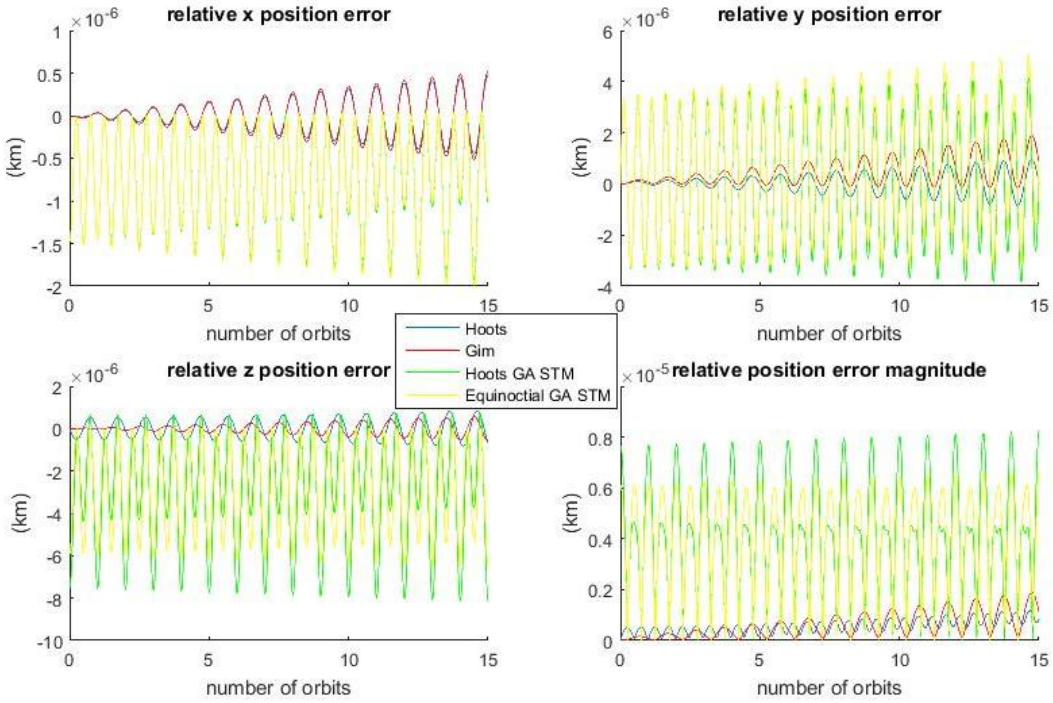


**Figure 7.7: Relative position error for geostationary orbit**

The final comparison to Reference [19] is Figure 7.7, which shows the relative position error over 15 orbits for a formation in geostationary orbit. Because the chief's orbit is equatorial, both Kinoshita theory and the nonsingular-element STM are singular and are not shown. For this scenario, the chief has the following initial osculating equinoctial elements: $a$ is 42,164.1598 kilometers, $\Psi$ is 116 degrees, and $\tilde{q}_1 = \tilde{q}_2 = p_1 = p_2 = 0$. The differential elements are as follows: $\delta a$ is 0, $\delta\Psi$ is 6.7944e-4 degrees, $\delta\tilde{q}_1$ is 5.3291e-6, $\delta\tilde{q}_2$ is 2.5992e-6, $\delta p_1$ is 2.5992e-6, and $\delta p_2$ is 5.3291e-6.

Note that in many cases the STM errors are nonzero even at the initial time. In order to propagate the relative orbit accurately with an STM, the relative initial conditions must themselves undergo a linearizing transformation–this transformation introduces an offset at the initial time, but prevents an accumulating error over the course of the propagation, as discussed in Chapter VI.

Finally, Figure 7.8 shows the importance of the equinoctial-elements version of the PCO initial conditions derived in Chapter III. The truth and analytical models use $J_2$ as the only perturbation, and the

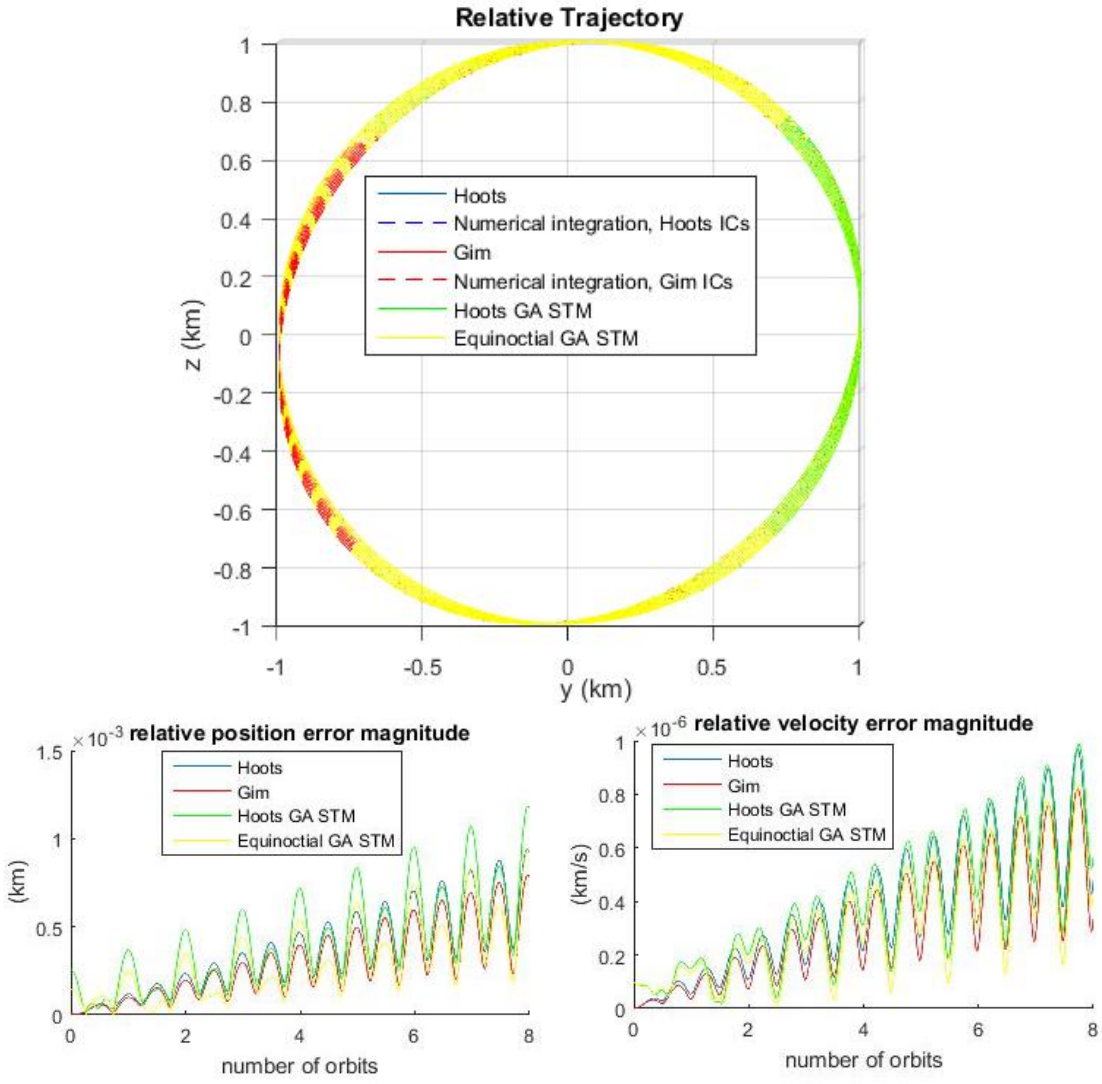


**Figure 7.8: PCO about equatorial chief orbit**

direct-differencing models are first-order. The chief's semi-major axis is 7100 kilometers, its eccentricity is 0.01, and its inclination is 0. The deputy's PCO radius is 1 kilometer, and its initial phase angle (meaning the phase angle when the chief passes the ECI 1-direction) is 0. Simulating this formation would be impossible without the new PCO definition. In the $y$-$z$ trajectory plot, note that the shape remains mostly circular over 8 orbits.

# CHAPTER VIII

# SUMMARY AND CONCLUSIONS

This dissertation explored new alternatives for modeling perturbed satellite relative motion, with a goal of achieving greater flexibility, simplicity, computational efficiency, and accuracy.

First, this study extended Hoots theory, an analytical averaging-method perturbation solution to the Zonal Problem, to include zonal harmonic $J_6$ at first order, and harmonics $J_2$ through $J_4$ at second order (truncated at 0th order in the chief's eccentricity). This study also supplied the needed first-order long-period terms for nonsingular-elements theory. In addition, it developed a hybrid numerical/analytical osculating-to-mean conversion algorithm for initial conditions, allowing simulations with osculating elements given as inputs. Later, this study used the Hoots elements to derive a closed-form relative motion model, a Gim-Alfriend State Transition Matrix.

This study also defined the parameters of linearized, bounded, unperturbed relative motion in terms of differential orbit elements; and it explained in detail the geometry of Projected Circular Orbits and PCO parameters $\rho$ and $\alpha$. For the first time, this study used equinoctial elements to define the PCO initial conditions, removing the singularity for equatorial chief orbits.

In addition, this study compared alternatives for along-track drift prevention, derived second-order versions of the drift-mitigation conditions, and developed a method for preventing all along-track secular motion. The new method can be implemented in formations about any chief orbit by sacrificing one degree of freedom in designing the formation geometry. This study also found certain non-drifting PCO formations about certain special chief orbits.

Finally, this study explained in detail the sources of modeling error: input noise amplified by numerical integration, linearized relative coordinates, the approximations inherent in analytical solutions to the Zonal Problem, truncation due to numerical solutions of Kepler's Equation, and singularities for certain variable choices. This study predicted and verified the order of magnitude of modeling error from each source.

Although various orbit theories and orbit elements sets are compared in the chapters of this study, it does not attempt to prove that one orbit theory is better than all others–such a thing can perhaps not be proven. Instead, this study represents one step in pursuit of a theory which balances speed and accuracy in predicting relative motion results for formation-flying applications.

In general, no choice of variables guarantees lower error for all orbits. However, there are three characteristics that are valuable about the Hoots elements: they have no singularities, they require only one solution of Kepler's Equation at each time step (even when using a GA STM), and they have already existing a second-order orbit theory and a GA STM–both derived in this dissertation. The Poincaré elements and the equinoctial elements share the first characteristic; the equinoctial elements share the second, and they already have a first-order theory and a GA STM. Therefore, these element sets also merit further study.

## VIII.A SUGGESTIONS FOR FUTURE WORK

There are a number of areas in which it would be desirable to continue the work addressed in this study. Although the modeling error has been well characterized here, it would be helpful to illustrate the error using the Yan-Alfriend modeling error index, in order to compare to other studies in the literature. In addition, quantifying the computational efficiency of each model would be revealing, and would be more meaningful to mission planners and software designers than simply counting algorithm steps.

Orbit theory has been exhaustively studied for generations, but in light of the results here, it may be beneficial to write a new second-order solution to the Zonal Problem in terms of the equinoctial elements (using $\Lambda$) and the Poincaré elements. Also, with modern computer algebra techniques, it should be possible using a Lie-series method to extend to second order the generating function for a single-step transformation, of the kind used by Alfriend and Velez in 1975 [15]. For any of these methods, a second-order generating function that does not use eccentricity expansions would be an improvement.

In the field of satellite relative motion, it will be straightforward to extend the Hoots-element GA STM to second order; extending the mean secular rates in $\bar{\phi}_x$ would be especially beneficial. In addition, a closed-form model of perturbed relative motion, such as a GA STM, should be developed using the Poincaré

elements. Finally, the geometric analysis performed here for PCO formations could be easily applied to other similar formations, such as the the General Circular Orbit and the near-PCO for elliptical chief orbits; the initial conditions for each one could then be defined in terms of equinoctial elements, allowing for formations about the equator. Finally, fast, accurate relative motion models of the type studied here would lend themselves well to improving the investigation of the conjunction analysis problem, important for Space Situational Awareness, as well as other important operational problems.

The method derived here for eliminating along-track secular motion should be developed further. In particular, it should be studied as an optimization problem, to see if it is possible to minimize the secular motion with a single degree of freedom, making available the full range of formation geometries. Also, in some circumstances, it may be desirable to treat increasing along-track separation due to long-period oscillations as a drift; if the period of the apsidal rotation is many days, some applications may not be able to tolerate a separation from the desired formation geometry for that long. For these cases, the prospect of augmenting the drift-prevention condition with a term to mitigate long-period changes should be explored.

# REFERENCES


[1] K. T. Alfriend, S. R. Vadali, P. Gurfil, J. P. How, and L. S. Breger, *Spacecraft Formation Flying: Dynamics, Control and Navigation*. Oxford: Elsevier, 2010.

[2] D. A. Vallado, *Fundamentals of Astrodynamics and Applications*. El Segundo: Microcosm Press, 4th ed., 2013.

[3] H. Schaub and J. L. Junkins, *Analytical Mechanics of Space Systems*. Reston: AIAA, 2nd ed., 2009.

[4] D. Brouwer, "Solution of the problem of artificial satellite theory without drag," *The Astronomical Journal*, vol. 64, no. 11, pp. 378–397, 1959.

[5] H. Von Zeipel, "Recherches sur le mouvement des petites planètes," *Arkiv för Matematik, Astronomi och Fysik*, vol. 11, No. 1 and No. 7, 1916, Vol. 12, No. 9, 1917, and Vol. 13, No. 3, 1918.

[6] Y. Kozai, "Second-order solution of artificial satellite theory without air drag," *The Astronomical Journal*, vol. 67, no. 7, pp. 446–461, 1962.

[7] R. H. Lyddane, "Small eccentricities or inclinations in the Brouwer theory of the artificial satellite," *The Astronomical Journal*, vol. 68, no. 8, pp. 555–558, 1963.

[8] F. R. Hoots, "A nonsingular reformulation of the Brouwer geopotential theory," American Astronautical Society Paper 79-137, June 1979.

[9] F. R. Hoots, "Reformulation of the Brouwer geopotential theory for improved computational efficiency," *Celestial Mechanics*, vol. 24, no. 4, pp. 367–375, 1981.

[10] G. Hori, "Theory of general perturbations with unspecified canonical variables," *Publications of the Astronomical Society of Japan*, vol. 18, no. 4, pp. 287–296, 1966.

[11] H. Kinoshita, "Third-order solution of an artificial satellite theory," Special Report #379, Smithsonian Astrophysical Observatory, 1977.

[12] A. Deprit, "Canonical transformations depending on a small parameter," *Celestial Mechanics*, vol. 1, no. 1, pp. 12–30, 1969.

[13] A. Deprit and A. Rom, "The main problem of artificial satellite theory for small and moderate eccentricities," *Celestial Mechanics*, vol. 2, no. 2, pp. 166–206, 1970.

[14] A. A. Kamel, "Expansion formulae in canonical transformations depending on a small parameter," *Celestial Mechanics*, vol. 1, no. 2, pp. 190–199, 1969.

[15] K. T. Alfriend and C. E. Velez, "The application of general perturbation theories to the artificial satellite problem," *Acta Astronautica*, vol. 2, no. 7–8, pp. 577–591, 1975.

[16] W. H. Clohessy and R. S. Wiltshire, "Terminal guidance system for satellite rendezvous," *Journal of the Aerospace Sciences*, vol. 27, pp. 653–658, 674, September 1960.

[17] G. W. Hill, "Researches in the lunar theory," *American Journal of Mathematics*, vol. 1, no. 1, pp. 5–26, 129–147, 245–260, 1878.

[18] D. Gim and K. T. Alfriend, "State transition matrix of relative motion for the perturbed noncircular reference orbit," *Journal of Guidance, Control, and Dynamics*, vol. 26, no. 6, pp. 956–971, 2003.

[19] D. Gim, *A Precise Analytic Solution to the Relative Motion of Formation Flying Satellites*. Dissertation, Texas A&M University, 2002.

[20] H. Yan, S. R. Vadali, and K. T. Alfriend, "State transition matrix for relative motion including higher-order gravity perturbations," American Astronautical Society Paper 13-793, August 2013.

[21] J. L. Garrison, T. G. Gardner, and P. Axelrad, "Relative motion in highly elliptical orbits," American Astronautical Society Paper 95-194, February 1995.

[22] H. Schaub, "Relative orbit geometry through classical orbital element differences," *Journal of Guidance, Control, and Dynamics*, vol. 27, no. 5, pp. 839–848, 2004.

[23] S. R. Vadali, K. T. Alfriend, and S. Vaddi, "Hill's equations, mean orbital elements, and formation flying of satellites," American Astronautical Society Paper 00-258, March 2000.

[24] S. D'Amico and O. Montenbruck, "Proximity operations of formation-flying spacecraft using an eccentricity/inclination vector separation," *Journal of Guidance, Control, and Dynamics*, vol. 29, no. 3, pp. 554–563, 2006.

[25] Y. He, M. Xu, and X. Chen, "Distance-based relative orbital elements determination for formation flying system," *Acta Astronautica*, vol. 118, no. 1–2, pp. 109–122, 2016.

[26] T. A. Lovell and S. G. Tragesser, "Guidance for relative motion of low earth orbit spacecraft based on relative orbit elements," AIAA Paper 2004-4988, August 2004.

[27] K. T. Alfriend, H. Schaub, and D. Gim, "Gravitational perturbations, nonlinearity and circular orbit assumption effects on formation flying control strategies," American Astronautical Society Paper 00-012, February 2000.

[28] P. Sengupta and S. R. Vadali, "Relative motion and the geometry of formations in Keplerian elliptic orbits," *Journal of Guidance, Control, and Dynamics*, vol. 30, no. 4, pp. 953–964, 2007.

[29] F. Jiang, J. Li, H. Baoyin, and Y. Gao, "Study on relative orbit geometry of spacecraft formations in elliptical reference orbits," *Journal of Guidance, Control, and Dynamics*, vol. 31, no. 1, pp. 123–134, 2008.

[30] J. L. Junkins, M. R. Akella, and K. T. Alfriend, "Non-Gaussian error propagation in orbital mechanics," *Journal of the Astronautical Sciences*, vol. 44, no. 4, pp. 541–563, 1996.

[31] G. W. Hill, "Motion of a system of material points under the action of gravitation," *The Astronomical Journal*, vol. 27, no. 22-23, pp. 171–182, 1913.

[32] E. T. Whittaker, *A Treatise on the Analytical Dynamics of Particles and Rigid Bodies*. New York: Dover Publications, 4th ed., 1944.

[33] A. Deprit, "The elimination of the parallax in satellite theory," *Celestial Mechanics*, vol. 24, no. 2, pp. 111–153, 1981.

[34] K. T. Alfriend and S. L. Coffey, "Elimination of the perigee in the satellite problem," *Celestial Mechanics*, vol. 32, no. 2, pp. 163–172, 1984.

[35] M. Lara, J. F. San-Juan, and L. M. López-Ochoa, "Proper averaging via parallax elimination," American Astronautical Society Paper 13-722, August 2013.

[36] M. Lara, J. F. San-Juan, and L. M. López-Ochoa, "Delaunay variables approach to the elimination of the perigee in artificial satellite theory," *Celestial Mechanics and Dynamical Astronomy*, vol. 120, no. 1, pp. 39–56, 2014.

[37] K. Aksnes, "A second-order artificial satellite theory based on an intermediate orbit," *The Astronomical Journal*, vol. 75, no. 9, pp. 1066–1076, 1970.

[38] B. Mahajan, S. R. Vadali, and K. T. Alfriend, "Analytic solution for satellite relative motion: the complete zonal gravitational problem," American Astronautical Society Paper 16-262, February 2016.

[39] K. T. Alfriend and H. Yan, "Evaluation and comparison of relative motion theories," *Journal of Guidance, Control, and Dynamics*, vol. 28, no. 2, pp. 254–261, 2005.

[40] K. Fujimoto, K. T. Alfriend, and S. R. Vadali, "Bridging dynamical modeling effort and sensor accuracy in relative spacecraft navigation," American Astronautical Society Paper 15-677, August 2015.

[41] S. R. Vadali, "An analytical solution for relatve motion of satellites," in *Dynamics and Control of Systems and Structures in Space 2002*, Cranfield University, Cranfield, UK, July 2002.

[42] S. S. Vaddi, K. T. Alfriend, S. R. Vadali, and P. Sengupta, "Formation establishment and reconfiguration using impulsive control," *Journal of Guidance, Control, and Dynamics*, vol. 28, no. 2, pp. 262–268, 2005.

[43] S. R. Vadali, P. Sengupta, H. Yan, and K. T. Alfriend, "Fundamental frequencies of satellite relative motion and control of formations," *Journal of Guidance, Control, and Dynamics*, vol. 31, no. 5, pp. 1239–1248, 2008.

[44] H. Schaub and K. T. Alfriend, "$J_2$ invariant relative orbits for spacecraft formations," *Celestial Mechanics and Dynamical Astronomy*, vol. 79, no. 2, pp. 77–95, 2001.

[45] Y. Kozai, "The motion of a close earth satellite," *The Astronomical Journal*, vol. 64, no. 11, pp. 367–377, 1959.

[46] C. W. T. Roscoe, *Satellite Formation Design in Orbits of High Eccentricity for Missions with Performance Criteria Specified over a Region of Interest*. Dissertation, Texas A&M University, 2012.

[47] A. J. Sinclair, R. E. Sherrill, and T. A. Lovell, "Calibration of linearized solutions for satellite relative motion," *Journal of Guidance, Control, and Dynamics*, vol. 37, no. 4, pp. 1362–1367, 2014.

# APPENDIX A

# SECOND-ORDER CORRECTION TERMS

The expressions in this appendix all assume canonical units, so that $\mu = 1$ and $Re = 1$. It was explained in Chapter II that only terms of 0th order in eccentricity are to be included in the second-order corrections, but the forms of the expressions below are not strictly 0th order: their terms contain factors of various powers of $1/G$. Since a factor with a power of $k$ is

$$\frac{1}{G^k} = \frac{1}{L^k(1-e^2)^{k/2}} = \frac{1}{L^k}\left(1 + \frac{k}{2}e^2 + \mathcal{O}(e^4)\right)$$

the expressions below differ from 0th order in $e$ by a quantity of order $e^2 J_2^2$. To recover strictly 0th-order terms, simply replace $G$ below with $L$, and $H$ with $L\theta$, where $\theta = H/G = \cos i$.

## A.1 SHORT-PERIOD CORRECTION FOR NONSINGULAR ELEMENTS

The second-order short-period corrections to the nonsingular elements $\underline{z}$ due to $J_2$ are found in Kinsoshita [11]. However, the corrections due to $J_3$ and $J_4$ are given here. All variables on the right-hand side of the equations in this section are intermediate variables, but the prime symbol has been dropped for brevity.

The $J_3$ term is $\{\underline{z}', S_{23}\}$, and the $J_4$ term is $\{\underline{z}', S_{24}\}$. The corrections, derived using Maxima, are

$$\begin{aligned}
\{L', S_{23}\} = &-\frac{J_3\sqrt{G^2-H^2}}{8G^8}\Big[\left(5\sin\left(3l+3g\right) - 15\sin\left(l+g\right)\right)H^2 \\
&+ \left(-5\sin\left(3l+3g\right) + 3\sin\left(l+g\right)\right)G^2\Big] \\
\{\lambda', S_{23}\} = &\frac{J_3\sqrt{G^2-H^2}}{24G^9(H^2-G^2)}\Big[\left(40\cos\left(3l+3g\right) - 360\cos\left(l+g\right)\right)H^4 \\
&+ \left(-65\cos\left(3l+3g\right) + 369\cos\left(l+g\right)\right)G^2H^2 + \left(25\cos\left(3l+3g\right) - 45\cos\left(l+g\right)\right)G^4\Big] \\
\{q_1', S_{23}\} = &-\frac{J_3\sqrt{G^2-H^2}}{32G^8L}\Big[\left(25\sin\left(4l+4g\right) - 80\sin\left(2l+2g\right)\right)H^2 \\
&+ \left(-25\sin\left(4l+4g\right) + 8\sin\left(2l+2g\right)\right)G^2\Big] \\
\{q_2', S_{23}\} = &\frac{J_3\sqrt{G^2-H^2}}{32G^8L}\Big[\left(25\cos\left(4l+4g\right) - 100\cos\left(2l+2g\right)\right)H^2 \\
&+ \left(-25\cos\left(4l+4g\right) + 28\cos\left(2l+2g\right)\right)G^2\Big]
\end{aligned}$$

$$\{h', S_{23}\} = -\frac{J_3 H\sqrt{G^2-H^2}}{8G^8(H^2-G^2)}\Big[\left(5\cos\left(3l+3g\right)-45\cos\left(l+g\right)\right)H^2$$
$$+\left(-5\cos\left(3l+3g\right)+33\cos\left(l+g\right)\right)G^2\Big]$$

and

$$\{L', S_{24}\} = -\frac{5J_4(H^2-G^2)}{64G^{11}}\Big[\left(7\cos\left(4l+4g\right)-28\cos\left(2l+2g\right)\right)H^2$$
$$+\left(-7\cos\left(4l+4g\right)+4\cos\left(2l+2g\right)\right)G^2\Big]$$
$$\{\lambda', S_{24}\} = -\frac{5J_4}{256G^{12}}\Big[\left(77\sin\left(4l+4g\right)-616\sin\left(2l+2g\right)\right)H^4$$
$$+\left(-126\sin\left(4l+4g\right)+576\sin\left(2l+2g\right)\right)G^2H^2$$
$$+\left(49\sin\left(4l+4g\right)-56\sin\left(2l+2g\right)\right)G^4\Big]$$
$$\{q_1', S_{24}\} = -\frac{J_4}{128G^{11}L}\Big[\left(91\cos\left(5l+5g\right)-385\cos\left(3l+3g\right)+1190\cos\left(l+g\right)\right)H^4$$
$$+\left(-182\cos\left(5l+5g\right)+410\cos\left(3l+3g\right)-1060\cos\left(l+g\right)\right)G^2H^2$$
$$+\left(91\cos\left(5l+5g\right)-25\cos\left(3l+3g\right)+110\cos\left(l+g\right)\right)G^4\Big]$$
$$\{q_2', S_{24}\} = -\frac{J_4}{128G^{11}L}\Big[\left(91\sin\left(5l+5g\right)-455\sin\left(3l+3g\right)+910\sin\left(l+g\right)\right)H^4$$
$$+\left(-182\sin\left(5l+5g\right)+550\sin\left(3l+3g\right)-740\sin\left(l+g\right)\right)G^2H^2$$
$$+\left(91\sin\left(5l+5g\right)-95\sin\left(3l+3g\right)+70\sin\left(l+g\right)\right)G^4\Big]$$
$$\{h', S_{24}\} = \frac{5J_4H}{64G^{11}}\left[\left(7\sin\left(4l+4g\right)-56\sin\left(2l+2g\right)\right)H^2+\left(-7\sin\left(4l+4g\right)+32\sin\left(2l+2g\right)\right)G^2\right]$$

Of course, since $H$ is a constant of the motion even under zonal harmonic perturbations, $\{H', S_{23}+S_{24}\} = 0$.

## A.2 SHORT-PERIOD CORRECTION FOR HOOTS ELEMENTS

All variables on the right-hand side of the equations in this section are intermediate variables, but the prime symbol has been dropped for brevity.

There are two second-order terms in Eq. 2.4 that depend on $J_2$: $\{\underline{y}', S_{22}\}$ and $\frac{1}{2}\{\{\underline{y}', S_1\}, S_1\}$.

$$\{y_1', S_{22}\} = \frac{J_2^2}{256G^4L^6}\Big(39\cos(4l+4g)H^4 + 1546\cos(2l+2g)H^4 - 777H^4 - 30\cos(4l+4g)G^2H^2 - 1800\cos(2l+2g)G^2H^2 + 18G^2H^2 - 9\cos(4l+4g)G^4 + 254\cos(2l+2g)G^4 + 39G^4\Big)$$

$$\{y_2', S_{22}\} = -\frac{J_2^2}{256G^4L^9}\Big(-21\sin(4l+4g)H^4 + 542\sin(2l+2g)H^4 + 42\sin(4l+4g)G^2H^2 - 552\sin(2l+2g)G^2H^2 - 21\sin(4l+4g)G^4 + 10\sin(2l+2g)G^4\Big)$$

$$\{y_3', S_{22}\} = -\frac{J_2^2}{256G^4L^9}\Big(39\cos(4l+4g)H^4 + 1402\cos(2l+2g)H^4 - 777H^4 - 54\cos(4l+4g)G^2H^2 - 1704\cos(2l+2g)G^2H^2 + 18G^2H^2 + 15\cos(4l+4g)G^4 + 302\cos(2l+2g)G^4 + 39G^4\Big)$$

$$\{y_4', S_{22}\} = \frac{J_2^2}{2^{17/2}G^5L^8}\sqrt{\frac{G-H}{G}}\Big[6HL\Big(18\sin(3l+3g)H^3 + 30\sin(l+g)H^3 - 6\sin(3l+3g)GH^2 + 6\sin(l+g)GH^2 - 8\sin(3l+3g)G^2H - 6\sin(l+g)G^2H - \sin(5l+5g)G^3 - \sin(3l+3g)G^3 + 2\sin(l+g)G^3\Big) + G\left(H^2-G^2\right)\Big(21\sin(5l+5g)H^2 - 269\sin(3l+3g)H^2 - 290\sin(l+g)H^2 + 94\sin(3l+3g)G^2 + 94\sin(l+g)G^2\Big)\Big]$$

$$\{y_5', S_{22}\} = \frac{J_2^2}{2^{17/2}G^5L^8}\sqrt{\frac{G-H}{G}}\Big[6HL\Big(18\cos(3l+3g)H^3 - 30\cos(l+g)H^3 - 6\cos(3l+3g)GH^2 - 6\cos(l+g)GH^2 - 12\cos(3l+3g)G^2H + 6\cos(l+g)G^2H - \cos(5l+5g)G^3 - 3\cos(3l+3g)G^3 - 2\cos(l+g)G^3\Big) + G\left(H^2-G^2\right)\Big(21\cos(5l+5g)H^2 - 311\cos(3l+3g)H^2 + 290\cos(l+g)H^2 + 94\cos(3l+3g)G^2 - 94\cos(l+g)G^2\Big)\Big]$$

$$\{y_6', S_{22}\} = \frac{J_2^2(H-G)}{128G^5L^8}\Big(144\sin(2l+2g)H^3L + 6\sin(4l+4g)G^2HL - 48\sin(2l+2g)G^2HL + 21\sin(4l+4g)GH^3 - 290\sin(2l+2g)GH^3 + 21\sin(4l+4g)G^2H^2 - 290\sin(2l+2g)G^2H^2 + 94\sin(2l+2g)G^3H + 94\sin(2l+2g)G^4\Big)$$

Following a similar process, replacing $\{\underline{y}', S_1\}$ with the short-period terms of Hoots's first-order corrections,

$$\frac{1}{2}\{\{y_1', S_1\}, S_1\} = \frac{J_2^2}{64G^8L^3}\Big[\Big(9\cos(4l+4g) - 108\cos(2l+2g) - 21\Big)H^4L + \Big(-18\cos(4l+4g) + 108\cos(2l+2g) + 30\Big)G^2H^2L + \Big(9\cos(4l+4g) - 9\Big)G^4L + \Big(-14\cos(4l+4g) - 153\cos(2l+2g) + 83\Big)GH^4 + \Big(28\cos(4l+4g) + 204\cos(2l+2g) - 58\Big)G^3H^2 + \Big(-14\cos(4l+4g) - 51\cos(2l+2g) + 11\Big)G^5\Big]$$

$$\frac{1}{2}\{\{y_2', S_1\}, S_1\} = -\frac{J_2^2}{32G^8L^6}\Big[9\sin(4l+4g)(H^2-G^2)L + \Big(-13\sin(4l+4g) - 45\sin(2l+2g)\Big)GH^2 + \Big(13\sin(4l+4g) + 15\sin(2l+2g)\Big)G^3\Big]$$

$$\frac{1}{2}\{\{y_3', S_1\}, S_1\} = \frac{J_2^2}{64G^8L^6}\Big[\Big(18\cos(4l+4g) + 108\cos(2l+2g) - 42\Big)H^4L + \Big(-36\cos(4l+4g) - 108\cos(2l+2g) + 60\Big)G^2H^2L + \Big(18\cos(4l+4g) - 18\Big)G^4L + \Big(-17\cos(4l+4g) + 45\cos(2l+2g) + 250\Big)GH^4 + \Big(34\cos(4l+4g) - 60\cos(2l+2g) - 176\Big)G^3H^2 + \Big(-17\cos(4l+4g) + 15\cos(2l+2g) + 34\Big)G^5\Big]$$

$$\frac{1}{2}\{\{y_4', S_1\}, S_1\} = \frac{J_2^2\sqrt{G-H}}{2^{19/2}G^9L^5}\Big[2\sin(l+g)\Big(30H^4L + 126GH^3L - 3G^2H^2L - 72G^3HL - 9G^4L + 120GH^4 - 80G^2H^3 - 320G^3H^2 + 32G^4H + 56G^5\Big) + \sin(5l+5g)(H-G)^2\Big(120H^2L + 120GHL + 27G^2L - 88GH^2 - 80G^2H + 8G^3\Big) - 3\sin(3l+3g)G(H-G)\Big(4H^2L + GHL + 3G^2L - 104H^3 - 136GH^2 + 40G^2H + 40G^3\Big)\Big]$$

$$\frac{1}{2}\{\{y_5', S_1\}, S_1\} = \frac{J_2^2\sqrt{G-H}}{2^{19/2}G^9L^5}\Big[2\cos(l+g)\Big(30H^4L + 126GH^3L - 3G^2H^2L - 72G^3HL - 9G^4L - 24GH^4 + 64G^2H^3 + 208G^3H^2 - 16G^4H - 40G^5\Big) + \cos(5l+5g)(H-G)^2\Big(120H^2L + 120GHL + 27G^2L - 88GH^2 - 80G^2H + 8G^3\Big) + 3\cos(3l+3g)G(H-G)\Big(4H^2L + GHL + 3G^2L + 184H^3 + 248GH^2 + 8G^2H - 24G^3\Big)\Big]$$

$$\frac{1}{2}\left\{\left\{y_6',S_1\right\},S_1\right\}=\frac{J_2^2(H-G)}{128G^8L^5}\Big[63\sin\left(4l+4g\right)H^3L-9\sin\left(4l+4g\right)GH^2L-45\sin\left(4l+4g\right)G^2HL$$
$$-9\sin\left(4l+4g\right)G^3L+\Big(-64\sin\left(4l+4g\right)+144\sin\left(2l+2g\right)\Big)GH^3$$
$$+\Big(8\sin\left(4l+4g\right)+144\sin\left(2l+2g\right)\Big)G^2H^2+\Big(64\sin\left(4l+4g\right)$$
$$-144\sin\left(2l+2g\right)\Big)G^3H+\Big(-8\sin\left(4l+4g\right)-48\sin\left(2l+2g\right)\Big)G^4\Big]$$

The $J_3$ term in Eq. 2.4 is $\left\{\underline{y}',S_{23}\right\}$, and the $J_4$ term is $\left\{\underline{y}',S_{24}\right\}$. The corrections, derived using Maxima, are

$$\left\{y_1',S_{23}\right\}=-\frac{J_3L\sqrt{G^2-H^2}}{32G^8}\Big[\left(5\sin\left(3l+3g\right)-30\sin\left(l+g\right)\right)H^2$$
$$+\left(-5\sin\left(3l+3g\right)+6\sin\left(l+g\right)\right)G^2\Big]$$
$$\left\{y_2',S_{23}\right\}=-\frac{3J_3\sqrt{G^2-H^2}}{32G^8L^2}\Big[\left(5\cos\left(3l+3g\right)-30\cos\left(l+g\right)\right)H^2$$
$$+\left(-5\cos\left(3l+3g\right)+6\cos\left(l+g\right)\right)G^2\Big]$$
$$\left\{y_3',S_{23}\right\}=-\frac{3J_3\sqrt{G^2-H^2}}{32G^8L^2}\Big[\left(5\sin\left(3l+3g\right)-10\sin\left(l+g\right)\right)H^2$$
$$+\left(-5\sin\left(3l+3g\right)+2\sin\left(l+g\right)\right)G^2\Big]$$
$$\left\{y_4',S_{23}\right\}=-\frac{J_3(H+G)}{2^{11/2}3G^9L}\sqrt{\frac{H+G}{G}}\Big\{\Big[\Big(65\cos\left(4l+4g\right)-580\cos\left(2l+2g\right)-765\Big)H^4$$
$$+\Big(-15\cos\left(4l+4g\right)+60\cos\left(2l+2g\right)-45\Big)GH^3+\Big(-115\cos\left(4l+4g\right)$$
$$+584\cos\left(2l+2g\right)+747\Big)G^2H^2+\Big(15\cos\left(4l+4g\right)-24\cos\left(2l+2g\right)+9\Big)G^3H$$
$$+\Big(50\cos\left(4l+4g\right)-40\cos\left(2l+2g\right)-90\Big)G^4\Big]L+\Big(-45\cos\left(4l+4g\right)$$
$$+225\cos\left(2l+2g\right)+270\Big)GH^4+\Big(90\cos\left(4l+4g\right)-234\cos\left(2l+2g\right)-324\Big)G^3H^2$$
$$+\Big(-45\cos\left(4l+4g\right)+9\cos\left(2l+2g\right)+54\Big)G^5\Big\}$$

$$\{y_5', S_{23}\} = \frac{J_3(H-G)}{2^{11/2}3G^9L(H+G)}\sqrt{\frac{H+G}{G}}\Big\{\Big[\Big(65\sin(4l+4g) - 770\sin(2l+2g)\Big)H^3$$
$$+ \Big(50\sin(4l+4g) - 740\sin(2l+2g)\Big)GH^2 + \Big(-65\sin(4l+4g)$$
$$+ 134\sin(2l+2g)\Big)G^2H + \Big(-50\sin(4l+4g) + 140\sin(2l+2g)\Big)G^3\Big]L$$
$$+ \Big(-45\sin(4l+4g) + 315\sin(2l+2g)\Big)GH^3 + \Big(-45\sin(4l+4g)$$
$$+ 315\sin(2l+2g)\Big)G^2H^2 + \Big(45\sin(4l+4g) - 99\sin(2l+2g)\Big)G^3H$$
$$+ \Big(45\sin(4l+4g) - 99\sin(2l+2g)\Big)G^4\Big\}$$
$$\{y_6', S_{23}\} = \frac{J_3\sqrt{G^2-H^2}}{G^9L(H+G)}\Big\{\Big[\Big(80\cos(3l+3g) - 720\cos(l+g)\Big)H^3 + \Big(50\cos(3l+3g)$$
$$- 450\cos(l+g)\Big)GH^2 + \Big(-80\cos(3l+3g) + 288\cos(l+g)\Big)G^2H$$
$$+ \Big(-50\cos(3l+3g) + 90\cos(l+g)\Big)G^3\Big]L + \Big(-45\cos(3l+3g)$$
$$+ 270\cos(l+g)\Big)GH^3 + \Big(-45\cos(3l+3g) + 270\cos(l+g)\Big)G^2H^2$$
$$+ \Big(45\cos(3l+3g) - 54\cos(l+g)\Big)G^3H + \Big(45\cos(3l+3g) - 54\cos(l+g)\Big)G^4\Big\}$$

and

$$\{y_1', S_{24}\} = -\frac{J_4L}{64G^{11}}\Big[\Big(7\cos(4l+4g) - 140\cos(2l+2g) - 525\Big)H^4 + \Big(-14\cos(4l+4g)$$
$$+ 160\cos(2l+2g) + 450\Big)G^2H^2 + \Big(7\cos(4l+4g) - 20\cos(2l+2g) - 45\Big)G^4\Big]$$
$$\{y_2', S_{24}\} = \frac{J_4(H^2-G^2)}{16G^{11}L^2}\Big[\Big(7\sin(4l+4g) - 70\sin(2l+2g)\Big)H^2 + \Big(-7\sin(4l+4g)$$
$$+ 10\sin(2l+2g)\Big)G^2\Big]$$
$$\{y_3', S_{24}\} = -\frac{J_4}{64G^{11}L^2}\Big[\Big(28\cos(4l+4g) + 525\Big)H^4 + \Big(-56\cos(4l+4g) - 450\Big)G^2H^2$$
$$+ \Big(28\cos(4l+4g) + 45\Big)G^4\Big]$$

$$\{y_4', S_{24}\} = -\frac{J_4}{2^{19/2}G^{12}L}\sqrt{\frac{G-H}{G}}\Big\{\Big[\Big(315\sin(5l+5g) - 2345\sin(3l+3g) - 3360\sin(l+g)\Big)H^4$$
$$+ \Big(-70\sin(5l+5g) + 350\sin(3l+3g) - 280\sin(l+g)\Big)GH^3$$
$$+ \Big(-560\sin(5l+5g) + 2140\sin(3l+3g) + 2920\sin(l+g)\Big)G^2H^2$$
$$+ \Big(70\sin(5l+5g) - 110\sin(3l+3g) + 40\sin(l+g)\Big)G^3H + \Big(245\sin(5l+5g)$$
$$- 35\sin(3l+3g) - 280\sin(l+g)\Big)G^4\Big]L + \Big(-224\sin(5l+5g) + 2016\sin(3l+3g)$$
$$+ 2240\sin(l+g)\Big)GH^4 + \Big(448\sin(5l+5g) - 2112\sin(3l+3g)$$
$$- 2560\sin(l+g)\Big)G^3H^2 + \Big(-224\sin(5l+5g) + 96\sin(3l+3g)$$
$$+ 320\sin(l+g)\Big)G^5\Big\}$$
$$\{y_5', S_{24}\} = -\frac{J_4}{2^{19/2}G^{12}L}\sqrt{\frac{G-H}{G}}\Big\{\Big[\Big(315\cos(5l+5g) - 3255\cos(3l+3g) + 3360\cos(l+g)\Big)H^4$$
$$+ \Big(-70\cos(5l+5g) + 210\cos(3l+3g) + 280\cos(l+g)\Big)GH^3$$
$$+ \Big(-560\cos(5l+5g) + 3540\cos(3l+3g) - 2920\cos(l+g)\Big)G^2H^2$$
$$+ \Big(70\cos(5l+5g) + 30\cos(3l+3g) - 40\cos(l+g)\Big)G^3H + \Big(245\cos(5l+5g)$$
$$- 525\cos(3l+3g) + 280\cos(l+g)\Big)G^4\Big]L + \Big(-224\cos(5l+5g)$$
$$+ 2464\cos(3l+3g) - 2240\cos(l+g)\Big)GH^4 + \Big(448\cos(5l+5g) - 3008\cos(3l+3g)$$
$$+ 2560\cos(l+g)\Big)G^3H^2 + \Big(-224\cos(5l+5g) + 544\cos(3l+3g)$$
$$- 320\cos(l+g)\Big)G^5\Big\}$$
$$\{y_6', S_{24}\} = -\frac{J_4(H-G)}{256G^{12}L}\Big\{\Big[\Big(385\sin(4l+4g) - 3080\sin(2l+2g)\Big)H^3 + \Big(245\sin(4l+4g)$$
$$- 1960\sin(2l+2g)\Big)GH^2 + \Big(-385\sin(4l+4g) + 920\sin(2l+2g)\Big)G^2H$$
$$+ \Big(-245\sin(4l+4g) + 280\sin(2l+2g)\Big)G^3\Big]L + \Big(-224\sin(4l+4g)$$
$$+ 2240\sin(2l+2g)\Big)GH^2(H+G) + \Big(224\sin(4l+4g)$$
$$- 320\sin(2l+2g)\Big)G^3(H+G)\Big\}$$

### A.3 LONG-PERIOD CORRECTION FOR HOOTS ELEMENTS

All variables on the right-hand side of the equations in this section are mean variables, but the double-prime symbol has been dropped for brevity. At 0th order in $e$, several of the second-order terms in Eq. 2.5 vanish. Those that do not are listed here.

The corrections due to $J_3$ in the term $\left\{\underline{y}'', S_{23}^*\right\}$ are

$$\{y_1'', S_{23}^*\} = -\frac{J_3 \sin(l+g)}{32G^3L^4}\frac{\sqrt{G^2-H^2}}{5H^2-G^2}\left(345H^4-157G^2H^2+4G^4\right)$$

$$\{y_2'', S_{23}^*\} = -\frac{J_3 \cos(l+g)}{32G^3L^7}\frac{\sqrt{G^2-H^2}}{5H^2-G^2}\left(345H^4-157G^2H^2+4G^4\right)$$

$$\{y_3'', S_{23}^*\} = \frac{J_3 \sin(l+g)}{32G^3L^7}\frac{\sqrt{G^2-H^2}}{5H^2-G^2}\left(345H^4-157G^2H^2+4G^4\right)$$

$$\{y_4'', S_{23}^*\} = -\frac{J_3}{2^{11/2}G^3L^6}\sqrt{\frac{G-H}{G}}\frac{\sqrt{G^2-H^2}}{5H^2-G^2}\left(345H^4-157G^2H^2+4G^4\right)\left(\cos(2l+2g)+1\right)$$

$$\{y_5'', S_{23}^*\} = \frac{J_3}{2^{11/2}G^3L^6}\sqrt{\frac{G-H}{G}}\frac{\sqrt{G^2-H^2}}{5H^2-G^2}\left(345H^4-157G^2H^2+4G^4\right)\sin(2l+2g)$$

$$\{y_6'', S_{23}^*\} = -\frac{J_3 \cos(l+g)}{16G^3L^6}\frac{\sqrt{G^2-H^2}}{5H^2-G^2}\left(345H^4-157G^2H^2+4G^4\right)$$

The corrections due to coupled $J_3$ and $J_4$ in the term $\left\{\underline{y}'', S_{234}^*\right\}$ are

$$\{y_1'', S_{234}^*\} = \frac{5}{64}\frac{J_3J_4}{J_2^2}\frac{\sin(l+g)}{G^3L^4}\frac{\sqrt{G^2-H^2}}{5H^2-G^2}\left(217H^4-168G^2H^2+15G^4\right)$$

$$\{y_2'', S_{234}^*\} = \frac{5}{64}\frac{J_3J_4}{J_2^2}\frac{\cos(l+g)}{G^3L^7}\frac{\sqrt{G^2-H^2}}{5H^2-G^2}\left(217H^4-168G^2H^2+15G^4\right)$$

$$\{y_3'', S_{234}^*\} = -\frac{5}{64}\frac{J_3J_4}{J_2^2}\frac{\sin(l+g)}{G^3L^7}\frac{\sqrt{G^2-H^2}}{5H^2-G^2}\left(217H^4-168G^2H^2+15G^4\right)$$

$$\{y_4'', S_{234}^*\} = -\frac{5}{2^{13/2}}\frac{J_3J_4}{J_2^2}\frac{H-G}{G^3L^6(5H^2-G^2)}\sqrt{\frac{H+G}{G}}\left(217H^4-168G^2H^2+15G^4\right)\Big(\cos(2l+2g)+1\Big)$$

$$\{y_5'', S_{234}^*\} = \frac{5}{2^{13/2}}\frac{J_3J_4}{J_2^2}\frac{H-G}{G^3L^6(5H^2-G^2)}\sqrt{\frac{H+G}{G}}\left(217H^4-168G^2H^2+15G^4\right)\sin(2l+2g)$$

$$\{y_6'', S_{234}^*\} = \frac{5}{32}\frac{J_3J_4}{J_2^2}\frac{\cos(l+g)}{G^3L^6}\frac{\sqrt{G^2-H^2}}{5H^2-G^2}\left(217H^4-168G^2H^2+15G^4\right)$$

The corrections due to $J_3$ in the term $\frac{1}{2}\left\{\left\{\underline{y}'', S_{12}^*\right\}, S_{13}^*\right\}$ (where $\left\{\underline{y}'', S_{12}^*\right\}$ can be replaced by the long-period $J_2$ terms in Hoots's first-order corrections) are

$$\frac{1}{2}\left\{\{y_1'', S_{12}^*\}, S_{13}^*\right\} = \frac{J_3 \sin(l+g)}{32G^7}\frac{(H^2-G^2)\sqrt{G^2-H^2}}{5H^2-G^2}\left(15H^2-2G^2\right)$$

$$\frac{1}{2}\left\{\{y_2'', S_{12}^*\}, S_{13}^*\right\} = \frac{J_3 \cos(l+g)}{32G^7L^3}\frac{(H^2-G^2)\sqrt{G^2-H^2}}{5H^2-G^2}\left(15H^2-2G^2\right)$$

$$\frac{1}{2}\left\{\left\{y_3'',S_{12}^*\right\},S_{13}^*\right\}=-\frac{J_3\sin\left(l+g\right)}{32G^7L^3}\frac{(H^2-G^2)\sqrt{G^2-H^2}}{5H^2-G^2}\left(15H^2-2G^2\right)$$
$$\frac{1}{2}\left\{\left\{y_4'',S_{12}^*\right\},S_{13}^*\right\}=-\frac{J_3}{2^{11/2}G^6L^2}\frac{(H-G)^2(H+G)}{5H^2-G^2}\sqrt{\frac{H+G}{G}}\left(15H^2-2G^2\right)\left(\cos\left(2l+2g\right)+1\right)$$
$$\frac{1}{2}\left\{\left\{y_5'',S_{12}^*\right\},S_{13}^*\right\}=\frac{J_3}{2^{11/2}G^6L^2}\frac{(H-G)^2(H+G)}{5H^2-G^2}\sqrt{\frac{H+G}{G}}\left(15H^2-2G^2\right)\sin\left(2l+2g\right)$$
$$\frac{1}{2}\left\{\left\{y_6'',S_{12}^*\right\},S_{13}^*\right\}=\frac{J_3\cos\left(l+g\right)}{16G^7L^2}\frac{(H^2-G^2)\sqrt{G^2-H^2}}{5H^2-G^2}\left(15H^2-2G^2\right)$$

The corrections due to $J_3$ in the term $\frac{1}{2}\left\{\left\{\underline{y}'',S_{13}^*\right\},S_{13}^*\right\}$ (where $\left\{\underline{y}'',S_{13}^*\right\}$ can be replaced by the long-period $J_3$ terms in Hoots's first-order corrections) are

$$\frac{1}{2}\left\{\left\{y_1'',S_{13}^*\right\},S_{13}^*\right\}=-\frac{J_3^2}{J_2^2}\frac{H^2-G^2}{8G^3L}\left(\cos\left(2l+2g\right)+1\right)$$
$$\frac{1}{2}\left\{\left\{y_2'',S_{13}^*\right\},S_{13}^*\right\}=\frac{J_3^2}{J_2^2}\frac{H^2-G^2}{4G^3L^4}\sin\left(2l+2g\right)$$
$$\frac{1}{2}\left\{\left\{y_3'',S_{13}^*\right\},S_{13}^*\right\}=\frac{J_3^2}{J_2^2}\frac{H^2-G^2}{8G^3L^4}\left(2\cos\left(2l+2g\right)+1\right)$$
$$\frac{1}{2}\left\{\left\{y_4'',S_{13}^*\right\},S_{13}^*\right\}=-\frac{J_3^2}{J_2^2}\frac{1}{2^{11/2}G^3L^3}\sqrt{\frac{G-H}{G}}\Big[\left(2G\sin\left(l+g\right)-9\sin\left(3l+3g\right)-9\sin\left(l+g\right)\right)H^2$$
$$+2\sin\left(l+g\right)G^2H+9\left(\sin\left(3l+3g\right)+\sin\left(l+g\right)\right)G^2\Big]$$
$$\frac{1}{2}\left\{\left\{y_5'',S_{13}^*\right\},S_{13}^*\right\}=-\frac{J_3^2}{J_2^2}\frac{H+G}{2^{11/2}G^3L^3}\sqrt{\frac{G-H}{G}}\Big(2GH\cos\left(l+g\right)-9H\cos\left(3l+3g\right)-7H\cos\left(l+g\right)$$
$$+9G\cos\left(3l+3g\right)+7G\cos\left(l+g\right)\Big)$$
$$\frac{1}{2}\left\{\left\{y_6'',S_{13}^*\right\},S_{13}^*\right\}=\frac{5}{16}\frac{J_3^2}{J_2^2}\frac{H^2-G^2}{G^3L^3}\sin\left(2l+2g\right)$$

Finally, the corrections in the term $\frac{1}{2}\left\{\left\{\underline{y}'',S_{14}^*\right\},S_{13}^*\right\}$ (where $\left\{\underline{y}'',S_{14}^*\right\}$ can be replaced by the long-period $J_4$ terms in Hoots's first-order corrections) are

$$\frac{1}{2}\left\{\left\{y_1'',S_{14}^*\right\},S_{13}^*\right\}=\frac{5}{64}\frac{J_3J_4}{J_2^2}\frac{\sin\left(l+g\right)}{G^4L^3}\frac{(H^2-G^2)\sqrt{G^2-H^2}}{5H^2-G^2}\left(7H^2-G^2\right)$$
$$\frac{1}{2}\left\{\left\{y_2'',S_{14}^*\right\},S_{13}^*\right\}=\frac{5}{64}\frac{J_3J_4}{J_2^2}\frac{\cos\left(l+g\right)}{G^4L^6}\frac{(H^2-G^2)\sqrt{G^2-H^2}}{5H^2-G^2}\left(7H^2-G^2\right)$$
$$\frac{1}{2}\left\{\left\{y_3'',S_{14}^*\right\},S_{13}^*\right\}=-\frac{5}{64}\frac{J_3J_4}{J_2^2}\frac{\sin\left(l+g\right)}{G^4L^6}\frac{(H^2-G^2)\sqrt{G^2-H^2}}{5H^2-G^2}\left(7H^2-G^2\right)$$
$$\frac{1}{2}\left\{\left\{y_4'',S_{14}^*\right\},S_{13}^*\right\}=-\frac{5}{2^{13/2}}\frac{J_3J_4}{J_2^2}\frac{(H-G)^2(H+G)}{G^4L^5(5H^2-G^2)}\sqrt{\frac{G+H}{G}}\left(7H^2-G^2\right)\left(\cos\left(2l+2g\right)+1\right)$$
$$\frac{1}{2}\left\{\left\{y_5'',S_{14}^*\right\},S_{13}^*\right\}=\frac{5}{2^{13/2}}\frac{J_3J_4}{J_2^2}\frac{(H-G)^2(H+G)}{G^4L^5(5H^2-G^2)}\sqrt{\frac{G+H}{G}}\left(7H^2-G^2\right)\sin\left(2l+2g\right)$$
$$\frac{1}{2}\left\{\left\{y_6'',S_{14}^*\right\},S_{13}^*\right\}=\frac{5}{32}\frac{J_3J_4}{J_2^2}\frac{\cos\left(l+g\right)}{G^4L^5}\frac{(H^2-G^2)\sqrt{G^2-H^2}}{5H^2-G^2}\left(7H^2-G^2\right)$$

At higher powers of $e$, of course, there would be several additional terms in the second-order long-period corrections.

# APPENDIX B

# ELEMENTS OF $D^{(lp)}$ AND $D^{(sp)}$

## B.1 LONG-PERIOD

$$D_{11}^{(lp)} = R_e^2 J_2 \left( \frac{-p_{50}}{8p_{51}y_1^3y_3^2} \right) \left( y_5^2 + y_4^2 - 1 \right) \left( y_1y_3^2y_5^2 - 2\mu y_5^2 + 2y_1y_2y_3y_4y_5 - y_1y_3^2y_4^2 + 2\mu y_4^2 \right)$$

$$D_{21}^{(lp)} = R_e^2 J_2 \left( \frac{-p_{50}}{4p_{51}y_1^4y_3} \right) \left( y_5^2 + y_4^2 - 1 \right) \left( y_1y_2y_3y_5^2 - 2y_1y_3^2y_4y_5 + 3\mu y_4y_5 - y_1y_2y_3y_4^2 \right)$$

$$\begin{aligned} D_{31}^{(lp)} = R_e^2 J_2 \left( \frac{p_{50}}{8p_{51}y_1^5y_3^3} \right) \left( y_5^2 + y_4^2 - 1 \right) \left( 2y_1^2y_2^2y_3^2y_5^2 + 3\mu y_1y_3^2y_5^2 - 4\mu^2y_5^2 - 4y_1^2y_2y_3^3y_4y_5 \right. \\ \left. + 12\mu y_1y_2y_3y_4y_5 - 2y_1^2y_2^2y_3^2y_4^2 - 3\mu y_1y_3^2y_4^2 + 4\mu^2y_4^2 \right) \end{aligned}$$

$$\begin{aligned} D_{41}^{(lp)} = R_e^2 J_2 \left( \frac{1}{16p_{51}^2y_1^5y_3^4} \right) \left( 4p_1y_1^2y_2y_3^3y_5^3 + 4p_1y_1^2y_2y_3^3y_4^2y_5 - 2p_1y_1^2y_2y_3^3y_5 - p_2y_1^2y_3^4y_4 + p_4y_1^2y_2^2y_3^2 \right. \\ \left. + 3p_4\mu y_1y_3^2 - 3p_3\mu y_1y_2y_3 - 2p_5\mu^2 \right) \end{aligned}$$

$$\begin{aligned} D_{51}^{(lp)} = R_e^2 J_2 \left( \frac{1}{16p_{51}^2y_1^5y_3^4} \right) \left( 4p_6y_1^2y_2y_3^3y_5^2 + 4p_6y_1^2y_2y_3^3y_4^2 + p_7y_1^2y_3^4 - 2p_6y_1^2y_2y_3^3 - p_8y_1^2y_2^2y_3^2 \right. \\ \left. - 3p_8\mu y_1y_3^2 + 3p_{10}\mu y_1y_2y_3 + 2p_9\mu^2 \right) \end{aligned}$$

$$\begin{aligned} D_{61}^{(lp)} = R_e^2 J_2 \left( \frac{1}{8p_{51}^2y_1^5y_3^4} \right) \left( 4p_{12}y_1^2y_2y_3^3y_5^4 - 2p_{11}y_1^2y_3^4y_5^2 - 2p_{12}y_1^2y_2y_3^3y_5^2 - 3p_{14}\mu y_1y_2y_3y_5^2 \right. \\ - 4p_{12}y_1^2y_2y_3^3y_4^2 - 2p_{11}y_1^2y_3^4y_4^2 + 2p_{12}y_1^2y_2y_3^3y_4^2 + 3p_{14}\mu y_1y_2y_3y_4^2 + 2p_{13}y_1^2y_2^2y_3^2 \\ \left. + 6p_{13}\mu y_1y_3^2 - 4p_{15}\mu^2 \right) \end{aligned}$$

$$D_{12}^{(lp)} = R_e^2 J_2 \left( \frac{p_{50}}{4p_{51}y_1y_3} \right) y_4y_5 \left( y_5^2 + y_4^2 - 1 \right)$$

$$D_{22}^{(lp)} = R_e^2 J_2 \left( \frac{p_{50}}{8p_{51}y_1^2} \right) \left( y_5^2 - y_4^2 \right) \left( y_5^2 + y_4^2 - 1 \right)$$

$$D_{32}^{(lp)} = R_e^2 J_2 \left( \frac{-p_{50}}{4p_{51}y_1^3y_3^2} \right) \left( y_5^2 + y_4^2 - 1 \right) \left( y_1y_2y_3y_5^2 - y_1y_3^2y_4y_5 + 2\mu y_4y_5 - y_1y_2y_3y_4^2 \right)$$

$$D_{42}^{(lp)} = R_e^2 J_2 \left( \frac{-1}{16p_{51}^2y_1^3y_3^3} \right) \left( 2p_1y_1y_3^2y_5^3 + 2p_1y_1y_3^2y_4^2y_5 - p_1y_1y_3^2y_5 + p_4y_1y_2y_3 - p_3\mu \right)$$

$$D_{52}^{(lp)} = R_e^2 J_2 \left( \frac{-1}{16p_{51}^2y_1^3y_3^3} \right) \left( 2p_6y_1y_3^2y_5^2 + 2p_6y_1y_3^2y_4^2 - p_6y_1y_3^2 - p_8y_1y_2y_3 + p_{10}\mu \right)$$

$$D_{62}^{(lp)} = R_e^2 J_2 \left( \frac{-1}{8p_{51}^2 y_1^3 y_3^3} \right) \left( 2p_{12} y_1 y_3^2 y_5^4 - p_{12} y_1 y_3^2 y_5^2 - p_{14} \mu y_5^2 - 2p_{12} y_1 y_3^2 y_4^4 + p_{12} y_1 y_3^2 y_4^2 + p_{14} \mu y_4^2 \right.$$
$$\left. + 2p_{13} y_1 y_2 y_3 \right)$$

$$D_{13}^{(lp)} = R_e^2 J_2 \left( \frac{p_{50}}{4p_{51} y_1^2 y_3^3} \right) \left( y_5^2 + y_4^2 - 1 \right) \left( \mu y_5^2 - y_1 y_2 y_3 y_4 y_5 - \mu y_4^2 \right)$$

$$D_{23}^{(lp)} = R_e^2 J_2 \left( \frac{-p_{50}}{4p_{51} y_1^3 y_3^2} \right) y_4 y_5 \left( y_5^2 + y_4^2 - 1 \right) \left( y_1 y_3^2 + \mu \right)$$

$$D_{33}^{(lp)} = R_e^2 J_2 \left( \frac{p_{50}}{8p_{51} y_1^4 y_3^4} \right) \left( y_5^2 + y_4^2 - 1 \right) \left( y_1^2 y_2^2 y_3^2 y_5^2 + \mu y_1 y_3^2 y_5^2 - 3\mu^2 y_5^2 + 8\mu y_1 y_2 y_3 y_4 y_5 \right.$$
$$\left. - y_1^2 y_2^2 y_3^2 y_4^2 - \mu y_1 y_3^2 y_4^2 + 3\mu^2 y_4^2 \right)$$

$$D_{43}^{(lp)} = R_e^2 J_2 \left( \frac{1}{16p_{51}^2 y_1^4 y_3^5} \right) \left( 2p_1 y_1^2 y_2 y_3^3 y_5^3 + 2p_1 y_1^2 y_2 y_3^3 y_4^2 y_5 - p_1 y_1^2 y_2 y_3^3 y_5 + p_4 y_1^2 y_2^2 y_3^2 + 2p_4 \mu y_1 y_3^2 \right.$$
$$\left. - 3p_3 \mu y_1 y_2 y_3 - 2p_5 \mu^2 \right)$$

$$D_{53}^{(lp)} = R_e^2 J_2 \left( \frac{1}{16p_{51}^2 y_1^4 y_3^5} \right) \left( 2p_6 y_1^2 y_2 y_3^3 y_5^2 + 2p_6 y_1^2 y_2 y_3^3 y_4^2 - p_6 y_1^2 y_2 y_3^3 - p_8 y_1^2 y_2^2 y_3^2 - 2p_8 \mu y_1 y_3^2 \right.$$
$$\left. + 3p_{10} \mu y_1 y_2 y_3 + 2p_9 \mu^2 \right)$$

$$D_{63}^{(lp)} = R_e^2 J_2 \left( \frac{1}{8p_{51}^2 y_1^4 y_3^5} \right) \left( 2p_{12} y_1^2 y_2 y_3^3 y_5^4 - p_{12} y_1^2 y_2 y_3^3 y_5^2 - 3p_{14} \mu y_1 y_2 y_3 y_5^2 - 2p_{12} y_1^2 y_2 y_3^3 y_4^4 \right.$$
$$\left. + p_{12} y_1^2 y_2 y_3^3 y_4^2 + 3p_{14} \mu y_1 y_2 y_3 y_4^2 + 2p_{13} y_1^2 y_2^2 y_3^2 + 4p_{13} \mu y_1 y_3^2 - 4p_{15} \mu^2 \right)$$

$$D_{14}^{(lp)} = R_e^2 J_2 \left( \frac{-1}{4p_{51}^2 y_1^2 y_3^2} \right) \left( p_{16} y_1 y_3^2 - p_{17} y_1 y_2 y_3 - p_{16} \mu \right)$$

$$D_{24}^{(lp)} = R_e^2 J_2 \left( \frac{-1}{4p_{51}^2 y_1^3 y_3} \right) \left( p_{17} y_1 y_3^2 - p_{16} y_1 y_2 y_3 - p_{17} \mu \right)$$

$$D_{34}^{(lp)} = R_e^2 J_2 \left( \frac{1}{4p_{51}^2 y_1^4 y_3^3} \right) \left( p_{17} y_1^2 y_2 y_3^3 + p_{16} y_1^2 y_2^2 y_3^2 + p_{16} \mu y_1 y_3^2 - 2p_{17} \mu y_1 y_2 y_3 - p_{16} \mu^2 \right)$$

$$D_{44}^{(lp)} = R_e^2 J_2 \left( \frac{-1}{32p_{51}^3 y_1^4 y_3^4} \right) \left( 8p_{19} y_1^2 y_2 y_3^3 y_4 y_5 - 8p_{18} \mu y_1 y_2 y_3 y_4 y_5 - p_{20} y_1^2 y_3^4 + p_{21} y_1^2 y_2^2 y_3^2 \right.$$
$$\left. + 2p_{21} \mu y_1 y_3^2 - p_{22} \mu^2 \right)$$

$$D_{54}^{(lp)} = R_e^2 J_2 \left( \frac{-1}{16p_{51}^3 y_1^4 y_3^4} \right) \left( p_{23} y_1^2 y_3^4 y_4 y_5 - p_{24} y_1^2 y_2^2 y_3^2 y_4 y_5 - 2p_{24} \mu y_1 y_3^2 y_4 y_5 + p_{25} \mu^2 y_4 y_5 \right.$$
$$\left. + p_{26} y_1^2 y_2 y_3^3 + p_{27} \mu y_1 y_2 y_3 \right)$$

$$D_{64}^{(lp)} = R_e^2 J_2 \left( \frac{1}{8p_{51}^3 y_1^4 y_3^4} \right) \left( p_{30} y_1^2 y_3^4 y_5 - p_{31} y_1^2 y_2^2 y_3^2 y_5 - 2p_{31} \mu y_1 y_3^2 y_5 + p_{32} \mu^2 y_5 \right.$$
$$\left. + 2p_{28} y_1^2 y_2 y_3^3 y_4 - 2p_{29} \mu y_1 y_2 y_3 y_4 \right)$$

$$D_{15}^{(lp)} = R_e^2 J_2 \left( \frac{1}{4p_{51}^2 y_1^2 y_3^2} \right) \left( p_{33} y_1 y_3^2 + p_{34} y_1 y_2 y_3 - p_{33} \mu \right)$$

$$D_{25}^{(lp)} = R_e^2 J_2 \left( \frac{-1}{4p_{51}^2 y_1^3 y_3} \right) \left( p_{34} y_1 y_3^2 + p_{33} y_1 y_2 y_3 - p_{34} \mu \right)$$

$$D_{35}^{(lp)} = R_e^2 J_2 \left( \frac{1}{4p_{51}^2 y_1^4 y_3^3} \right) \left( p_{34} y_1^2 y_2 y_3^3 - p_{33} y_1^2 y_2^2 y_3^2 - p_{33} \mu y_1 y_3^2 - 2p_{34} \mu y_1 y_2 y_3 + p_{33} \mu^2 \right)$$

$$D_{45}^{(lp)} = R_e^2 J_2 \left( \frac{1}{16p_{51}^3 y_1^4 y_3^4} \right) \left( p_{35} y_1^2 y_3^4 y_4 y_5 - p_{36} y_1^2 y_2^2 y_3^2 y_4 y_5 - 2p_{36} \mu y_1 y_3^2 y_4 y_5 + p_{37} \mu^2 y_4 y_5 \right.$$
$$\left. - p_{38} y_1^2 y_2 y_3^3 + p_{39} \mu y_1 y_2 y_3 \right)$$

$$D_{55}^{(lp)} = R_e^2 J_2 \left( \frac{-1}{32p_{51}^3 y_1^4 y_3^4} \right) \left( 8p_{40} y_1^2 y_2 y_3^3 y_4 y_5 + 8p_{41} \mu y_1 y_2 y_3 y_4 y_5 + p_{42} y_1^2 y_3^4 - p_{43} y_1^2 y_2^2 y_3^2 \right.$$
$$\left. - 2p_{43} \mu y_1 y_3^2 + p_{44} \mu^2 \right)$$

$$D_{65}^{(lp)} = R_e^2 J_2 \left( \frac{-1}{8p_{51}^3 y_1^4 y_3^4} \right) \left( 2p_{46} y_1^2 y_2 y_3^3 y_5 - 2p_{47} \mu y_1 y_2 y_3 y_5 - p_{45} y_1^2 y_3^4 y_4 + p_{48} y_1^2 y_2^2 y_3^2 y_4 \right.$$
$$\left. + 2p_{48} \mu y_1 y_3^2 y_4 - p_{49} \mu^2 y_4 \right)$$

$$D_{16}^{(lp)} = D_{26}^{(lp)} = D_{36}^{(lp)} = D_{46}^{(lp)} = D_{56}^{(lp)} = D_{66}^{(lp)} = 0$$

where $p_1$ through $p_{50}$ are a set of polynomial functions in $y_4$ and $y_5$, listed below.

### B.2 SHORT-PERIOD

$$D_{11}^{(sp)} = R_e^2 J_2 \left( \frac{-\mu}{2\pi_{26} y_1^3 y_3^3} \right) \left( 10\pi_1 \mu^3 + \pi_3 \mu^2 - \pi_4 \mu + 2\pi_2 \right)$$

$$D_{21}^{(sp)} = R_e^2 J_2 \left( \frac{\mu}{2\pi_{26} y_1^4 y_3^3} \right) \left( 7\pi_1 \mu^3 y_2 + \pi_6 \mu^2 - \pi_7 \mu + 3\pi_5 \right)$$

$$D_{31}^{(sp)} = R_e^2 J_2 \left( \frac{\mu}{2\pi_{26} y_1^5 y_3^3} \right) \left( 2\pi_8 \mu^3 + \pi_{10} \mu^2 - \pi_{11} \mu + 3\pi_9 \right)$$

$$D_{41}^{(sp)} = R_e^2 J_2 \left( \frac{\mu}{2\pi_{26} y_1^5 y_3^4} \right) \left( 24\pi_{12} \Gamma \mu y_5 + 2\pi_{13} \mu^3 + \pi_{15} \mu^2 - \pi_{16} \mu + 3\pi_{14} \right)$$

$$D_{51}^{(sp)} = R_e^2 J_2 \left( \frac{-\mu}{2\pi_{26} y_1^5 y_3^4} \right) \left( 24\pi_{12} \Gamma \mu y_4 + 2\pi_{17} \mu^3 - \pi_{19} \mu^2 + \pi_{20} \mu + 3\pi_{18} \right)$$

$$D_{61}^{(sp)} = R_e^2 J_2 \left( \frac{\mu}{2\pi_{26} y_1^5 y_3^4} \right) \left( 2\pi_{21} \mu^3 + \pi_{23} \mu^2 + 12\pi_{25} \Gamma \mu - \pi_{24} \mu + 3\pi_{22} \right)$$

$$D_{12}^{(sp)} = R_e^2 J_2 \left( \frac{\mu}{2\pi_{26} y_1 y_3^3} \right) \pi_1 y_2 \left( 3y_1^2 y_3^4 + 2y_1^2 y_2^2 y_3^2 - 5\mu y_1 y_3^2 - 4\kappa \mu y_3 - 2\mu^2 \right)$$

$$D_{22}^{(sp)} = R_e^2 J_2 \left( \frac{-\mu}{2\pi_{26} y_1^3 y_3^3} \right) \pi_1 \big( 3y_1^3 y_2^2 y_3^4 - 2\mu y_1^2 y_3^4 - \kappa\mu y_1 y_3^3 + 2y_1^3 y_2^4 y_3^2 - 6\mu y_1^2 y_2^2 y_3^2$$
$$+ 3\mu^2 y_1 y_3^2 - 4\kappa\mu y_1 y_2^2 y_3 + 4\kappa\mu^2 y_3 - 2\mu^2 y_1 y_2^2 + 2\mu^3 \big)$$

$$D_{32}^{(sp)} = R_e^2 J_2 \left( \frac{\mu}{2\pi_{26} y_1^3 y_3^2} \right) \big( 2\pi_{27}\mu^2 + \pi_{28}\mu - \pi_{29} \big)$$

$$D_{42}^{(sp)} = R_e^2 J_2 \left( \frac{-\mu}{2\pi_{26} y_1^3 y_3^4} \right) \big( 24\pi_{38}\mu^3 y_5 + \pi_{30}\mu^2 - \pi_{31}\mu + \pi_{32} \big)$$

$$D_{52}^{(sp)} = R_e^2 J_2 \left( \frac{\mu}{2\pi_{26} y_1^3 y_3^4} \right) \big( 24\pi_{38}\mu^3 y_4 + \pi_{33}\mu^2 - \pi_{34}\mu + \pi_{35} \big)$$

$$D_{62}^{(sp)} = R_e^2 J_2 \left( \frac{-\mu}{2\pi_{26} y_1^3 y_3^4} \right) \big( 12\pi_{40}\mu^3 + 2\pi_{36}\mu^2 - \pi_{37}\mu + \pi_{39} \big)$$

$$D_{13}^{(sp)} = R_e^2 J_2 \left( \frac{-\mu}{2\pi_{26} y_1^2 y_3^4} \right) \big( 12\pi_1\mu^3 + 2\pi_{41}\mu^2 - \pi_{42}\mu + \pi_{43} \big)$$

$$D_{23}^{(sp)} = R_e^2 J_2 \left( \frac{\mu}{2\pi_{26} y_1^3 y_3^4} \right) \big( 6\pi_1\mu^3 y_2 + \pi_{44}\mu^2 - 2\pi_{46}\mu + \pi_{45} \big)$$

$$D_{33}^{(sp)} = R_e^2 J_2 \left( \frac{\mu}{2\pi_{26} y_1^4 y_3^4} \right) \big( 2\pi_{47}\mu^3 + 2\pi_{48}\mu^2 - \pi_{49}\mu + \pi_{50} \big)$$

$$D_{43}^{(sp)} = R_e^2 J_2 \left( \frac{\mu}{2\pi_{26} y_1^4 y_3^5} \right) \big( 24\pi_{12}\Gamma\mu y_5 + 2\pi_{51}\mu^3 + \pi_{52}\mu^2 - \pi_{53}\mu + \pi_{54} \big)$$

$$D_{53}^{(sp)} = R_e^2 J_2 \left( \frac{-\mu}{2\pi_{26} y_1^4 y_3^5} \right) \big( 24\pi_{12}\Gamma\mu y_4 + 2\pi_{55}\mu^3 - \pi_{56}\mu^2 + \pi_{58}\mu + \pi_{57} \big)$$

$$D_{63}^{(sp)} = R_e^2 J_2 \left( \frac{\mu}{2\pi_{26} y_1^4 y_3^5} \right) \big( 8\pi_{59}\mu^3 + 2\pi_{60}\mu^2 + 12\pi_{25}\Gamma\mu - \pi_{61}\mu + \pi_{62} \big)$$

$$D_{14}^{(sp)} = R_e^2 J_2 \left( \frac{-2\mu}{y_1^3 y_3^3 (\kappa y_3 + \mu)} \right) \big( \pi_{63}\mu - \pi_{64} \big)$$

$$D_{24}^{(sp)} = R_e^2 J_2 \left( \frac{-2\mu}{y_1^3 y_3^3 (y_1^2 y_3^3 + y_1^2 y_2^2 y_3 - 2\mu y_1 y_3 - \kappa\mu)} \right) \big( 6\pi_{65}\mu^2 y_2 y_4 + \pi_{66}\mu - \pi_{67} \big)$$

$$D_{34}^{(sp)} = R_e^2 J_2 \left( \frac{-2\mu}{y_1^4 y_3^3 (\kappa y_3 + \mu)} \right) \big( 2\mu^2 y_4^3 - \mu^2 y_4 + \pi_{68}\mu + \pi_{69} \big)$$

$$D_{44}^{(sp)} = R_e^2 J_2 \left( \frac{-\mu}{4 y_1^4 y_3^4 (\kappa y_3 + \mu)} \right) \big( 120\pi_{65}\Gamma\kappa\mu y_3 y_4 y_5 + 120\pi_{65}\Gamma\mu^2 y_4 y_5 - \pi_{71}\mu^2 + \pi_{72}\mu + 4\pi_{70} \big)$$

$$D_{54}^{(sp)} = R_e^2 J_2 \left( \frac{\mu}{2 y_1^4 y_3^4 (\kappa y_3 + \mu)} \right) \big( 6\pi_{73}\Gamma\kappa\mu y_3 + 6\pi_{73}\Gamma\mu^2 - \pi_{74}\mu^2 - \pi_{75}\mu + \pi_{76} \big)$$

$$D_{64}^{(sp)} = R_e^2 J_2 \left( \frac{-\mu}{y_1^4 y_3^4 (\kappa y_3 + \mu)} \right) \big( 12\pi_{77}\Gamma\kappa\mu y_3 y_4 + 12\pi_{77}\Gamma\mu^2 y_4 - \pi_{78}\mu^2 + \pi_{80}\mu + 2\pi_{79} \big)$$

$$D_{15}^{(sp)} = R_e^2 J_2 \left( \frac{-2\mu}{y_1^3 y_3^3 (\kappa y_3 + \mu)} \right) \big( \pi_{81}\mu - \pi_{82} \big)$$

$$D_{25}^{(sp)} = R_e^2 J_2 \left( \frac{-2\mu}{y_1^3 y_3^3 (y_1^2 y_3^3 + y_1^2 y_2^2 y_3 - 2\mu y_1 y_3 - \kappa\mu)} \right) \big( 6\pi_{65}\mu^2 y_2 y_5 - \pi_{84}\mu - \pi_{83} \big)$$

$$D_{35}^{(sp)} = R_e^2 J_2 \left( \frac{2\mu}{y_1^4 y_3^3 (\kappa y_3 + \mu)} \right) \left( 2\mu^2 y_5^3 - \mu^2 y_5 + \pi_{85}\mu - \pi_{86} \right)$$

$$D_{45}^{(sp)} = R_e^2 J_2 \left( \frac{-\mu}{2y_1^4 y_3^4 (\kappa y_3 + \mu)} \right) \left( 6\pi_{88}\Gamma\kappa\mu y_3 + 6\pi_{88}\Gamma\mu^2 - \pi_{87}\mu^2 - \pi_{89}\mu + \pi_{90} \right)$$

$$D_{55}^{(sp)} = R_e^2 J_2 \left( \frac{\mu}{4y_1^4 y_3^4 (\kappa y_3 + \mu)} \right) \left( 120\pi_{65}\Gamma\kappa\mu y_3 y_4 y_5 + 120\pi_{65}\Gamma\mu^2 y_4 y_5 - \pi_{91}\mu^2 + \pi_{93}\mu + 4\pi_{92} \right)$$

$$D_{65}^{(sp)} = R_e^2 J_2 \left( \frac{-\mu}{y_1^4 y_3^4 (\kappa y_3 + \mu)} \right) \left( 12\pi_{77}\Gamma\kappa\mu y_3 y_5 + 12\pi_{77}\Gamma\mu^2 y_5 - \pi_{94}\mu^2 - \pi_{95}\mu + 2\pi_{96} \right)$$

$$D_{16}^{(sp)} = D_{26}^{(sp)} = D_{36}^{(sp)} = D_{46}^{(sp)} = D_{56}^{(sp)} = D_{66}^{(sp)} = 0$$

where $\Gamma$ is the difference between eccentric and true anomaly; $\kappa = \sqrt{y_1 \left( 2\mu - y_1 y_2^2 - y_1 y_3^2 \right)}$; and $\pi_1$ through $\pi_{96}$ are a set of polynomial functions in $y_1$, $y_2$, $y_3$, $y_4$, $y_5$, and $\kappa$, listed below. In terms of Hoots position elements,

$$\Gamma = \text{atan2}\left( \kappa y_2 \, , y_1 y_3^2 + y_1 y_2^2 - \mu \right) - \text{atan2}\left( y_1 y_2 y_3 \, , y_1 y_3^2 - \mu \right)$$

where $\text{atan2}$ is the quadrant-specific inverse tangent function.

### B.3 POLYNOMIAL FUNCTIONS USED IN THE SENSITIVITY MATRIX

$$\begin{aligned}
p_1 = {} & 300y_5^{10} + 1200y_4^2 y_5^8 - 750y_5^8 + 1800y_4^4 y_5^6 - 2400y_4^2 y_5^6 + 720y_5^6 + 1200y_4^6 y_5^4 - 2700y_4^4 y_5^4 \\
& + 1750y_4^2 y_5^4 - 330y_5^4 + 300y_4^8 y_5^2 - 1200y_4^6 y_5^2 + 1340y_4^4 y_5^2 - 560y_4^2 y_5^2 + 74y_5^2 - 150y_4^8 \\
& + 310y_4^6 - 230y_4^4 + 70y_4^2 - 7 \\
p_2 = {} & 300y_5^{12} + 1800y_4^2 y_5^{10} - 750y_5^{10} + 4500y_4^4 y_5^8 - 4050y_4^2 y_5^8 + 840y_5^8 + 6000y_4^6 y_5^6 \\
& - 8700y_4^4 y_5^6 + 4000y_4^2 y_5^6 - 565y_5^6 + 4500y_4^8 y_5^4 - 9300y_4^6 y_5^4 + 6960y_4^4 y_5^4 - 2205y_4^2 y_5^4 \\
& + 244y_5^4 + 1800y_4^{10} y_5^2 - 4950y_4^8 y_5^2 + 5280y_4^6 y_5^2 - 2715y_4^4 y_5^2 + 668y_4^2 y_5^2 - 62y_5^2 \\
& + 300y_4^{12} - 1050y_4^{10} + 1480y_4^8 - 1075y_4^6 + 424y_4^4 - 86y_4^2 + 7
\end{aligned}$$

$$
\begin{aligned}
p_3 = y_5\big(&1200y_5^{12} + 5400y_4^2y_5^{10} - 3600y_5^{10} + 9000y_4^4y_5^8 - 12900y_4^2y_5^8 + 4250y_5^8 + 6000y_4^6y_5^6 \\
&- 15600y_4^4y_5^6 + 11460y_4^2y_5^6 - 2500y_5^6 - 5400y_4^6y_5^4 + 8880y_4^4y_5^4 - 4650y_4^2y_5^4 + 766y_5^4 \\
&- 1800y_4^{10}y_5^2 + 2400y_4^8y_5^2 + 380y_4^6y_5^2 - 1800y_4^4y_5^2 + 848y_4^2y_5^2 - 116y_5^2 - 600y_4^{12} \\
&+ 1500y_4^{10} - 1290y_4^8 + 350y_4^6 + 82y_4^4 - 56y_4^2 + 7\big) \\
p_4 = y_4\big(&1500y_5^{12} + 7800y_4^2y_5^{10} - 4350y_5^{10} + 16500y_4^4y_5^8 - 18450y_4^2y_5^8 + 4960y_5^8 \\
&+ 18000y_4^6y_5^6 - 30300y_4^4y_5^6 + 16360y_4^2y_5^6 - 2805y_5^6 + 10500y_4^8y_5^4 - 23700y_4^6y_5^4 \\
&+ 19320y_4^4y_5^4 - 6685y_4^2y_5^4 + 820y_5^4 + 3000y_4^{10}y_5^2 - 8550y_4^8y_5^2 + 9400y_4^6y_5^2 \\
&- 4955y_4^4y_5^2 + 1244y_4^2y_5^2 - 118y_5^2 + 300y_4^{12} - 1050y_4^{10} + 1480y_4^8 - 1075y_4^6 \\
&+ 424y_4^4 - 86y_4^2 + 7\big) \\
p_5 = y_4\big(&2700y_5^{12} + 13800y_4^2y_5^{10} - 7950y_5^{10} + 28500y_4^4y_5^8 - 32850y_4^2y_5^8 + 9080y_5^8 \\
&+ 30000y_4^6y_5^6 - 51900y_4^4y_5^6 + 28720y_4^2y_5^6 - 5045y_5^6 + 16500y_4^8y_5^4 - 38100y_4^6y_5^4 \\
&+ 31680y_4^4y_5^4 - 11165y_4^2y_5^4 + 1396y_5^4 + 4200y_4^{10}y_5^2 - 12150y_4^8y_5^2 + 13520y_4^6y_5^2 \\
&- 7195y_4^4y_5^2 + 1820y_4^2y_5^2 - 174y_5^2 + 300y_4^{12} - 1050y_4^{10} + 1480y_4^8 - 1075y_4^6 \\
&+ 424y_4^4 - 86y_4^2 + 7\big) \\
p_6 = y_4\big(&300y_4^2y_5^8 - 150y_5^8 + 1200y_4^4y_5^6 - 1200y_4^2y_5^6 + 310y_5^6 + 1800y_4^6y_5^4 - 2700y_4^4y_5^4 \\
&+ 1340y_4^2y_5^4 - 230y_5^4 + 1200y_4^8y_5^2 - 2400y_4^6y_5^2 + 1750y_4^4y_5^2 - 560y_4^2y_5^2 + 70y_5^2 \\
&+ 300y_4^10 - 750y_4^8 + 720y_4^6 - 330y_4^4 + 74y_4^2 - 7\big) \\
p_7 = y_5\big(&300y_5^{12} + 1800y_4^2y_5^{10} - 1050y_5^{10} + 4500y_4^4y_5^8 - 4950y_4^2y_5^8 + 1480y_5^8 + 6000y_4^6y_5^6 \\
&- 9300y_4^4y_5^6 + 5280y_4^2y_5^6 - 1075y_5^6 + 4500y_4^8y_5^4 - 8700y_4^6y_5^4 + 6960y_4^4y_5^4 \\
&- 2715y_4^2y_5^4 + 424y_5^4 + 1800y_4^{10}y_5^2 - 4050y_4^8y_5^2 + 4000y_4^6y_5^2 - 2205y_4^4y_5^2 \\
&+ 668y_4^2y_5^2 - 86y_5^2 + 300y_4^{12} - 750y_4^{10} + 840y_4^8 - 565y_4^6 + 244y_4^4 - 62y_4^2 + 7\big)
\end{aligned}
$$

$$
\begin{aligned}
p_8 = y_5\big(&300y_5^{12} + 3000y_4^2y_5^{10} - 1050y_5^{10} + 10500y_4^4y_5^8 - 8550y_4^2y_5^8 + 1480y_5^8 \\
&+ 18000y_4^6y_5^6 - 23700y_4^4y_5^6 + 9400y_4^2y_5^6 - 1075y_5^6 + 16500y_4^8y_5^4 - 30300y_4^6y_5^4 \\
&+ 19320y_4^4y_5^4 - 4955y_4^2y_5^4 + 424y_5^4 + 7800y_4^{10}y_5^2 - 18450y_4^8y_5^2 + 16360y_4^6y_5^2 \\
&- 6685y_4^4y_5^2 + 1244y_4^2y_5^2 - 86y_5^2 + 1500y_4^{12} - 4350y_4^{10} + 4960y_4^8 - 2805y_4^6 \\
&+ 820y_4^4 - 118y_4^2 + 7\big) \\
p_9 = y_5\big(&300y_5^{12} + 4200y_4^2y_5^{10} - 1050y_5^{10} + 16500y_4^4y_5^8 - 12150y_4^2y_5^8 + 1480y_5^8 \\
&+ 30000y_4^6y_5^6 - 38100y_4^4y_5^6 + 13520y_4^2y_5^6 - 1075y_5^6 + 28500y_4^8y_5^4 - 51900y_4^6y_5^4 \\
&+ 31680y_4^4y_5^4 - 7195y_4^2y_5^4 + 424y_5^4 + 13800y_4^{10}y_5^2 - 32850y_4^8y_5^2 + 28720y_4^6y_5^2 \\
&- 11165y_4^4y_5^2 + 1820y_4^2y_5^2 - 86y_5^2 + 2700y_4^{12} - 7950y_4^{10} + 9080y_4^8 - 5045y_4^6 \\
&+ 1396y_4^4 - 174y_4^2 + 7\big) \\
p_{10} = y_4\big(&600y_5^{12} + 1800y_4^2y_5^{10} - 1500y_5^{10} - 2400y_4^2y_5^8 + 1290y_5^8 - 6000y_4^6y_5^6 + 5400y_4^4y_5^6 \\
&- 380y_4^2y_5^6 - 350y_5^6 - 9000y_4^8y_5^4 + 15600y_4^6y_5^4 - 8880y_4^4y_5^4 + 1800y_4^2y_5^4 - 82y_5^4 \\
&- 5400y_4^{10}y_5^2 + 12900y_4^8y_5^2 - 11460y_4^6y_5^2 + 4650y_4^4y_5^2 - 848y_4^2y_5^2 + 56y_5^2 \\
&- 1200y_4^{12} + 3600y_4^{10} - 4250y4^8 + 2500y_4^6 - 766y_4^4 + 116y_4^2 - 7\big) \\
p_{11} = y_4y_5\big(&150y_5^8 + 600y_4^2y_5^6 - 300y_5^6 + 900y_4^4y_5^4 - 900y_4^2y_5^4 + 205y_5^4 + 600y_4^6y_5^2 \\
&- 900y_4^4y_5^2 + 410y_4^2y_5^2 - 50y_5^2 + 150y_4^8 - 300y_4^6 + 205y_4^4 - 50y_4^2 + 2\big) \\
p_{12} = &150y_5^8 + 600y_4^2y_5^6 - 300y_5^6 + 900y_4^4y_5^4 - 900y_4^2y_5^4 + 210y_5^4 + 600y_4^6y_5^2 - 900y_4^4y_5^2 \\
&+ 420y_4^2y_5^2 - 60y_5^2 + 150y_4^8 - 300y_4^6 + 210y_4^4 - 60y_4^2 + 7 \\
p_{13} = y_4y_5\big(&450y_5^{10} + 2250y_4^2y_5^8 - 1200y_5^8 + 4500y_4^4y_5^6 - 4800y_4^2y_5^6 + 1235y_5^6 + 4500y_4^6y_5^4 \\
&- 7200y_4^4y_5^4 + 3705y_4^2y_5^4 - 610y_5^4 + 2250y_4^8y_5^2 - 4800y_4^6y_5^2 + 3705y_4^4y_5^2 \\
&- 1220y_4^2y_5^2 + 146y_5^2 + 450y_4^{10} - 1200y_4^8 + 1235y_4^6 - 610y_4^4 + 146y_4^2 - 14\big)
\end{aligned}
$$

$$
\begin{aligned}
p_{14} &= 600y_5^{10} + 3000y_4^2y_5^8 - 1650y_5^8 + 6000y_4^4y_5^6 - 6600y_4^2y_5^6 + 1750y_5^6 + 6000y_4^6y_5^4 \\
&\quad - 9900y_4^4y_5^4 + 5250y_4^2y_5^4 - 890y_5^4 + 3000y_4^8y_5^2 - 6600y_4^6y_5^2 + 5250y_4^4y_5^2 \\
&\quad - 1780y_4^2y_5^2 + 218y_5^2 + 600y_4^{10} - 1650y_4^8 + 1750y_4^6 - 890y_4^4 + 218y_4^2 - 21 \\
p_{15} &= y_4y_5\big(750y_5^{10} + 3750y_4^2y_5^8 - 2100y_5^8 + 7500y_4^4y_5^6 - 8400y_4^2y_5^6 + 2265y_5^6 + 7500y_4^6y_5^4 \\
&\quad - 12600y_4^4y_5^4 + 6795y_4^2y_5^4 - 1170y_5^4 + 3750y_4^8y_5^2 - 8400y_4^6y_5^2 + 6795y_4^4y_5^2 \\
&\quad - 2340y_4^2y_5^2 + 290y_5^2 + 750y_4^{10} - 2100y_4^8 + 2265y_4^6 - 1170y_4^4 + 290y_4^2 - 28\big) \\
p_{16} &= y_4\big(300y_4^2y_5^8 - 150y_5^8 + 1200y_4^4y_5^6 - 1200y_4^2y_5^6 + 310y_5^6 + 1800y_4^6y_5^4 - 2700y_4^4y_5^4 \\
&\quad + 1340y_4^2y_5^4 - 230y_5^4 + 1200y_4^8y_5^2 - 2400y_4^6y_5^2 + 1750y_4^4y_5^2 - 560y_4^2y_5^2 + 70y_5^2 \\
&\quad + 300y_4^{10} - 750y_4^8 + 720y_4^6 - 330y_4^4 + 74y_4^2 - 7\big) \\
p_{17} &= y_5\big(150y_5^{10} + 1050y_4^2y_5^8 - 450y_5^8 + 2700y_4^4y_5^6 - 2400y_4^2y_5^6 + 515y_5^6 + 3300y_4^6y_5^4 \\
&\quad - 4500y_4^4y_5^4 + 1955y_4^2y_5^4 - 280y_5^4 + 1950y_4^8y_5^2 - 3600y_4^6y_5^2 + 2365y_4^4y_5^2 \\
&\quad - 660y_4^2y_5^2 + 72y_5^2 + 450y_4^{10} - 1050y_4^8 + 925y_4^6 - 380y_4^4 + 76y_4^2 - 7\big) \\
p_{18} &= 1500y_5^{14} + 6000y_4^2y_5^{12} - 3750y_5^{12} + 4500y_4^4y_5^{10} - 9000y_4^2y_5^{10} + 3100y_5^{10} \\
&\quad - 15000y_4^6y_5^8 + 11250y_4^4y_5^8 - 650y_4^2y_5^8 - 475y_5^8 - 37500y_4^8y_5^6 + 60000y_4^6y_5^6 \\
&\quad - 33600y_4^4y_5^6 + 7900y_4^2y_5^6 - 685y_5^6 - 36000y_4^{10}y_5^4 + 78750y_4^8y_5^4 - 65900y_4^6y_5^4 \\
&\quad + 26550y_4^4y_5^4 - 5235y_4^2y_5^4 + 405y_5^4 - 16500y_4^{12}y_5^2 + 45000y_4^{10}y_5^2 - 49100y_4^8y_5^2 \\
&\quad + 27500y_4^6y_5^2 - 8415y_4^4y_5^2 + 1350y_4^2y_5^2 - 86y_5^2 - 3000y_4^{14} + 9750y_4^{12} - 13050y_4^{10} \\
&\quad + 9325y_4^8 - 3865y_4^6 + 945y_4^4 - 128y_4^2 + 7
\end{aligned}
$$

$$
\begin{aligned}
p_{19} = {} & 1500y_5^{14} + 9000y_4^2y_5^{12} - 5250y_5^{12} + 22500y_4^4y_5^{10} - 27000y_4^2y_5^{10} + 7700y_5^{10} \\
& + 30000y_4^6y_5^8 - 56250y_4^4y_5^8 + 33050y_4^2y_5^8 - 6175y_5^8 + 22500y_4^8y_5^6 - 60000y_4^6y_5^6 \\
& + 55200y_4^4y_5^6 - 21200y_4^2y_5^6 + 2935y_5^6 + 9000y_4^{10}y_5^4 - 33750y_4^8y_5^4 + 44300y_4^6y_5^4 \\
& - 26550y_4^4y_5^4 + 7485y_4^2y_5^4 - 825y_5^4 + 1500y_4^{12}y_5^2 - 9000y_4^{10}y_5^2 + 16700y_4^8y_5^2 \\
& - 14200y_4^6y_5^2 + 6165y_4^4y_5^2 - 1350y_4^2y_5^2 + 124y_5^2 - 750y_4^{12} + 2250y_4^{10} - 2675y_4^8 \\
& + 1615y_4^6 - 525y_4^4 + 90y_4^2 - 7 \\
p_{20} = {} & 1500y_5^{16} + 18000y_4^2y_5^{14} - 5250y_5^{14} + 84000y_4^4y_5^{12} - 60750y_4^2y_5^{12} + 8250y_5^{12} \\
& + 210000y_4^6y_5^{10} - 254250y_4^4y_5^{10} + 89700y_4^2y_5^{10} - 7775y_5^{10} + 315000y_4^8y_5^8 \\
& - 543750y_4^6y_5^8 + 324350y_4^4y_5^8 - 75675y_4^2y_5^8 + 4885y_5^8 + 294000y_4^{10}y_5^6 \\
& - 663750y_4^8y_5^6 + 565400y_4^6y_5^6 - 223550y_4^4y_5^6 + 39300y_4^2y_5^6 - 2095y_5^6 \\
& + 168000y_4^{12}y_5^4 - 470250y_4^{10}y_5^4 + 523350y_4^8y_5^4 - 294350y_4^6y_5^4 + 87030y_4^4y_5^4 \\
& - 12405y_4^2y_5^4 + 589y_5^4 + 54000y_4^{14}y_5^2 - 180750y_4^{12}y_5^2 + 248900y_4^{10}y_5^2 \\
& - 181875y_4^8y_5^2 + 75700y_4^6y_5^2 - 17805y_4^4y_5^2 + 2154y_4^2y_5^2 - 97y_5^2 + 7500y_4^{16} \\
& - 29250y_4^{14} + 48050y_4^{12} - 43175y_4^{10} + 23085y_4^8 - 7495y_4^6 + 1445y_4^4 - 153y_4^2 + 7 \\
p_{21} = {} & 7500y_5^{16} + 72000y_4^2y_5^{14} - 29250y_5^{14} + 282000y_4^4y_5^{12} - 240750y_4^2y_5^{12} + 48050y_5^{12} \\
& + 600000y_4^6y_5^{10} - 794250y_4^4y_5^{10} + 331500y_4^2y_5^{10} - 43175y_5^{10} + 765000y_4^8y_5^8 \\
& - 1383750y_4^6y_5^8 + 893550y_4^4y_5^8 - 242475y_4^2y_5^8 + 23085y_5^8 + 600000y_4^{10}y_5^6 \\
& - 1383750y_4^8y_5^6 + 1220200y_4^6y_5^6 - 511550y_4^4y_5^6 + 101340y_4^2y_5^6 - 7495y_5^6 \\
& + 282000y_4^{12}y_5^4 - 794250y_4^{10}y_5^4 + 893550y_4^8y_5^4 - 511550y_4^6y_5^4 + 156510y_4^4y_5^4 \\
& - 24165y_4^2y_5^4 + 1445y_5^4 + 72000y_4^{14}y_5^2 - 240750y_4^{12}y_5^2 + 331500y_4^{10}y_5^2 \\
& - 242475y_4^8y_5^2 + 101340y_4^6y_5^2 - 24165y_4^4y_5^2 + 3042y_4^2y_5^2 - 153y_5^2 + 7500y_4^{16} \\
& - 29250y_4^{14} + 48050y_4^{12} - 43175y_4^{10} + 23085y_4^8 - 7495y_4^6 + 1445y_4^4 - 153y_4^2 + 7
\end{aligned}
$$

$$
\begin{aligned}
p_{22} = {} & 13500y_5^{16} + 126000y_4^2y_5^{14} - 53250y_5^{14} + 480000y_4^4y_5^{12} - 420750y_4^2y_5^{12} + 87850y_5^{12} \\
& + 990000y_4^6y_5^{10} - 1334250y_4^4y_5^{10} + 573300y_4^2y_5^{10} - 78575y_5^{10} + 1215000y_4^8y_5^8 \\
& - 2223750y_4^6y_5^8 + 1462750y_4^4y_5^8 - 409275y_4^2y_5^8 + 41285y_5^8 + 906000y_4^{10}y_5^6 \\
& - 2103750y_4^8y_5^6 + 1875000y_4^6y_5^6 - 799550y_4^4y_5^6 + 163380y_4^2y_5^6 - 12895y_5^6 \\
& + 396000y_4^{12}y_5^4 - 1118250y_4^{10}y_5^4 + 1263750y_4^8y_5^4 - 728750y_4^6y_5^4 + 225990y_4^4y_5^4 \\
& - 35925y_4^2y_5^4 + 2301y_5^4 + 90000y_4^{14}y_5^2 - 300750y_4^{12}y_5^2 + 414100y_4^{10}y_5^2 \\
& - 303075y_4^8y_5^2 + 126980y_4^6y_5^2 - 30525y_4^4y_5^2 + 3930y_4^2y_5^2 - 209y_5^2 + 7500y_4^{16} \\
& - 29250y_4^{14} + 48050y_4^{12} - 43175y_4^{10} + 23085y_4^8 - 7495y_4^6 + 1445y_4^4 - 153y_4^2 + 7 \\
p_{23} = {} & 3000y_5^{14} + 21000y_4^2y_5^{12} - 9750y_5^{12} + 63000y_4^4y_5^{10} - 58500y_4^2y_5^{10} + 12850y_5^{10} \\
& + 105000y_4^6y_5^8 - 146250y_4^4y_5^8 + 64450y_4^2y_5^8 - 8625y_5^8 + 105000y_4^8y_5^6 \\
& - 195000y_4^6y_5^6 + 129300y_4^4y_5^6 - 35200y_4^2y_5^6 + 2965y_5^6 + 63000y_4^{10}y_5^4 \\
& - 146250y_4^8y_5^4 + 129700y_4^6y_5^4 - 53850y_4^4y_5^4 + 9675y_4^2y_5^4 - 405y_5^4 + 21000y_4^{12}y_5^2 \\
& - 58500y_4^{10}y_5^2 + 65050y_4^8y_5^2 - 36600y_4^6y_5^2 + 10455y_4^4y_5^2 - 1170y_4^2y_5^2 - 22y_5^2 \\
& + 3000y_4^{14} - 9750y_4^{12} + 13050y_4^{10} - 9325y_4^8 + 3745y_4^6 - 765y_4^4 + 38y_4^2 + 8 \\
p_{24} = {} & 9000y_5^{14} + 69000y_4^2y_5^{12} - 33750y_5^{12} + 225000y_4^4y_5^{10} - 220500y_4^2y_5^{10} + 52650y_5^{10} \\
& + 405000y_4^6y_5^8 - 596250y_4^4y_5^8 + 284850y_4^2y_5^8 - 44025y_5^8 + 435000y_4^8y_5^6 \\
& - 855000y_4^6y_5^6 + 612900y_4^4y_5^6 - 189400y_4^2y_5^6 + 21165y_5^6 + 279000y_4^{10}y_5^4 \\
& - 686250y_4^8y_5^4 + 656100y_4^6y_5^4 - 304050y_4^4y_5^4 + 67995y_4^2y_5^4 - 5805y_5^4 \\
& + 99000y_4^{12}y_5^2 - 292500y_4^{10}y_5^2 + 349650y_4^8y_5^2 - 216000y_4^6y_5^2 + 72495y_4^4y_5^2 \\
& - 12450y_4^2y_5^2 + 834y_5^2 + 15000y_4^{14} - 51750y_4^{12} + 74250y_4^{10} - 57325y_4^8 \\
& + 25665y_4^6 - 6645y_4^4 + 910y_4^2 - 48
\end{aligned}
$$

$$
\begin{aligned}
p_{25} = {} & 15000y_5^{14} + 117000y_4^2y_5^{12} - 57750y_5^{12} + 387000y_4^4y_5^{10} - 382500y_4^2y_5^{10} + 92450y_5^{10} \\
& + 705000y_4^6y_5^8 - 1046250y_4^4y_5^8 + 505250y_4^2y_5^8 - 79425y_5^8 + 765000y_4^8y_5^6 \\
& - 1515000y_4^6y_5^6 + 1096500y_4^4y_5^6 - 343600y_4^2y_5^6 + 39365y_5^6 + 495000y_4^{10}y_5^4 \\
& - 1226250y_4^8y_5^4 + 1182500y_4^6y_5^4 - 554250y_4^4y_5^4 + 126315y_4^2y_5^4 - 11205y_5^4 \\
& + 177000y_4^{12}y_5^2 - 526500y_4^{10}y_5^2 + 634250y_4^8y_5^2 - 395400y_4^6y_5^2 + 134535y_4^4y_5^2 \\
& - 23730y_4^2y_5^2 + 1690y_5^2 + 27000y_4^{14} - 93750y_4^{12} + 135450y_4^{10} - 105325y_4^8 \\
& + 47585y_4^6 - 12525y_4^4 + 1782y_4^2 - 104 \\
p_{26} = {} & 9000y_4^2y_5^{14} - 1500y_5^{14} + 69000y_4^4y_5^{12} - 45000y_4^2y_5^{12} + 5350y_5^{12} + 225000y_4^6y_5^{10} \\
& - 256500y_4^4y_5^{10} + 86700y_4^2y_5^{10} - 8000y_5^{10} + 405000y_4^8y_5^8 - 660000y_4^6y_5^8 \\
& + 375050y_4^4y_5^8 - 85650y_4^2y_5^8 + 6470y_5^8 + 435000y_4^{10}y_5^6 - 922500y_4^8y_5^6 \\
& + 740200y_4^6y_5^6 - 276600y_4^4y_5^6 + 47370y_4^2y_5^6 - 3040y_5^6 + 279000y_4^{12}y_5^4 \\
& - 729000y_4^{10}y_5^4 + 757050y_4^8y_5^4 - 395900y_4^6y_5^4 + 108570y_4^4y_5^4 - 14730y_4^2y_5^4 \\
& + 825y_5^4 + 99000y_4^{14}y_5^2 - 307500y_4^{12}y_5^2 + 392300y_4^{10}y_5^2 - 264600y_4^8y_5^2 \\
& + 100910y_4^6y_5^2 - 21540y_4^4y_5^2 + 2394y_4^2y_5^2 - 119y_5^2 + 15000y_4^{16} - 54000y_4^{14} \\
& + 81750y_4^{12} - 67650y_4^{10} + 33240y_4^8 - 9850y_4^6 + 1705y_4^4 - 159y_4^2 + 7
\end{aligned}
$$

$$
\begin{aligned}
p_{27} = {} & 3000y_5^{16} + 9000y_4^2y_5^{14} - 10500y_5^{14} - 39000y_4^4y_5^{12} - 9000y_4^2y_5^{12} + 14550y_5^{12} \\
& - 255000y_4^6y_5^{10} + 220500y_4^4y_5^{10} - 25500y_4^2y_5^{10} - 9700y_5^{10} - 585000y_4^8y_5^8 \\
& + 870000y_4^6y_5^8 - 410350y_4^4y_5^8 + 55350y_4^2y_5^8 + 2630y_5^8 - 717000y_4^{10}y_5^6 \\
& + 1462500y_4^8y_5^6 - 1095400y_4^6y_5^6 + 357600y_4^4y_5^6 - 43650y_4^2y_5^6 + 340y_5^6 \\
& - 501000y_4^{12}y_5^4 + 1287000y_4^{10}y_5^4 - 1297350y_4^8y_5^4 + 643700y_4^6y_5^4 - 159450y_4^4y_5^4 \\
& + 16950y_4^2y_5^4 - 397y_5^4 - 189000y_4^{14}y_5^2 + 583500y_4^{12}y_5^2 - 735100y_4^{10}y_5^2 \\
& + 484500y_4^8y_5^2 - 177430y_4^6y_5^2 + 35040y_4^4y_5^2 - 3234y_4^2y_5^2 + 91y_5^2 - 30000y_4^{16} \\
& + 108000y_4^{14} - 162850y_4^{12} + 133350y_4^{10} - 64260y_4^8 + 18430y_4^6 - 3005y_4^4 \\
& + 243y_4^2 - 7 \\
p_{28} = {} & 3000y_4^2y_5^{12} - 750y_5^{12} + 18000y_4^4y_5^{10} - 13500y_4^2y_5^{10} + 2250y_5^{10} + 45000y_4^6y_5^8 \\
& - 56250y_4^4y_5^8 + 22050y_4^2y_5^8 - 2700y_5^8 + 60000y_4^8y_5^6 - 105000y_4^6y_5^6 + 65700y_4^4y_5^6 \\
& - 17400y_4^2y_5^6 + 1690y_5^6 + 45000y_4^{10}y_5^4 - 101250y_4^8y_5^4 + 87300y_4^6y_5^4 - 36000y_4^4y_5^4 \\
& + 7170y_4^2y_5^4 - 585y_5^4 + 18000y_4^{12}y_5^2 - 49500y_4^{10}y_5^2 + 54450y_4^8y_5^2 - 30600y_4^6y_5^2 \\
& + 9270y_4^4y_5^2 - 1470y_4^2y_5^2 + 105y_5^2 + 3000y_4^{14} - 9750y_4^{12} + 13050y_4^{10} - 9300y_4^8 \\
& + 3790y_4^6 - 885y_4^4 + 113y_4^2 - 7 \\
p_{29} = {} & 6000y_4^2y_5^{12} - 2250y_5^{12} + 36000y_4^4y_5^{10} - 31500y_4^2y_5^{10} + 6850y_5^{10} + 90000y_4^6y_5^8 \\
& - 123750y_4^4y_5^8 + 55750y_4^2y_5^8 - 8400y_5^8 + 120000y_4^8y_5^6 - 225000y_4^6y_5^6 \\
& + 154500y_4^4y_5^6 - 46500y_4^2y_5^6 + 5310y_5^6 + 90000y_4^{10}y_5^4 - 213750y_4^8y_5^4 \\
& + 197500y_4^6y_5^4 - 89100y_4^4y_5^4 + 19890y_4^2y_5^4 - 1815y_5^4 + 36000y_4^{12}y_5^2 \\
& - 103500y_4^{10}y_5^2 + 120250y_4^8y_5^2 - 72300y_4^6y_5^2 + 23850y_4^4y_5^2 - 4170y_4^2y_5^2 + 315y_5^2 \\
& + 6000y_4^{14} - 20250y_4^{12} + 28350y_4^{10} - 21300y_4^8 + 9270y_4^6 - 2355y_4^4 + 331y_4^2 - 21
\end{aligned}
$$

$$
\begin{aligned}
p_{30} = {} & 750y_5^{14} + 6750y_4^2y_5^{12} - 2250y_5^{12} + 24750y_4^4y_5^{10} - 18000y_4^2y_5^{10} + 2675y_5^{10} \\
& + 48750y_4^6y_5^8 - 56250y_4^4y_5^8 + 18825y_4^2y_5^8 - 1575y_5^8 + 56250y_4^8y_5^6 - 90000y_4^6y_5^6 \\
& + 48550y_4^4y_5^6 - 9750y_4^2y_5^6 + 465y_5^6 + 38250y_4^{10}y_5^4 - 78750y_4^8y_5^4 + 59450y_4^6y_5^4 \\
& - 19800y_4^4y_5^4 + 2565y_4^2y_5^4 - 60y_5^4 + 14250y_4^{12}y_5^2 - 36000y_4^{10}y_5^2 + 35175y_4^8y_5^2 \\
& - 16650y_4^6y_5^2 + 3735y_4^4y_5^2 - 300y_4^2y_5^2 + 2y_5^2 + 2250y_4^{14} - 6750y_4^{12} + 8125y_4^{10} \\
& - 5025y_4^8 + 1635y_4^6 - 240y_4^4 + 6y_4^2 \\
p_{31} = {} & 2250y_5^{14} + 20250y_4^2y_5^{12} - 8250y_5^{12} + 74250y_4^4y_5^{10} - 63000y_4^2y_5^{10} + 12625y_5^{10} + 146250y_4^6y_5^8 \\
& - 191250y_4^4y_5^8 + 79275y_4^2y_5^8 - 10425y_5^8 + 168750y_4^8y_5^6 - 300000y_4^6y_5^6 + 190850y_4^4y_5^6 \\
& - 51450y_4^2y_5^6 + 5015y_5^6 + 114750y_4^{10}y_5^4 - 258750y_4^8y_5^4 + 223150y_4^6y_5^4 - 91800y_4^4y_5^4 \\
& + 18075y_4^2y_5^4 - 1410y_5^4 + 42750y_4^{12}y_5^2 - 117000y_4^{10}y_5^2 + 127725y_4^8y_5^2 - 70950y_4^6y_5^2 \\
& + 21105y_4^4y_5^2 - 3240y_4^2y_5^2 + 216y_5^2 + 6750y_4^{14} - 21750y_4^{12} + 28775y_4^{10} - 20175y_4^8 + 8045y_4^6 \\
& - 1830y_4^4 + 228y_4^2 - 14 \\
p_{32} = {} & 3750y_5^{14} + 33750y_4^2y_5^{12} - 14250y_5^{12} + 123750y_4^4y_5^{10} - 108000y_4^2y_5^{10} + 22575y_5^{10} + 243750y_4^6y_5^8 \\
& - 326250y_4^4y_5^8 + 139725y_4^2y_5^8 - 19275y_5^8 + 281250y_4^8y_5^6 - 510000y_4^6y_5^6 + 333150y_4^4y_5^6 \\
& - 93150y_4^2y_5^6 + 9565y_5^6 + 191250y_4^{10}y_5^4 - 438750y_4^8y_5^4 + 386850y_4^6y_5^4 - 163800y_4^4y_5^4 \\
& + 33585y_4^2y_5^4 - 2760y_5^4 + 71250y_4^{12}y_5^2 - 198000y_4^{10}y_5^2 + 220275y_4^8y_5^2 - 125250y_4^6y_5^2 \\
& + 38475y_4^4y_5^2 - 6180y_4^2y_5^2 + 430y_5^2 + 11250y_4^{14} - 36750y_4^{12} + 49425y_4^{10} - 35325y_4^8 \\
& + 14455y_4^6 - 3420y_4^4 + 450y_4^2 - 28 \\
p_{33} = {} & y_5\Big(300y_5^{10} + 1200y_4^2y_5^8 - 750y_5^8 + 1800y_4^4y_5^6 - 2400y_4^2y_5^6 + 720y_5^6 + 1200y_4^6y_5^4 - 2700y_4^4y_5^4 \\
& + 1750y_4^2y_5^4 - 330y_5^4 + 300y_4^8y_5^2 - 1200y_4^6y_5^2 + 1340y_4^4y_5^2 - 560y_4^2y_5^2 + 74y_5^2 - 150y_4^8 + 310y_4^6 \\
& - 230y_4^4 + 70y_4^2 - 7\Big)
\end{aligned}
$$

$$
\begin{aligned}
p_{34} = y_4\Big(&450y_5^{10} + 1950y_4^2y_5^8 - 1050y_5^8 + 3300y_4^4y_5^6 - 3600y_4^2y_5^6 + 925y_5^6 + 2700y_4^6y_5^4 - 4500y_4^4y_5^4 \\
&+ 2365y_4^2y_5^4 - 380y_5^4 + 1050y_4^8y_5^2 - 2400y_4^6y_5^2 + 1955y_4^4y_5^2 - 660y_4^2y_5^2 + 76y_5^2 + 150y_4^{10} \\
&- 450y_4^8 + 515y_4^6 - 280y_4^4 + 72y_4^2 - 7\Big)
\end{aligned}
$$

$$
\begin{aligned}
p_{35} = &3000y_5^{14} + 21000y_4^2y_5^{12} - 9750y_5^{12} + 63000y_4^4y_5^{10} - 58500y_4^2y_5^{10} + 13050y_5^{10} + 105000y_4^6y_5^8 \\
&- 146250y_4^4y_5^8 + 65050y_4^2y_5^8 - 9325y_5^8 + 105000y_4^8y_5^6 - 195000y_4^6y_5^6 + 129700y_4^4y_5^6 \\
&- 36600y_4^2y_5^6 + 3745y_5^6 + 63000y_4^{10}y_5^4 - 146250y_4^8y_5^4 + 129300y_4^6y_5^4 - 53850y_4^4y_5^4 \\
&+ 10455y_4^2y_5^4 - 765y_5^4 + 21000y_4^{12}y_5^2 - 58500y_4^{10}y_5^2 + 64450y_4^8y_5^2 - 35200y_4^6y_5^2 + 9675y_4^4y_5^2 \\
&- 1170y_4^2y_5^2 + 38y_5^2 + 3000y_4^{14} - 9750y_4^{12} + 12850y_4^{10} - 8625y_4^8 + 2965y_4^6 - 405y_4^4 - 22y_4^2 \\
&+ 8
\end{aligned}
$$

$$
\begin{aligned}
p_{36} = &15000y_5^{14} + 99000y_4^2y_5^{12} - 51750y_5^{12} + 279000y_4^4y_5^{10} - 292500y_4^2y_5^{10} + 74250y_5^{10} + 435000y_4^6y_5^8 \\
&- 686250y_4^4y_5^8 + 349650y_4^2y_5^8 - 57325y_5^8 + 405000y_4^8y_5^6 - 855000y_4^6y_5^6 + 656100y_4^4y_5^6 \\
&- 216000y_4^2y_5^6 + 25665y_5^6 + 225000y_4^{10}y_5^4 - 596250y_4^8y_5^4 + 612900y_4^6y_5^4 - 304050y_4^4y_5^4 \\
&+ 72495y_4^2y_5^4 - 6645y_5^4 + 69000y_4^{12}y_5^2 - 220500y_4^{10}y_5^2 + 284850y_4^8y_5^2 - 189400y_4^6y_5^2 \\
&+ 67995y_4^4y_5^2 - 12450y_4^2y_5^2 + 910y_5^2 + 9000y_4^{14} - 33750y_4^{12} + 52650y_4^{10} - 44025y_4^8 + 21165y_4^6 \\
&- 5805y_4^4 + 834y_4^2 - 48
\end{aligned}
$$

$$
\begin{aligned}
p_{37} = &27000y_5^{14} + 177000y_4^2y_5^{12} - 93750y_5^{12} + 495000y_4^4y_5^{10} - 526500y_4^2y_5^{10} + 135450y_5^{10} \\
&+ 765000y_4^6y_5^8 - 1226250y_4^4y_5^8 + 634250y_4^2y_5^8 - 105325y_5^8 + 705000y_4^8y_5^6 - 1515000y_4^6y_5^6 \\
&+ 1182500y_4^4y_5^6 - 395400y_4^2y_5^6 + 47585y_5^6 + 387000y_4^{10}y_5^4 - 1046250y_4^8y_5^4 + 1096500y_4^6y_5^4 \\
&- 554250y_4^4y_5^4 + 134535y_4^2y_5^4 - 12525y_5^4 + 117000y_4^{12}y_5^2 - 382500y_4^{10}y_5^2 + 505250y_4^8y_5^2 \\
&- 343600y_4^6y_5^2 + 126315y_4^4y_5^2 - 23730y_4^2y_5^2 + 1782y_5^2 + 15000y_4^{14} - 57750y_4^{12} + 92450y_4^{10} \\
&- 79425y_4^8 + 39365y_4^6 - 11205y_4^4 + 1690y_4^2 - 104
\end{aligned}
$$

$$
\begin{aligned}
p_{38} = {} & 15000y_5^{16} + 99000y_4^2y_5^{14} - 54000y_5^{14} + 279000y_4^4y_5^{12} - 307500y_4^2y_5^{12} + 81750y_5^{12} + 435000y_4^6y_5^{10} \\
& - 729000y_4^4y_5^{10} + 392300y_4^2y_5^{10} - 67650y_5^{10} + 405000y_4^8y_5^8 - 922500y_4^6y_5^8 + 757050y_4^4y_5^8 \\
& - 264600y_4^2y_5^8 + 33240y_5^8 + 225000y_4^{10}y_5^6 - 660000y_4^8y_5^6 + 740200y_4^6y_5^6 - 395900y_4^4y_5^6 \\
& + 100910y_4^2y_5^6 - 9850y_5^6 + 69000y_4^12y_5^4 - 256500y_4^{10}y_5^4 + 375050y_4^8y_5^4 - 276600y_4^6y_5^4 \\
& + 108570y_4^4y_5^4 - 21540y_4^2y_5^4 + 1705y_5^4 + 9000y_4^{14}y_5^2 - 45000y_4^{12}y_5^2 + 86700y_4^{10}y_5^2 - 85650y_4^8y_5^2 \\
& + 47370y_4^6y_5^2 - 14730y_4^4y_5^2 + 2394y_4^2y_5^2 - 159y_5^2 - 1500y_4^{14} + 5350y_4^{12} - 8000y_4^{10} + 6470y_4^8 \\
& - 3040y_4^6 + 825y_4^4 - 119y_4^2 + 7 \\
p_{39} = {} & 30000y_5^{16} + 189000y_4^2y_5^{14} - 108000y_5^{14} + 501000y_4^4y_5^{12} - 583500y_4^2y_5^{12} + 162850y_5^{12} \\
& + 717000y_4^6y_5^{10} - 1287000y_4^4y_5^{10} + 735100y_4^2y_5^{10} - 133350y_5^{10} + 585000y_4^8y_5^8 - 1462500y_4^6y_5^8 \\
& + 1297350y_4^4y_5^8 - 484500y_4^2y_5^8 + 64260y_5^8 + 255000y_4^{10}y_5^6 - 870000y_4^8y_5^6 + 1095400y_4^6y_5^6 \\
& - 643700y_4^4y_5^6 + 177430y_4^2y_5^6 - 18430y_5^6 + 39000y_4^{12}y_5^4 - 220500y_4^{10}y_5^4 + 410350y_4^8y_5^4 \\
& - 357600y_4^6y_5^4 + 159450y_4^4y_5^4 - 35040y_4^2y_5^4 + 3005y_5^4 - 9000y_4^{14}y_5^2 + 9000y_4^{12}y_5^2 + 25500y_4^{10}y_5^2 \\
& - 55350y_4^8y_5^2 + 43650y_4^6y_5^2 - 16950y_4^4y_5^2 + 3234y_4^2y_5^2 - 243y_5^2 - 3000y_4^{16} + 10500y_4^{14} \\
& - 14550y_4^{12} + 9700y_4^{10} - 2630y_4^8 - 340y_4^6 + 397y_4^4 - 91y_4^2 + 7 \\
p_{40} = {} & 1500y_4^2y_5^{12} - 750y_5^{12} + 9000y_4^4y_5^{10} - 9000y_4^2y_5^{10} + 2250y_5^{10} + 22500y_4^6y_5^8 - 33750y_4^4y_5^8 \\
& + 16700y_4^2y_5^8 - 2675y_5^8 + 30000y_4^8y_5^6 - 60000y_4^6y_5^6 + 44300y_4^4y_5^6 - 14200y_4^2y_5^6 + 1615y_5^6 \\
& + 22500y_4^{10}y_5^4 - 56250y_4^8y_5^4 + 55200y_4^6y_5^4 - 26550y_4^4y_5^4 + 6165y_4^2y_5^4 - 525y_5^4 + 9000y_4^{12}y_5^2 \\
& - 27000y_4^{10}y_5^2 + 33050y_4^8y_5^2 - 21200y_4^6y_5^2 + 7485y_4^4y_5^2 - 1350y_4^2y_5^2 + 90y_5^2 + 1500y_4^{14} \\
& - 5250y_4^{12} + 7700y_4^{10} - 6175y_4^8 + 2935y_4^6 - 825y_4^4 + 124y_4^2 - 7
\end{aligned}
$$

$$
\begin{aligned}
p_{41} = {} & 3000y_5^{14} + 16500y_4^2y_5^{12} - 9750y_5^{12} + 36000y_4^4y_5^{10} - 45000y_4^2y_5^{10} + 13050y_5^{10} + 37500y_4^6y_5^8 \\
& - 78750y_4^4y_5^8 + 49100y_4^2y_5^8 - 9325y_5^8 + 15000y_4^8y_5^6 - 60000y_4^6y_5^6 + 65900y_4^4y_5^6 - 27500y_4^2y_5^6 \\
& + 3865y_5^6 - 4500y_4^{10}y_5^4 - 11250y_4^8y_5^4 + 33600y_4^6y_5^4 - 26550y_4^4y_5^4 + 8415y_4^2y_5^4 - 945y_5^4 \\
& - 6000y_4^{12}y_5^2 + 9000y_4^{10}y_5^2 + 650y_4^8y_5^2 - 7900y_4^6y_5^2 + 5235y_4^4y_5^2 - 1350y_4^2y_5^2 + 128y_5^2 \\
& - 1500y_4^{14} + 3750y_4^{12} - 3100y_4^{10} + 475y_4^8 + 685y_4^6 - 405y_4^4 + 86y_4^2 - 7 \\
p_{42} = {} & 7500y_5^{16} + 54000y_4^2y_5^{14} - 29250y_5^{14} + 168000y_4^4y_5^{12} - 180750y_4^2y_5^{12} + 48050y_5^{12} + 294000y_4^6y_5^{10} \\
& - 470250y_4^4y_5^{10} + 248900y_4^2y_5^{10} - 43175y_5^{10} + 315000y_4^8y_5^8 - 663750y_4^6y_5^8 + 523350y_4^4y_5^8 \\
& - 181875y_4^2y_5^8 + 23085y_5^8 + 210000y_4^{10}y_5^6 - 543750y_4^8y_5^6 + 565400y_4^6y_5^6 - 294350y_4^4y_5^6 \\
& + 75700y_4^2y_5^6 - 7495y_5^6 + 84000y_4^{12}y_5^4 - 254250y_4^{10}y_5^4 + 324350y_4^8y_5^4 - 223550y_4^6y_5^4 \\
& + 87030y_4^4y_5^4 - 17805y_4^2y_5^4 + 1445y_5^4 + 18000y_4^{14}y_5^2 - 60750y_4^{12}y_5^2 + 89700y_4^{10}y_5^2 - 75675y_4^8y_5^2 \\
& + 39300y_4^6y_5^2 - 12405y_4^4y_5^2 + 2154y_4^2y_5^2 - 153y_5^2 + 1500y_4^{16} - 5250y_4^{14} + 8250y_4^{12} - 7775y_4^{10} \\
& + 4885y_4^8 - 2095y_4^6 + 589y_4^4 - 97y_4^2 + 7 \\
p_{43} = {} & 7500y_5^{16} + 72000y_4^2y_5^{14} - 29250y_5^{14} + 282000y_4^4y_5^{12} - 240750y_4^2y_5^{12} + 48050y_5^{12} + 600000y_4^6y_5^{10} \\
& - 794250y_4^4y_5^{10} + 331500y_4^2y_5^{10} - 43175y_5^{10} + 765000y_4^8y_5^8 - 1383750y_4^6y_5^8 + 893550y_4^4y_5^8 \\
& - 242475y_4^2y_5^8 + 23085y_5^8 + 600000y_4^{10}y_5^6 - 1383750y_4^8y_5^6 + 1220200y_4^6y_5^6 - 511550y_4^4y_5^6 \\
& + 101340y_4^2y_5^6 - 7495y_5^6 + 282000y_4^{12}y_5^4 - 794250y_4^{10}y_5^4 + 893550y_4^8y_5^4 - 511550y_4^6y_5^4 \\
& + 156510y_4^4y_5^4 - 24165y_4^2y_5^4 + 1445y_5^4 + 72000y_4^{14}y_5^2 - 240750y_4^{12}y_5^2 + 331500y_4^{10}y_5^2 \\
& - 242475y_4^8y_5^2 + 101340y_4^6y_5^2 - 24165y_4^4y_5^2 + 3042y_4^2y_5^2 - 153y_5^2 + 7500y_4^{16} - 29250y_4^{14} \\
& + 48050y_4^{12} - 43175y_4^{10} + 23085y_4^8 - 7495y_4^6 + 1445y_4^4 - 153y_4^2 + 7
\end{aligned}
$$

$$
\begin{aligned}
p_{44} = {} & 7500y_5^{16} + 90000y_4^2y_5^{14} - 29250y_5^{14} + 396000y_4^4y_5^{12} - 300750y_4^2y_5^{12} + 48050y_5^{12} + 906000y_4^6y_5^{10} \\
& - 1118250y_4^4y_5^{10} + 414100y_4^2y_5^{10} - 43175y_5^{10} + 1215000y_4^8y_5^8 - 2103750y_4^6y_5^8 + 1263750y_4^4y_5^8 \\
& - 303075y_4^2y_5^8 + 23085y_5^8 + 990000y_4^{10}y_5^6 - 2223750y_4^8y_5^6 + 1875000y_4^6y_5^6 - 728750y_4^4y_5^6 \\
& + 126980y_4^2y_5^6 - 7495y_5^6 + 480000y_4^{12}y_5^4 - 1334250y_4^{10}y_5^4 + 1462750y_4^8y_5^4 - 799550y_4^6y_5^4 \\
& + 225990y_4^4y_5^4 - 30525y_4^2y_5^4 + 1445y_5^4 + 126000y_4^{14}y_5^2 - 420750y_4^{12}y_5^2 + 573300y_4^{10}y_5^2 \\
& - 409275y_4^8y_5^2 + 163380y_4^6y_5^2 - 35925y_4^4y_5^2 + 3930y_4^2y_5^2 - 153y_5^2 + 13500y_4^{16} - 53250y_4^{14} \\
& + 87850y_4^{12} - 78575y_4^{10} + 41285y_4^8 - 12895y_4^6 + 2301y_4^4 - 209y_4^2 + 7 \\
p_{45} = {} & 2250y_5^{14} + 14250y_4^2y_5^{12} - 6750y_5^{12} + 38250y_4^4y_5^{10} - 36000y_4^2y_5^{10} + 8125y_5^{10} + 56250y_4^6y_5^8 \\
& - 78750y_4^4y_5^8 + 35175y_4^2y_5^8 - 5025y_5^8 + 48750y_4^8y_5^6 - 90000y_4^6y_5^6 + 59450y_4^4y_5^6 - 16650y_4^2y_5^6 \\
& + 1635y_5^6 + 24750y_4^{10}y_5^4 - 56250y_4^8y_5^4 + 48550y_4^6y_5^4 - 19800y_4^4y_5^4 + 3735y_4^2y_5^4 - 240y_5^4 \\
& + 6750y_4^{12}y_5^2 - 18000y_4^{10}y_5^2 + 18825y_4^8y_5^2 - 9750y_4^6y_5^2 + 2565y_4^4y_5^2 - 300y_4^2y_5^2 + 6y_5^2 + 750y_4^{14} \\
& - 2250y_4^{12} + 2675y_4^{10} - 1575y_4^8 + 465y_4^6 - 60y_4^4 + 2y_4^2 \\
p_{46} = {} & 3000y_5^{14} + 18000y_4^2y_5^{12} - 9750y_5^{12} + 45000y_4^4y_5^{10} - 49500y_4^2y_5^{10} + 13050y_5^{10} + 60000y_4^6y_5^8 \\
& - 101250y_4^4y_5^8 + 54450y_4^2y_5^8 - 9300y_5^8 + 45000y_4^8y_5^6 - 105000y_4^6y_5^6 + 87300y_4^4y_5^6 - 30600y_4^2y_5^6 \\
& + 3790y_5^6 + 18000y_4^{10}y_5^4 - 56250y_4^8y_5^4 + 65700y_4^6y_5^4 - 36000y_4^4y_5^4 + 9270y_4^2y_5^4 - 885y_5^4 \\
& + 3000y_4^{12}y_5^2 - 13500y_4^{10}y_5^2 + 22050y_4^8y_5^2 - 17400y_4^6y_5^2 + 7170y_4^4y_5^2 - 1470y_4^2y_5^2 + 113y_5^2 \\
& - 750y_4^{12} + 2250y_4^{10} - 2700y_4^8 + 1690y_4^6 - 585y_4^4 + 105y_4^2 - 7 \\
p_{47} = {} & 6000y_5^{14} + 36000y_4^2y_5^{12} - 20250y_5^{12} + 90000y_4^4y_5^{10} - 103500y_4^2y_5^{10} + 28350y_5^{10} + 120000y_4^6y_5^8 \\
& - 213750y_4^4y_5^8 + 120250y_4^2y_5^8 - 21300y_5^8 + 90000y_4^8y_5^6 - 225000y_4^6y_5^6 + 197500y_4^4y_5^6 \\
& - 72300y_4^2y_5^6 + 9270y_5^6 + 36000y_4^{10}y_5^4 - 123750y_4^8y_5^4 + 154500y_4^6y_5^4 - 89100y_4^4y_5^4 \\
& + 23850y_4^2y_5^4 - 2355y_5^4 + 6000y_4^{12}y_5^2 - 31500y_4^{10}y_5^2 + 55750y_4^8y_5^2 - 46500y_4^6y_5^2 + 19890y_4^4y_5^2 \\
& - 4170y_4^2y_5^2 + 331y_5^2 - 2250y_4^{12} + 6850y_4^{10} - 8400y_4^8 + 5310y_4^6 - 1815y_4^4 + 315y_4^2 - 21
\end{aligned}
$$

$$
\begin{aligned}
p_{48} = {} & 6750y_5^{14} + 42750y_4^2y_5^{12} - 21750y_5^{12} + 114750y_4^4y_5^{10} - 117000y_4^2y_5^{10} + 28775y_5^{10} + 168750y_4^6y_5^8 \\
& - 258750y_4^4y_5^8 + 127725y_4^2y_5^8 - 20175y_5^8 + 146250y_4^8y_5^6 - 300000y_4^6y_5^6 + 223150y_4^4y_5^6 \\
& - 70950y_4^2y_5^6 + 8045y_5^6 + 74250y_4^{10}y_5^4 - 191250y_4^8y_5^4 + 190850y_4^6y_5^4 - 91800y_4^4y_5^4 \\
& + 21105y_4^2y_5^4 - 1830y_5^4 + 20250y_4^{12}y_5^2 - 63000y_4^{10}y_5^2 + 79275y_4^8y_5^2 - 51450y_4^6y_5^2 + 18075y_4^4y_5^2 \\
& - 3240y_4^2y_5^2 + 228y_5^2 + 2250y_4^{14} - 8250y_4^{12} + 12625y_4^{10} - 10425y_4^8 + 5015y_4^6 - 1410y_4^4 \\
& + 216y_4^2 - 14 \\
p_{49} = {} & 11250y_5^{14} + 71250y_4^2y_5^{12} - 36750y_5^{12} + 191250y_4^4y_5^{10} - 198000y_4^2y_5^{10} + 49425y_5^{10} + 281250y_4^6y_5^8 \\
& - 438750y_4^4y_5^8 + 220275y_4^2y_5^8 - 35325y_5^8 + 243750y_4^8y_5^6 - 510000y_4^6y_5^6 + 386850y_4^4y_5^6 \\
& - 125250y_4^2y_5^6 + 14455y_5^6 + 123750y_4^{10}y_5^4 - 326250y_4^8y_5^4 + 333150y_4^6y_5^4 - 163800y_4^4y_5^4 \\
& + 38475y_4^2y_5^4 - 3420y_5^4 + 33750y_4^{12}y_5^2 - 108000y_4^{10}y_5^2 + 139725y_4^8y_5^2 - 93150y_4^6y_5^2 \\
& + 33585y_4^4y_5^2 - 6180y_4^2y_5^2 + 450y_5^2 + 3750y_4^{14} - 14250y_4^{12} + 22575y_4^{10} - 19275y_4^8 + 9565y_4^6 \\
& - 2760y_4^4 + 430y_4^2 - 28 \\
p_{50} = {} & 30y_5^4 + 60y_4^2y_5^2 - 30y_5^2 + 30y_4^4 - 30y_4^2 + 7 \\
p_{51} = {} & 5y_5^4 + 10y_4^2y_5^2 - 5y_5^2 + 5y_4^4 - 5y_4^2 + 1
\end{aligned}
$$

$$
\begin{aligned}
\pi_1 = {} & 6y_5^4 + 12y_4^2y_5^2 - 6y_5^2 + 6y_4^4 - 6y_4^2 + 1 \\
\pi_2 = {} & y_1^2y_3^2(y_2^2 + y_3^2)\big(6y_1y_3^2y_5^4 - 8\kappa y_3y_5^4 + 12y_1y_2^2y_5^4 + 12y_1y_3^2y_4^2y_5^2 - 12\kappa y_3y_4^2y_5^2 \\
& + 24y_1y_2^2y_4^2y_5^2 - 6y_1y_3^2y_5^2 + 8\kappa y_3y_5^2 - 12y_1y_2^2y_5^2 + 6y_1y_3^2y_4^4 - 4\kappa y_3y_4^4 + 12y_1y_2^2y_4^4 \\
& - 6y_1y_3^2y_4^2 + 4\kappa y_3y_4^2 - 12y_1y_2^2y_4^2 + y_1y_3^2 - \kappa y_3 + 2y_1y_2^2\big) \\
\pi_3 = {} & 130y_1y_3^2y_5^4 + 124\kappa y_3y_5^4 - 24y_1y_2^2y_5^4 + 228y_1y_3^2y_4^2y_5^2 + 240\kappa y_3y_4^2y_5^2 - 48y_1y_2^2y_4^2y_5^2 - 130y_1y_3^2y_5^2 \\
& - 124kappay_3y_5^2 + 24y_1y_2^2y_5^2 + 98y_1y_3^2y_4^4 + 116\kappa y_3y_4^4 - 24y_1y_2^2y_4^4 - 98y_1y_3^2y_4^2 - 116\kappa y_3y_4^2 \\
& + 24y_1y_2^2y_4^2 + 19y_1y_3^2 + 20\kappa y_3 - 4y_1y_2^2
\end{aligned}
$$

$$\pi_4 = y_1 y_3 \Big( 104 y_1 y_3^3 y_5^4 + 10\kappa y_3^2 y_5^4 + 122 y_1 y_2^2 y_3 y_5^4 + 48\kappa y_2^2 y_5^4 + 192 y_1 y_3^3 y_4^2 y_5^2 + 36\kappa y_3^2 y_4^2 y_5^2 + 228 y_1 y_2^2 y_3 y_4^2 y_5^2 + 96\kappa y_2^2 y_4^2 y_5^2 - 104 y_1 y_3^3 y_5^2 - 10\kappa y_3^2 y_5^2 - 122 y_1 y_2^2 y_3 y_5^2 - 48\kappa y_2^2 y_5^2 + 88 y_1 y_3^3 y_4^4 + 26\kappa y_3^2 y_4^4 + 106 y_1 y_2^2 y_3 y_4^4 + 48\kappa y_2^2 y_4^4 - 88 y_1 y_3^3 y_4^2 - 26\kappa y_3^2 y_4^2 - 106 y_1 y_2^2 y_3 y_4^2 - 48\kappa y_2^2 y_4^2 + 16 y_1 y_3^3 + 3\kappa y_3^2 + 19 y_1 y_2^2 y_3 + 8\kappa y_2^2 \Big)$$

$$\pi_5 = y_1^2 y_3^2 \left( y_2^2 + y_3^2 \right) \Big( 6 y_1 y_2^3 y_5^4 - 8\kappa y_3^2 y_4 y_5^3 + 12 y_1 y_2^3 y_4^2 y_5^2 - 6 y_1 y_2^3 y_5^2 - 8\kappa y_3^2 y_4^3 y_5 + 8\kappa y_3^2 y_4 y_5 + 6 y_1 y_2^3 y_4^4 - 6 y_1 y_2^3 y_4^2 + y_1 y_2^3 \Big)$$

$$\pi_6 = 66 y_1 y_2 y_3^2 y_5^4 + 84\kappa y_2 y_3 y_5^4 - 18 y_1 y_2^3 y_5^4 + 96 y_1 y_3^3 y_4 y_5^3 + 24\kappa y_3^2 y_4 y_5^3 + 132 y_1 y_2 y_3^2 y_4^2 y_5^2 + 168\kappa y_2 y_3 y_4^2 y_5^2 - 36 y_1 y_2^3 y_4^2 y_5^2 - 66 y_1 y_2 y_3^2 y_5^2 - 84\kappa y_2 y_3 y_5^2 + 18 y_1 y_2^3 y_5^2 + 96 y_1 y_3^3 y_4^3 y_5 + 24\kappa y_3^2 y_4^3 y_5 - 96 y_1 y_3^3 y_4 y_5 - 24\kappa y_3^2 y_4 y_5 + 66 y_1 y_2 y_3^2 y_4^4 + 84\kappa y_2 y_3 y_4^4 - 18 y_1 y_2^3 y_4^4 - 66 y_1 y_2 y_3^2 y_4^2 - 84\kappa y_2 y_3 y_4^2 + 18 y_1 y_2^3 y_4^2 + 11 y_1 y_2 y_3^2 + 14\kappa y_2 y_3 - 3 y_1 y_2^3$$

$$\pi_7 = y_1 y_3 \Big( 48 y_1 y_2 y_3^3 y_5^4 + 24\kappa y_2 y_3^2 y_5^4 + 78 y_1 y_2^3 y_3 y_5^4 + 36\kappa y_2^3 y_5^4 + 48 y_1 y_3^4 y_4 y_5^3 - 48\kappa y_3^3 y_4 y_5^3 + 48 y_1 y_2^2 y_3^2 y_4 y_5^3 + 96 y_1 y_2 y_3^3 y_4^2 y_5^2 + 48\kappa y_2 y_3^2 y_4^2 y_5^2 + 156 y_1 y_2^3 y_3 y_4^2 y_5^2 + 72\kappa y_2^3 y_4^2 y_5^2 - 48 y_1 y_2 y_3^3 y_5^2 - 24\kappa y_2 y_3^2 y_5^2 - 78 y_1 y_2^3 y_3 y_5^2 - 36\kappa y_2^3 y_5^2 + 48 y_1 y_3^4 y_4^3 y_5 - 48\kappa y_3^3 y_4^3 y_5 + 48 y_1 y_2^2 y_3^2 y_4^3 y_5 - 48 y_1 y_3^4 y_4 y_5 + 48\kappa y_3^3 y_4 y_5 - 48 y_1 y_2^2 y_3^2 y_4 y_5 + 48 y_1 y_2 y_3^3 y_4^4 + 24\kappa y_2 y_3^2 y_4^4 + 78 y_1 y_2^3 y_3 y_4^4 + 36\kappa y_2^3 y_4^4 - 48 y_1 y_2 y_3^3 y_4^2 - 24\kappa y_2 y_3^2 y_4^2 - 78 y_1 y_2^3 y_3 y_4^2 - 36\kappa y_2^3 y_4^2 + 8 y_1 y_2 y_3^3 + 4\kappa y_2 y_3^2 + 13 y_1 y_2^3 y_3 + 6\kappa y_2^3 \Big)$$

$$\pi_8 = 58 y_1 y_3 y_5^4 + 4\kappa y_5^4 + 84 y_1 y_3 y_4^2 y_5^2 - 58 y_1 y_3 y_5^2 - 4\kappa y_5^2 + 26 y_1 y_3 y_4^4 - 4\kappa y_4^4 - 26 y_1 y_3 y_4^2 + 4\kappa y_4^2 + 7 y_1 y_3$$

$$\pi_9 = y_1^3 y_3^3 \left( y_2^2 + y_3^2 \right) \Big( 6 y_1 y_3^2 y_5^4 + 12 y_1 y_2^2 y_5^4 + 8\kappa y_2 y_4 y_5^3 + 12 y_1 y_3^2 y_4^2 y_5^2 - 12\kappa y_3 y_4^2 y_5^2 + 24 y_1 y_2^2 y_4^2 y_5^2 - 6 y_1 y_3^2 y_5^2 - 12 y_1 y_2^2 y_5^2 + 8\kappa y_2 y_4^3 y_5 - 8\kappa y_2 y_4 y_5 + 6 y_1 y_3^2 y_4^4 - 12\kappa y_3 y_4^4 + 12 y_1 y_2^2 y_4^4 - 6 y_1 y_3^2 y_4^2 + 12\kappa y_3 y_4^2 - 12 y_1 y_2^2 y_4^2 + y_1 y_3^2 - \kappa y_3 + 2 y_1 y_2^2 \Big)$$

$$\pi_{10} = y_1 y_3 \Big( 74 y_1 y_3^2 y_5^4 + 166 \kappa y_3 y_5^4 - 52 y_1 y_2^2 y_5^4 - 96 y_1 y_2 y_3 y_4 y_5^3 - 24 \kappa y_2 y_4 y_5^3 + 324 y_1 y_3^2 y_4^2 y_5^2$$
$$+ 336 \kappa y_3 y_4^2 y_5^2 - 72 y_1 y_2^2 y_4^2 y_5^2 - 74 y_1 y_3^2 y_5^2 - 166 \kappa y_3 y_5^2 + 52 y_1 y_2^2 y_5^2 - 96 y_1 y_2 y_3 y_4^3 y_5$$
$$- 24 \kappa y_2 y_4^3 y_5 + 96 y_1 y_2 y_3 y_4 y_5 + 24 \kappa y_2 y_4 y_5 + 250 y_1 y_3^2 y_4^4 + 170 \kappa y_3 y_4^4 - 20 y_1 y_2^2 y_4^4$$
$$- 250 y_1 y_3^2 y_4^2 - 170 \kappa y_3 y_4^2 + 20 y_1 y_2^2 y_4^2 + 27 y_1 y_3^2 + 28 \kappa y_3 - 6 y_1 y_2^2 \Big)$$

$$\pi_{11} = y_1^2 y_3^2 \Big( 102 y_1 y_3^3 y_5^4 + 68 \kappa y_3^2 y_5^4 + 132 y_1 y_2^2 y_3 y_5^4 + 80 \kappa y_2^2 y_5^4 - 48 y_1 y_2 y_3^2 y_4 y_5^3 + 48 \kappa y_2 y_3 y_4 y_5^3$$
$$- 48 y_1 y_2^3 y_4 y_5^3 + 276 y_1 y_3^3 y_4^2 y_5^2 + 48 \kappa y_3^2 y_4^2 y_5^2 + 336 y_1 y_2^2 y_3 y_4^2 y_5^2 + 144 \kappa y_2^2 y_4^2 y_5^2 - 102 y_1 y_3^3 y_5^2$$
$$- 68 \kappa y_3^2 y_5^2 - 132 y_1 y_2^2 y_3 y_5^2 - 80 \kappa y_2^2 y_5^2 - 48 y_1 y_2 y_3^2 y_4^3 y_5 + 48 \kappa y_2 y_3 y_4^3 y_5 - 48 y_1 y_2^3 y_4^3 y_5$$
$$+ 48 y_1 y_2 y_3^2 y_4 y_5 - 48 \kappa y_2 y_3 y_4 y_5 + 48 y_1 y_2^3 y_4 y_5 + 174 y_1 y_3^3 y_4^4 - 20 \kappa y_3^2 y_4^4 + 204 y_1 y_2^2 y_3 y_4^4$$
$$+ 64 \kappa y_2^2 y_4^4 - 174 y_1 y_3^3 y_4^2 + 20 \kappa y_3^2 y_4^2 - 204 y_1 y_2^2 y_3 y_4^2 - 64 \kappa y_2^2 y_4^2 + 23 y_1 y_3^3 + 4 \kappa y_3^2 + 28 y_1 y_2^2 y_3$$
$$+ 12 \kappa y_2^2 \Big)$$

$$\pi_{12} = \pi_{26} \pi_{38}$$

$$\pi_{13} = 90 y_1 y_2 y_5^5 + 72 y_1 y_3 y_4 y_5^4 + 18 \kappa y_4 y_5^4 + 180 y_1 y_2 y_4^2 y_5^3 - 90 y_1 y_2 y_5^3 + 80 y_1 y_3 y_4^3 y_5^2 + 20 \kappa y_4^3 y_5^2$$
$$- 68 y_1 y_3 y_4 y_5^2 - 17 \kappa y_4 y_5^2 + 90 y_1 y_2 y_4^4 y_5 - 90 y_1 y_2 y_4^2 y_5 + 18 y_1 y_2 y_5 + 8 y_1 y_3 y_4^5 + 2 \kappa y_4^5$$
$$- 12 y_1 y_3 y_4^3 - 3 \kappa y_4^3 + 4 y_1 y_3 y_4 + \kappa y_4$$

$$\pi_{14} = y_1^3 y_3^2 \left( y_2^2 + y_3^2 \right) \Big( 24 y_1 y_2 y_3^2 y_5^5 - 32 \kappa y_2 y_3 y_5^5 + 30 y_1 y_2^3 y_5^5 + 20 \kappa y_3^2 y_4 y_5^4 + 48 y_1 y_2 y_3^2 y_4^2 y_5^3$$
$$- 52 \kappa y_2 y_3 y_4^2 y_5^3 + 60 y_1 y_2^3 y_4^2 y_5^3 - 24 y_1 y_2 y_3^2 y_5^3 + 32 \kappa y_2 y_3 y_5^3 - 30 y_1 y_2^3 y_5^3 + 24 \kappa y_3^2 y_4^3 y_5^2$$
$$- 18 \kappa y_3^2 y_4 y_5^2 + 24 y_1 y_2 y_3^2 y_4^4 y_5 - 20 \kappa y_2 y_3 y_4^4 y_5 + 30 y_1 y_2^3 y_4^4 y_5 - 24 y_1 y_2 y_3^2 y_4^2 y_5 + 22 \kappa y_2 y_3 y_4^2 y_5$$
$$- 30 y_1 y_2^3 y_4^2 y_5 + 5 y_1 y_2 y_3^2 y_5 - 6 \kappa y_2 y_3 y_5 + 6 y_1 y_2^3 y_5 + 4 \kappa y_3^2 y_4^5 - 6 \kappa y_3^2 y_4^3 + 2 \kappa y_3^2 y_4 \Big)$$

$$\pi_{15} = y_1\Big(756y_1y_2y_3^2y_5^5 + 504\kappa y_2y_3y_5^5 - 90y_1y_2^3y_5^5 - 312y_1y_3^3y_4y_5^4 + 12\kappa y_3^2y_4y_5^4 - 72y_1y_2^2y_3y_4y_5^4$$
$$+ 1368y_1y_2y_3^2y_4^2y_5^3 + 972\kappa y_2y_3y_4^2y_5^3 - 180y_1y_2^3y_4^2y_5^3 - 756y_1y_2y_3^2y_5^3 - 504\kappa y_2y_3y_5^3$$
$$+ 90y_1y_2^3y_5^3 - 368y_1y_3^3y_4^3y_5^2 + 8\kappa y_3^2y_4^3y_5^2 - 80y_1y_2^2y_3y_4^3y_5^2 + 284y_1y_3^3y_4y_5^2 - 14\kappa y_3^2y_4y_5^2$$
$$+ 68y_1y_2^2y_3y_4y_5^2 + 612y_1y_2y_3^2y_4^4y_5 + 468\kappa y_2y_3y_4^4y_5 - 90y_1y_2^3y_4^4y_5 - 636y_1y_2y_3^2y_4^2y_5$$
$$- 474\kappa y_2y_3y_4^2y_5 + 90y_1y_2^3y_4^2y_5 + 145y_1y_2y_3^2y_5 + 99\kappa y_2y_3y_5 - 18y_1y_2^3y_5 - 56y_1y_3^3y_4^5$$
$$- 4\kappa y_3^2y_4^5 - 8y_1y_2^2y_3y_4^5 + 84y_1y_3^3y_4^3 + 6\kappa y_3^2y_4^3 + 12y_1y_2^2y_3y_4^3 - 28y_1y_3^3y_4 - 2\kappa y_3^2y_4$$
$$- 4y_1y_2^2y_3y_4\Big)$$
$$\pi_{16} = y_1^2y_3\Big(576y_1y_2y_3^3y_5^5 - 24\kappa y_2y_3^2y_5^5 + 606y_1y_2^3y_3y_5^5 + 180\kappa y_2^3y_5^5 - 120y_1y_3^4y_4y_5^4 + 156\kappa y_3^3y_4y_5^4$$
$$- 120y_1y_2^2y_3^2y_4y_5^4 + 36\kappa y_2^2y_3y_4y_5^4 + 1080y_1y_2y_3^3y_4^2y_5^3 + 24\kappa y_2y_3^2y_4^2y_5^3 + 1140y_1y_2^3y_3y_4^2y_5^3$$
$$+ 360\kappa y_2^3y_4^2y_5^3 - 576y_1y_2y_3^3y_5^3 + 24\kappa y_2y_3^2y_5^3 - 606y_1y_2^3y_3y_5^3 - 180\kappa y_2^3y_5^3 - 144y_1y_3^4y_4^3y_5^2$$
$$+ 184\kappa y_3^3y_4^3y_5^2 - 144y_1y_2^2y_3^2y_4^3y_5^2 + 40\kappa y_2^2y_3y_4^3y_5^2 + 108y_1y_3^4y_4y_5^2 - 142\kappa y_3^3y_4y_5^2$$
$$+ 108y_1y_2^2y_3^2y_4y_5^2 - 34\kappa y_2^2y_3y_4y_5^2 + 504y_1y_2y_3^3y_4^4y_5 + 48\kappa y_2y_3^2y_4^4y_5 + 534y_1y_2^3y_3y_4^4y_5$$
$$+ 180\kappa y_2^3y_4^4y_5 - 516y_1y_2y_3^3y_4^2y_5 - 36\kappa y_2y_3^2y_4^2y_5 - 546y_1y_2^3y_3y_4^2y_5 - 180\kappa y_2^3y_4^2y_5$$
$$+ 113y_1y_2y_3^3y_5 - 2\kappa y_2y_3^2y_5 + 118y_1y_2^3y_3y_5 + 36\kappa y_2^3y_5 - 24y_1y_3^4y_4^5 + 28\kappa y_3^3y_4^5 - 24y_1y_2^2y_3^2y_4^5$$
$$+ 4\kappa y_2^2y_3y_4^5 + 36y_1y_3^4y_4^3 - 42\kappa y_3^3y_4^3 + 36y_1y_2^2y_3^2y_4^3 - 6\kappa y_2^2y_3y_4^3 - 12y_1y_3^4y_4 + 14\kappa y_3^3y_4$$
$$- 12y_1y_2^2y_3^2y_4 + 2\kappa y_2^2y_3y_4\Big)$$
$$\pi_{17} = 8y_1y_3y_5^5 + 2\kappa y_5^5 + 90y_1y_2y_4y_5^4 + 80y_1y_3y_4^2y_5^3 + 20\kappa y_4^2y_5^3 - 12y_1y_3y_5^3 - 3\kappa y_5^3 + 180y_1y_2y_4^3y_5^2$$
$$- 90y_1y_2y_4y_5^2 + 72y_1y_3y_4^4y_5 + 18\kappa y_4^4y_5 - 68y_1y_3y_4^2y_5 - 17\kappa y_4^2y_5 + 4y_1y_3y_5 + \kappa y_5$$
$$+ 90y_1y_2y_5^5 - 90y_1y_2y_4^3 + 18y_1y_2y_4$$
$$\pi_{18} = y_1^3y_3^2\left(y_2^2 + y_3^2\right)\Big(4\kappa y_3^2y_5^5 + 24y_1y_2y_3^2y_4y_5^4 - 28\kappa y_2y_3y_4y_5^4 + 30y_1y_2^3y_4y_5^4 + 24\kappa y_3^2y_4^2y_5^3 - 6\kappa y_3^2y_5^3$$
$$+ 48y_1y_2y_3^2y_4^3y_5^2 - 44\kappa y_2y_3y_4^3y_5^2 + 60y_1y_2^3y_4^3y_5^2 - 24y_1y_2y_3^2y_4y_5^2 + 26\kappa y_2y_3y_4y_5^2 - 30y_1y_2^3y_4y_5^2$$
$$+ 20\kappa y_3^2y_4^4y_5 - 18\kappa y_3^2y_4^2y_5 + 2\kappa y_3^2y_5 + 24y_1y_2y_3^2y_4^5 - 16\kappa y_2y_3y_4^5 + 30y_1y_2^3y_4^5 - 24y_1y_2y_3^2y_4^3$$
$$+ 16\kappa y_2y_3y_4^3 - 30y_1y_2^3y_4^3 + 5y_1y_2y_3^2y_4 - 4\kappa y_2y_3y_4 + 6y_1y_2^3y_4\Big)$$

$$\pi_{19} = y_1\Big(56y_1y_3^3y_5^5 + 4\kappa y_3^2y_5^5 + 8y_1y_2^2y_3y_5^5 - 708y_1y_2y_3^2y_4y_5^4 - 492\kappa y_2y_3y_4y_5^4 + 90y_1y_2^3y_4y_5^4$$
$$+ 368y_1y_3^3y_4^2y_5^3 - 8\kappa y_3^2y_4^2y_5^3 + 80y_1y_2^2y_3y_4^2y_5^3 - 84y_1y_3^3y_5^3 - 6 * \kappa y_3^2y_5^3 - 12y_1y_2^2y_3y_5^3$$
$$- 1272y_1y_2y_3^2y_4^3y_5^2 - 948\kappa y_2y_3y_4^3y_5^2 + 180y_1y_2^3y_4^3y_5^2 + 684y_1y_2y_3^2y_4y_5^2 + 486\kappa y_2y_3y_4y_5^2$$
$$- 90y_1y_2^3y_4y_5^2 + 312y_1y_3^3y_4^4y_5 - 12\kappa y_3^2y_4^4y_5 + 72y_1y_2^2y_3y_4^4y_5 - 284y_1y_3^3y_4^2y_5 + 14\kappa y_3^2y_4^2y_5$$
$$- 68y_1y_2^2y_3y_4^2y_5 + 28y_1y_3^3y_5 + 2\kappa y_3^2y_5 + 4y_1y_2^2y_3y_5 - 564y_1y_2y_3^2y_4^5 - 456\kappa y_2y_3y_4^5$$
$$+ 90y_1y_2^3y_4^5 + 564y_1y_2y_3^2y_4^3 + 456\kappa y_2y_3y_4^3 - 90y_1y_2^3y_4^3 - 121y_1y_2y_3^2y_4 - 93\kappa y_2y_3y_4$$
$$+ 18y_1y_2^3y_4\Big)$$

$$\pi_{20} = y_1^2y_3\Big(24y_1y_3^4y_5^5 - 28\kappa y_3^3y_5^5 + 24y_1y_2^2y_3^2y_5^5 - 4\kappa y_2^2y_3y_5^5 - 552y_1y_2y_3^3y_4y_5^4 - 582y_1y_2^3y_3y_4y_5^4$$
$$- 180\kappa y_2^3y_4y_5^4 + 144y_1y_3^4y_4^2y_5^3 - 184\kappa y_3^3y_4^2y_5^3 + 144y_1y_2^2y_3^2y_4^2y_5^3 - 40\kappa y_2^2y_3y_4^2y_5^3 - 36y_1y_3^4y_5^3$$
$$+ 42\kappa y_3^3y_5^3 - 36y_1y_2^2y_3^2y_5^3 + 6\kappa y_2^2y_3y_5^3 - 1032y_1y_2y_3^3y_4^3y_5^2 - 72\kappa y_2y_3^2y_4^3y_5^2 - 1092y_1y_2^3y_3y_4^3y_5^2$$
$$- 360\kappa y_2^3y_4^3y_5^2 + 540y_1y_2y_3^3y_4y_5^2 + 12\kappa y_2y_3^2y_4y_5^2 + 570y_1y_2^3y_3y_4y_5^2 + 180\kappa y_2^3y_4y_5^2$$
$$+ 120y_1y_3^4y_4^4y_5 - 156\kappa y_3^3y_4^4y_5 + 120y_1y_2^2y_3^2y_4^4y_5 - 36\kappa y_2^2y_3y_4^4y_5 - 108y_1y_3^4y_4^2y_5$$
$$+ 142\kappa y_3^3y_4^2y_5 - 108y_1y_2^2y_3^2y_4^2y_5 + 34\kappa y_2^2y_3y_4^2y_5 + 12y_1y_3^4y_5 - 14\kappa y_3^3y_5 + 12y_1y_2^2y_3^2y_5$$
$$- 2\kappa y_2^2y_3y_5 - 480y_1y_2y_3^3y_4^5 - 72\kappa y_2y_3^2y_4^5 - 510y_1y_2^3y_3y_4^5 - 180\kappa y_2^3y_4^5 + 480y_1y_2y_3^3y_4^3$$
$$+ 72\kappa y_2y_3^2y_4^3 + 510y_1y_2^3y_3y_4^3 + 180\kappa y_2^3y_4^3 - 101y_1y_2y_3^3y_4 - 10\kappa y_2y_3^2y_4 - 106y_1y_2^3y_3y_4$$
$$- 36\kappa y_2^3y_4\Big)$$

$$\pi_{21} = 90y_1y_2y_5^4 + 80y_1y_3y_4y_5^3 + 20\kappa y_4y_5^3 + 180y_1y_2y_4^2y_5^2 - 72y_1y_2y_5^2 + 80y_1y_3y_4^3y_5 + 20\kappa y_4^3y_5$$
$$- 64y_1y_3y_4y_5 - 16\kappa y_4y_5 + 90y_1y_2y_4^4 - 72y_1y_2y_4^2 + 9y_1y_2$$

$$\pi_{22} = y_1^3y_3^2\left(y_2^2 + y_3^2\right)\Big(24y_1y_2y_3^2y_5^4 - 32\kappa y_2y_3y_5^4 + 30y_1y_2^3y_5^4 + 24\kappa y_3^2y_4y_5^3 + 48y_1y_2y_3^2y_4^2y_5^2$$
$$- 48\kappa y_2y_3y_4^2y_5^2 + 60y_1y_2^3y_4^2y_5^2 - 18y_1y_2y_3^2y_5^2 + 24\kappa y_2y_3y_5^2 - 24y_1y_2^3y_5^2 + 24\kappa y_3^2y_4^3y_5$$
$$- 16\kappa y_3^2y_4y_5 + 24y_1y_2y_3^2y_4^4 - 16\kappa y_2y_3y_4^4 + 30y_1y_2^3y_4^4 - 18y_1y_2y_3^2y_4^2 + 12\kappa y_2y_3y_4^2 - 24y_1y_2^3y_4^2$$
$$+ 2y_1y_2y_3^2 - 2\kappa y_2y_3 + 3y_1y_2^3\Big)$$

$$\pi_{23} = y_1\Big(756y_1y_2y_3^2y_5^4 + 504\kappa y_2y_3y_5^4 - 90y_1y_2^3y_5^4 - 368y_1y_3^3y_4y_5^3 + 8\kappa y_3^2y_4y_5^3 - 80y_1y_2^2y_3y_4y_5^3$$
$$+ 1320y_1y_2y_3^2y_4^2y_5^2 + 960\kappa y_2y_3y_4^2y_5^2 - 180y_1y_2^3y_4^2y_5^2 - 594y_1y_2y_3^2y_5^2 - 402\kappa y_2y_3y_5^2$$
$$+ 72y_1y_2^3y_5^2 - 368y_1y_3^3y_4^3y_5 + 8\kappa y_3^2y_4^3y_5 - 80y_1y_2^2y_3y_4^3y_5 + 256y_1y_3^3y_4y_5 - 16\kappa y_3^2y_4y_5$$
$$+ 64y_1y_2^2y_3y_4y_5 + 564y_1y_2y_3^2y_4^4 + 456\kappa y_2y_3y_4^4 - 90y_1y_2^3y_4^4 - 450y_1y_2y_3^2y_4^2 - 366\kappa y_2y_3y_4^2$$
$$+ 72y_1y_2^3y_4^2 + 64y_1y_2y_3^2 + 48\kappa y_2y_3 - 9y_1y_2^3\Big)$$

$$\pi_{24} = y_1^2y_3\Big(576y_1y_2y_3^3y_5^4 - 24\kappa y_2y_3^2y_5^4 + 606y_1y_2^3y_3y_5^4 + 180\kappa y_2^3y_5^4 - 144y_1y_3^4y_4y_5^3 + 184\kappa y_3^3y_4y_5^3$$
$$- 144y_1y_2^2y_3^2y_4y_5^3 + 40\kappa y_2^2y_3y_4y_5^3 + 1056y_1y_2y_3^3y_4^2y_5^2 + 48\kappa y_2y_3^2y_4^2y_5^2 + 1116y_1y_2^3y_3y_4^2y_5^2$$
$$+ 360\kappa y_2^3y_4^2y_5^2 - 450y_1y_2y_3^3y_5^2 + 12\kappa y_2y_3^2y_5^2 - 480y_1y_2^3y_3y_5^2 - 144\kappa y_2^3y_5^2 - 144y_1y_3^4y_4^3y_5$$
$$+ 184\kappa y_3^3y_4^3y_5 - 144y_1y_2^2y_3^2y_4^3y_5 + 40\kappa y_2^2y_3y_4^3y_5 + 96y_1y_3^4y_4y_5 - 128\kappa y_3^3y_4y_5 + 96y_1y_2^2y_3^2y_4y_5$$
$$- 32\kappa y_2^2y_3y_4y_5 + 480y_1y_2y_3^3y_4^4 + 72\kappa y_2y_3^2y_4^4 + 510y_1y_2^3y_3y_4^4 + 180\kappa y_2^3y_4^4 - 378y_1y_2y_3^3y_4^2$$
$$- 60\kappa y_2y_3^2y_4^2 - 408y_1y_2^3y_3y_4^2 - 144\kappa y_2^3y_4^2 + 50y_1y_2y_3^3 + 4\kappa y_2y_3^2 + 55y_1y_2^3y_3 + 18\kappa y_2^3\Big)$$

$$\pi_{25} = \pi_{26}\pi_{40}$$

$$\pi_{26} = \kappa y_1^2y_3^4 + 2\mu y_1^2y_3^3 + \kappa y_1^2y_2^2y_3^2 - 2\kappa\mu y_1y_3^2 + 2\mu y_1^2y_2^2y_3 - 4\mu^2y_1y_3 - \kappa\mu^2$$

$$\pi_{27} = 6y_1y_2y_5^4 + 16y_1y_3y_4y_5^3 + 4\kappa y_4y_5^3 + 12y_1y_2y_4^2y_5^2 - 6y_1y_2y_5^2 + 16y_1y_3y_4^3y_5 + 4\kappa y_4^3y_5$$
$$- 16y_1y_3y_4y_5 - 4\kappa y_4y_5 + 6y_1y_2y_4^4 - 6y_1y_2y_4^2 + y_1y_2$$

$$\pi_{28} = y_1y_3\Big(30y_1y_2y_3y_5^4 + 24\kappa y_2y_5^4 - 16y_1y_3^2y_4y_5^3 + 16\kappa y_3y_4y_5^3 - 16y_1y_2^2y_4y_5^3 + 60y_1y_2y_3y_4^2y_5^2$$
$$+ 48\kappa y_2y_4^2y_5^2 - 30y_1y_2y_3y_5^2 - 24\kappa y_2y_5^2 - 16y_1y_3^2y_4^3y_5 + 16\kappa y_3y_4^3 * y_5 - 16y_1y_2^2y_4^3y_5$$
$$+ 16y_1y_3^2y_4y_5 - 16\kappa y_3y_4y_5 + 16y_1y_2^2y_4y_5 + 30y_1y_2y_3y_4^4 + 24\kappa y_2y_4^4 - 30y_1y_2y_3y_4^2 - 24\kappa y_2y_4^2$$
$$+ 5y_1y_2y_3 + 4\kappa y_2\Big)$$

$$\pi_{29} = y_1^2y_3^2\Big(18y_1y_2y_3^2y_5^4 + 12y_1y_2^3y_5^4 + 8\kappa y_3^2y_4y_5^3 + 8\kappa y_2^2y_4y_5^3 + 36y_1y_2y_3^2y_4^2y_5^2 + 24y_1y_2^3y_4^2y_5^2$$
$$- 18y_1y_2y_3^2y_5^2 - 12y_1y_2^3y_5^2 + 8\kappa y_3^2y_4^3y_5 + 8\kappa y_2^2y_4^3y_5 - 8\kappa y_3^2y_4y_5 - 8\kappa y_2^2y_4y_5 + 18y_1y_2y_3^2y_4^4$$
$$+ 12y_1y_2^3y_4^4 - 18y_1y_2y_3^2y_4^2 - 12y_1y_2^3y_4^2 + 3y_1y_2y_3^2 + 2y_1y_2^3\Big)$$

$$\pi_{30} = y_5\Big(260y_1y_3^2y_5^4 + 248\kappa y_3y_5^4 - 60y_1y_2^2y_5^4 + 472y_1y_3^2y_4^2y_5^2 + 484\kappa y_3y_4^2y_5^2 - 120y_1y_2^2y_4^2y_5^2$$
$$- 260y_1y_3^2y_5^2 - 248\kappa y_3y_5^2 + 60y_1y_2^2y_5^2 + 212y_1y_3^2y_4^4 + 236\kappa y_3y_4^4 - 60y_1y_2^2y_4^4 - 220y_1y_3^2y_4^2$$
$$- 238\kappa y_3y_4^2 + 60y_1y_2^2y_4^2 + 50y_1y_3^2 + 49\kappa y_3 - 12y_1y_2^2\Big)$$

$$\pi_{31} = y_1y_3y_5\Big(208y_1y_3^3y_5^4 + 20\kappa y_3^2y_5^4 + 274y_1y_2^2y_3y_5^4 + 120\kappa y_2^2y_5^4 + 392y_1y_3^3y_4^2y_5^2 + 64\kappa y_3^2y_4^2y_5^2$$
$$+ 524y_1y_2^2y_3y_4^2y_5^2 + 240\kappa y_2^2y_4^2y_5^2 - 208y_1y_3^3y_5^2 - 20\kappa y_3^2y_5^2 - 274y_1y_2^2y_3y_5^2 - 120\kappa y_2^2y_5^2$$
$$+ 184y_1y_3^3y_4^4 + 44\kappa y_3^2y_4^4 + 250y_1y_2^2y_3y_4^4 + 120\kappa y_2^2y_4^4 - 188y_1y_3^3y_4^2 - 40\kappa y_3^2y_4^2 - 254y_1y_2^2y_3y_4^2$$
$$- 120\kappa y_2^2y_4^2 + 41y_1y_3^3 + 5\kappa y_3^2 + 54y_1y_2^2y_3 + 24\kappa y_2^2\Big)$$

$$\pi_{32} = y_1^2y_3^2\Big(24y_1y_3^4y_5^4 - 32\kappa y_3^3y_5^4 + 90y_1y_2^2y_3^2y_5^4 - 32\kappa y_2^2y_3y_5^4 + 60y_1y_2^4y_5^4 + 48y_1y_3^4y_4^2y_5^2 - 52\kappa y_3^3y_4^2y_5^2$$
$$+ 180y_1y_2^2y_3^2y_4^2y_5^2 - 52\kappa y_2^2y_3y_4^2y_5^2 + 120y_1y_2^4y_4^2y_5^2 - 24y_1y_3^4y_5^2 + 32\kappa y_3^3y_5^2 - 90y_1y_2^2y_3^2y_5^2$$
$$+ 32\kappa y_2^2y_3y_5^2 - 60y_1y_2^4y_5^2 + 24y_1y_3^4y_4^4 - 20\kappa y_3^3y_4^4 + 90y_1y_2^2y_3^2y_4^4 - 20\kappa y_2^2y_3y_4^4 + 60y_1y_2^4y_4^4$$
$$- 24y_1y_3^4y_4^2 + 22\kappa y_3^3y_4^2 - 90y_1y_2^2y_3^2y_4^2 + 22\kappa y_2^2y_3y_4^2 - 60y_1y_2^4y_4^2 + 5y_1y_3^4 - 6\kappa y_3^3 + 18y_1y_2^2y_3^2$$
$$- 6\kappa y_2^2y_3 + 12y_1y_2^4\Big)$$

$$\pi_{33} = y_4\Big(244y_1y_3^2y_5^4 + 244\kappa y_3y_5^4 - 60y_1y_2^2y_5^4 + 440y_1y_3^2y_4^2y_5^2 + 476\kappa y_3y_4^2y_5^2 - 120y_1y_2^2y_4^2y_5^2$$
$$- 236y_1y_3^2y_5^2 - 242\kappa y_3y_5^2 + 60y_1y_2^2y_5^2 + 196y_1y_3^2y_4^4 + 232\kappa y_3y_4^4 - 60y_1y_2^2y_4^4 - 196y_1y_3^2y_4^2$$
$$- 232\kappa y_3y_4^2 + 60y_1y_2^2y_4^2 + 42y_1y_3^2 + 47\kappa y_3 - 12y_1y_2^2\Big)$$

$$\pi_{34} = y_1y_3y_4\Big(200y_1y_3^3y_5^4 + 28\kappa y_3^2y_5^4 + 266y_1y_2^2y_3y_5^4 + 120\kappa y_2^2y_5^4 + 376y_1y_3^3y_4^2y_5^2 + 80\kappa y_3^2y_4^2y_5^2$$
$$+ 508y_1y_2^2y_3y_4^2y_5^2 + 240\kappa y_2^2y_4^2y_5^2 - 196y_1y_3^3y_5^2 - 32kappay_3^2y_5^2 - 262y_1y_2^2y_3y_5^2 - 120\kappa y_2^2y_5^2$$
$$+ 176y_1y_3^3y_4^4 + 52kappay_3^2y_4^4 + 242y_1y_2^2y_3y_4^4 + 120\kappa y_2^2y_4^4 - 176y_1y_3^3y_4^2 - 52\kappa y_3^2y_4^2$$
$$- 242y_1y_2^2y_3y_4^2 - 120\kappa y_2^2y_4^2 + 37y_1y_3^3 + 9\kappa y_3^2 + 50y_1y_2^2y_3 + 24\kappa y_2^2\Big)$$

$$\pi_{35} = y_1^2 y_3^2 y_4 \Big( 24 y_1 y_3^4 y_5^4 - 28\kappa y_3^3 y_5^4 + 90 y_1 y_2^2 y_3^2 y_5^4 - 28\kappa y_2^2 y_3 y_5^4 + 60 y_1 y_2^4 y_5^4 + 48 y_1 y_3^4 y_4^2 y_5^2$$
$$- 44\kappa y_3^3 y_4^2 y_5^2 + 180 y_1 y_2^2 y_3^2 y_4^2 y_5^2 - 44\kappa y_2^2 y_3 y_4^2 y_5^2 + 120 y_1 y_2^4 y_4^2 y_5^2 - 24 y_1 y_3^4 y_5^2 + 26\kappa y_3^3 y_5^2$$
$$- 90 y_1 y_2^2 y_3^2 y_5^2 + 26\kappa y_2^2 y_3 y_5^2 - 60 y_1 y_2^4 y_5^2 + 24 y_1 y_3^4 y_4^4 - 16\kappa y_3^3 y_4^4 + 90 y_1 y_2^2 y_3^2 y_4^4 - 16\kappa y_2^2 y_3 y_4^4$$
$$+ 60 y_1 y_2^4 y_4^4 - 24 y_1 y_3^4 y_4^2 + 16\kappa y_3^3 y_4^2 - 90 y_1 y_2^2 y_3^2 y_4^2 + 16\kappa y_2^2 y_3 y_4^2 - 60 y_1 y_2^4 y_4^2 + 5 y_1 y_3^4 - 4\kappa y_3^3$$
$$+ 18 y_1 y_2^2 y_3^2 - 4\kappa y_2^2 y_3 + 12 y_1 y_2^4 \Big)$$

$$\pi_{36} = 130 y_1 y_3^2 y_5^4 + 124\kappa y_3 y_5^4 - 30 y_1 y_2^2 y_5^4 + 228 y_1 y_3^2 y_4^2 y_5^2 + 240 kappa y_3 y_4^2 y_5^2 - 60 y_1 y_2^2 y_4^2 y_5^2$$
$$- 102 y_1 y_3^2 y_5^2 - 99\kappa y_3 y_5^2 + 24 y_1 y_2^2 y_5^2 + 98 y_1 y_3^2 y_4^4 + 116\kappa y_3 y_4^4 - 30 y_1 y_2^2 y_4^4 - 78 y_1 y_3^2 y_4^2$$
$$- 93\kappa y_3 y_4^2 + 24 y_1 y_2^2 y_4^2 + 11 y_1 y_3^2 + 12\kappa y_3 - 3 y_1 y_2^2$$

$$\pi_{37} = y_1 y_3 \Big( 208 y_1 y_3^3 y_5^4 + 20\kappa y_3^2 y_5^4 + 274 y_1 y_2^2 y_3 y_5^4 + 120\kappa y_2^2 y_5^4 + 384 y_1 y_3^3 y_4^2 y_5^2 + 72\kappa y_3^2 y_4^2 y_5^2$$
$$+ 516 y_1 y_2^2 y_3 y_4^2 y_5^2 + 240\kappa y_2^2 y_4^2 y_5^2 - 162 y_1 y_3^3 y_5^2 - 18\kappa y_3^2 y_5^2 - 216 y_1 y_2^2 y_3 y_5^2 - 96\kappa y_2^2 y_5^2$$
$$+ 176 y_1 y_3^3 y_4^4 + 52\kappa y_3^2 y_4^4 + 242 y_1 y_2^2 y_3 y_4^4 + 120\kappa y_2^2 y_4^4 - 138 y_1 y_3^3 y_4^2 - 42\kappa y_3^2 y_4^2 - 192 y_1 y_2^2 y_3 y_4^2$$
$$- 96\kappa y_2^2 y_4^2 + 18 y_1 y_3^3 + 4\kappa y_3^2 + 25 y_1 y_2^2 y_3 + 12\kappa y_2^2 \Big)$$

$$\pi_{38} = 5 y_5^4 + 10 y_4^2 y_5^2 - 5 y_5^2 + 5 y_4^4 - 5 y_4^2 + 1$$

$$\pi_{39} = y_1^2 y_3^2 \Big( 24 y_1 y_3^4 y_5^4 - 32\kappa y_3^3 y_5^4 + 90 y_1 y_2^2 y_3^2 y_5^4 - 32\kappa y_2^2 y_3 y_5^4 + 60 y_1 y_2^4 y_5^4 + 48 y_1 y_3^4 y_4^2 y_5^2 - 48\kappa y_3^3 y_4^2 y_5^2$$
$$+ 180 y_1 y_2^2 y_3^2 y_4^2 y_5^2 - 48\kappa y_2^2 y_3 y_4^2 y_5^2 + 120 y_1 y_2^4 y_4^2 y_5^2 - 18 y_1 y_3^4 y_5^2 + 24\kappa y_3^3 y_5^2 - 72 y_1 y_2^2 y_3^2 y_5^2$$
$$+ 24\kappa y_2^2 y_3 y_5^2 - 48 y_1 y_2^4 y_5^2 + 24 y_1 y_3^4 y_4^4 - 16\kappa y_3^3 y_4^4 + 90 y_1 y_2^2 y_3^2 y_4^4 - 16\kappa y_2^2 y_3 y_4^4 + 60 y_1 y_2^4 y_4^4$$
$$- 18 y_1 y_3^4 y_4^2 + 12\kappa y_3^3 y_4^2 - 72 y_1 y_2^2 y_3^2 y_4^2 + 12\kappa y_2^2 y_3 y_4^2 - 48 y_1 y_2^4 y_4^2 + 2 y_1 y_3^4 - 2\kappa y_3^3 + 9 y_1 y_2^2 y_3^2$$
$$- 2\kappa y_2^2 y_3 + 6 y_1 y_2^4 \Big)$$

$$\pi_{40} = 10 y_5^4 + 20 y_4^2 y_5^2 - 8 y_5^2 + 10 y_4^4 - 8 y_4^2 + 1$$

$$\pi_{41} = 74 y_1 y_3^2 y_5^4 + 74\kappa y_3 y_5^4 - 18 y_1 y_2^2 y_5^4 + 132 y_1 y_3^2 y_4^2 y_5^2 + 144\kappa y_3 y_4^2 y_5^2 - 36 y_1 y_2^2 y_4^2 y_5^2 - 74 y_1 y_3^2 y_5^2$$
$$- 74\kappa y_3 y_5^2 + 18 y_1 y_2^2 y_5^2 + 58 y_1 y_3^2 y_4^4 + 70\kappa y_3 y_4^4 - 18 y_1 y_2^2 y_4^4 - 58 y_1 y_3^2 y_4^2 - 70\kappa y_3 y_4^2$$
$$+ 18 y_1 y_2^2 y_4^2 + 11 y_1 y_3^2 + 12\kappa y_3 - 3 y_1 y_2^2$$

$$\pi_{42} = y_1 y_3 \Big( 116 y_1 y_3^3 y_5^4 + 16 \kappa y_3^2 y_5^4 + 158 y_1 y_2^2 y_3 y_5^4 + 72 \kappa y_2^2 y_5^4 + 216 y_1 y_3^3 y_4^2 y_5^2 + 48 \kappa y_3^2 y_4^2 y_5^2$$
$$+ 300 y_1 y_2^2 y_3 y_4^2 y_5^2 + 144 \kappa y_2^2 y_4^2 y_5^2 - 116 y_1 y_3^3 y_5^2 - 16 \kappa y_3^2 y_5^2 - 158 y_1 y_2^2 y_3 y_5^2 - 72 \kappa y_2^2 y_5^2$$
$$+ 100 y_1 y_3^3 y_4^4 + 32 \kappa y_3^2 y_4^4 + 142 y_1 y_2^2 y_3 y_4^4 + 72 \kappa y_2^2 y_4^4 - 100 y_1 y_3^3 y_4^2 - 32 \kappa y_3^2 y_4^2 - 142 y_1 y_2^2 y_3 y_4^2$$
$$- 72 \kappa y_2^2 y_4^2 + 18 y_1 y_3^3 + 4 \kappa y_3^2 + 25 y_1 y_2^2 y_3 + 12 \kappa y_2^2 \Big)$$

$$\pi_{43} = y_1^2 y_3^2 \Big( 12 y_1 y_3^4 y_5^4 - 16 \kappa y_3^3 y_5^4 + 54 y_1 y_2^2 y_3^2 y_5^4 - 16 \kappa y_2^2 y_3 y_5^4 + 36 y_1 y_2^4 y_5^4 + 24 y_1 y_3^4 y_4^2 y_5^2 - 24 \kappa y_3^3 y_4^2 y_5^2$$
$$+ 108 y_1 y_2^2 y_3^2 y_4^2 y_5^2 - 24 \kappa y_2^2 y_3 y_4^2 y_5^2 + 72 y_1 y_2^4 y_4^2 y_5^2 - 12 y_1 y_3^4 y_5^2 + 16 \kappa y_3^3 y_5^2 - 54 y_1 y_2^2 y_3^2 y_5^2$$
$$+ 16 \kappa y_2^2 y_3 y_5^2 - 36 y_1 y_2^4 y_5^2 + 12 y_1 y_3^4 y_4^4 - 8 \kappa y_3^3 y_4^4 + 54 y_1 y_2^2 y_3^2 y_4^4 - 8 \kappa y_2^2 y_3 y_4^4 + 36 y_1 y_2^4 y_4^4$$
$$- 12 y_1 y_3^4 y_4^2 + 8 \kappa y_3^3 y_4^2 - 54 y_1 y_2^2 y_3^2 y_4^2 + 8 \kappa y_2^2 y_3 y_4^2 - 36 y_1 y_2^4 y_4^2 + 2 y_1 y_3^4 - 2 \kappa y_3^3 + 9 y_1 y_2^2 y_3^2$$
$$- 2 \kappa y_2^2 y_3 + 6 y_1 y_2^4 \Big)$$

$$\pi_{44} = 60 y_1 y_2 y_3^2 y_5^4 + 72 \kappa y_2 y_3 y_5^4 - 18 y_1 y_2^3 y_5^4 + 32 y_1 y_3^3 y_4 y_5^3 + 8 \kappa y_3^2 y_4 y_5^3 + 120 y_1 y_2 y_3^2 y_4^2 y_5^2$$
$$+ 144 \kappa y_2 y_3 y_4^2 y_5^2 - 36 y_1 y_2^3 y_4^2 y_5^2 - 60 y_1 y_2 y_3^2 y_5^2 - 72 \kappa y_2 y_3 y_5^2 + 18 y_1 y_2^3 y_5^2 + 32 y_1 y_3^3 y_4^3 y_5$$
$$+ 8 \kappa y_3^2 y_4^3 y_5 - 32 y_1 y_3^3 y_4 y_5 - 8 \kappa y_3^2 y_4 y_5 + 60 y_1 y_2 y_3^2 y_4^4 + 72 \kappa y_2 y_3 y_4^4 - 18 y_1 y_2^3 y_4^4 - 60 y_1 y_2 y_3^2 y_4^2$$
$$- 72 \kappa y_2 y_3 y_4^2 + 18 y_1 y_2^3 y_4^2 + 10 y_1 y_2 y_3^2 + 12 \kappa y_2 y_3 - 3 y_1 y_2^3$$

$$\pi_{45} = y_1^2 y_3^2 \Big( 24 y_1 y_2^3 y_3^2 y_5^4 + 18 y_1 y_2^5 y_5^4 - 8 \kappa y_3^4 y_4 y_5^3 - 8 \kappa y_2^2 y_3^2 y_4 y_5^3 + 48 y_1 y_2^3 y_3^2 y_4^2 y_5^2 + 36 y_1 y_2^5 y_4^2 y_5^2$$
$$- 24 y_1 y_2^3 y_3^2 y_5^2 - 18 y_1 y_2^5 y_5^2 - 8 \kappa y_3^4 y_4^3 y_5 - 8 \kappa y_2^2 y_3^2 y_4^3 y_5 + 8 \kappa y_3^4 y_4 y_5 + 8 \kappa y_2^2 y_3^2 y_4 y_5$$
$$+ 24 y_1 y_2^3 y_3^2 y_4^4 + 18 y_1 y_2^5 y_4^4 - 24 y_1 y_2^3 y_3^2 y_4^2 - 18 y_1 y_2^5 y_4^2 + 4 y_1 y_2^3 y_3^2 + 3 y_1 y_2^5 \Big)$$

$$\pi_{46} = y_1 y_3 \Big( 24 y_1 y_2 y_3^3 y_5^4 + 12 \kappa y_2 y_3^2 y_5^4 + 36 y_1 y_2^3 y_3 y_5^4 + 18 \kappa y_2^3 y_5^4 + 8 y_1 y_3^4 y_4 y_5^3 - 8 \kappa y_3^3 y_4 y_5^3$$
$$+ 8 y_1 y_2^2 y_3^2 y_4 y_5^3 + 48 y_1 y_2 y_3^3 y_4^2 y_5^2 + 24 \kappa y_2 y_3^2 y_4^2 y_5^2 + 72 y_1 y_2^3 y_3 y_4^2 y_5^2 + 36 \kappa y_2^3 y_4^2 y_5^2 - 24 y_1 y_2 y_3^3 y_5^2$$
$$- 12 \kappa y_2 y_3^2 y_5^2 - 36 y_1 y_2^3 y_3 y_5^2 - 18 \kappa y_2^3 y_5^2 + 8 y_1 y_3^4 y_4^3 y_5 - 8 \kappa y_3^3 y_4^3 y_5 + 8 y_1 y_2^2 y_3^2 y_4^3 y_5 - 8 y_1 y_3^4 y_4 y_5$$
$$+ 8 \kappa y_3^3 y_4 y_5 - 8 y_1 y_2^2 y_3^2 y_4 y_5 + 24 y_1 y_2 y_3^3 y_4^4 + 12 \kappa y_2 y_3^2 y_4^4 + 36 y_1 y_2^3 y_3 y_4^4 + 18 \kappa y_2^3 y_4^4 + 3 \kappa y_2^3$$
$$- 24 y_1 y_2 y_3^3 y_4^2 - 12 \kappa y_2 y_3^2 y_4^2 - 36 y_1 y_2^3 y_3 y_4^2 - 18 \kappa y_2^3 y_4^2 + 4 y_1 y_2 y_3^3 + 2 \kappa y_2 y_3^2 + 6 y_1 y_2^3 y_3 \Big)$$

$$\pi_{47} = 36 y_1 y_3 y_5^4 + 3 \kappa y_5^4 + 48 y_1 y_3 y_4^2 y_5^2 - 36 y_1 y_3 y_5^2 - 3 \kappa y_5^2 + 12 y_1 y_3 y_4^4 - 3 \kappa y_4^4 - 12 y_1 y_3 y_4^2 + 3 \kappa y_4^2$$
$$+ 4 y_1 y_3$$

$$\pi_{48} = y_1 y_3 \Big( 24 y_1 y_3^2 y_5^4 + 51 \kappa y_3 y_5^4 - 18 y_1 y_2^2 y_5^4 - 32 y_1 y_2 y_3 y_4 y_5^3 - 8 \kappa y_2 y_4 y_5^3 + 84 y_1 y_3^2 y_4^2 y_5^2 + 96 \kappa y_3 y_4^2 y_5^2$$
$$- 24 y_1 y_2^2 y_4^2 y_5^2 - 24 y_1 y_3^2 y_5^2 - 51 \kappa y_3 y_5^2 + 18 y_1 y_2^2 y_5^2 - 32 y_1 y_2 y_3 y_4^3 y_5 - 8 \kappa y_2 y_4^3 y_5$$
$$+ 32 y_1 y_2 y_3 y_4 y_5 + 8 \kappa y_2 y_4 y_5 + 60 y_1 y_3^2 y_4^4 + 45 \kappa y_3 y_4^4 - 6 y_1 y_2^2 y_4^4 - 60 y_1 y_3^2 y_4^2 - 45 \kappa y_3 y_4^2$$
$$+ 6 y_1 y_2^2 y_4^2 + 7 y_1 y_3^2 + 8 \kappa y_3 - 2 y_1 y_2^2 \Big)$$

$$\pi_{49} = y_1^2 y_3^2 \Big( 54 y_1 y_3^3 y_5^4 + 36 \kappa y_3^2 y_5^4 + 84 y_1 y_2^2 y_3 y_5^4 + 54 \kappa y_2^2 y_5^4 - 32 y_1 y_2 y_3^2 y_4 y_5^3 + 32 \kappa y_2 y_3 y_4 y_5^3$$
$$- 32 y_1 y_2^3 y_4 y_5^3 + 132 y_1 y_3^3 y_4^2 y_5^2 + 36 \kappa y_3^2 y_4^2 y_5^2 + 192 y_1 y_2^2 y_3 y_4^2 y_5^2 + 96 \kappa y_2^2 y_4^2 y_5^2 - 54 y_1 y_3^3 y_5^2$$
$$- 36 \kappa y_3^2 y_5^2 - 84 y_1 y_2^2 y_3 y_5^2 - 54 \kappa y_2^2 y_5^2 - 32 y_1 y_2 y_3^2 y_4^3 y_5 + 32 \kappa y_2 y_3 y_4^3 y_5 - 32 y_1 y_2^3 y_4^3 y_5$$
$$+ 32 y_1 y_2 y_3^2 y_4 y_5 - 32 \kappa y_2 y_3 y_4 y_5 + 32 y_1 y_2^3 y_4 y_5 + 78 y_1 y_3^3 y_4^4 + 108 y_1 y_2^2 y_3 y_4^4 + 42 \kappa y_2^2 y_4^4$$
$$- 78 y_1 y_3^3 y_4^2 - 108 y_1 y_2^2 y_3 y_4^2 - 42 kappa y_2^2 y_4^2 + 11 y_1 y_3^3 + 3 \kappa y_3^2 + 16 y_1 y_2^2 y_3 + 8 \kappa y_2^2 \Big)$$

$$\pi_{50} = y_1^3 y_3^3 \Big( 6 y_1 y_3^4 y_5^4 + 36 y_1 y_2^2 y_3^2 y_5^4 + 24 y_1 y_2^4 y_5^4 + 16 \kappa y_2 y_3^2 y_4 y_5^3 + 16 \kappa y_2^3 y_4 y_5^3 + 12 y_1 y_3^4 y_4^2 y_5^2$$
$$- 12 \kappa y_3^3 y_4^2 y_5^2 + 72 y_1 y_2^2 y_3^2 y_4^2 y_5^2 - 12 \kappa y_2^2 y_3 y_4^2 y_5^2 + 48 y_1 y_2^4 y_4^2 y_5^2 - 6 y_1 y_3^4 y_5^2 - 36 y_1 y_2^2 y_3^2 y_5^2$$
$$- 24 y_1 y_2^4 y_5^2 + 16 \kappa y_2 y_3^2 y_4^3 y_5 + 16 \kappa y_2^3 y_4^3 y_5 - 16 \kappa y_2 y_3^2 y_4 y_5 - 16 \kappa y_2^3 y_4 y_5 + 6 y_1 y_3^4 y_4^4 - 12 \kappa y_3^3 y_4^4$$
$$+ 36 y_1 y_2^2 y_3^2 y_4^4 - 12 \kappa y_2^2 y_3 y_4^4 + 24 y_1 y_2^4 y_4^4 - 6 y_1 y_3^4 y_4^2 + 12 \kappa y_3^3 y_4^2 - 36 y_1 y_2^2 y_3^2 y_4^2 + 12 \kappa y_2^2 y_3 y_4^2$$
$$- 24 y_1 y_2^4 y_4^2 + y_1 y_3^4 - \kappa y_3^3 + 6 y_1 y_2^2 y_3^2 - \kappa y_2^2 y_3 + 4 y_1 y_2^4 \Big)$$

$$\pi_{51} = 120 y_1 y_2 y_5^5 + 72 y_1 y_3 y_4 y_5^4 + 18 \kappa y_4 y_5^4 + 240 y_1 y_2 y_4^2 y_5^3 - 120 y_1 y_2 y_5^3 + 80 y_1 y_3 y_4^3 y_5^2 + 20 \kappa y_4^3 y_5^2$$
$$- 68 y_1 y_3 y_4 y_5^2 - 17 \kappa y_4 y_5^2 + 120 y_1 y_2 y_4^4 y_5 - 120 y_1 y_2 y_4^2 y_5 + 24 y_1 y_2 y_5 + 8 y_1 y_3 y_4^5 + 2 \kappa y_4^5$$
$$- 12 y_1 y_3 y_4^3 - 3 \kappa y_4^3 + 4 y_1 y_3 y_4 + \kappa y_4$$

$$\pi_{52} = y_1 \Big( 852 y_1 y_2 y_3^2 y_5^5 + 624 \kappa y_2 y_3 y_5^5 - 120 y_1 y_2^3 y_5^5 - 232 y_1 y_3^3 y_4 y_5^4 + 32 \kappa y_3^2 y_4 y_5^4 - 72 y_1 y_2^2 y_3 y_4 y_5^4$$
$$+ 1560 y_1 y_2 y_3^2 y_4^2 y_5^3 + 1212 \kappa y_2 y_3 y_4^2 y_5^3 - 240 y_1 y_2^3 y_4^2 y_5^3 - 852 y_1 y_2 y_3^2 y_5^3 - 624 \kappa y_2 y_3 y_5^3$$
$$+ 120 y_1 y_2^3 y_5^3 - 272 y_1 y_3^3 y_4^3 y_5^2 + 32 \kappa y_3^2 y_4^3 y_5^2 - 80 y_1 y_2^2 y_3 y_4^3 y_5^2 + 212 y_1 y_3^3 y_4 y_5^2 - 32 \kappa y_3^2 y_4 y_5^2$$
$$+ 68 y_1 y_2^2 y_3 y_4 y_5^2 + 708 y_1 y_2 y_3^2 y_4^4 y_5 + 588 \kappa y_2 y_3 y_4^4 y_5 - 120 y_1 y_2^3 y_4^4 y_5 - 732 y_1 y_2 y_3^2 y_4^2 y_5$$
$$- 594 \kappa y_2 y_3 y_4^2 y_5 + 120 y_1 y_2^3 y_4^2 y_5 + 164 y_1 y_2 y_3^2 y_5 + 123 \kappa y_2 y_3 y_5 - 24 y_1 y_2^3 y_5 - 40 y_1 y_3^3 y_4^5$$
$$- 8 y_1 y_2^2 y_3 y_4^5 + 60 y_1 y_3^3 y_4^3 + 12 y_1 y_2^2 y_3 y_4^3 - 20 y_1 y_3^3 y_4 - 4 y_1 y_2^2 y_3 y_4 \Big)$$

$$\pi_{53} = y_1^2 y_3 \Big( 648 y_1 y_2 y_3^3 y_5^5 + 12\kappa y_2 y_3^2 y_5^5 + 726 y_1 y_2^3 y_3 y_5^5 + 240\kappa y_2^3 y_5^5 - 80 y_1 y_3^4 y_4 y_5^4 + 116\kappa y_3^3 y_4 y_5^4$$
$$- 80 y_1 y_2^2 y_3^2 y_4 y_5^4 + 36\kappa y_2^2 y_3 y_4 y_5^4 + 1224 y_1 y_2 y_3^3 y_4^2 y_5^3 + 96\kappa y_2 y_3^2 y_4^2 y_5^3 + 1380 y_1 y_2^3 y_3 y_4^2 y_5^3$$
$$+ 480\kappa y_2^3 y_4^2 y_5^3 - 648 y_1 y_2 y_3^3 y_5^3 - 12\kappa y_2 y_3^2 y_5^3 - 726 y_1 y_2^3 y_3 y_5^3 - 240\kappa y_2^3 y_5^3 - 96 y_1 y_3^4 y_4^3 y_5^2$$
$$+ 136\kappa y_3^3 y_4^3 y_5^2 - 96 y_1 y_2^2 y_3^2 y_4^3 y_5^2 + 40\kappa y_2^2 y_3 y_4^3 y_5^2 + 72 y_1 y_3^4 y_4 y_5^2 - 106\kappa y_3^3 y_4 y_5^2 + 72 y_1 y_2^2 y_3^2 y_4 y_5^2$$
$$- 34\kappa y_2^2 y_3 y_4 y_5^2 + 576 y_1 y_2 y_3^3 y_4^4 y_5 + 84\kappa y_2 y_3^2 y_4^4 y_5 + 654 y_1 y_2^3 y_3 y_4^4 y_5 + 240\kappa y_2^3 y_4^4 y_5$$
$$- 588 y_1 y_2 y_3^3 y_4^2 y_5 - 72\kappa y_2 y_3^2 y_4^2 y_5 - 666 y_1 y_2^3 y_3 y_4^2 y_5 - 240\kappa y_2^3 y_4^2 y_5 + 127 y_1 y_2 y_3^3 y_5 + 5\kappa y_2 y_3^2 y_5$$
$$+ 142 y_1 y_2^3 y_3 y_5 + 48\kappa y_2^3 y_5 - 16 y_1 y_3^4 y_4^5 + 20\kappa y_3^3 y_4^5 - 16 y_1 y_2^2 y_3^2 y_4^5 + 4\kappa y_2^2 y_3 y_4^5 + 24 y_1 y_3^4 y_4^3$$
$$- 30\kappa y_3^3 y_4^3 + 24 y_1 y_2^2 y_3^2 y_4^3 - 6\kappa y_2^2 y_3 y_4^3 - 8 y_1 y_3^4 y_4 + 10\kappa y_3^3 y_4 - 8 y_1 y_2^2 y_3^2 y_4 + 2\kappa y_2^2 y_3 y_4 \Big)$$
$$\pi_{54} = y_1^3 y_3^2 \Big( 72 y_1 y_2 y_3^4 y_5^5 - 96\kappa y_2 y_3^3 y_5^5 + 198 y_1 y_2^3 y_3^2 y_5^5 - 96\kappa y_2^3 y_3 y_5^5 + 120 y_1 y_2^5 y_5^5 + 40\kappa y_3^4 y_4 y_5^4$$
$$+ 40\kappa y_2^2 y_3^2 y_4 y_5^4 + 144 y_1 y_2 y_3^4 y_4^2 y_5^3 - 156\kappa y_2 y_3^3 y_4^2 y_5^3 + 396 y_1 y_2^3 y_3^2 y_4^2 y_5^3 - 156\kappa y_2^3 y_3 y_4^2 y_5^3$$
$$+ 240 y_1 y_2^5 y_4^2 y_5^3 - 72 y_1 y_2 y_3^4 y_5^3 + 96\kappa y_2 y_3^3 y_5^3 - 198 y_1 y_2^3 y_3^2 y_5^3 + 96\kappa y_2^3 y_3 y_5^3 - 120 y_1 y_2^5 y_5^3$$
$$+ 48\kappa y_3^4 y_4^3 y_5^2 + 48\kappa y_2^2 y_3^2 y_4^3 y_5^2 - 36\kappa y_3^4 y_4 y_5^2 - 36\kappa y_2^2 y_3^2 y_4 y_5^2 + 72 y_1 y_2 y_3^4 y_4^4 y_5 - 60\kappa y_2 y_3^3 y_4^4 y_5$$
$$+ 198 y_1 y_2^3 y_3^2 y_4^4 y_5 - 60\kappa y_2^3 y_3 y_4^4 y_5 + 120 y_1 y_2^5 y_4^4 y_5 - 72 y_1 y_2 y_3^4 y_4^2 y_5 + 66\kappa y_2 y_3^3 y_4^2 y_5$$
$$- 198 y_1 y_2^3 y_3^2 y_4^2 y_5 + 66\kappa y_2^3 y_3 y_4^2 y_5 - 120 y_1 y_2^5 y_4^2 y_5 + 15 y_1 y_2 y_3^4 y_5 - 18\kappa y_2 y_3^3 y_5 + 40 y_1 y_2^3 y_3^2 y_5$$
$$- 18\kappa y_2^3 y_3 y_5 + 24 y_1 y_2^5 y_5 + 8\kappa y_3^4 y_4^5 + 8\kappa y_2^2 y_3^2 y_4^5 - 12\kappa y_3^4 y_4^3 - 12\kappa y_2^2 y_3^2 y_4^3 + 4\kappa y_3^4 y_4$$
$$+ 4\kappa y_2^2 y_3^2 y_4 \Big)$$
$$\pi_{55} = 8 y_1 y_3 y_5^5 + 2\kappa y_5^5 + 120 y_1 y_2 y_4 y_5^4 + 80 y_1 y_3 y_4^2 y_5^3 + 20\kappa y_4^2 y_5^3 - 12 y_1 y_3 y_5^3 - 3\kappa y_5^3 + 240 y_1 y_2 y_4^3 y_5^2$$
$$- 120 y_1 y_2 y_4 y_5^2 + 72 y_1 y_3 y_4^4 y_5 + 18\kappa y_4^4 y_5 - 68 y_1 y_3 y_4^2 y_5 - 17\kappa y_4^2 y_5 + 4 y_1 y_3 y_5 + \kappa y_5$$
$$+ 120 y_1 y_2 y_4^5 - 120 y_1 y_2 y_4^3 + 24 y_1 y_2 y_4$$

$$\pi_{56} = y_1\Big(40y_1y_3^3y_5^5 + 8y_1y_2^2y_3y_5^5 - 804y_1y_2y_3^2y_4y_5^4 - 612\kappa y_2y_3y_4y_5^4 + 120y_1y_2^3y_4y_5^4 + 272y_1y_3^3y_4^2y_5^3$$
$$- 32\kappa y_3^2y_4^2y_5^3 + 80y_1y_2^2y_3y_4^2y_5^3 - 60y_1y_3^3y_5^3 - 12y_1y_2^2y_3y_5^3 - 1464y_1y_2y_3^2y_4^3y_5^2$$
$$- 1188\kappa y_2y_3y_4^3y_5^2 + 240y_1y_2^3y_4^3y_5^2 + 780y_1y_2y_3^2y_4y_5^2 + 606\kappa y_2y_3y_4y_5^2 - 120y_1y_2^3y_4y_5^2$$
$$+ 232y_1y_3^3y_4^4y_5 - 32\kappa y_3^2y_4^4y_5 + 72y_1y_2^2y_3y_4^4y_5 - 212y_1y_3^3y_4^2y_5 + 32\kappa y_3^2y_4^2y_5 - 68y_1y_2^2y_3y_4^2y_5$$
$$+ 20y_1y_3^3y_5 + 4y_1y_2^2y_3y_5 - 660y_1y_2y_3^2y_4^5 - 576\kappa y_2y_3y_4^5 + 120y_1y_2^3y_4^5 + 660y_1y_2y_3^2y_4^3$$
$$+ 576\kappa y_2y_3y_4^3 - 120y_1y_2^3y_4^3 - 140y_1y_2y_3^2y_4 - 117\kappa y_2y_3y_4 + 24y_1y_2^3y_4\Big)$$

$$\pi_{57} = y_1^3y_3^2\Big(8\kappa y_3^4y_5^5 + 8\kappa y_2^2y_3^2y_5^5 + 72y_1y_2y_3^4y_4y_5^4 - 84\kappa y_2y_3^3y_4y_5^4 + 198y_1y_2^3y_3^2y_4y_5^4 - 84\kappa y_2^3y_3y_4y_5^4$$
$$+ 120y_1y_2^5y_4y_5^4 + 48\kappa y_3^4y_4^2y_5^3 + 48\kappa y_2^2y_3^2y_4^2y_5^3 - 12\kappa y_3^4y_5^3 - 12\kappa y_2^2y_3^2y_5^3 + 144y_1y_2y_3^4y_4^3y_5^2$$
$$- 132\kappa y_2y_3^3y_4^3y_5^2 + 396y_1y_2^3y_3^2y_4^3y_5^2 - 132\kappa y_2^3y_3y_4^3y_5^2 + 240y_1y_2^5y_4^3y_5^2 - 72y_1y_2y_3^4y_4y_5^2$$
$$+ 78\kappa y_2y_3^3y_4y_5^2 - 198y_1y_2^3y_3^2y_4y_5^2 + 78\kappa y_2^3y_3y_4y_5^2 - 120y_1y_2^5y_4y_5^2 + 40\kappa y_3^4y_4^4y_5$$
$$+ 40\kappa y_2^2y_3^2y_4^4y_5 - 36\kappa y_3^4y_4^2y_5 - 36\kappa y_2^2y_3^2y_4^2y_5 + 4\kappa y_3^4y_5 + 4\kappa y_2^2y_3^2y_5 + 72y_1y_2y_3^4y_4^5$$
$$- 48\kappa y_2y_3^3y_4^5 + 198y_1y_2^3y_3^2y_4^5 - 48\kappa y_2^3y_3y_4^5 + 120y_1y_2^5y_4^5 - 72y_1y_2y_3^4y_4^3 + 48\kappa y_2y_3^3y_4^3$$
$$- 198y_1y_2^3y_3^2y_4^3 + 48\kappa y_2^3y_3y_4^3 - 120y_1y_2^5y_4^3 + 15y_1y_2y_3^4y_4 - 12\kappa y_2y_3^3y_4 + 40y_1y_2^3y_3^2y_4$$
$$- 12\kappa y_2^3y_3y_4 + 24y_1y_2^5y_4\Big)$$

$$\pi_{58} = y_1^2y_3\Big(16y_1y_3^4y_5^5 - 20\kappa y_3^3y_5^5 + 16y_1y_2^2y_3^2y_5^5 - 4\kappa y_2^2y_3y_5^5 - 624y_1y_2y_3^3y_4y_5^4 - 36\kappa y_2y_3^2y_4y_5^4$$
$$- 702y_1y_2^3y_3y_4y_5^4 - 240\kappa y_2^3y_4y_5^4 + 96y_1y_3^4y_4^2y_5^3 - 136\kappa y_3^3y_4^2y_5^3 + 96y_1y_2^2y_3^2y_4^2y_5^3$$
$$- 40\kappa y_2^2y_3y_4^2y_5^3 - 24y_1y_3^4y_5^3 + 30\kappa y_3^3y_5^3 - 24y_1y_2^2y_3^2y_5^3 + 6\kappa y_2^2y_3y_5^3 - 1176y_1y_2y_3^3y_4^3y_5^2$$
$$- 144\kappa y_2y_3^2y_4^3y_5^2 - 1332y_1y_2^3y_3y_4^3y_5^2 - 480\kappa y_2^3y_4^3y_5^2 + 612y_1y_2y_3^3y_4y_5^2 + 48\kappa y_2y_3^2y_4y_5^2$$
$$+ 690y_1y_2^3y_3y_4y_5^2 + 240\kappa y_2^3y_4y_5^2 + 80y_1y_3^4y_4^4y_5 - 116\kappa y_3^3y_4^4y_5 + 80y_1y_2^2y_3^2y_4^4y_5$$
$$- 36\kappa y_2^2y_3y_4^4y_5 - 72y_1y_3^4y_4^2y_5 + 106\kappa y_3^3y_4^2y_5 - 72y_1y_2^2y_3^2y_4^2y_5 + 34\kappa y_2^2y_3y_4^2y_5 + 8y_1y_3^4y_5$$
$$- 10\kappa y_3^3y_5 + 8y_1y_2^2y_3^2y_5 - 2\kappa y_2^2y_3y_5 - 552y_1y_2y_3^3y_4^5 - 108\kappa y_2y_3^2y_4^5 - 630y_1y_2^3y_3y_4^5$$
$$- 240\kappa y_2^3y_4^5 + 552y_1y_2y_3^3y_4^3 + 108\kappa y_2y_3^2y_4^3 + 630y_1y_2^3y_3y_4^3 + 240\kappa y_2^3y_4^3 - 115y_1y_2y_3^3y_4$$
$$- 17\kappa y_2y_3^2y_4 - 130y_1y_2^3y_3y_4 - 48\kappa y_2^3y_4\Big)$$

$$\pi_{59} = 30y_1y_2y_5^4 + 20y_1y_3y_4y_5^3 + 5\kappa y_4y_5^3 + 60y_1y_2y_4^2y_5^2 - 24y_1y_2y_5^2 + 20y_1y_3y_4^3y_5 + 5\kappa y_4^3y_5$$
$$- 16y_1y_3y_4y_5 - 4\kappa y_4y_5 + 30y_1y_2y_4^4 - 24y_1y_2y_4^2 + 3y_1y_2$$

$$\pi_{60} = y_1\Big(426y_1y_2y_3^2y_5^4 + 312\kappa y_2y_3y_5^4 - 60y_1y_2^3y_5^4 - 136y_1y_3^3y_4y_5^3 + 16\kappa y_3^2y_4y_5^3 - 40y_1y_2^2y_3y_4y_5^3$$
$$+ 756y_1y_2y_3^2y_4^2y_5^2 + 600\kappa y_2y_3y_4^2y_5^2 - 120y_1y_2^3y_4^2y_5^2 - 336y_1y_2y_3^2y_5^2 - 249\kappa y_2y_3y_5^2 + 48y_1y_2^3y_5^2$$
$$- 136y_1y_3^3y_4^3y_5 + 16\kappa y_3^2y_4^3y_5 - 40y_1y_2^2y_3y_4^3y_5 + 96y_1y_3^3y_4y_5 - 16\kappa y_3^2y_4y_5 + 32y_1y_2^2y_3y_4y_5$$
$$+ 330y_1y_2y_3^2y_4^4 + 288\kappa y_2y_3y_4^4 - 60y_1y_2^3y_4^4 - 264y_1y_2y_3^2y_4^2 - 231\kappa y_2y_3y_4^2 + 48y_1y_2^3y_4^2$$
$$+ 37y_1y_2y_3^2 + 30kappay_2y_3 - 6y_1y_2^3\Big)$$

$$\pi_{61} = y_1^2y_3\Big(648y_1y_2y_3^3y_5^4 + 12\kappa y_2y_3^2y_5^4 + 726y_1y_2^3y_3y_5^4 + 240\kappa y_2^3y_5^4 - 96y_1y_3^4y_4y_5^3 + 136\kappa y_3^3y_4y_5^3$$
$$- 96y_1y_2^2y_3^2y_4y_5^3 + 40\kappa y_2^2y_3y_4y_5^3 + 1200y_1y_2y_3^3y_4^2y_5^2 + 120\kappa y_2y_3^2y_4^2y_5^2 + 1356y_1y_2^3y_3y_4^2y_5^2$$
$$+ 480\kappa y_2^3y_4^2y_5^2 - 510y_1y_2y_3^3y_5^2 - 18\kappa y_2y_3^2y_5^2 - 576y_1y_2^3y_3y_5^2 - 192\kappa y_2^3y_5^2 - 96y_1y_3^4y_4^3y_5$$
$$+ 136\kappa y_3^3y_4^3y_5 - 96y_1y_2^2y_3^2y_4^3y_5 + 40\kappa y_2^2y_3y_4^3y_5 + 64y_1y_3^4y_4y_5 - 96\kappa y_3^3y_4y_5 + 64y_1y_2^2y_3^2y_4y_5$$
$$- 32\kappa y_2^2y_3y_4y_5 + 552y_1y_2y_3^3y_4^4 + 108\kappa y_2y_3^2y_4^4 + 630y_1y_2^3y_3y_4^4 + 240\kappa y_2^3y_4^4 - 438y_1y_2y_3^3y_4^2$$
$$- 90\kappa y_2y_3^2y_4^2 - 504y_1y_2^3y_3y_4^2 - 192\kappa y_2^3y_4^2 + 58y_1y_2y_3^3 + 8\kappa y_2y_3^2 + 67y_1y_2^3y_3 + 24\kappa y_2^3\Big)$$

$$\pi_{62} = y_1^3y_3^2\Big(72y_1y_2y_3^4y_5^4 - 96\kappa y_2y_3^3y_5^4 + 198y_1y_2^3y_3^2y_5^4 - 96\kappa y_2^3y_3y_5^4 + 120y_1y_2^5y_5^4 + 48\kappa y_3^4y_4y_5^3$$
$$+ 48\kappa y_2^2y_3^2y_4y_5^3 + 144y_1y_2y_3^4y_4^2y_5^2 - 144\kappa y_2y_3^3y_4^2y_5^2 + 396y_1y_2^3y_3^2y_4^2y_5^2 - 144\kappa y_2^3y_3y_4^2y_5^2$$
$$+ 240y_1y_2^5y_4^2y_5^2 - 54y_1y_2y_3^4y_5^2 + 72\kappa y_2y_3^3y_5^2 - 156y_1y_2^3y_3^2y_5^2 + 72\kappa y_2^3y_3y_5^2 - 96y_1y_2^5y_5^2$$
$$+ 48\kappa y_3^4y_4^3y_5 + 48\kappa y_2^2y_3^2y_4^3y_5 - 32\kappa y_3^4y_4y_5 - 32\kappa y_2^2y_3^2y_4y_5 + 72y_1y_2y_3^4y_4^4 - 48\kappa y_2y_3^3y_4^4$$
$$+ 198y_1y_2^3y_3^2y_4^4 - 48\kappa y_2^3y_3y_4^4 + 120y_1y_2^5y_4^4 - 54y_1y_2y_3^4y_4^2 + 36\kappa y_2y_3^3y_4^2 - 156y_1y_2^3y_3^2y_4^2$$
$$+ 36\kappa y_2^3y_3y_4^2 - 96y_1y_2^5y_4^2 + 6y_1y_2y_3^4 - 6\kappa y_2y_3^3 + 19y_1y_2^3y_3^2 - 6\kappa y_2^3y_3 + 12y_1y_2^5\Big)$$

$$\pi_{63} = y_4\left(24y_1y_3y_5^2 + 12\kappa y_5^2 + 22y_1y_3y_4^2 + 12\kappa y_4^2 - 11y_1y_3 - 6\kappa\right)$$

$$\pi_{64} = y_1y_3y_4\Big(6y_1y_3^2y_5^2 - 6\kappa y_3y_5^2 + 12y_1y_2^2y_5^2 + 6y_1y_3^2y_4^2 - 4\kappa y_3y_4^2 + 12y_1y_2^2y_4^2 - 3y_1y_3^2 + 2\kappa y_3$$
$$- 6y_1y_2^2\Big)$$

$$\pi_{65} = 2y_5^2 + 2y_4^2 - 1$$

$$\pi_{66} = 4y_1y_3^3y_5^3 + 2\kappa y_3^2y_5^3 - 6y_1y_2y_3^2y_4y_5^2 + 12\kappa y_2y_3y_4y_5^2 - 6y_1y_2^3y_4y_5^2 + 12y_1y_3^3y_4^2y_5 + 6\kappa y_3^2y_4^2y_5$$
$$- 4y_1y_3^3y_5 - 2\kappa y_3^2y_5 - 6y_1y_2y_3^2y_4^3 + 12\kappa y_2y_3y_4^3 - 6y_1y_2^3y_4^3 + 3y_1y_2y_3^2y_4 - 6\kappa y_2y_3y_4$$
$$+ 3y_1y_2^3y_4$$

$$\pi_{67} = y_1y_3\Big(2y_1y_3^4y_5^3 + 2y_1y_2^2y_3^2y_5^3 + 6\kappa y_2^3y_4y_5^2 + 6y_1y_3^4y_4^2y_5 + 6y_1y_2^2y_3^2y_4^2y_5 - 2y_1y_3^4y_5 - 2y_1y_2^2y_3^2y_5$$
$$+ 6\kappa y_2^3y_4^3 - 3\kappa y_2^3y_4\Big)$$

$$\pi_{68} = y_3\Big(2y_1y_2y_5^3 - 24y_1y_3y_4y_5^2 - 12\kappa y_4y_5^2 + 6y_1y_2y_4^2y_5 - 2y_1y_2y_5 - 30y_1y_3y_4^3 - 10\kappa y_4^3 + 15y_1y_3y_4$$
$$+ 5\kappa y_4\Big)$$

$$\pi_{69} = y_1y_3^2\Big(2\kappa y_2y_5^3 + 6y_1y_3^2y_4y_5^2 - 6\kappa y_3y_4y_5^2 + 12y_1y_2^2y_4y_5^2 + 6\kappa y_2y_4^2y_5 - 2\kappa y_2y_5 + 6y_1y_3^2y_4^3$$
$$- 12\kappa y_3y_4^3 + 12y_1y_2^2y_4^3 - 3y_1y_3^2y_4 + 6\kappa y_3y_4 - 6y_1y_2^2y_4\Big)$$

$$\pi_{70} = y_1y_3\Big(10\kappa y_3^2y_5^4 + 48y_1y_2y_3^2y_4y_5^3 - 52\kappa y_2y_3y_4y_5^3 + 60y_1y_2^3y_4y_5^3 + 36\kappa y_3^2y_4^2y_5^2 - 9\kappa y_3^2y_5^2$$
$$+ 48y_1y_2y_3^2y_4^3y_5 - 40\kappa y_2y_3y_4^3y_5 + 60y_1y_2^3y_4^3y_5 - 24y_1y_2y_3^2y_4y_5 + 22\kappa y_2y_3y_4y_5 - 30y_1y_2^3y_4y_5$$
$$+ 10\kappa y_3^2y_4^4 - 9\kappa y_3^2y_4^2 + \kappa y_3^2\Big)$$

$$\pi_{71} = 18y_5^4 + 60y_4^2y_5^2 - 17y_5^2 + 10y_4^4 - 9y_4^2 + 1$$

$$\pi_{72} = 40y_1y_3^2y_5^4 - 18\kappa y_3y_5^4 - 736y_1y_2y_3y_4y_5^3 - 240\kappa y_2y_4y_5^3 + 144y_1y_3^2y_4^2y_5^2 - 60\kappa y_3y_4^2y_5^2 - 36y_1y_3^2y_5^2$$
$$+ 17\kappa y_3y_5^2 - 688y_1y_2y_3y_4^3y_5 - 240\kappa y_2y_4^3y_5 + 352y_1y_2y_3y_4y_5 + 120\kappa y_2y_4y_5 + 40y_1y_3^2y_4^4$$
$$- 10\kappa y_3y_4^4 - 36y_1y_3^2y_4^2 + 9\kappa y_3y_4^2 + 4y_1y_3^2 - \kappa y_3$$

$$\pi_{73} = 5y_5^4 + 30y_4^2y_5^2 - 5y_5^2 + 25y_4^4 - 15y_4^2 + 1$$

$$\pi_{74} = y_4y_5\left(20y_5^2 + 36y_4^2 - 17\right)$$

$$\pi_{75} = 94y_1y_2y_3y_5^4 + 30\kappa y_2y_5^4 - 48y_1y_3^2y_4y_5^3 + 20\kappa y_3y_4y_5^3 + 528y_1y_2y_3y_4^2y_5^2 + 180\kappa y_2y_4^2y_5^2$$
$$- 92y_1y_2y_3y_5^2 - 30\kappa y_2y_5^2 - 80y_1y_3^2y_4^3y_5 + 36\kappa y_3y_4^3y_5 + 36y_1y_3^2y_4y_5 - 17\kappa y_3y_4y_5$$
$$+ 410y_1y_2y_3y_4^4 + 150\kappa y_2y_4^4 - 246y_1y_2y_3y_4^2 - 90\kappa y_2y_4^2 + 17y_1y_2y_3 + 6\kappa y_2$$

$$\pi_{76} = y_1 y_3 \Big( 24 y_1 y_2 y_3^2 y_5^4 - 28 \kappa y_2 y_3 y_5^4 + 30 y_1 y_2^3 y_5^4 + 48 \kappa y_3^2 y_4 y_5^3 + 144 y_1 y_2 y_3^2 y_4^2 y_5^2 - 132 \kappa y_2 y_3 y_4^2 y_5^2 + 180 y_1 y_2^3 y_4^2 y_5^2 - 24 y_1 y_2 y_3^2 y_5^2 + 26 \kappa y_2 y_3 y_5^2 - 30 y_1 y_2^3 y_5^2 + 80 \kappa y_3^2 y_4^3 y_5 - 36 \kappa y_3^2 y_4 y_5 + 120 y_1 y_2 y_3^2 y_4^4 - 80 \kappa y_2 y_3 y_4^4 + 150 y_1 y_2^3 y_4^4 - 72 y_1 y_2 y_3^2 y_4^2 + 48 \kappa y_2 y_3 y_4^2 - 90 y_1 y_2^3 y_4^2 + 5 y_1 y_2 y_3^2 - 4 \kappa y_2 y_3 + 6 y_1 y_2^3 \Big)$$

$$\pi_{77} = 5 y_5^2 + 5 y_4^2 - 2$$

$$\pi_{78} = y_5 (5 y_5^2 + 15 y_4^2 - 4)$$

$$\pi_{79} = y_1 y_3 \Big( 6 \kappa y_3^2 y_5^3 + 24 y_1 y_2 y_3^2 y_4 y_5^2 - 24 \kappa y_2 y_3 y_4 y_5^2 + 30 y_1 y_2^3 y_4 y_5^2 + 18 \kappa y_3^2 y_4^2 y_5 - 4 \kappa y_3^2 y_5 + 24 y_1 y_2 y_3^2 y_4^3 - 16 \kappa y_2 y_3 y_4^3 + 30 y_1 y_2^3 y_4^3 - 9 y_1 y_2 y_3^2 y_4 + 6 \kappa y_2 y_3 y_4 - 12 y_1 y_2^3 y_4 \Big)$$

$$\pi_{80} = 12 y_1 y_3^2 y_5^3 - 5 \kappa y_3 y_5^3 - 180 y_1 y_2 y_3 y_4 y_5^2 - 60 \kappa y_2 y_4 y_5^2 + 36 y_1 y_3^2 y_4^2 y_5 - 15 \kappa y_3 y_4^2 y_5 - 8 y_1 y_3^2 y_5 + 4 \kappa y_3 y_5 - 164 y_1 y_2 y_3 y_4^3 - 60 \kappa y_2 y_4^3 + 66 y_1 y_2 y_3 y_4 + 24 \kappa y_2 y_4$$

$$\pi_{81} = y_5 \left( 26 y_1 y_3 y_5^2 + 12 \kappa y_5^2 + 24 y_1 y_3 y_4^2 + 12 \kappa y_4^2 - 13 y_1 y_3 - 6 \kappa \right)$$

$$\pi_{82} = y_1 y_3 y_5 \Big( 6 y_1 y_3^2 y_5^2 - 8 \kappa y_3 y_5^2 + 12 y_1 y_2^2 y_5^2 + 6 y_1 y_3^2 y_4^2 - 6 \kappa y_3 y_4^2 + 12 y_1 y_2^2 y_4^2 - 3 y_1 y_3^2 + 4 \kappa y_3 - 6 y_1 y_2^2 \Big)$$

$$\pi_{83} = y_1 y_3 \Big( 6 \kappa y_2^3 y_5^3 + 6 y_1 y_3^4 y_4 y_5^2 + 6 y_1 y_2^2 y_3^2 y_4 y_5^2 + 6 \kappa y_2^3 y_4^2 y_5 - 3 \kappa y_2^3 y_5 + 2 y_1 y_3^4 y_4^3 + 2 y_1 y_2^2 y_3^2 y_4^3 - 2 y_1 y_3^4 y_4 - 2 y_1 y_2^2 y_3^2 y_4 \Big)$$

$$\pi_{84} = 6 y_1 y_2 y_3^2 y_5^3 - 12 \kappa y_2 y_3 y_5^3 + 6 y_1 y_2^3 y_5^3 - 12 y_1 y_3^3 y_4 y_5^2 - 6 \kappa y_3^2 y_4 y_5^2 + 6 y_1 y_2 y_3^2 y_4^2 y_5 - 12 \kappa y_2 y_3 y_4^2 y_5 + 6 y_1 y_2^3 y_4^2 y_5 - 3 y_1 y_2 y_3^2 y_5 + 6 \kappa y_2 y_3 y_5 - 3 y_1 y_2^3 y_5 - 4 y_1 y_3^3 y_4^3 - 2 \kappa y_3^2 y_4^3 + 4 y_1 y_3^3 y_4 + 2 \kappa y_3^2 y_4$$

$$\pi_{85} = y_3 \Big( 18 y_1 y_3 y_5^3 + 14 \kappa y_5^3 - 6 y_1 y_2 y_4 y_5^2 + 24 y_1 y_3 y_4^2 y_5 + 12 \kappa y_4^2 y_5 - 9 y_1 y_3 y_5 - 7 \kappa y_5 - 2 y_1 y_2 y_4^3 + 2 y_1 y_2 y_4 \Big)$$

$$\pi_{86} = y_1 y_3^2 \Big( 6 y_1 y_3^2 y_5^3 + 12 y_1 y_2^2 y_5^3 + 6 \kappa y_2 y_4 y_5^2 + 6 y_1 y_3^2 y_4^2 y_5 - 6 \kappa y_3 y_4^2 y_5 + 12 y_1 y_2^2 y_4^2 y_5 - 3 y_1 y_3^2 y_5 - 6 y_1 y_2^2 y_5 + 2 \kappa y_2 y_4^3 - 2 \kappa y_2 y_4 \Big)$$

$$\pi_{87} = y_4 y_5 \left( 36 y_5^2 + 20 y_4^2 - 17 \right)$$

$$\pi_{88} = 25 y_5^4 + 30 y_4^2 y_5^2 - 15 y_5^2 + 5 y_4^4 - 5 y_4^2 + 1$$

$$\pi_{89} = 490y_1y_2y_3y_5^4 + 150\kappa y_2y_5^4 - 80y_1y_3^2y_4y_5^3 + 36\kappa y_3y_4y_5^3 + 552y_1y_2y_3y_4^2y_5^2 + 180\kappa y_2y_4^2y_5^2$$
$$- 294y_1y_2y_3y_5^2 - 90\kappa y_2y_5^2 - 48y_1y_3^2y_4^3y_5 + 20\kappa y_3y_4^3y_5 + 36y_1y_3^2y_4y_5 - 17\kappa y_3y_4y_5$$
$$+ 86y_1y_2y_3y_4^4 + 30\kappa y_2y_4^4 - 88y_1y_2y_3y_4^2 - 30\kappa y_2y_4^2 + 19y_1y_2y_3 + 6\kappa y_2$$

$$\pi_{90} = y_1y_3\Big(120y_1y_2y_3^2y_5^4 - 160\kappa y_2y_3y_5^4 + 150y_1y_2^3y_5^4 + 80\kappa y_3^2y_4y_5^3 + 144y_1y_2y_3^2y_4^2y_5^2 - 156\kappa y_2y_3y_4^2y_5^2$$
$$+ 180y_1y_2^3y_4^2y_5^2 - 72y_1y_2y_3^2y_5^2 + 96\kappa y_2y_3y_5^2 - 90y_1y_2^3y_5^2 + 48\kappa y_3^2y_4^3y_5 - 36\kappa y_3^2y_4y_5$$
$$+ 24y_1y_2y_3^2y_4^4 - 20\kappa y_2y_3y_4^4 + 30y_1y_2^3y_4^4 - 24y_1y_2y_3^2y_4^2 + 22\kappa y_2y_3y_4^2 - 30y_1y_2^3y_4^2 + 5y_1y_2y_3^2$$
$$- 6\kappa y_2y_3 + 6y_1y_2^3\Big)$$

$$\pi_{91} = 10y_5^4 + 60y_4^2y_5^2 - 9y_5^2 + 18y_4^4 - 17y_4^2 + 1$$

$$\pi_{92} = y_1y_3\Big(10\kappa y_3^2y_5^4 + 48y_1y_2y_3^2y_4y_5^3 - 56\kappa y_2y_3y_4y_5^3 + 60y_1y_2^3y_4y_5^3 + 36\kappa y_3^2y_4^2y_5^2 - 9\kappa y_3^2y_5^2$$
$$+ 48y_1y_2y_3^2y_4^3y_5 - 44\kappa y_2y_3y_4^3y_5 + 60y_1y_2^3y_4^3y_5 - 24y_1y_2y_3^2y_4y_5 + 26\kappa y_2y_3y_4y_5 - 30y_1y_2^3y_4y_5$$
$$+ 10\kappa y_3^2y_4^4 - 9\kappa y_3^2y_4^2 + \kappa y_3^2\Big)$$

$$\pi_{93} = 40y_1y_3^2y_5^4 - 10\kappa y_3y_5^4 - 752y_1y_2y_3y_4y_5^3 - 240\kappa y_2y_4y_5^3 + 144y_1y_3^2y_4^2y_5^2 - 60\kappa y_3y_4^2y_5^2 - 36y_1y_3^2y_5^2$$
$$+ 9\kappa y_3y_5^2 - 704y_1y_2y_3y_4^3y_5 - 240\kappa y_2y_4^3y_5 + 368y_1y_2y_3y_4y_5 + 120\kappa y_2y_4y_5 + 40y_1y_3^2y_4^4$$
$$- 18\kappa y_3y_4^4 - 36y_1y_3^2y_4^2 + 17\kappa y_3y_4^2 + 4y_1y_3^2 - \kappa y_3$$

$$\pi_{94} = y_4\left(15y_5^2 + 5y_4^2 - 4\right)$$

$$\pi_{95} = 196y_1y_2y_3y_5^3 + 60\kappa y_2y_5^3 - 36y_1y_3^2y_4y_5^2 + 15\kappa y_3y_4y_5^2 + 180y_1y_2y_3y_4^2y_5 + 60\kappa y_2y_4^2y_5$$
$$- 78y_1y_2y_3y_5 - 24\kappa y_2y_5 - 12y_1y_3^2y_4^3 + 5\kappa y_3y_4^3 + 8y_1y_3^2y_4 - 4\kappa y_3y_4$$

$$\pi_{96} = y_1y_3\Big(24y_1y_2y_3^2y_5^3 - 32\kappa y_2y_3y_5^3 + 30y_1y_2^3y_5^3 + 18\kappa y_3^2y_4y_5^2 + 24y_1y_2y_3^2y_4^2y_5 - 24\kappa y_2y_3y_4^2y_5$$
$$+ 30y_1y_2^3y_4^2y_5 - 9y_1y_2y_3^2y_5 + 12\kappa y_2y_3y_5 - 12y_1y_2^3y_5 + 6\kappa y_3^2y_4^3 - 4\kappa y_3^2y_4\Big)$$

# APPENDIX C

# ELEMENTS OF $\bar{\phi}_{\bar{y}}(t, t_0)$

$$\bar{\phi}_{\bar{y}}(t, t_0) = \mathcal{J}(t)\bar{\phi}_{\bar{x}}(t, t_0)\mathcal{J}^{-1}(t_0)$$

where all matrices are computed using chief mean element values. With the exception of $\mathcal{J}(t)$, all element values are taken at the initial time.

The nonzero elements of $\mathcal{J}$ are

$$\mathcal{J}_{11} = \eta^2/(e\cos f + 1)$$

$$\mathcal{J}_{21} = -(ne\sin f)/(2\eta)$$

$$\mathcal{J}_{31} = -n(e\cos f + 1)/(2\eta)$$

$$\mathcal{J}_{12} = (a\sin f\cos l)/\eta - a\cos f\sin l$$

$$\mathcal{J}_{22} = na(e\cos f + 1)^2(\eta\sin f\sin l + \cos f\cos l)/\eta^4$$

$$\mathcal{J}_{32} = \left(na(e\cos f + 1)(e\cos^2 f + \cos f - e)\sin l\right)/\eta^3 - \left(na(e\cos f + 1)^2\sin f\cos l\right)/\eta^4$$

$$\begin{aligned}\mathcal{J}_{42} = {} & \left((e\cos f + 2)\sin f\cos u\sin(i/2)\sin l\right)/\eta^2 \\ & + \left(\cos f(e\cos f + 2)\cos u\sin(i/2)\cos l\right)/\eta^3 \\ & + \left(e\left(\frac{\eta^2}{\eta+1} + 1\right)\cos u\sin(i/2)\cos l\right)/\eta^3\end{aligned}$$

$$\begin{aligned}\mathcal{J}_{52} = {} & -\left((e\cos f + 2)\sin f\sin u\sin(i/2)\sin l\right)/\eta^2 \\ & - \left(\cos f(e\cos f + 2)\sin u\sin(i/2)\cos l\right)/\eta^3 \\ & - \left(e\left(\frac{\eta^2}{\eta+1} + 1\right)\sin u\sin(i/2)\cos l\right)/\eta^3\end{aligned}$$

$$\begin{aligned}\mathcal{J}_{62} = {} & \left((e\cos f + 2)\sin f\sin l\right)/\eta^2 + \left(\cos f(e\cos f + 2)\cos l\right)/\eta^3 \\ & + \left(e\left(\frac{\eta^2}{\eta+1} + 1\right)\cos l\right)/\eta^3\end{aligned}$$

$$\mathcal{J}_{13} = -(a\sin f\sin l)/\eta - a\cos f\cos l$$

$$\mathcal{J}_{23} = na(e\cos f + 1)^2(\eta \sin f \cos l - \cos f \sin l)/\eta^4$$

$$\mathcal{J}_{33} = \left(na(e\cos f + 1)(e\cos^2 f + \cos f - e)\cos l\right)/\eta^3 + \left(na(e\cos f + 1)^2 \sin f \sin l\right)/\eta^4$$

$$\begin{aligned}\mathcal{J}_{43} = &\left((e\cos f + 2)\sin f \cos u \sin(i/2)\cos l\right)/\eta^2 \\ &- \left(\cos f(e\cos f + 2)\cos u \sin(i/2)\sin l\right)/\eta^3 \\ &- \left(e\left(\frac{\eta^2}{\eta+1} + 1\right)\cos u \sin(i/2)\sin l\right)/\eta^3\end{aligned}$$

$$\begin{aligned}\mathcal{J}_{53} = &-\left((e\cos f + 2)\sin f \sin u \sin(i/2)\cos l\right)/\eta^2 \\ &+ \left(\cos f(e\cos f + 2)\sin u \sin(i/2)\sin l\right)/\eta^3 \\ &+ \left(e\left(\frac{\eta^2}{\eta+1} + 1\right)\sin u \sin(i/2)\sin l\right)/\eta^3\end{aligned}$$

$$\begin{aligned}\mathcal{J}_{63} = &\left((e\cos f + 2)\sin f \cos l\right)/\eta^2 - \left(\cos f(e\cos f + 2)\sin l\right)/\eta^3 \\ &- \left(e\left(\frac{\eta^2}{\eta+1} + 1\right)\sin l\right)/\eta^3\end{aligned}$$

$$\mathcal{J}_{44} = \sin u \sin h - \cos u \cos h$$

$$\mathcal{J}_{54} = \cos u \sin h + \sin u \cos h$$

$$\mathcal{J}_{45} = \cos u \sin h + \sin u \cos h$$

$$\mathcal{J}_{55} = \cos u \cos h - \sin u \sin h$$

$$\mathcal{J}_{46} = \cos u \sin(i/2)$$

$$\mathcal{J}_{56} = -\sin u \sin(i/2)$$

$$\mathcal{J}_{66} = 1$$

where $\eta = \sqrt{1-e^2}$ and $u = f + g$.

The elements of $\bar{\phi}_{\bar{x}}(t, t_0)$ are below. (These expressions are valid only for canonical units, where $R_e = 1$ and $\mu = 1$.)

$$\bar{\phi}_{\bar{x}(11)} = 1$$

$$\bar{\phi}_{\bar{x}(21)} = \frac{1}{4y_1^6 y_3^3}\big[ -21k_1^3 k_2 J_2\big( -\sin(E-\kappa y_2)\sin[(t-t_0)(f_1J_2+f_2)]$$
$$+\cos(E-\kappa y_2)\cos[(t-t_0)(f_1J_2+f_2)]\big)P_1(t-t_0)$$
$$-6\kappa k_1^2 k_2 y_1^3 y_3^3\big( -\sin(E-\kappa y_2)\sin[(t-t_0)(f_1J_2+f_2)]$$
$$+\cos(E-\kappa y_2)\cos[(t-t_0)(f_1J_2+f_2)]\big)(t-t_0)\big]$$

$$\bar{\phi}_{\bar{x}(31)} = \frac{1}{4y_1^6 y_3^3}\big[ -21k_1^3 k_2 J_2\big( -\cos(E-\kappa y_2)\sin[(t-t_0)(f_1J_2+f_2)]$$
$$-\sin(E-\kappa y_2)\cos[(t-t_0)(f_1J_2+f_2)]\big)P_1(t-t_0)$$
$$-6\kappa k_1^2 k_2 y_1^3 y_3^3\big( -\cos(E-\kappa y_2)\sin[(t-t_0)(f_1J_2+f_2)]$$
$$-\sin(E-\kappa y_2)\cos[(t-t_0)(f_1J_2+f_2)]\big)(t-t_0)\big]$$

$$\bar{\phi}_{\bar{x}(41)} = \frac{1}{4y_1^7 y_3^4}\big[ -21\kappa k_1^2 J_2\big( -y_5\sin y_6\sin[f_3(t-t_0)J_2] + y_4\cos y_6\sin[f_3(t-t_0)J_2]$$
$$+y_4\sin y_6\cos[f_3(t-t_0)J_2] + y_5\cos y_6\cos[f_3(t-t_0)J_2]\big)P_2(t-t_0)\big]$$

$$\bar{\phi}_{\bar{x}(51)} = \frac{1}{4y_1^7 y_3^4}\big[ -21\kappa k_1^2 J_2\big( -y_4\sin y_6\sin[f_3(t-t_0)J_2] - y_5\cos y_6\sin[f_3(t-t_0)J_2]$$
$$-y_5\sin y_6\cos[f_3(t-t_0)J_2] + y_4\cos y_6\cos[f_3(t-t_0)J_2]\big)P_2(t-t_0)\big]$$

$$\bar{\phi}_{\bar{x}(61)} = \frac{1}{4y_1^7 y_3^4}\big(-21k_1^2 J_2 P_3(t-t_0) - 6\kappa k_1^2 y_1^4 y_3^4 (t-t_0)\big)$$

$$\bar{\phi}_{\bar{x}(22)} = \frac{1}{2y_1^7 y_3^5}\big[ -9k_1 k_2^2 y_1 J_2\big( -\cos^2(E-\kappa y_2)\sin[(t-t_0)(f_1J_2+f_2)]$$
$$+\sin[(t-t_0)(f_1J_2+f_2)]$$
$$-\cos(E-\kappa y_2)\sin(E-\kappa y_2)\cos[(t-t_0)(f_1J_2+f_2)]\big)P_1(t-t_0)$$
$$+2y_1^7 y_3^5\cos[(t-t_0)(f_1J_2+f_2)]\big]$$

$$\bar{\phi}_{\bar{x}(32)} = \frac{1}{2y_1^7 y_3^5}\big[9k_1 k_2^2 y_1 J_2\big(\cos^2(E-\kappa y_2)\cos[(t-t_0)(f_1J_2+f_2)]$$
$$-\cos[(t-t_0)(f_1J_2+f_2)]$$
$$-\cos(E-\kappa y_2)\sin(E-\kappa y_2)\sin[(t-t_0)(f_1J_2+f_2)]\big)P_1(t-t_0)$$
$$-2y_1^7 y_3^5\sin[(t-t_0)(f_1J_2+f_2)]\big]$$

$$\bar{\phi}_{\bar{x}(42)} = \frac{1}{y_1^7 y_3^6}\big[6\kappa k_2 \sin(E-\kappa y_2)J_2\big(-y_5 \sin y_6 \sin[f_3(t-t_0)J_2]$$
$$+ y_4 \cos y_6 \sin[f_3(t-t_0)J_2] + y_4 \sin y_6 \cos[f_3(t-t_0)J_2]$$
$$+ y_5 \cos y_6 \cos[f_3(t-t_0)J_2]\big)P_2(t-t_0)\big]$$
$$\bar{\phi}_{\bar{x}(52)} = \frac{1}{y_1^7 y_3^6}\big[6\kappa k_2 \sin(E-\kappa y_2)J_2\big(-y_4 \sin y_6 \sin[f_3(t-t_0)J_2]$$
$$- y_5 \cos y_6 \sin[f_3(t-t_0)J_2] - y_5 \sin y_6 \cos[f_3(t-t_0)J_2]$$
$$+ y_4 \cos y_6 \cos[f_3(t-t_0)J_2]\big)P_2(t-t_0)\big]$$
$$\bar{\phi}_{\bar{x}(62)} = \frac{1}{2y_1^7 y_3^6}\left(3\kappa k_2 \sin(E-\kappa y_2)J_2 P_4(t-t_0)\right)$$
$$\bar{\phi}_{\bar{x}(23)} = \frac{1}{2y_1^7 y_3^5}\big[9k_1 k_2^2 y_1 \cos(E-\kappa y_2)J_2\big(-\sin(E-\kappa y_2)\sin[(t-t_0)(f_1J_2+f_2)]$$
$$+ \cos(E-\kappa y_2)\cos[(t-t_0)(f_1J_2+f_2)]\big)P_1(t-t_0)$$
$$+ 2y_1^7 y_3^5 \sin[(t-t_0)(f_1J_2+f_2)]\big]$$
$$\bar{\phi}_{\bar{x}(33)} = \frac{1}{2y_1^7 y_3^5}\big[9k_1 k_2^2 y_1 \cos(E-\kappa y_2)J_2\big(-\cos(E-\kappa y_2)\sin[(t-t_0)(f_1J_2+f_2)]$$
$$- \sin(E-\kappa y_2)\cos[(t-t_0)(f_1J_2+f_2)]\big)P_1(t-t_0)$$
$$+ 2y_1^7 y_3^5 \cos[(t-t_0)(f_1J_2+f_2)]\big]$$
$$\bar{\phi}_{\bar{x}(43)} = \frac{1}{y_1^7 y_3^6}\big[6\kappa k_2 \cos(E-\kappa y_2)J_2\big(-y_5 \sin y_6 \sin[f_3(t-t_0)J_2]$$
$$+ y_4 \cos y_6 \sin[f_3(t-t_0)J_2] + y_4 \sin y_6 \cos[f_3(t-t_0)J_2]$$
$$+ y_5 \cos y_6 \cos[f_3(t-t_0)J_2]\big)P_2(t-t_0)\big]$$
$$\bar{\phi}_{\bar{x}(53)} = \frac{1}{y_1^7 y_3^6}\big[6\kappa k_2 \cos(E-\kappa y_2)J_2\big(-y_4 \sin y_6 \sin[f_3(t-t_0)J_2]$$
$$- y_5 \cos y_6 \sin[f_3(t-t_0)J_2] - y_5 \sin y_6 \cos[f_3(t-t_0)J_2]$$
$$+ y_4 \cos y_6 \cos[f_3(t-t_0)J_2]\big)P_2(t-t_0)\big]$$
$$\bar{\phi}_{\bar{x}(63)} = \frac{1}{2y_1^7 y_3^6}\left(3\kappa k_2 \cos(E-\kappa y_2)J_2 P_4(t-t_0)\right)$$
$$\bar{\phi}_{\bar{x}(24)} = \frac{1}{y_1^5 y_3^3}\big[18k_1^2 k_2\left(y_5 \sin y_6 - y_4 \cos y_6\right)J_2\big(-\sin(E-\kappa y_2)\sin[(t-t_0)(f_1J_2+f_2)]$$
$$+ \cos(E-\kappa y_2)\cos[(t-t_0)(f_1J_2+f_2)]\big)P_2(t-t_0)\big]$$

$$\bar{\phi}_{\bar{x}(34)} = \frac{1}{y_1^5 y_3^3}\big[18k_1^2k_2\,(y_5\sin y_6 - y_4\cos y_6)\,J_2\big(-\cos\left(E-\kappa y_2\right)\sin\left[(t-t_0)(f_1J_2+f_2)\right]$$

$$-\sin\left(E-\kappa y_2\right)\cos\left[(t-t_0)(f_1J_2+f_2)\right]\big)P_2(t-t_0)\big]$$

$$\bar{\phi}_{\bar{x}(44)} = \frac{1}{y_1^6 y_3^4}\big[-6\kappa k_1 J_2\,(-f_4\sin\left[f_3(t-t_0)J_2\right] - f_5\cos\left[f_3(t-t_0)J_2\right])\,(t-t_0)$$

$$+y_1^6y_3^4\cos\left[f_3(t-t_0)J_2\right]\big]$$

$$\bar{\phi}_{\bar{x}(54)} = \frac{1}{y_1^6 y_3^4}\big[6\kappa k_1 J_2\,(-f_5\sin\left[f_3(t-t_0)J_2\right] + f_4\cos\left[f_3(t-t_0)J_2\right])\,(t-t_0)$$

$$-y_1^6y_3^4\sin\left[f_3(t-t_0)J_2\right]\big]$$

$$\bar{\phi}_{\bar{x}(64)} = \frac{1}{y_1^6 y_3^4}\,(6k_1(y_5\sin y_6 - y_4\cos y_6)J_2P_5(t-t_0))$$

$$\bar{\phi}_{\bar{x}(25)} = \frac{1}{y_1^5 y_3^3}\big[18k_1^2k_2\,(y_4\sin y_6 + y_5\cos y_6)\,J_2\big(-\sin\left(E-\kappa y_2\right)\sin\left[(t-t_0)(f_1J_2+f_2)\right]$$

$$+\cos\left(E-\kappa y_2\right)\cos\left[(t-t_0)(f_1J_2+f_2)\right]\big)P_2(t-t_0)\big]$$

$$\bar{\phi}_{\bar{x}(35)} = \frac{1}{y_1^5 y_3^3}\big[18k_1^2k_2\,(y_4\sin y_6 + y_5\cos y_6)\,J_2\big(-\cos\left(E-\kappa y_2\right)\sin\left[(t-t_0)(f_1J_2+f_2)\right]$$

$$-\sin\left(E-\kappa y_2\right)\cos\left[(t-t_0)(f_1J_2+f_2)\right]\big)P_2(t-t_0)\big]$$

$$\bar{\phi}_{\bar{x}(45)} = \frac{1}{y_1^6 y_3^4}\big[6\kappa k_1 J_2\big(-f_5\sin\left[f_3(t-t_0)J_2\right] + 2y_4y_5\cos y_6\sin y_6\cos\left[f_3(t-t_0)J_2\right]$$

$$+y_5^2\cos^2 y_6\cos\left[f_3(t-t_0)J_2\right] - y_4^2\cos^2 y_6\cos\left[f_3(t-t_0)J_2\right]$$

$$+y_4^2\cos\left[f_3(t-t_0)J_2\right]\big)(t-t_0) + y_1^6y_3^4\sin\left[f_3(t-t_0)J_2\right]\big]$$

$$\bar{\phi}_{\bar{x}(55)} = \frac{1}{y_1^6 y_3^4}\big[6\kappa k_1 J_2\big(-f_5\cos\left[f_3(t-t_0)J_2\right] - 2y_4y_5\cos y_6\sin y_6\sin\left[f_3(t-t_0)J_2\right]$$

$$-y_5^2\cos^2 y_6\sin\left[f_3(t-t_0)J_2\right] + y_4^2\cos^2 y_6\sin\left[f_3(t-t_0)J_2\right]$$

$$-y_4^2\sin\left[f_3(t-t_0)J_2\right]\big)(t-t_0) + y_1^6y_3^4\cos\left[f_3(t-t_0)J_2\right]\big]$$

$$\bar{\phi}_{\bar{x}(65)} = \frac{1}{y_1^6 y_3^4}\,(6k_1(y_4\sin y_6 + y_5\cos y_6)J_2P_5(t-t_0))$$

$$\bar{\phi}_{\bar{x}(66)} = 1$$

$$\bar{\phi}_{\bar{x}(12)} = \bar{\phi}_{\bar{x}(13)} = \bar{\phi}_{\bar{x}(14)} = \bar{\phi}_{\bar{x}(15)} = 0$$

$$\bar{\phi}_{\bar{x}(16)} = \bar{\phi}_{\bar{x}(26)} = \bar{\phi}_{\bar{x}(36)} = \bar{\phi}_{\bar{x}(46)} = \bar{\phi}_{\bar{x}(56)} = 0$$

where $k_1 = 2 - y_1 y_2^2 - y_1 y_3^2$, $k_2 = \sqrt{1 - k_1 y_1 y_3^2} = e$, $\kappa = \sqrt{k_1 y_1}$,

$$P_1 = 6y_5^4 + 12y_4^2 y_5^2 - 6y_5^2 + 6y_4^4 - 6y_4^2 + 1$$

$$P_2 = 2y_5^2 + 2y_4^2 - 1$$

$$P_3 = 6k_1 y_1 y_3 y_5^4 + 10\kappa y_5^4 + 12k_1 y_1 y_3 y_4^2 y_5^2 + 20\kappa y_4^2 y_5^2 - 6k_1 y_1 y_3 y_5^2 - 8\kappa y_5^2 + 6k_1 y_1 y_3 y_4^4$$
$$+ 10\kappa y_4^4 - 6k_1 y_1 y_3 y_4^2 - 8\kappa y_4^2 + k_1 y_1 y_3 + \kappa$$

$$P_4 = 18\kappa y_3 y_5^4 + 40y_5^4 + 36\kappa y_3 y_4^2 y_5^2 + 80y_4^2 y_5^2 - 18\kappa y_3 y_5^2 - 32y_5^2 + 18\kappa y_3 y_4^4 + 40y_4^4$$
$$- 18\kappa y_3 y_4^2 - 32y_4^2 + 3\kappa y_3 + 4$$

$$P_5 = 6k_1 y_1 y_3 y_5^2 + 10\kappa y_5^2 + 6k_1 y_1 y_3 y_4^2 + 10\kappa y_4^2 - 3k_1 y_1 y_3 - 4\kappa$$

and

$$f_1 = (3k_1^2 P_1)/(2y_1^5 y_3^3)$$

$$f_2 = (k_1/y_1)^{3/2}$$

$$f_3 = (3\kappa k_1^3 P_2)/\left(2(1 - 2k_2^2 + k_2^4)y_1^4\right)$$

$$f_4 = 2y_4 y_5 \cos y_6 \sin y_6 + y_5^2 \cos^2 y_6 - y_4^2 \cos^2 y_6 - y_5^2$$

$$f_5 = y_5^2 \cos y_6 \sin y_6 - y_4^2 \cos y_6 \sin y_6 - 2y_4 y_5 \cos^2 y_6 + y_4 y_5$$

# APPENDIX D

# ELEMENTS OF $\Sigma(t)$

$\Sigma(t) = A(t) + B(t)$, where the matrices are computed using the chief's osculating elements.

The nonzero elements of $A(t)$ are

$$A_{11} = A_{42} = A_{53} = 1$$

$$A_{51} = -y_3/y_1$$

$$A_{24} = 2y_1y_5$$

$$A_{34} = \left(2y_1(y_5-1)(y_5+1)\sqrt{-y_5^2-y_4^2+1}\right)/(y_5^2+y4^2-1)$$

$$A_{54} = 2y_2y_5$$

$$A_{64} = \left(2\sqrt{-y_5^2-y_4^2+1}\,(y_2y_5^2-y_3y_4y_5-y_2)\right)/(y_5^2+y_4^2-1)$$

$$A_{25} = -2y_1y_4$$

$$A_{35} = -\left(2y_1y_4y_5\sqrt{-y_5^2-y_4^2+1}\right)/(y_5^2+y4^2-1)$$

$$A_{55} = -2y_2y_4$$

$$A_{65} = -\left(2(y_2y_4y_5-y_3y_4^2+y_3)\sqrt{-y_5^2-y_4^2+1}\right)/(y_5^2+y_4^2-1)$$

$$A_{26} = -y_1(2y_5^2+2y_4^2-1)$$

$$A_{36} = -2y_1y_5\sqrt{-y_5^2-y_4^2+1}$$

$$A_{56} = -y_2(2y_5^2+2y_4^2-1)$$

$$A_{66} = -2(y_2y_5-y_3y_4)\sqrt{-y_5^2-y_4^2+1}$$

Accounting for $J_2$ only, $B(t)$ is

$$B(t) = \frac{6J_2R_e^2\mu y_4(2y_5^2+2y_4^2-1)}{y_1^3y_3}\begin{bmatrix} 0_{3x3} & 0_{3x3} \\ 0_{3x3} & B_{22} \end{bmatrix}$$

where

$$B_{22} = \begin{bmatrix} 0 & 0 & 0 \\ -2(y_5^2 - 1) & 2y_4 y_5 & 2y_5(y_5^2 + y_4^2 - 1) \\ -2y_5\sqrt{1 - y_4^2 - y_5^2} & 2y_4\sqrt{1 - y_4^2 - y_5^2} & (2y_5^2 + 2y_4^2 - 1)\sqrt{1 - y_4^2 - y_5^2} \end{bmatrix}$$

# APPENDIX E

# RELATIVE TRANSFORMATION MAP FOR WHITTAKER VARIABLES

## E.1 BACKGROUND

The set of orbit elements known as polar nodal variables, or Hill's variables [31], or Whittaker variables [32, p. 349], are $\underline{w} = \begin{bmatrix} r & u & h & \dot{r} & G & H \end{bmatrix}$, where $r$ is the radial distance to the orbiting satellite, $u$ is the argument of latitude, $h$ is the right ascension of the ascending node, $\dot{r}$ is the radial rate, $G$ is the angular momentum magnitude, and $H$ is the polar component of angular momentum. In terms of classical orbit elements $\underline{\text{oe}} = \begin{bmatrix} a & e & i & h & g & l \end{bmatrix}$ (where $a$ is the semi-major axis, $e$ is the eccentricity, $i$ is the inclination, $g$ is the argument of perigee, and $l$ is the mean anomaly), they are

$$
\begin{aligned}
r &= \frac{a\left(1-e^2\right)}{1+e\cos f} \\
u &= f+g \\
h &= h \\
\dot{r} &= \frac{\mu e}{\sqrt{\mu a\left(1-e^2\right)}}\sin f \\
G &= \sqrt{\mu a\left(1-e^2\right)} \\
H &= \sqrt{\mu a\left(1-e^2\right)}\cos i
\end{aligned}
$$

where $\mu$ is the Earth's gravitational parameter and $f(e,l)$ is the true anomaly. The inverse transformation is given by the following algorithm:

$$
\begin{aligned}
e\sin f &= \tfrac{\dot{r}G}{\mu} & e\cos f &= \tfrac{G^2}{\mu r}-1 \\
f &= \operatorname{atan2}\left(e\sin f, e\cos f\right) & e &= \sqrt{\left(e\sin f\right)^2+\left(e\cos f\right)^2} \\
E &= \operatorname{atan2}\left(\sin f\sqrt{1-e^2}, e+\cos f\right) & a &= \tfrac{G^2}{\mu\left(1-e^2\right)} \\
i &= \operatorname{acos}\tfrac{H}{G} & h &= h \\
g &= u-f & l &= E-e\sin E
\end{aligned}
\tag{E.1}
$$

where $E$ is the eccentric anomaly. Note that the formula for $f$ is invalid when $e = 0$; in other words, $f$ is undefined for circular orbits (and therefore so are $l$ and $g$).

Once an approximate solution to the Zonal Problem is posed in Whittaker elements, then it is possible to predict the relative motion of satellites not only by directly differencing the trajectories of the chief and deputy satellites, but also by constructing a closed-form relative motion model, such as the Gim-Alfriend State Transition Matrix (GA STM) [18], which approximates the relative motion using a succession of linear operators:

$$\begin{bmatrix} \underline{r}(t)^T & \underline{v}(t)^T \end{bmatrix}^T = \Sigma(t) D(t) \bar{\phi}_{\bar{w}}(t, t_0) D^{-1}(t_0) \Sigma^{-1}(t_0) \begin{bmatrix} \underline{r}(t_0)^T & \underline{v}(t_0)^T \end{bmatrix}^T \tag{E.2}$$

This is the same as Eq. 4.1 for the Hoots-elements STM, except that here $\bar{\phi}_{\bar{w}}(t, t_0)$ is the state transition matrix for the mean Whittaker elements.

This appendix develops the linearized transformation map $\Sigma$ and uses it to illustrate the chief difficulty with Whittaker elements: the singularity for zero inclination.

## E.2 RELATIVE TRANSFORMATION MAP $\Sigma$

Reference [18] reports expressions (shown in Chapter IV above) for the spherical curvilinear coordinates of a deputy satellite's relative position $\underline{r}(t)$ and velocity $\underline{v}(t)$ in terms of the chief's osculating nonsingular elements $\underline{ns} = \begin{bmatrix} a & u & i & q_1 = e\cos g & q_2 = e\sin g & h \end{bmatrix}$ and the deputy's relative osculating nonsingular elements ($\delta a$, $\delta u$, $\delta i$, $\delta q_1$, $\delta q_2$, and $\delta h$). These can be mapped into expressions in terms of the chief and relative Whittaker elements using Eqs. E.1 and the Jacobian matrix

$$\frac{\partial \underline{ns}}{\partial \underline{w}} = \begin{bmatrix} \frac{2\mu r G(\mu r - G)}{k} & 0 & 0 & \frac{2\mu r^4 \dot{r}}{k} & \frac{2\mu r^2 G}{k} & 0 \\ 0 & 1 & 0 & 0 & 0 & 0 \\ 0 & 0 & 0 & 0 & \frac{H}{G\sqrt{G^2 - H^2}} & \frac{-1}{\sqrt{G^2 - H^2}} \\ -\frac{G^2 \cos u}{\mu r^2} & \frac{r\dot{r}\cos u - (G^2 - \mu r)\sin u}{\mu r} & 0 & \frac{G \sin u}{\mu} & \frac{2G\cos u + r\dot{r}\sin u}{\mu r} & 0 \\ -\frac{G^2 \sin u}{\mu r^2} & \frac{r\dot{r}\sin u + (G^2 - \mu r)\cos u}{\mu r} & 0 & -\frac{G\cos u}{\mu} & \frac{2G\sin u - r\dot{r}\cos u}{\mu r} & 0 \\ 0 & 0 & 1 & 0 & 0 & 0 \end{bmatrix}$$

where $k = \left(G^2 + r^2\dot{r}^2 - 2\mu r\right)^2$. Some terms in $\underline{v}\,(t)$ depend on the perturbed rates of change in $u$ and $h$, which can be found from Gauss's Variational Equations in terms of the perturbing acceleration vector $\underline{a}_p$ due to the Earth's gravitational zonal harmonics [3]:

$$\dot{h} = \frac{a_h\, r \sin u}{G \sin i}$$
$$\dot{u} = \frac{G}{r^2} - \dot{h}\cos i$$

where $a_h$ is the component of $\underline{a}_p$ normal to the osculating orbit plane. Neglecting harmonics beyond $J_2$, a first-order perturbation theory gives $a_h$ as $-3R_e^2 J_2\left(\mu/r^4\right)\sin i \cos i \sin u$, where $R_e$ is the average radius of the Earth.

In the resulting expressions for $\underline{r}(t)$ and $\underline{v}(t)$, the coefficients of the differential Whittaker elements are then formed into matrix $\Sigma(t)$, so that

$$\begin{bmatrix} \underline{r}(t) \\ \\ \underline{v}(t) \end{bmatrix} = \Sigma(t)\,\underline{\delta w}(t) \tag{E.3}$$

The portion of the transformation due to the perturbing acceleration can be partitioned into a separate map $B(t)$, so that $\Sigma(t) = A(t) + B(t)$. The elements of $A(t)$ and $B(t)$ are listed below.

### E.2.1 Singularity for Equatorial Chief Orbits

It is important to discuss the case of equatorial orbits, when $i = 0$ (or, in terms of Whittaker elements, $H = G$). In this case, $h$ is undefined, and certain elements of the $A(t)$ matrix become singular. Specifically, they contribute the following terms to the cross-track motion:

$$z_{singular} = r \sin u \left(\frac{\frac{H}{G}\delta G - \delta H}{\sqrt{G^2 - H^2}}\right)$$
$$\dot{z}_{singular} = \frac{G\cos u + r\dot{r}\sin u}{r}\left(\frac{\frac{H}{G}\delta G - \delta H}{\sqrt{G^2 - H^2}}\right)$$

Note that in both expressions, the factor in parentheses contributing the singularity is $\delta i$ (compare to Eq. 7.92 in Reference [1], which also contains $z_{singular}$).

It can be shown that, for near-equatorial orbits, the size of the difference $\delta G - \delta H$ is smaller than first order in the relative coordinates (that is, the first variation of $H = G\cos i$ is $\delta H = \delta G \cos i - G\,\delta i \sin i$,

which evaluates to $\delta H = \delta G$ when $i = 0$). Using the near-equatorial approximation $\delta H = \delta G$ gives

$$\delta i = -\frac{\delta G}{G}\frac{\sqrt{G-H}}{\sqrt{G+H}}$$

This new expression is no longer singular; however, it also vanishes for the case of interest ($H = G$). It turns out that all the other cross-track terms also vanish for equatorial orbits, meaning that Eq. E.3 is unable to model any cross-track relative motion–it simply degenerates to the zeroth-order approximation that both chief and deputy orbits are equatorial.

An alternative approximation (more accurate than $\delta H = \delta G$) can be found by solving for $\delta i$ from the second variation of $H$, and then setting $H = G$:

$$\delta i^2 = \frac{2}{G}\left(\delta G - \delta H\right)$$

This shows that the real cross-track motion is of $\mathcal{O}(\frac{1}{2})$ in the differential Whittaker elements. In other words, a linearized model using Whittaker elements is not suitable for modeling relative motion near $i = 0$.

### E.3 ELEMENTS OF $\Sigma(t)$

$\Sigma(t) = A(t) + B(t)$, where the matrices are computed using the chief's osculating elements.

The nonzero elements of $A(t)$ are

$$A_{11} = 1$$

$$A_{22} = r$$

$$A_{23} = \frac{rH}{G}$$

$$A_{33} = \frac{r\cos u\sqrt{G^2-H^2}}{-G}$$

$$A_{35} = \frac{rH\sin u}{G\sqrt{G^2-H^2}}$$

$$A_{36} = \frac{-r\sin u}{\sqrt{G^2-H^2}}$$

$$A_{41} = \frac{4\mu^2 r\dot{r}(G^2-\mu r)}{G^2 k}$$

$$A_{44} = \frac{\mu^2 r^2(G^2+5r^2\dot{r}^2-2\mu r)}{-G^2 k}$$

$$A_{45} = \frac{4\mu^2 r^2\dot{r}(2G^2+r^2\dot{r}^2-2\mu r)}{-G^3 k}$$

$$A_{51} = \frac{-2G}{r^2}$$

$$A_{52} = \dot{r}$$

$$A_{53} = \frac{\dot{r}H}{G}$$

$$A_{55} = \frac{1}{r}$$

$$A_{63} = \frac{\left(G\sin u - r\dot{r}\cos u\right)\sqrt{G^2 - H^2}}{rG}$$

$$A_{65} = \frac{H\left(G\cos u + r\dot{r}\sin u\right)}{rG\sqrt{G^2 - H^2}}$$

$$A_{66} = \frac{G\cos u + r\dot{r}\sin u}{-r\sqrt{G^2 - H^2}}$$

where $k = \left(G^2 + r^2\dot{r}^2 - 2\mu r\right)^2$. As noted above, for equatorial orbits (when $H = G$), some of the cross-track elements become singular.

To first order in $J_2$, $B(t)$ is

$$B(t) = \frac{3J_2R_e^2\mu H\sin u}{r^2G^3}\mathcal{B}$$

where the nonzero elements of $\mathcal{B}$ are

$$\mathcal{B}_{53} = \frac{\cos u\left(G^2 - H^2\right)}{G}$$

$$\mathcal{B}_{55} = \frac{H\sin u}{-G}$$

$$\mathcal{B}_{56} = \sin u$$

$$\mathcal{B}_{62} = \sqrt{G^2 - H^2}$$

$$\mathcal{B}_{63} = \frac{H\sqrt{G^2 - H^2}}{G}$$